

ISOLATION AND STRUCTURE ELUCIDATION OF NEW COMPOUNDS FROM
CORNUS CONTROVERSA AND *DELPHINIUM CHRYSOTRICHUM*

by

Yangqing He

A Dissertation Submitted to the Faculty of
The Charles E. Schmidt College of Science
in Partial Fulfillment of the Requirements for the Degree of
Doctor of Philosophy

Florida Atlantic University

Boca Raton, FL

May 2014

ISOLATION AND STRUCTURE ELUCIDATION OF NEW COMPOUNDS FROM
CORNUS CONTROVERSA AND *DELPHINIUM CHRYSOTRICHUM*

by

Yangqing He

This dissertation was prepared under the direction of the candidate's dissertation advisor, Dr. Lyndon M. West, Department of Chemistry and Biochemistry, and has been approved by the members of his supervisory committee. It was submitted to the faculty of the Charles E. Schmidt College of Science and was accepted in partial fulfillment of the requirements for the degree of Doctor of Philosophy.

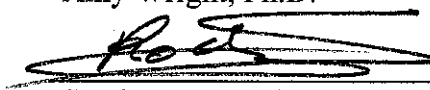
SUPERVISORY COMMITTEE:



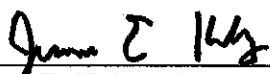
Lyndon M. West, Ph.D.
Dissertation Advisor



Amy Wright, Ph.D.



Stéphane P. Roche, Ph.D.



Jerome E. Haky, Ph.D.
Interim Chair, Department of Chemistry and Biochemistry



Russell Ivy, Ph.D.
Interim Dean, Charles E. Schmidt College of Science



Deborah L. Floyd, Ed.D.
Interim Dean, Graduate College

April 8, 2014

Date

ACKNOWLEDGEMENTS

First and foremost, I would like to express my deeply-felt gratitude to my advisor Dr. Lyndon M. West. I appreciate all his contributions of time, ideas, warm encouragement and thoughtful guidance to make my Ph.D. studying productive and stimulating. The joy and enthusiasm he has for the research was contagious and motivational for me, even during the tough time in the pursuit of my Ph.D. I am also thankful for the excellent example he has provided as a successful chemist and professor, as well as how patiently he is as a supervisor to his graduate students. His professional leadership, excellent scientific methods, and critical thinking have been, and will be, a great benefit to my scientific career.

A special thanks to my committee members: Dr. Amy Wright for always taking one day off from her research and driving two hours from Jupiter each times to provide helpful suggestion and warm encouragement. I want to express my gratitude to Dr. Stéphane P. Roche, Dr. Deguo Du and Dr. Cyril Párkányi, not only for their excellent comments and invaluable suggestions, but also for listening to me whenever I was excited about my research.

I would like to thank Dr. Jerome E. Haky, Salvatore Lepore, Andrew Terentis and Daniel T. de Lill for their outstanding teaching, patience, encouragement and support. I would especially like to thank Dr. Jerome E. Haky for always being willing to listening

and offer encouragement throughout my time at FAU. Also, I would like to thank Dr. Andrew Terentis for teaching me how to calculate NMR data with different software.

I would like to thank Dr. Mark T. Hamann at the University of Mississippi for collecting samples and offering support. Also, I would like to acknowledge Dr. Jiangnan Peng at the University of Texas Health Center at San Antonio for his valuable discussion and kind help on my manuscript.

I am grateful to all the members in our laboratory, their friendship and assistance has meant more to me than I could ever express. I could not complete my work without invaluable friendly assistance and their participation. Also I would like to thank all the faculty members, staff (especially Ms. Helena Szczesny, and Mr. Javier Riveria), library staff, and past and present students of Department of Chemistry and Biochemistry who helped me in different ways over the years.

I would like to thank the president and the leadership of College of Science of Xi'an University of Technology for giving me this opportunity to study abroad in the USA.

Lastly, I would give my special thanks to my family for their unconditional love, encouragement and enduring support. For my parents and sisters who supported me in all my pursuits. And most of all for my lovely son, Leon; I gratefully acknowledge your patience, understanding, as well as for the love you have missed from Dad during those separated years. And for my loving, supportive, encouraging, and patient wife Dr. Zhanying Ma whose faithful support during the final stages of this Ph.D. is so appreciated. Thanks both of you.

ABSTRACT

Author: Yangqing He
Title: Isolation and Structure Elucidation of New Compounds from *Cornus controversa* and *Delphinium chrysotrichum*
Institution: Florida Atlantic University
Dissertation Advisor: Dr. Lyndon M. West
Degree: Doctor of Philosophy
Year: 2014

The aim of this dissertation was to explore structurally unique secondary metabolites from herb medicinal plants *Cornus controversa* and *Delphinium chrysotrichum*.

The introduction in the first chapter provides a detailed review about the research progress of chemical constituents of the genus *Cornus*. In addition, its pharmacological activities were also summarized in this chapter to provide a framework for understanding the roles of medicinal herbs belong to genus *Cornus* as anti-diabetes therapeutics and to deliver useful information for further research.

In chapter two, seven new compounds, including one iridoid glucoside, cornoside A (**59**), five iridoid aglycones, cornolactones A – E (**60** – **64**) and one indenone glucoside, cornoside B (**65**), together with 10 known compounds have been isolated from the leaves of *Cornus controversa*. The structures of these compounds were established by interpretation of spectroscopic data. Cornolactone A (**61**) is the first natural

cis-fused tricyclic dilactone iridoid containing both a five- and six-membered lactone ring. Cornoside B (**65**) is the first alkaloid isolated from the genus *Cornus* bearing an indole-3-lactic acid-11- β -D-glucopyranoside skeleton.

In chapter three, we described the structure elucidation of three new diterpenoid alkaloids delphatisine D (**77**), chrysotrichumines A (**78**) and B (**79**), as well as 11 known compounds from the whole plants of *Delphinium chrysotrichum*. Delphatisine D (**77**) is a rare atisine-type alkaloid from genus *Delphinium* and is the C-15 epimer of spiramine C which bears an internal carbinolamine ether linkage (N–C–O–C) between C-7 and C-20. Chrysotrichumine A (**78**) is a rare natural C₁₉-diterpenoid alkaloid possessing a nitrone group between C-17 and C-19. In addition, their cytotoxic activity against human breast cancer cell lines of MCF-7 and MDA-MB-231 were also reported.

In chapter four, the detailed extraction and isolation procedures of the new compounds, cornosides A and B, cornolactones A – E, delphatisine D, chrysotrichumine A and B, as well as of all the known compounds were described. In addition, the experimental procedures for the determination of PPAR γ and LXR agonistic activities and the MTT cytotoxicity assay were listed in this chapter.

ISOLATION AND STRUCTURE ELUCIDATION OF NEW COMPOUNDS FROM
CORNUS CONTROVERSA AND *DELPHINIUM CHRYSOTRICHUM*

LIST OF TABLES	xi
LIST OF FIGURES	xii
CHAPTER 1: INTRODUCTION	
1.1 The Genus <i>Cornus</i> and its Anti-diabetic Activity	1
1.2 Research Progress on the Chemical Constituents and Bioactivities of <i>Cornus</i>	5
1.3 Summary	13
1.4 Research Objectives	14
CHAPTER 2: ISOLATION AND STRUCTURAL ELUCIDATION OF SEVEN NEW COMPOUNDS FROM <i>CORNUS CONTROVERSA</i>	
2.1 Background	17
2.2 Structure Elucidation of Cornosides A, B and Cornolactones A – E	18
2.3 Activity	73
2.4 Conclusion	73
CHAPTER 3: DELPHATISINE D AND CHRYSOTRICHUMINES A – B, THREE NEW DITERPENOID ALKALOIDS FROM <i>DELPHINIUM CHRYSOTRICHUM</i>	
3.1 Background	75
3.2 Structural Elucidation of Delpatisine D, Chrysotrichumine A and B	79
3.3 Cytotoxic Activity	109

3.4 Conclusion.....	109
CHAPTER 4: EXPERIMENTAL PROCEDURES	
4.1 General Experimental Procedures.....	110
4.2 Plant Material Collections.....	111
4.3 Extraction and Isolation of Cornosides A, B and Cornolactones A – E	111
4.4 Extraction and Isolation of Delphatisine D, Chrysotrichumine A and B.....	116
4.5 Determination of PPAR γ and LXR Agonistic Activities.....	119
4.6 MTT Cytotoxicity Assay.....	120
APPENDIX 1	122
APPENDIX 2	169
REFERENCES	190

LIST OF TABLES

Table 2.1 NMR Data of Cornoside A (59) in <i>d</i> ₆ -DMSO	27
Table 2.2 Comparison of ¹³ C NMR Data of compounds 59 and 70	27
Table 2.3 NMR Data of Cornoside A (59) in CD ₃ OD.....	31
Table 2.4 NMR Data for Cornolactone A (60) in CDCl ₃	34
Table 2.5 NMR Data for Cornolactone B (61) in CDCl ₃	42
Table 2.6 NMR Data for Cornolactone C (62) in CD ₃ OD	49
Table 2.7 NMR Data for Cornolactone D (63) in CDCl ₃	55
Table 2.8 NMR Data for Cornolactone E (64) in CDCl ₃	62
Table 2.9 NMR Data for Cornoside B (65) in CDCl ₃	68
Table 3.1 Comparison of ¹³ C NMR Data of compounds 77 and 90	83
Table 3.2 NMR Data for Delphatisine D (77) in CDCl ₃	84
Table 3.3 NMR Data for Chrysotrichumine A (78) in CDCl ₃	93
Table 3.4 Comparison of ¹³ C NMR Data of compounds 78 and 89	94
Table 3.5 NMR Data for Chrysotrichumine B (79) in CDCl ₃	101
Table 3.6 Comparison of ¹³ C NMR Data of compounds 79 and 86	104

LIST OF FIGURES

Figure 1.1 Structures of bioactivity compounds isolated from Genus <i>Cornus</i>	4
Figure 1.2 Chemical structures of iridoid glycosides isolated from <i>Cornus</i>	7
Figure 1.3 Chemical structures of anthocyanins isolated from <i>Cornus</i>	8
Figure 1.4 Chemical structures of flavanoids isolated from <i>Cornus</i>	10
Figure 1.5 Chemical structures of organic acids isolated from <i>Cornus</i>	12
Figure 1.6 New compounds isolated from <i>Cornus alternifolia</i>	15
Figure 2.1 Isolation scheme 1 for compounds 59 – 65	20
Figure 2.2 Isolation scheme 2 for compounds 59 – 65	21
Figure 2.3 Isolation scheme 3 for compounds 59 , 60 and 64	22
Figure 2.4 Isolation scheme 4 for compounds 59 , 60 and 64	23
Figure 2.5 Chemical structures of compounds 59 – 65	24
Figure 2.6 Ten known compounds isolated from <i>Cornus controversa</i>	25
Figure 2.7 Subfragments (A – C) of cornoside A (59).....	28
Figure 2.8 Key ^1H - ^1H COSY and HMBC correlations of cornoside A (59).....	29
Figure 2.9 Key NOESY correlations of cornoside A (59).....	30
Figure 2.10 ^1H NMR spectrum of cornoside A (59)	32
Figure 2.11 ^{13}C NMR spectrum of cornoside A (59).....	33
Figure 2.12 Isolated ^1H spin system of cornolactone A (60).....	35
Figure 2.13 Key ^1H - ^1H COSY and HMBC correlations of cornolactone A (60)	36

Figure 2.14 Key NOESY correlations of cornolactone A (60).....	37
Figure 2.15 ¹ H NMR spectrum of cornolactone A (60)	39
Figure 2.16 ¹³ C NMR spectrum of cornolactone A (60)	40
Figure 2.17 Subfragments (A – C) of cornolactone B (61)	42
Figure 2.18 Key ¹ H– ¹ H COSY and HMBC correlations of cornolactone B (61)	43
Figure 2.19 Key NOESY correlations of cornolactone B (61).....	44
Figure 2.20 ¹ H NMR spectrum of cornolactone B (61).....	46
Figure 2.21 ¹³ C NMR spectrum of cornolactone B (61).....	47
Figure 2.22 ¹ H NMR spectrum of cornolactone C (62).....	50
Figure 2.23 ¹³ C NMR spectrum of cornolactone C (62).....	51
Figure 2.24 Subfragments (A – C) of cornolactone C (62)	52
Figure 2.25 Key ¹ H– ¹ H COSY and HMBC correlations of cornolactone C (62)	53
Figure 2.26 Key NOESY correlations of cornolactone C (62).....	54
Figure 2.27 Subfragments (A – C) of cornolactone D (63).....	56
Figure 2.28 Key ¹ H– ¹ H COSY and HMBC correlations of cornolactone D (63)	57
Figure 2.29 Key NOESY correlations of cornolactone D (63).....	58
Figure 2.30 ¹ H NMR spectrum of cornolactone D (63)	59
Figure 2.31 ¹³ C NMR spectrum of cornolactone D (63)	60
Figure 2.32 Subfragments (A – C) of cornolactone E (64)	62
Figure 2.33 Key ¹ H– ¹ H COSY and HMBC correlations of cornolactone E (64).....	63
Figure 2.34 ¹ H NMR spectrum of cornolactone E (64).....	64
Figure 2.35 ¹³ C NMR spectrum of cornolactone E (64).....	65
Figure 2.36 Key NOESY correlations of cornolactone E (64).....	66

Figure 2.37 Isolated ^1H spin systems (A – C) of cornoside B (65)	68
Figure 2.38 Key ^1H - ^1H COSY and HMBC correlations of cornoside B (65)	69
Figure 2.39 ^1H NMR spectrum of cornoside B (65).....	71
Figure 2.40 ^{13}C NMR spectrum of cornoside B (65).....	72
Figure 2.41 Possible biosynthesis route to inversion of configuration at C-6 in 63 , 64 ..	74
Figure 3.1 Compounds previously isolated from <i>Delphinium chrysotrichum</i>	77
Figure 3.2 Chemical structures isolated from <i>Delphinium chrysotrichum</i>	78
Figure 3.3 Isolation scheme for delphatisine D (77).....	79
Figure 3.4 Isolation scheme for chrysotrichumines A (78) and B (79)	80
Figure 3.5 Substructures (A – G) of delphatisine D (77)	82
Figure 3.6 Chemical structures of isoatisine (91)	84
Figure 3.7 ^1H NMR spectrum of delphatisine D (77).....	85
Figure 3.8 ^{13}C NMR spectrum of delphatisine D (77).....	86
Figure 3.9 Key ^1H - ^1H COSY and HMBC correlations of delphatisine D (77)	87
Figure 3.10 ^1H NMR spectra of delphatisine D (77) and its acetic ester (77a)	89
Figure 3.11 Key NOESY correlations of delphatisine D (77).....	91
Figure 3.12 Substructures (A – D) of chrysotrichumine A (78).....	94
Figure 3.13 Key ^1H - ^1H COSY and HMBC correlations of chrysotrichumine A (78).....	95
Figure 3.14 ^1H NMR spectrum of chrysotrichumine A (78)	98
Figure 3.15 ^{13}C NMR spectrum of chrysotrichumine A (78).....	99
Figure 3.16 Key ROESY correlations of chrysotrichumine A (78).....	100
Figure 3.17 Substructures (A – E) of chrysotrichumine B (79)	102
Figure 3.18 Key ^1H - ^1H COSY and HMBC correlations of chrysotrichumine B (79)...	103

Figure 3.19 Key NOESY correlations of chrysotrichumine B (79).....	106
Figure 3.20 ^1H NMR spectrum of chrysotrichumine B (79).	107
Figure 3.21 ^{13}C NMR spectrum of chrysotrichumine B (79)	108

1. INTRODUCTION

1.1 The Genus *Cornus* and its Anti-diabetic Activity

The genus *Cornus* contains many medicinal plants. The genus *Cornus* belongs to the family Cornaceae and consists of approximately 55 species, distributed mainly in the northern hemisphere, including eastern Asia, southeastern and northern part of the United States.¹ These plants often assume a brilliant fall coloring and an attractive flower and fruit colors and are widely grown as ornamental plants throughout the United States. Many species of this genus have been commonly prescribed in traditional Chinese medicine as a tonic formula and considered to possess actions including invigoration of the liver and kidney, preservation of essence, and anti-diabetic activity. Such as in traditional Chinese medicine, “Liuwei Dihuang Wan” is a prescription for treating diabetic disorders.² *Cornus officinalis* is one of its six prescribed herb medicinal plants and plays key roles in the treatment of diabetes. This prescription has been used alone or modified by adding additional components for diabetic therapy in China and Japan for a long time.³ Furthermore, other interesting examples are the Chinese prescriptions Hachimijio-gan and Keishi-bukuryo-gan, both of which exhibited potential therapeutic effects against diabetic nephropathy, and had different functions in terms of their effects on metabolic disorders, especially on advanced glycation end-product (AGE) formation in Hachimi-jio-gan and oxidative stress in Keishi-bukuryo-gan. Both of them contain the

herb of *Cornus officinalis*.⁴ In addition, the use of the fruits from several plants of the genus *Cornus* as part of diet health foods has attracted considerable attention recently. *Cornus mas* (Cornelian cherry fruits) has been formerly fermented as a beverage in Europe, and now is used in Turkey in the concoction of a kind of sherbet.⁵

Up to now, there have been many studies focusing on the treatment of diabetes and its complications by extracts from several plants of the genus *Cornus* as part of traditional medicines because of their absence of toxic and/or side-effects. For example, *Cornus officinalis* is considered as one of the 25 plant-based drugs most frequently used in China, Japan, and Korea. Researchers have reported that its extract has anti-diabetic activity in streptozotocin-induced diabetic rats,⁶ and it was also regarded as the major active principle in the plasma glucose-lowering action of “Die-Huang-Wan” in normal rats.⁷

The genus *Cornus* is a rich source of diverse iridoid glycosides^{5,8} which have raised significant interest due to their wide range of fascinating bioactivities. Numerous bioactivities were recently reported including anti-diabetic,⁹ antioxidant,¹⁰ anti-inflammatory^{11,12} and antitumor activities.^{13,14} **Figure 1.1** shows nine compounds isolated from the genus *Cornus* whose anti-diabetic activity were well studied with different cell lines *in vitro* or *in vivo* using different models in rats. For example, morroniside (**1**) is an iridoid glycoside isolated from *C. officinalis* and has been identified as one component partly responsible for the protective effects of *C. officinalis* and “Hachimi-jio-gan” against diabetic renal damage in streptozotocin-induced diabetic rats.¹⁵ It can decrease increasing serum glucose and urinary protein levels for diabetic rats. The decreased levels of serum albumin and total protein in diabetic rats was significantly increased by

morrnonside administration at a dose of 100 mg/kg body weight.⁵ It also significantly reduced the enhanced levels of serum glycosylated protein, and serum and renal thiobarbituric acid-reactive substrates.¹⁵ Moreover, an analogue of morronside displayed effectively protective action of β -cells against diabetes mellitus.¹⁶ Additionally, morronside has also shown potential protective effects against oxidative stress-induced neurotoxic processes.¹⁰ Another example is loganin (**3**), which was isolated from *C. officinalis* and has exhibited significant anti-diabetic activity both in scopolamine-induced amnesic mice¹⁷ and streptozotocin-induced rats,¹⁸ as well as anti-inflammatory and anti-shock effects. Cornuside (**2**) could suppress the expression of cytokine-induced proinflammatory and adhesion molecules in the human umbilical vein endothelial cells.¹⁹ In addition, it has shown the protective effects of cultured rat cortical neurons against oxygen-glucose deprivation (OGD)-induced injuries and the ameliorative effects on mitochondrial energy metabolism.²⁰ In addition, **2** and **3** possess the effect of preventing the overexpression of transforming growth factor (TGF)- β_1 and matrixes in glomeruli with a diabetic model.²¹

In addition, other anti-diabetic compounds such as anthocyanins and triterpenoid acids also have been isolated from *Cornus*. For instance, three anthocyanins (**5** – **7**) were isolated from *C. alternifolia*, *C. controversa*, *C. kousa* and *Cornus florida*⁸ and exhibited potential abilities to decrease body weight, normalize glucose intolerance, preserve islet architecture, and showed an extremely elevated level of circulating insulin, and a dramatic decrease in liver lipids for the C57BL/6 mice fed the high-fat diet.²² In addition, ursolic acid (**8**) and oleanolic acid (**9**) have been reported to regulate mucin gene expression, and inhibit the production of mucin protein, by directly acting on airway

epithelial cells.²³ Ursolic acid (**8**) also exhibited a good hypoglycemic effect in alloxan-induced diabetic mice.²⁴

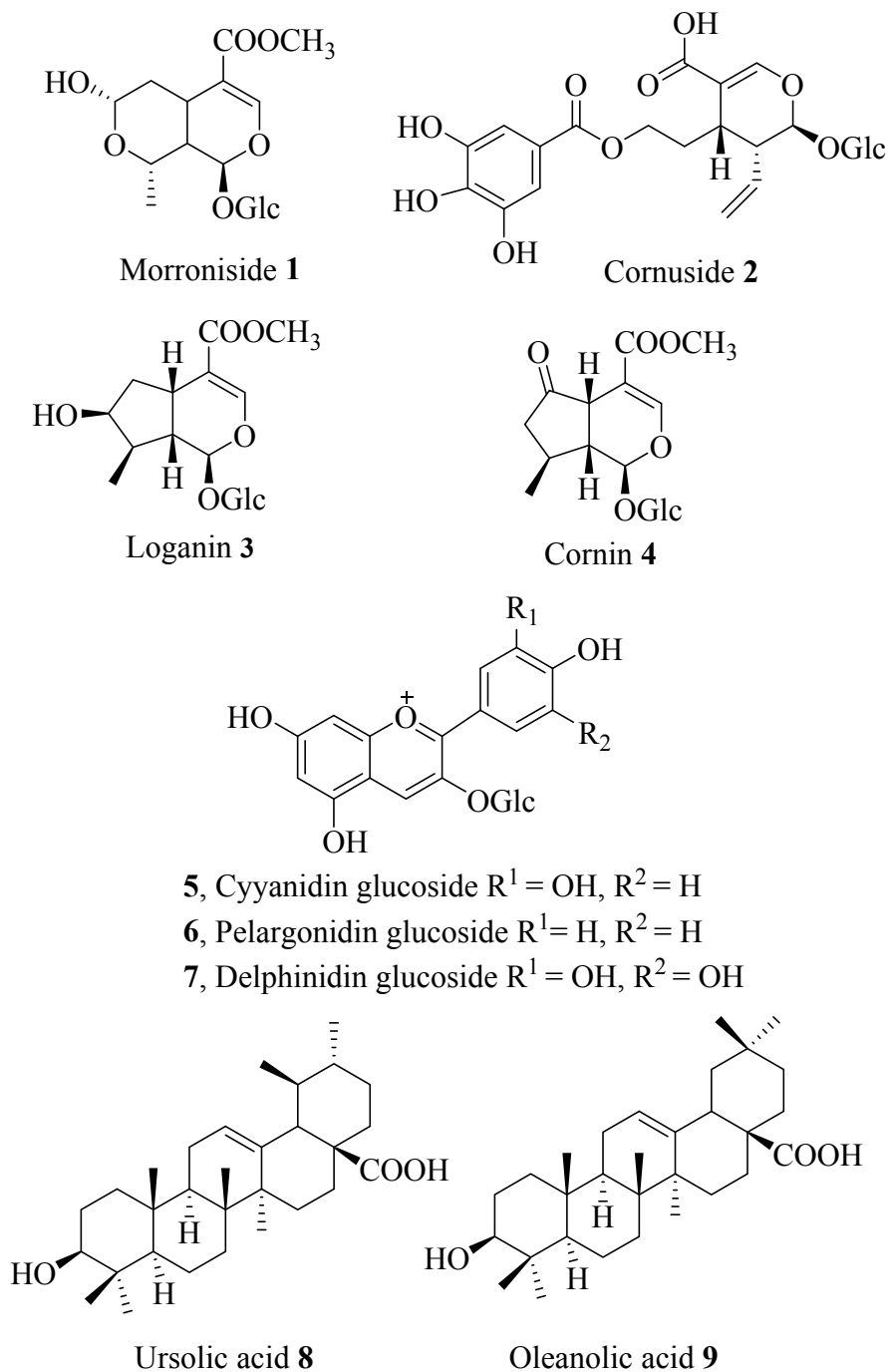


Figure 1.1 Structure of bioactivity compounds isolated from Genus *Cornus*.

Taking into consideration the potential anti-diabetic activities described above, as well as the wide distribution of this genus, it is fair to say that the plants of genus *Cornus* have reached their potential as a rich source of anti-diabetic drugs.

1.2 Research Progress on the Chemical Constituents and Bioactivities of Genus *Cornus*

Based on the information mentioned above, the genus *Cornus* is a rich source of diverse iridoid glycosides and anthocyanins, both of which have broad ranges of fascinating bioactivities. The chemical constituents of plants belonging to genus *Cornus* have been extensively studied in the past three decades. The previous chemical investigations of this genus have resulted in the isolation of over 200 compounds, which mainly include iridoid glycosides, anthocyanins, flavonoids, organic acid and esters. Herein, in order to provide useful information for further medicinal chemistry and pharmacological studies, the research progress on these chemical components over the past 20 years is reviewed in this chapter.

1.2.1 Iridoid glycosides and aglycone isolated from genus *Cornus*

Iridoid glycosides are the main active compounds of genus *Cornus* and a large portion of the iridoid glycosides were isolated from genus *Cornus*. So far, more than 20 iridoid glycosides and aglycone were produced by *Cornus* as shown in **Figure 1.2**.

Cornin (**4**) and dihydrocornin (**10**) were commonly isolated from *C. capitata*,²⁵ *C. officinalis*,²⁶ *C. alternifolia*,²⁷ *C. nuttallii*²⁸ and *C. florida*.²⁹ But in species *C. kousa*³⁰ only cornin has been found. Recently, cornin has been reported to display broad anti-cancer bioactivities against HCT-116 (colon), MCF-7 (breast), NCI-H460 (lung), SF-268 (central nervous system) and AGS (stomach) human tumor cell lines.³⁰ Compounds **11** and **12** were produced from *C. capitata* roots.²⁵ Loganin acid (**13**) and loganin were

isolated from *C. officinalis* exhibited potent anti-diabetic activity.^{17,18} Compounds geniposide (**14**), scandoside (**15**), scandoside methyl ester (**16**), monotropein (**18**) and golioside (**19**) were identified from *C. canadensis*.²⁸ Hastatoside (**17**) was an unusual iridoid glycoside that possesses a hydroxyl group at C-5 and has been isolated from *C. nuttallii* leaves.²⁸ Morroniside (**16**) as one of the most abundant iridoid glycosides in *C. officinalis*, has a potent effect in preventing diabetic complications such as diabetic angiopathy and the early stages of of diabetic nephropathy by regulating renal mesangial cell growth by inhibiting oxidative stress.^{29,31} And its derivatives **20** – **22** were also isolated from *C. officinalis* recently.^{16,32} Compound **24** exhibited effectively attenuated β -cell death in diabetes mellitus.¹⁶ However, no bioactivity for compounds **20** and **21** has been reported. Additionally, dehyromorroniaglycone (**23**), sweroside (**24**) and swertiamarin (**25**) were isolated from *C. officinalis* but no bioactivity have been reported.³³

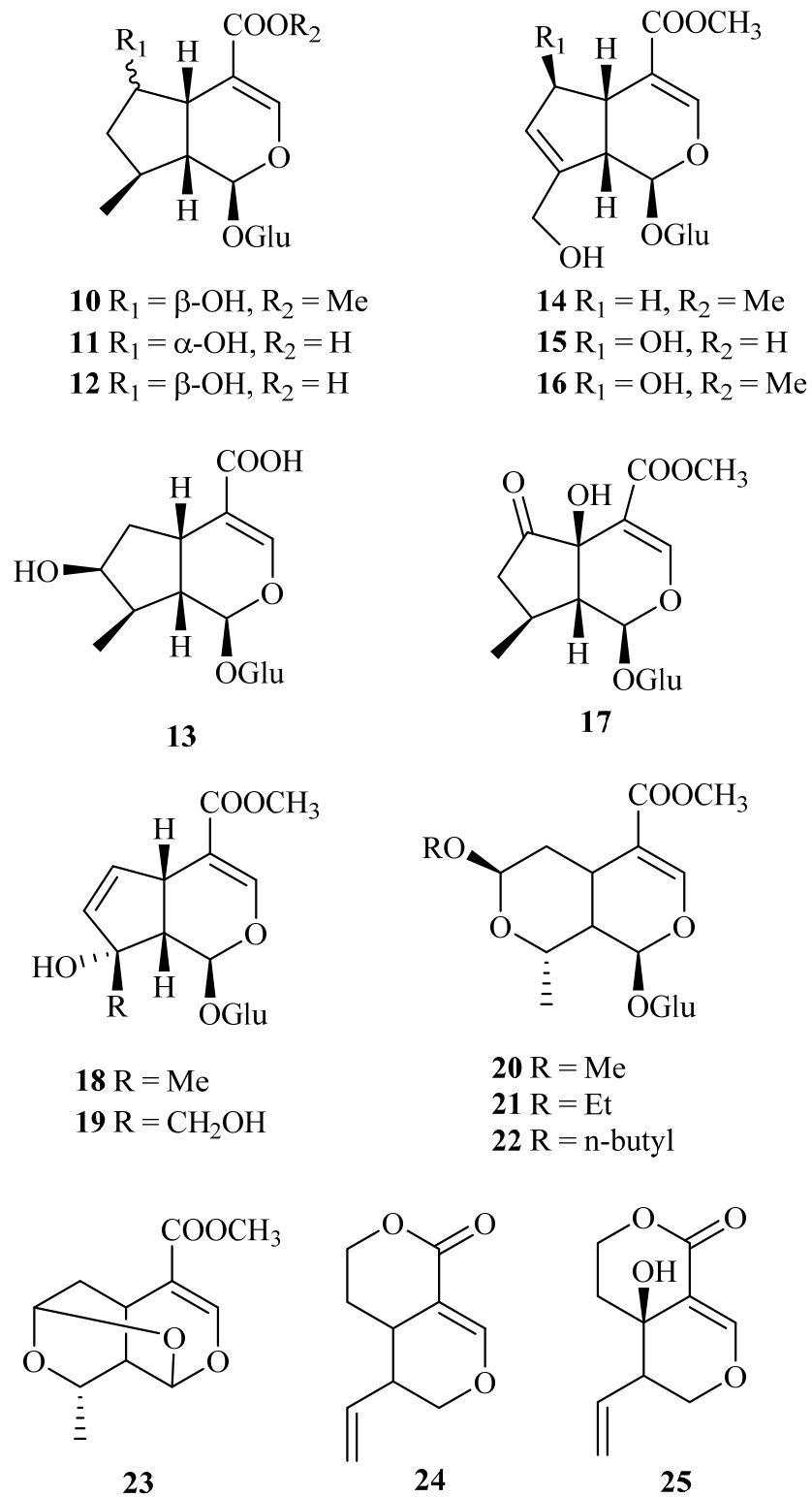


Figure 1.2 Chemical structures of iridoid glycosides isolated from *Cornus*.

1.2.2 Anthocyanins isolated from genus *Cornus*

Anthocyanins are one of the major classes of dietary polyphenols present and widely consumed in fruits and vegetables. Based upon their broad bioactivities described above, the food industry is interested in fruits and vegetables with a high content of bioactive anthocyanins to manufacture supplements with preventive and therapeutic uses. A number of anthocyanins have been isolated from *Cornus spp.* as shown in **Figure 1.3**. Delphinidin-3-glucoside (**26**), delphinidin-3-rutinoside (**27**) and cyaniding-3-glucoside (**28**) were isolated from both *C. alternifolia* and *C. controversa*.⁸ Compound **28** was also identified in *C. florida* and *C. kousa*.⁸ Furthermore, compounds **26** and **27** exhibited lipid peroxidation by 71% and 68%, respectively at 50 $\mu\text{g/mL}$. They also inhibited COX-1 enzymes by 39% and 49% and COX-2 by 54% and 48% at 100 $\mu\text{g/mL}$, respectively. And they both displayed growth inhibition against the tumor cell lines HCT-116 (colon), MCF-7 (breast), NCI-H460 (lung), SF-268 (central nervous system) and AGS (stomach) human tumor cell lines.

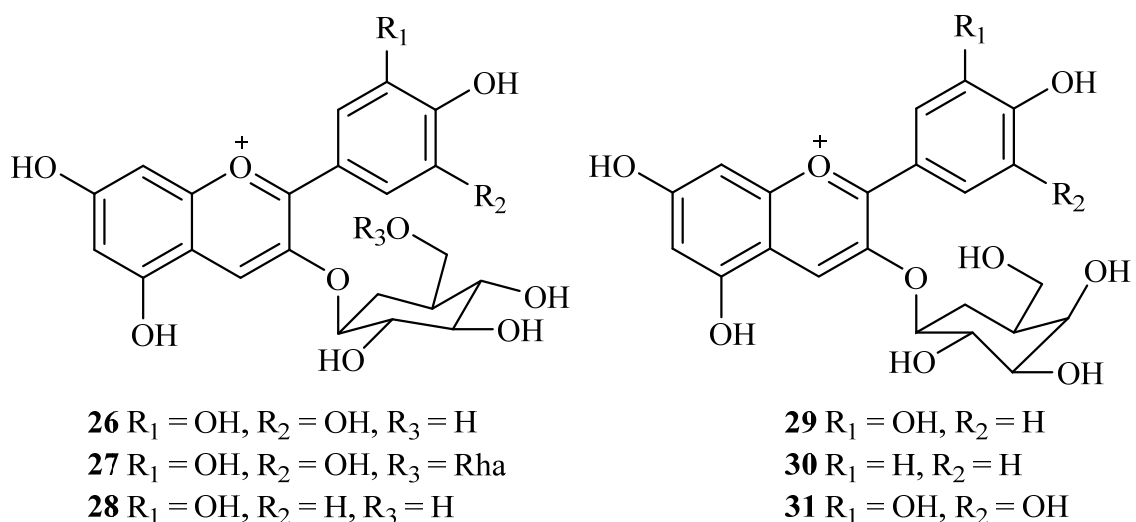


Figure 1.3 Chemical structures of anthocyanins isolated from *Cornus*.

Cyanidin-3-galactoside (**29**), pelargonidin-3-galactoside (**30**) and delphinidin-3-galactoside (**31**) are present in *C. mas*, *C. officinalis* and *C. controversa*. Compound **29** also has been purified from *C. florida*.^{5,8,22} Anthocyanins **29** – **31** show inhibition effects of COX-1 and COX-2 and antioxidant activities.⁵ Researchers also have recognized that compounds **29** – **31** (mixture) were able to ameliorate obesity and insulin resistance in C57BL/6 (high-fat diet induced) mice treated with the anthocyanins showed a 24% decrease in weight gain, as well as a decrease of lipid accumulation in the liver. These data indicated that anthocyanins **29** – **31** have the ability to improve certain metabolic parameters associated with diets high in saturated fats and obesity.²²

1.2.3 Flavonoids isolated from genus *Cornus*

In addition to the promising bioactivity of the iridoid glycosides and anthocyanins. *Cornus* also contains several interesting flavonoids. Flavonoids are one of the major classes of natural products with widespread distribution in fruits, vegetables, spices, tea and soy-based foodstuff and have received considerable attention for their chemistry and pharmacological activities. To date, over 15 flavonoids have been isolated from more than three species of *Cornus* spp., and their structures are shown in **Figure 1.4**.

Kaempferol (**32**), kaempferide (**33**), quercetin (**36**), isoquercitrin (**37**) and kyperoside (**38**) were isolated from *C. officinalis*.³² Compounds kaempferol-3-*O*-rhamnoside (**34**), myricetin-3-*O*-rhamnoside (**39**) were purified from *C. kousa*, which is a small deciduous tree widely found in China, Japan and Korea.³⁰ It bears sweet and edible fruits and now is used for the production of wine in many parts of China and Korea. Quercetin-3-*O*- β -D-glucuronide (**43**) and quercetin-3-*O*- β -D-glucuronide (**44**) were

isolated from *C. officinalis* with unusual substituents on the glucose moiety but no bioactivities have been reported so far.¹⁶

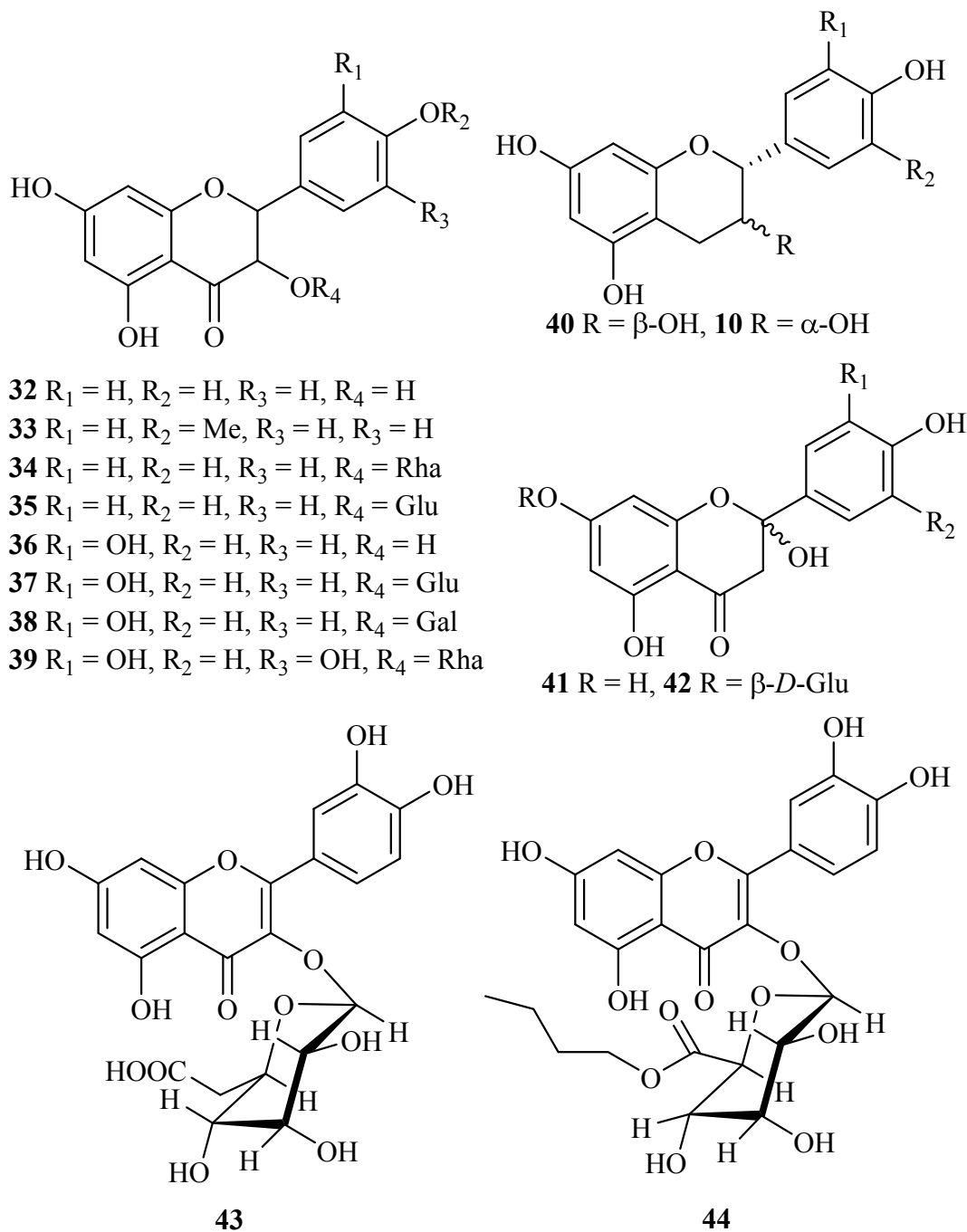


Figure 1.4 Chemical structures of flavonoids isolated from *Cornus*.

Interestingly, kaempferol-3-O-glucoside (**35**) has been found in both *C. kousa* fruits and *C. alternifolia* leaves, respectively.^{30,27} It was reported to have Fe²⁺ catalyzed lipid peroxidation activity. Furthermore, kaempferol-3-O- β -D-glucoside is an important chemotaxonomic marker and occurs widely in food plants such as black beans which are widely consumed throughout the world. Kaempferol-3-O- β -D-glucoside also has been found to have a mild inhibiting effect on the proliferation of HepG2 cells with an EC_{50} value of $306.4 \pm 131.3 \mu\text{M}$.³⁴ It has significant inhibitory activity against: 1) glycation bovine serum albumin (BSA) with an IC_{50} value of $0.32 \mu\text{M}$, 2) DPPH (2,2-diphenyl-1-picrylhydrazyl) radical scavenging activity ($IC_{50} = 86.10 \mu\text{M}$) and 3) xanthine oxidase inhibitory activity ($IC_{50} = 21.20 \mu\text{M}$).³⁵ Moreover, the kaempferol-3-O- β -D-glucoside moiety has been found to be essential for the bioactivity and effects of the flavonoid glycosides on the inhibition of tumor necrosis factor- α (TNF- α) production, decreased sensitivity of hepatocytes to TNF- α , and on the protection of hepatocytes against D-galactosamine (D-GalN).³⁶

1.2.4 Organic acids isolated from genus *Cornus*

So far, there are various organic acids and their derivatives have been isolated from *Cornus* spp. with interesting complex structures and potent antitumor and anti-diabetic activity, including betulinic acid (**45**), maslinic acid (**46**), arjunolic acid (**47**), 3-isoarjunolic acid (**48**),³⁷ gallic acid (**49**), caffeic acid (**50**), caftaric acid monomethyl ester (**51**),¹⁶ ellagic acid (**52**) and its two derivatives **53** and **54** (in **Figure 1.5**). Some of them are the main active components and played significant roles in *Cornus* spp.. For example, the ursonic acid and oleanolic acid (their structures are in **Figure 1.1**, compound **8** and **9**) which were isolated from several *Cornus* spp., such as *C. officinalis*, *C. mas* and *C.*

alternifolia have been confirmed as one of the anti-diabetic constituents in the Chinese traditional medicine *C. officinalis*.²³ The evidence that ursolic acid is a potent tyrosine phosphatase (PTP) 1B inhibitor further provided a potential explanation for the insulin sensitizing effect and stimulatory effect on glucose uptake from *C. officinalis*.³⁸

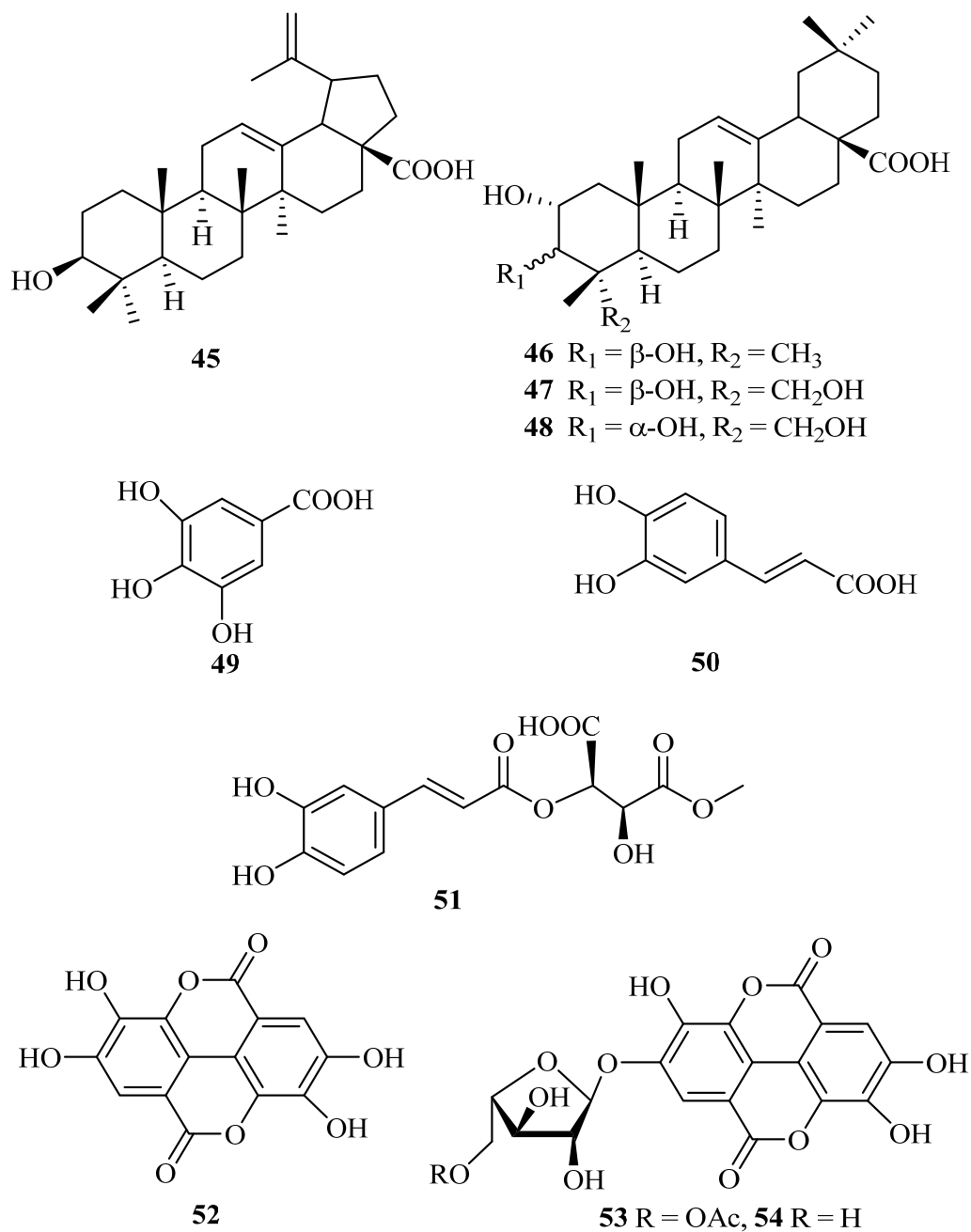


Figure 1.5 Chemical structures of organic acids and its derivatives isolated from *Cornus*.

It is worth noting that compounds **45** and **46** exhibited significant elastase inhibition activity with IC_{50} values of 10.81, 21.21 $\mu\text{g/mL}$, respectively. They have considerable value as cosmetic additives. Compound **51** exhibited significant insulin-mimetic effects on PEPCK mRNA expression.¹⁶ Furthermore, compounds **53** and **54** were evaluated for their anti-oxidative capacity in the medium of a high concentration of CuSO_4 , both of which acted as radical scavengers and/or antioxidants against the superoxide anion radicals and the peroxidation of linoleic acid.³⁹

Along with the various secondary metabolites as mentioned above, there are other kinds of compounds such as tannins, polysaccharides and glycoproteins have already been isolated from *Cornus* spp.. For their wide distribution and broad biological and pharmacological usefulness, *Cornus* spp. will continue to be a prolific source of novel, biologically active compounds.

1.3 Summary

Diabetes and its associated adverse cardiovascular conditions are increasingly prevalent in the world and are considered as one of the main threats to human health in the 21st century. Among two types of diabetic diseases, type 2 diabetes mellitus is the most common endocrine disease. It ranks high among the top 10 leading causes of death in the world and total number of people with diabetes is projected to rise from 289 million in 2010 to 439 million in 2030 worldwide. Diabetes treatments exhaust enormous amounts of resources including medicines, diets, physical training, and so on in all countries of the world. However, due to the side effects such as edema, weight gain and increased incidence of heart attack of the current available clinical medicine, TZDs and their derivatives have been tempered. Therefore, people have turned their focus to the

natural medicinal plants because they are highly diverse and often provide highly specific biological activities along with their nontoxic properties and fewer side effects.

The genus *Cornus* is a very convenient available source with wide distributions in the world and contain many medicinal plants. Many species of *Cornus* have been frequently used as herbs in traditional Chinese medicine, and their extracts exhibited potential effectiveness in treatment of diabetes. Furthermore, this genus is a rich source of diverse iridoid glucosides and anthocyanins, both of them have a wide range of fascinating bioactivities including anti-diabetic properties. Numerous research evidence has proved that the extracts or purified bioactivity compounds exhibit potential anti-diabetic properties as described in the above section.

1.4 Research Objectives

Previously, considering the broad usefulness profiles of *Cornus* spp. in traditional medicine as anti-diabetic drugs, we have been investigated the chemical constituents and their agonistic activities for peroxisome proliferator-activated receptors (PPAR α and PPAR γ) and liver X receptor (LXR) from the leaves *Cornus alternifolia*, which was collected in Oxford, Mississippi. As a result, three new iridoid glycosides, alternosides A – C (**55** – **57**) (in **Figure 1.6**) and a new megastigmane glycoside, cornalternoside (**58**), along with 10 known compounds were isolated from *C. alternifolia*.²⁷ Among them, compound **55** represents the first example of a naturally occurring iridoid glycoside with a β -glucopyranoside moiety at C-6 and shows weak activity on LXR. Interestingly, kaempferol 3-*O*-glucoside (**35**) exhibited significant agonistic activities for PPAR α and PPAR γ and LXR with EC_{50} values of 0.62, 3.0, and 1.8 μ M, respectively.

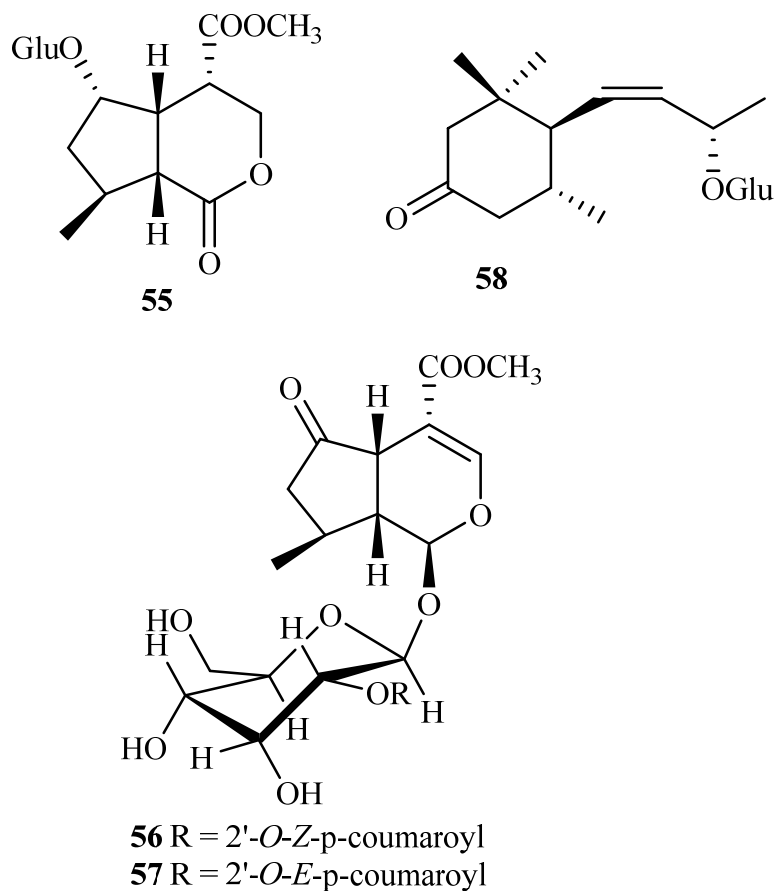


Figure 1.6 New compounds isolated from *Cornus alternifolia*.

In light of the above research results, and as a continuation to explore the potential natural PPARs and LXR agonists from genus *Cornus*, we also have studied the phytochemistry of a similar species of *Cornus controversal*. Initially, two compounds cornoside A (**59**) (its structure was shown in Chapter 2) and corin (**4**) were isolated. The structure of compound **59** was initially elucidated as an unprecedented skeleton with an unusual fused hexacyclic ring system (one five and one six membered lactone rings) and exhibited potent LXR agonist activity ($EC_{50} = 0.9 \mu\text{M}$). However, its stereochemistry was not determined due to a limited quantity of the sample, cornin (**4**) showed moderate LXR agonistic activity ($EC_{50} = 9.8 \mu\text{M}$).

The initial aim of this project is to isolate and purify additional quantities of cornosides A (**59**) to determine its absolute configuration. Furthermore, we propose to explore other structurally unique and new classes of nuclear receptor agonists for peroxisome proliferator activated receptors (PPARs) and liver X receptor (LXR) from this plant, which was collected from Oxford around the University of Mississippi.

In addition, as a continuing phytochemical investigation to find new diterpenoid alkaloids with potential anti-cancer activity from Chinese traditional medicine *Delphinium chrysotrichum* is another purpose of this dissertation. Specifically, we focused on the isolation and structure elucidation of the novel compounds from both medicinal plants.

2. ISOLATION AND STRUCTURAL ELUCIDATION OF SEVEN NEW COMPOUNDS FROM *CORNUS CONTROVERSA*

2.1 Background

Cornus controversa Hemsl. is a tree widely distributed in Korea, Northeastern China and the Southeastern United States. It is widely grown as an ornamental plant for its characteristic brilliant, colorful, and attractive flowers and fruits. Its extracts exhibited potential effectiveness in the treatment of diabetes and have been used traditionally in Chinese herbal medicine for its tonic, astringent and diuretic activities.⁴⁰ This plant is a rich source of diverse iridoid glycosides, which have aroused a lot of interest because of their wide range of fascinating bioactivities. Numerous biological activities were recently reported including anti-oxidant,¹⁰ anti-inflammatory,¹² anti-diabetic,^{15,18} anti-amnesic,¹⁷ and anti-malarial activities.⁴¹

Previous chemical investigations of *C. controversa* have resulted in the isolation of several compounds including flavonoids, phenolic compounds, terpenoids, tannins and anthocyanins.^{8,40} The anthocyanins impart bright colors to several fruits and vegetables and possess anti-inflammatory,^{5,8} anti-oxidative,⁵ anti-cancer⁸ and anti-diabetic activities.^{8,42} Taking into consideration the broad biological activities of iridoid glycosides and the anthocyanins, we investigated the chemical constituents of *C. controversa* collected from Oxford, Mississippi. A large scale extraction of the leaves of

C. controversa yielded one new iridoid glucoside, named cornoside A (**59**), and five new iridoid aglycones, cornolactones A – E (**60 – 64**), and an indole-3-lactic acid glucoside, named cornoside B (**65**) (**Figure 2.5**). Cornolactone A (**60**) was previously reported as a synthetic intermediate in the enantioselective synthesis of semperoside A,⁴³ however this is the first report of this compound from a natural source. In addition ten known compounds (**Figure 2.6**) were also isolated that included four iridoids, three megastigmane compounds, two ellagic acid derivatives, together with a flavonoid. The structures of all the compounds were assigned by detailed spectroscopic analysis or comparison with literature data. Cornoside A (**59**) is one of a small number of C₁₀ iridoid glucosides with a ring-opening between C-1 and O-2 and a γ -lactone linkage between C-6 and C-11. Cornolactone B (**61**) is the first natural *cis*-fused tricyclic dilactone iridoid containing both a five- and six-membered lactone ring. *In vitro*, cornoside A (**59**) exhibited significant liver X receptor (LXR) agonistic activity. Herein, we report the isolation, structure elucidation, and biological activity of the new compounds.

2.2 Structure Elucidation of Cornosides A, B, and Cornolactones A – E

The *Cornus controversa* leaves were collected in Oxford, Mississippi, in 2011 by Dr. Mark T. Hamann's group of the University of Mississippi. A 90% aqueous ethanol extract of the dried leaves of *C. controversa* (15 kg) was first fractionated on silica gel (step gradient elution hexane to EtOAc to MeOH). The 20% MeOH in EtOAc, was then subjected to column chromatography on polymeric HP-20 (step gradient elution 10% Me₂CO in H₂O to 100% Me₂CO). The 20% Me₂CO fraction was then subjected to repeated fractionation on either polymeric HP-20ss, reversed phase C-18, normal phase

Silica gel, or molecular exclusion Sephadex LH-20 column chromatography followed by a series of HPLC separations on either a PRP-1 column, C-8, or C-18 columns yielded cornosides A (**59**) and B (**65**), cornolactones A – E (**60** – **64**), and the known compounds cornin (**4**),²¹ dihydrocornin (**10**),²⁵ hastatoside (**17**),²⁸ isoquercitrin (**37**),³² alternosides A (**55**),²⁷ cornalternoside (**58**),²⁷ lauroside A (**66**),⁴⁴ (5*S*, 6*R*)-9-hydroxy-megastigm-7-en-3-one (**67**),⁴⁵ 3,3'-dimethyl-4'-*O*- β -D-glucopyranosyl ellagic acid (**68**)⁴⁶ and 3,4,3'-trimethyl-4'-*O*- β -D-glucopyranosyl ellagic acid (**69**).⁴⁷ The ¹H, ¹³C NMR and MS data of the known compounds matched well with that in the literature, respectively. The new compounds (**59** – **65**) were identified and assigned using detailed analysis of NMR spectroscopy and mass spectrometry.

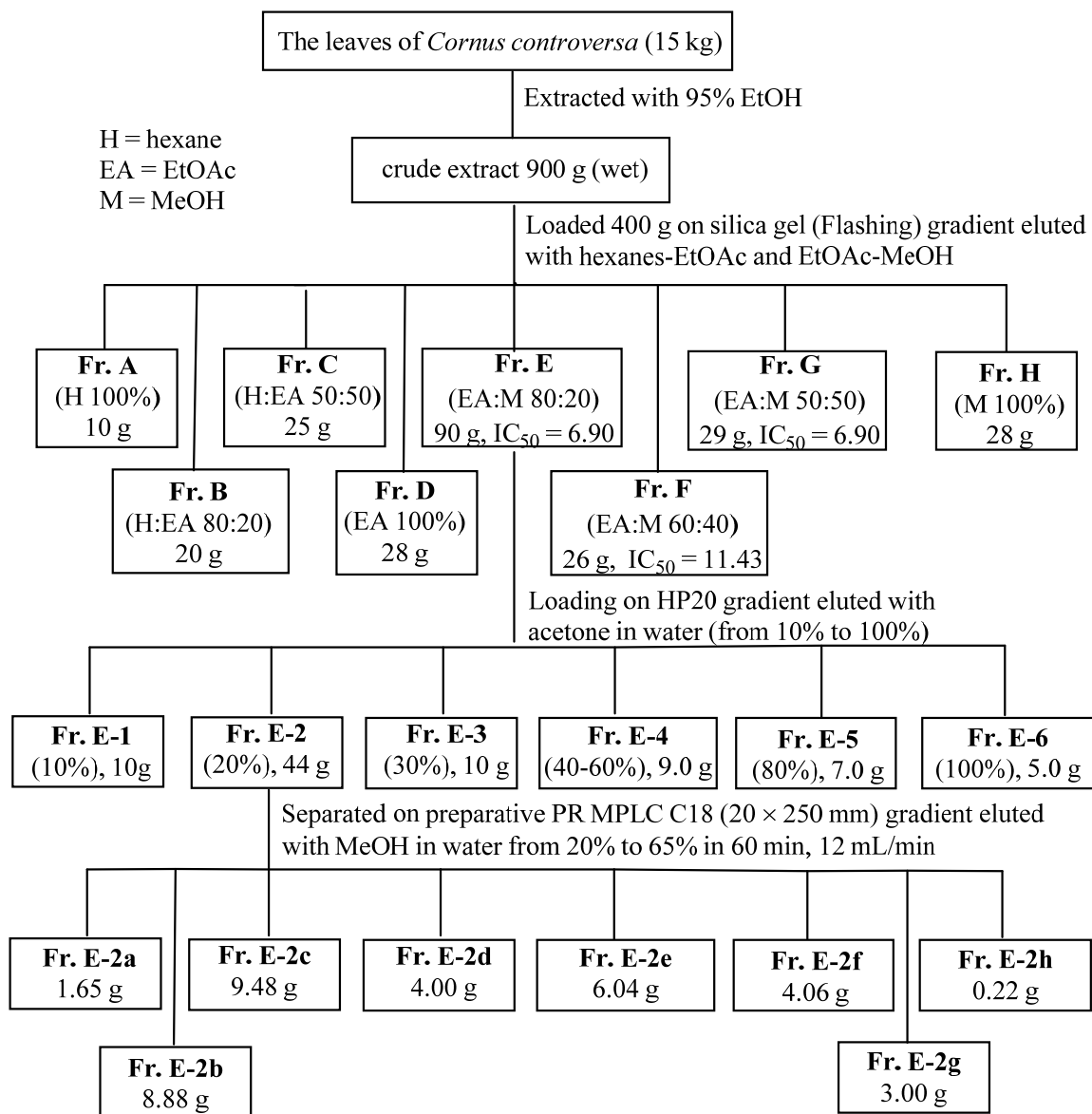


Figure 2.1 Isolation scheme 1 for new compounds 59 – 65.

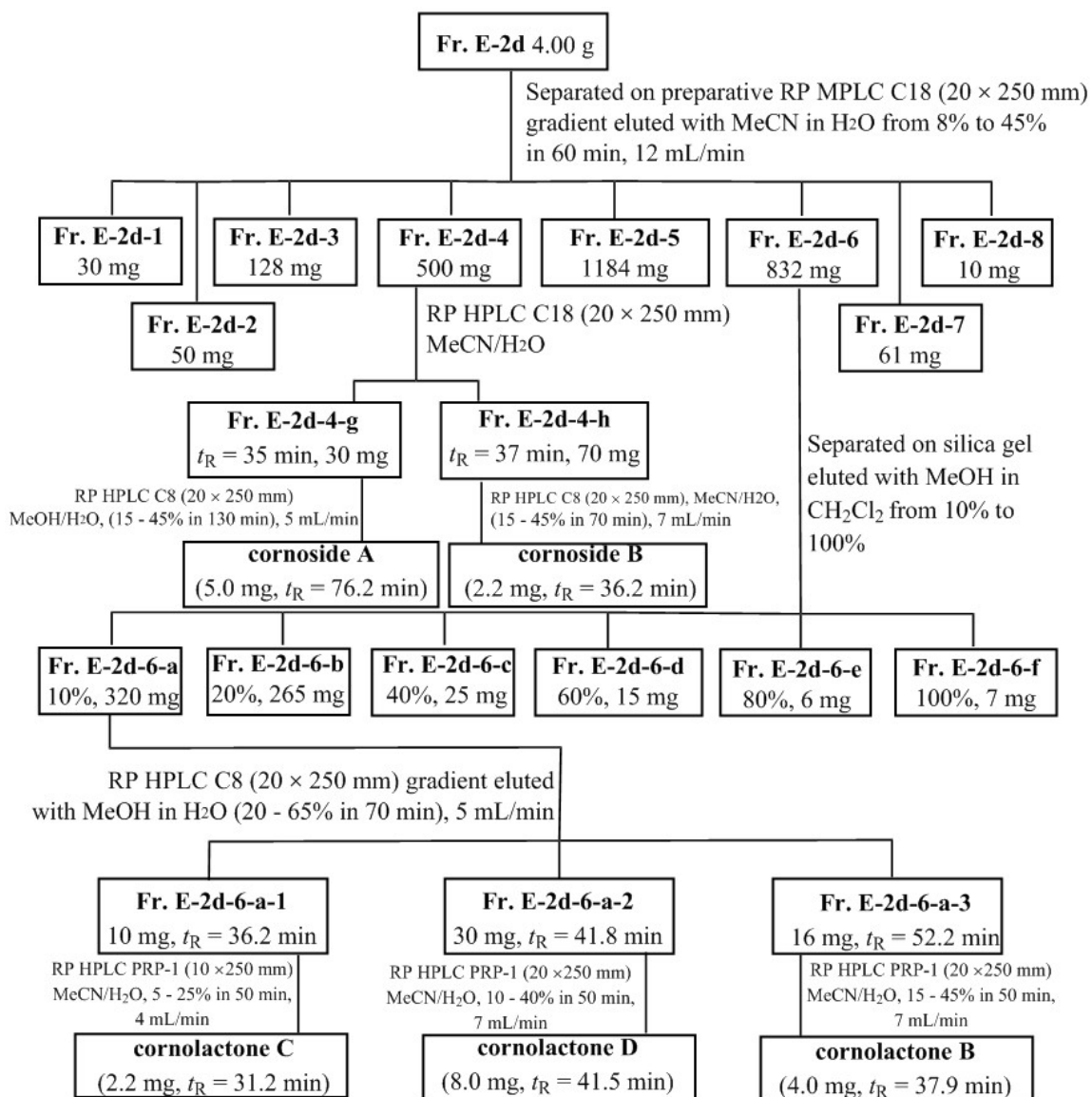


Figure 2.2 Isolation scheme 2 for new compounds **59** – **65**.

In order to collect more cornoside A (**59**), the rest of the crude extract was separated by similar procedures as shown in **Figures 2.3** and **2.4**. During this process, two more new compounds: cornolactones A (**60**) and E (**64**) were isolated.

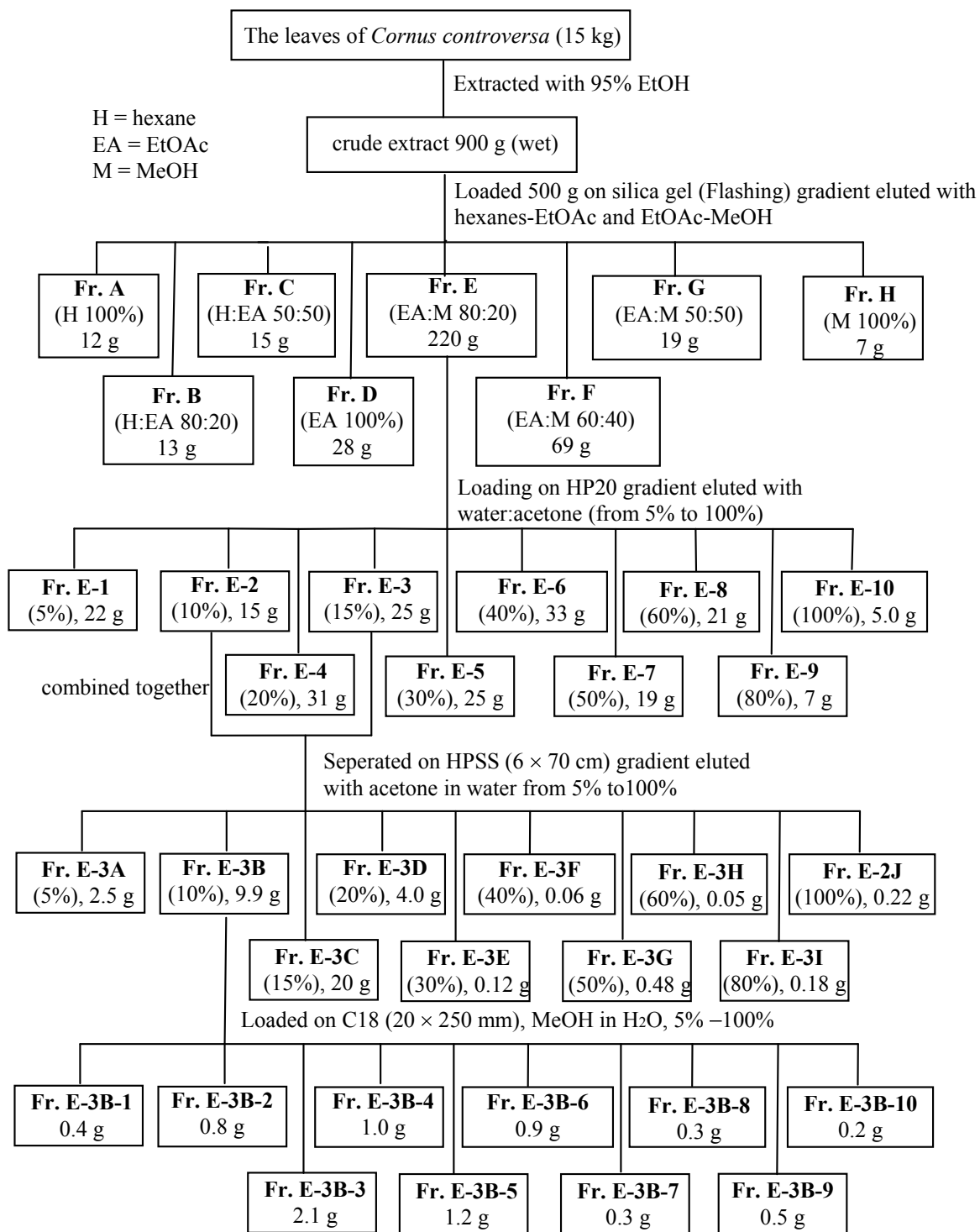


Figure 2.3 Isolation scheme 3 for cornoside A (59), cornolactones A (60) and E (64).

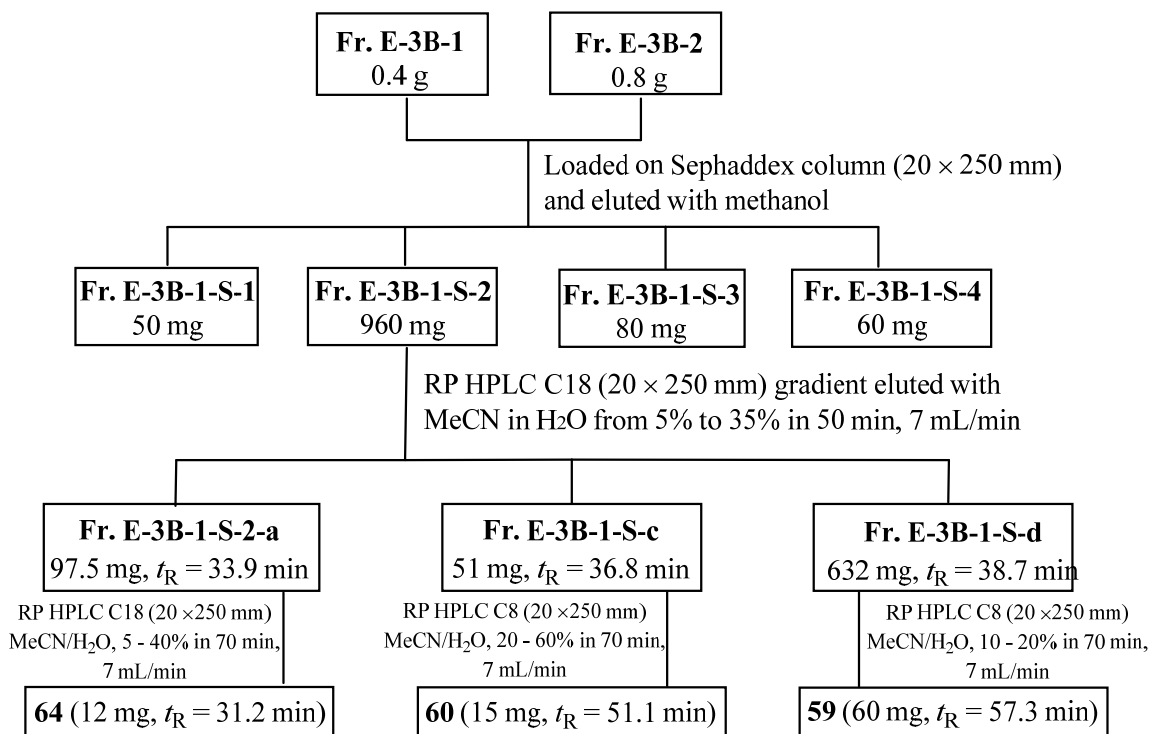


Figure 2.4 Isolation scheme 4 for cornosides A (**59**), cornolactones A (**60**) and E (**64**).

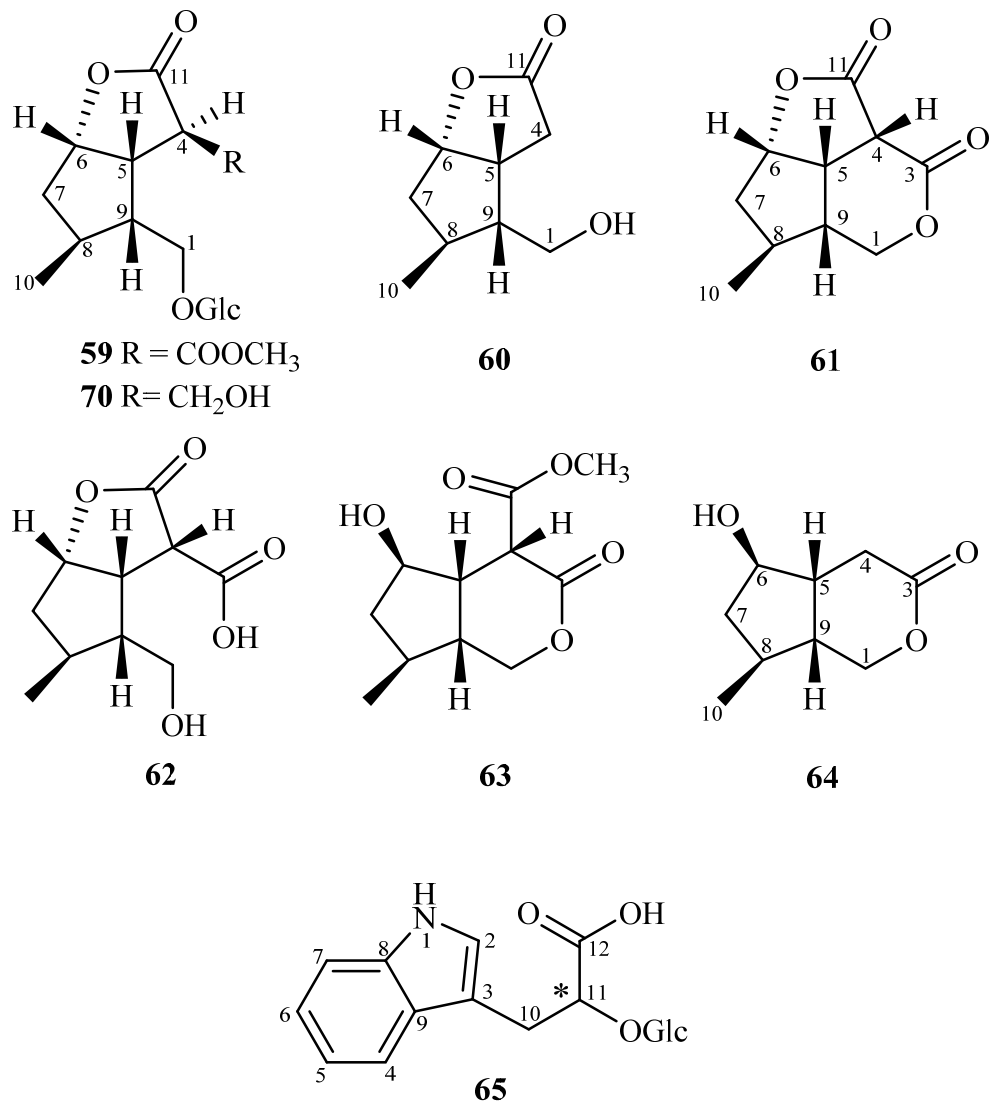


Figure 2.5 Chemical structures of seven new compounds (59 – 65).

Cornoside A (**59**) was obtained as a colorless gum, and the molecular formula $C_{17}H_{26}O_{10}$ was established on the basis of HRESIMS for the $[M + Na]^+$ at m/z 413.1417 (calcd 413.1418), which indicated 5 degrees of unsaturation. The IR spectrum showed characteristic absorptions for OH (3369 cm^{-1}) and C=O (1729 cm^{-1}). In the ^1H NMR spectrum (**Figure 2.10**) of **59**, in addition to the signals attributable to a glucose moiety and a methoxycarbonyl group, there were signals for the protons of an oxymethine [δ_{H} 5.03 (1H, t, $J = 6.8$ Hz, H-6)], four other methines [δ_{H} 3.94 (1H, d, $J = 5.6$ Hz, H-4); 3.37 (1H, q, $J = 7.2$ Hz, H-5); 1.90 (1H, m, H-8) and 1.83 (1H, m, H-9)], an oxymethylene [δ_{H} 3.98 (1H, dd, $J = 10.4, 3.6$ Hz, H-1a) and 3.38 (1H, m, H-1b)], a methylene group [δ_{H} 1.99 (1H, dd, $J = 13.6, 6.0$ Hz, H-7 α) and 1.47 (1H, ddd, $J = 13.6, 11.6, 6.0$ Hz, H-7 β)], and a methyl group [δ_{H} 0.95 (3H, d, $J = 5.6$ Hz)] (**Table 2.1**). ^{13}C NMR (**Figure 2.11**) and HSQC spectra revealed 17 carbon signals attributable to two carbonyl carbons, ten sp^3 methines, three sp^3 methylenes, one methoxyl and one methyl group. Among them, the signals at δ_{C} 103.0, 76.9, 76.7, 73.3, 70.1 and 61.1 were characteristic for a β -glucopyranosyl moiety,⁴⁸ which was further confirmed by the acid hydrolysis experiment (see experiment section in Charpt 4). A signal at δ_{C} 172.8 could be assigned to the lactone group, while resonances at δ_{C} 169.0 and 52.7 corresponded to a methoxycarbonyl group. Apart from the 3 degrees of unsaturation occupied by two carbonyl and a glucose moiety, the remaining 2 degrees of unsaturation indicated that **59** should possess a bicyclic system. The data summarized above suggested that **59** has the same molecular skeleton as that of gelsemiol 1-glucoside (**70**) (**Table 2.2**) except a methoxycarbonyl

instead of a hydroxymethyl group ($\delta_C = 61.0$ ppm) at C-4 of gelsemiol 1-glucoside (**70**).⁴⁹

The structure of **59** was further confirmed by detailed analysis of the 2D NMR spectra.

Table 2.1 NMR data of compound **59**. Measured at 400 MHz (^1H) and 100 MHz (^{13}C), in d_6 -DMSO, δ in ppm, J in Hz..

no.	δ_{H}	δ_{C}	HMBC (H \rightarrow C)	NOESY
1a	3.98, dd (10.4, 3.6)	66.7		
1b	3.38, overlapped		C-1', C-5, C-8, C-9	H-9, H-1a, H-10
3		169.0		
4	3.94, d (5.6)	47.8	C-3, C-5, C-6, C-9, C-11	H-8
5	3.37, q (7.2) ^a	45.5		
6	5.03, t (6.8)	83.6	C-8, C-9, C-11	H-5, H-7 α , H-7 β
7 α	1.99, dd (13.6, 6.0)	40.6	C-5, C-6, C-8, C-9	H-7 β
7 β	1.47, ddd (13.6, 11.6, 6.0)		C-8, C-10	H-6, H-7 α , H-10
8	1.90, m	32.0	C-1, C-7, C-9, C-10	
9	1.83, m	48.0		H-1b, H-10
10	0.95, d (5.6)	17.3	C-7, C-8, C-9	H-1b, H-7 β , H-8, H-9
11		172.8		
OMe	3.68, s	52.7	C-3	
1'	4.05, d (7.6)	103.0	C-1, C-3'	H-2', H-3'
2'	2.92, td (8.0, 4.4)	73.3		H-1'
3'	3.10, dd (17.6, 8.6)	76.7	C-4'	H-1'
4'	3.03, dd (18.0, 9.0)	70.1	C-6'	
5'	3.07, d (3.9)	76.9		
6a'	3.64, overlapped	61.1		
6b'	3.43, dd (11.7, 5.9)		C-5'	
OH-2'	4.72, d (4.3)		C-1', C-2', C-3'	
OH-3'	4.94, d (6.8)		C-2', C-3'	
OH-4'	4.93, d (7.2)		C-4'	
OH-6'	4.45, t (5.6)		C-5', C-6'	

^a J value obtained from 1D NOESY spectrum.

Table 2.2 Comparison of ^{13}C NMR Data of cornosides A (**59**)^a and (**70**)^b

position	59	70	position	59	70
1	66.7, CH ₂	70.5, CH ₂	11	172.8, C	182.6, C
3	169.0, C	61.0, CH ₂	OMe	52.7, CH ₃	
4	47.8, CH	51.0, CH	1'	103.0, CH	103.2, CH
5	45.5, CH	44.8, CH	2'	73.3, CH	73.9, CH
6	83.6, CH	86.5, CH	3'	76.7, CH	76.3, CH
7	40.6, CH ₂	41.6, CH ₂	4'	70.1, CH	70.4, CH
8	32.0, CH	33.3, CH	5'	76.9, CH	76.7, CH
9	47.9, CH	42.9, CH	6a'	61.1, CH	61.5, CH
10	17.3, CH ₃	17.2, CH ₃			

^a Measured in d_6 -DMSO, ^b Measured in D₂O;

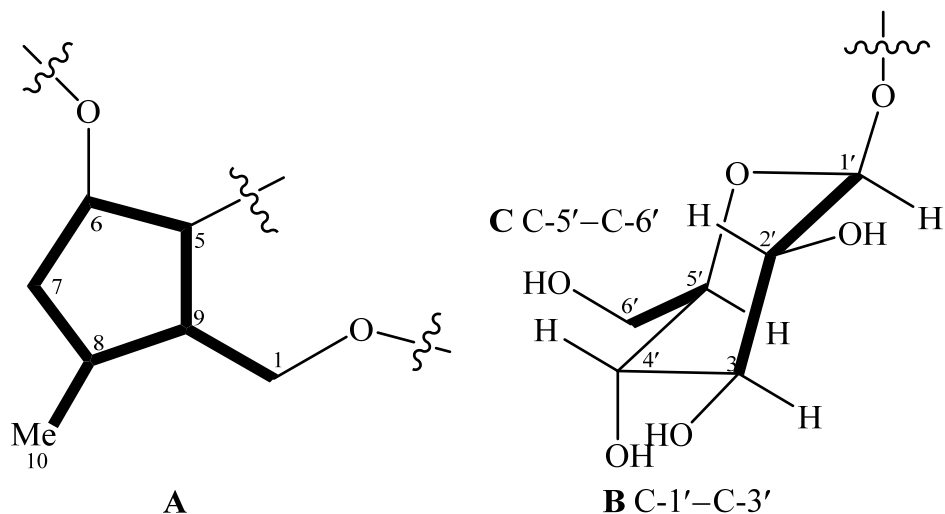


Figure 2.7 Subfragments (A – C) of cornoside A (**59**).

Analysis of the $^1\text{H} - ^1\text{H}$ COSY and gHSQC spectra of **59** allowed the establishment of three isolated subfragments (A – C) as drawn with bold lines in **Figure 2.7**. Fragment A was determined on the basis of COSY correlations between: H-1a (δ_{H} 3.98), H-1b (δ_{H} 3.38) and H-9 (δ_{H} 1.83), which is in turn coupled to H-5 (δ_{H} 3.37) and H-8 (δ_{H} 1.90); H-5 further correlated to H-6 (δ_{H} 5.03), which is in turn coupled to H₂-7 (δ_{H} 1.99, 1.47); H₂-7 is coupled to H-8 which is in turn correlated to H₃-10, which allowed to close the cyclopentyl ring system with a methyl substitution at C-8. In addition, clear COSY correlations between H-1' (δ_{H} 4.06) and H-2' (δ_{H} 2.92) and between a methine of H-5' (δ_{H} 3.07) and a methylene of H-6' (δ_{H} 3.65) allowed the establishment of fragments B and C. Furthermore, clearly correlations from the exchangeable proton of OH-C-2' observed at δ_{H} 4.72 (1H, d, $J = 4.3$ Hz) to H-2', from OH-C-3' observed at δ_{H} 4.95 (1H, dd, $J = 6.8, 4.8$ Hz) to H-3' and H-4', and from OH-C-6' at δ_{H} 4.45 (1H, t, $J = 5.6$ Hz) to H₂-6' were also observed in the $^1\text{H} - ^1\text{H}$ COSY spectrum.

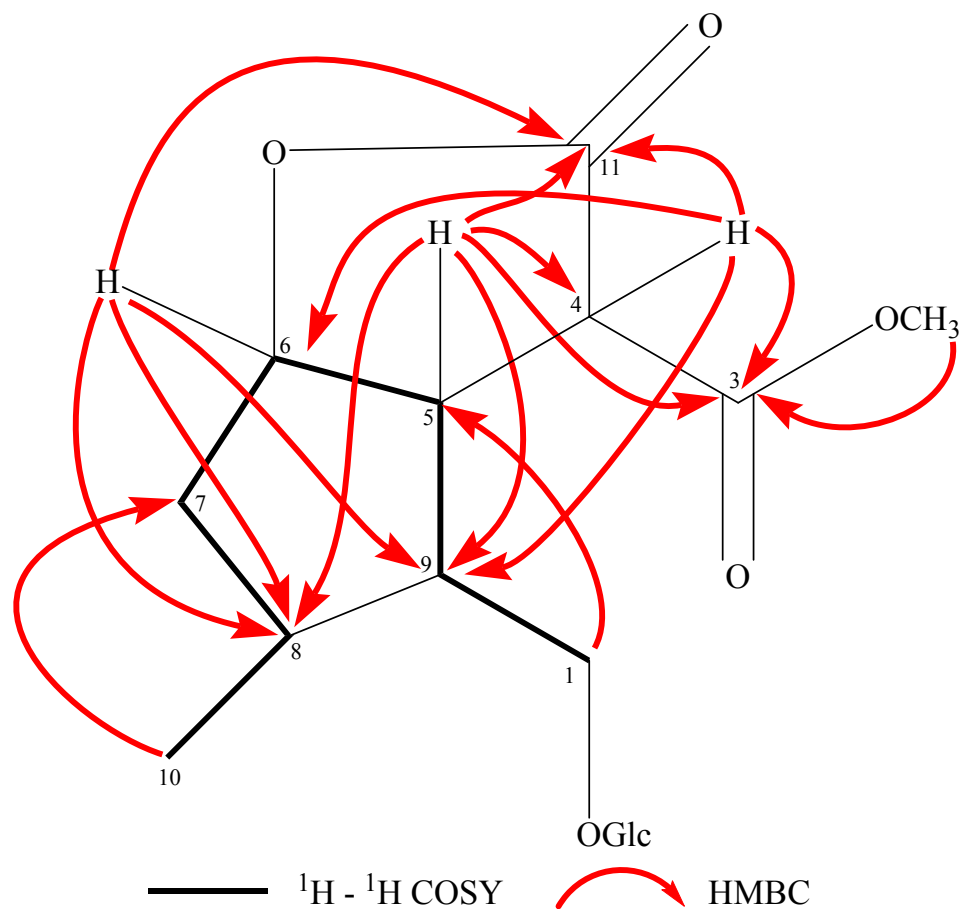


Figure 2.8 Key $^1\text{H} - ^1\text{H}$ COSY and HMBC correlations of cornoside A (**59**).

Remaining to be assigned were two ester carbonyl carbons C-3 (δ_{C} 169.0) and C-11 (δ_{C} 172.8), a methine H-4 (δ_{H} 3.94; δ_{C} 47.8), and a methoxy group (δ_{H} 3.68; δ_{C} 52.7). In the HMBC spectrum, the correlations between H-6 (δ_{H} 5.03) and the ester carbonyl carbon observed at δ_{C} 172.8 (C-11), and from H-5 (δ_{H} 3.37) to both C-4 and C-11 established the presence of a γ -lactone ring. A COSY correlation observed between H-5 and H-4 and an HMBC correlation from H-4 to C-11 further supported this assignment. Furthermore, HMBC correlations observed from H-4, H-5, and the methoxyl signal at δ_{H} 3.68 (3-OMe) to the remaining ester carbonyl carbon at δ_{C} 169.0 (C-3) established the connection of C-4 to C-3 and the presence of a methyl ester at C-3. Finally, the clear

HMBC correlations from H-1' (δ_{H} 4.05) to C-1 (δ_{C} 66.7) and from H-1 β (δ_{H} 3.98) to C-1' (δ_{C} 103.0) confirmed the glucosylation at C-1 and established the planar structure of **59** as depicted.

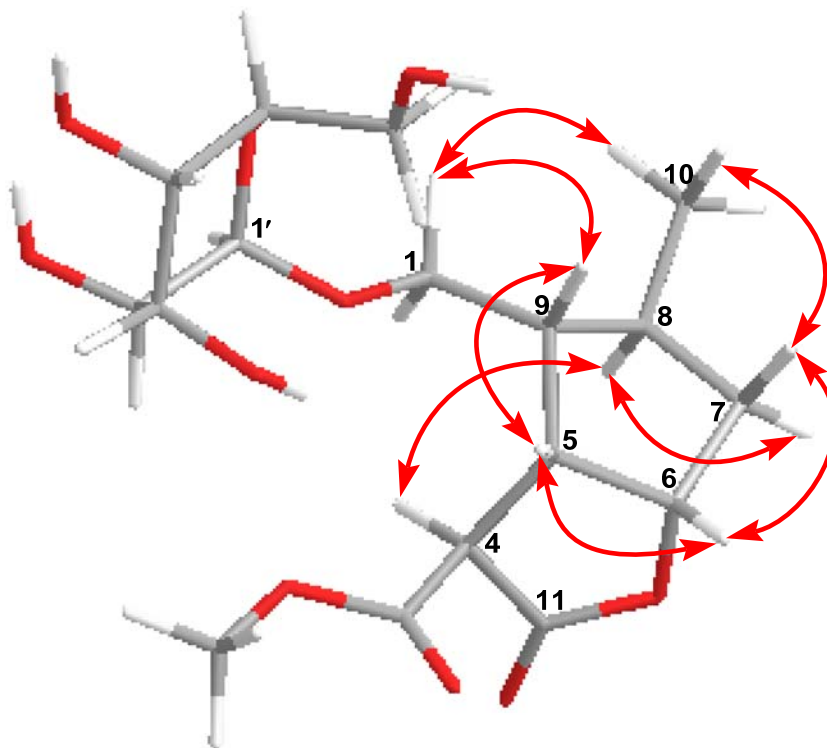


Figure 2.9 Key NOESY correlations of cornoside A (**59**).

The relative configuration of compound **59** was readily assigned as shown in **Figure 2.9** by NOESY correlations and the coupling patterns in the ^1H NMR spectrum. NOE correlations from H-5 to H-6 and H-9, together with correlations from H-7 β to H-6 and H₃-10 indicated that H-5, H-6, H-9 and Me-10 were on the same side of the cyclopentane ring in the β -orientation. This was further confirmed by 1D NOESY spectrum as H-6 was irradiated (A1-6). NOE correlations from H-8 to H-7 α , and H-1 confirmed the α -orientation of H-8 and the glucosylated side chain. A long range W-coupling in the COSY spectrum between Me-10 and H-7 α was consistent with the 1,2-

diaxial arrangement of these two groups. Finally, the α -orientation of H-4 was indicated by an NOE correlation observed between H-4 and H-8. This was further substantiated by a small coupling (5.6 Hz) observed between H-4 and H-5 that was similar to the coupling constants (*ca* 5.0 Hz in both cases) of the previously reported C-1 to O-2 ring-opened iridoids gelsemiol⁴⁹ and borryeriagenin.⁵⁰ This assignment was further confirmed by 1D NOESY correlations from H-4 to H-7 α and H-8 when both of them were irradiated (see A1-7 and A1-8). The absolute configuration of **59** is suggested based on biogenetic grounds that nearly all iridoids found in nature have a configuration of 5*S* and 9*R* and by analogy to the known co-isolated compounds that were found to have identical NMR data and comparable optical rotation values. Thus the structure of cornoside A (**59**) is therefore defined as 4*S*,5*S*,6*S*,8*S*,9*R*. Additional support for the absolute stereochemistry came from the isolation of cornolactone A (**60**), that was previously reported as a synthetic intermediate of the total synthesis of the iridoid semperoside A.⁴³

Table 2.3 NMR data of compound **59** measured in CD₃OD, δ in ppm, *J* in Hz..

no.	δ_{H}	δ_{C}	HMBC (H \rightarrow C)	NOESY
1a	4.08 (1H, dd, 10.2, 3..3)	68.8	C-5, C-9	H-9, H-1b, H-10
1b	3.46 (1H, dd, 10.2, 7.6)		C-9	H-9, H-1a, H-10
3		169.0		
4	3.23 (1H, m)	49.6		H-8
5	3.37 (1H, dd, 7.3, 7.1)	47.5	C-3, C-4, C-8, C-9, C-11	H-6, H-9
6	5.01 (1H, t, 6.2)	86.3	C-8, C-9, C-11	H-5, H-7 α , H-7 β
7 α	2.08 (1H, dd, 14.2, 5.9)	42.1	C-6, C-8	H-7 β
7 β	1.48 (1H, ddd, 14.2, 11.6, 5.8)		C-8	H-6, H-7 α , H-10
8	1.93 (1H, m)	33.9		H-4, H-7 α
9	1.88 (1H, m)	49.8		H-1a, H-1b, H-5
10	0.98 (3H, d, 6.0)	17.7	C-7, C-8, C-9	H-1a, H-7 β , H-9
11		175.5		
OMe	3.68 (3H, s)	52.3	C-3	
1'	4.18 (1H, d, 12.5)	104.6	C-1, C-3'	H-3', H-4'
2'	3.07 (1H, dd, 8.9, 7.9)	75.1	C-1', C-3'	
3'	3.19 (1H, d, 6.0)	78.2		H-1'
4'	3.22 (1H, m)	71.8		H-1'
5'	3.28 (1H, m)	78.2	C-4'	
6a'	3.80 (1H, d, 11.8)	63.0	C-4'	
6b'	3.60 (1H, dd, 11.8, 4.3)		C-5'	

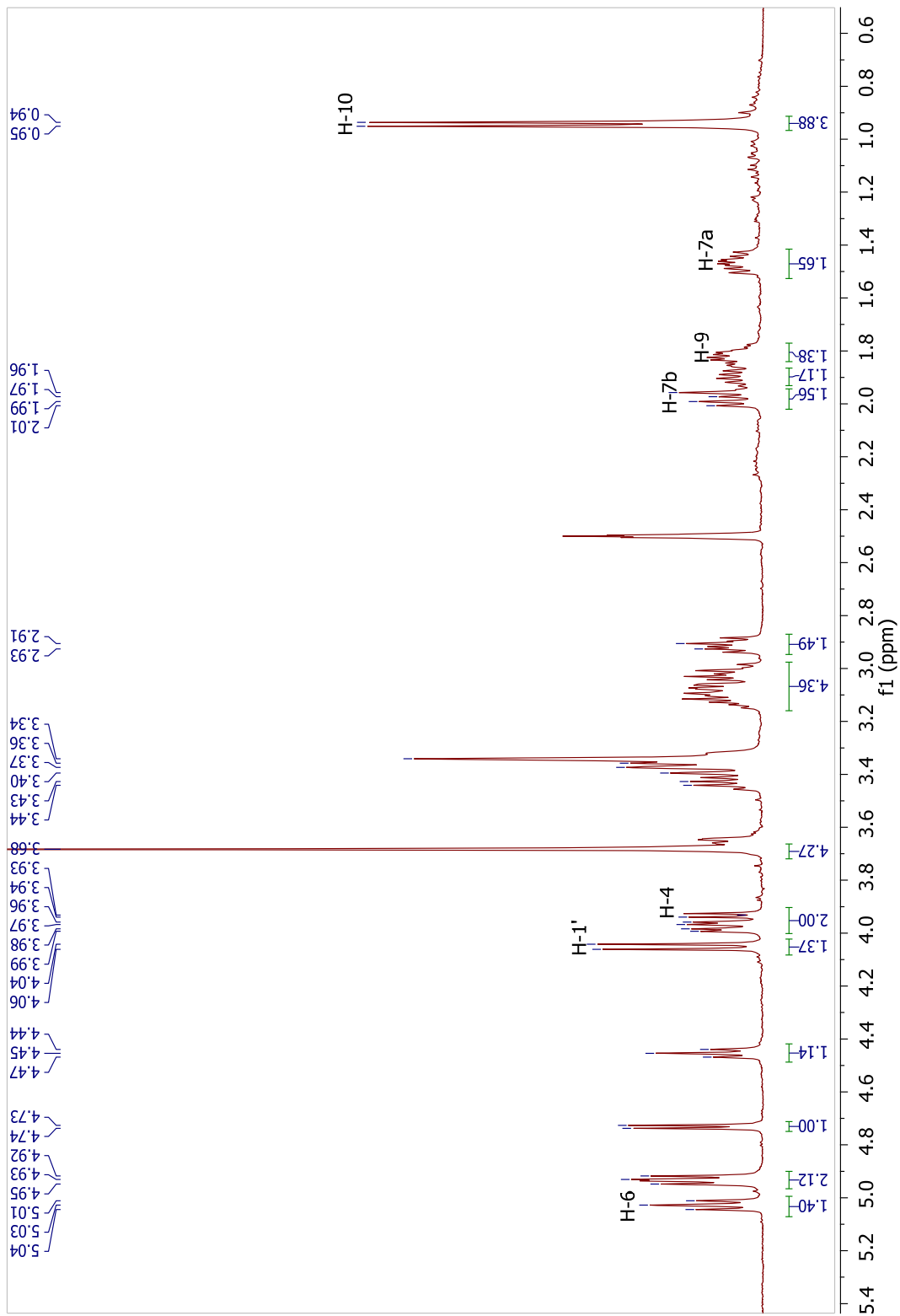


Figure 2.10 ^1H NMR spectrum of cornoside A (59), 400 MHz, in d_6 -DMSO

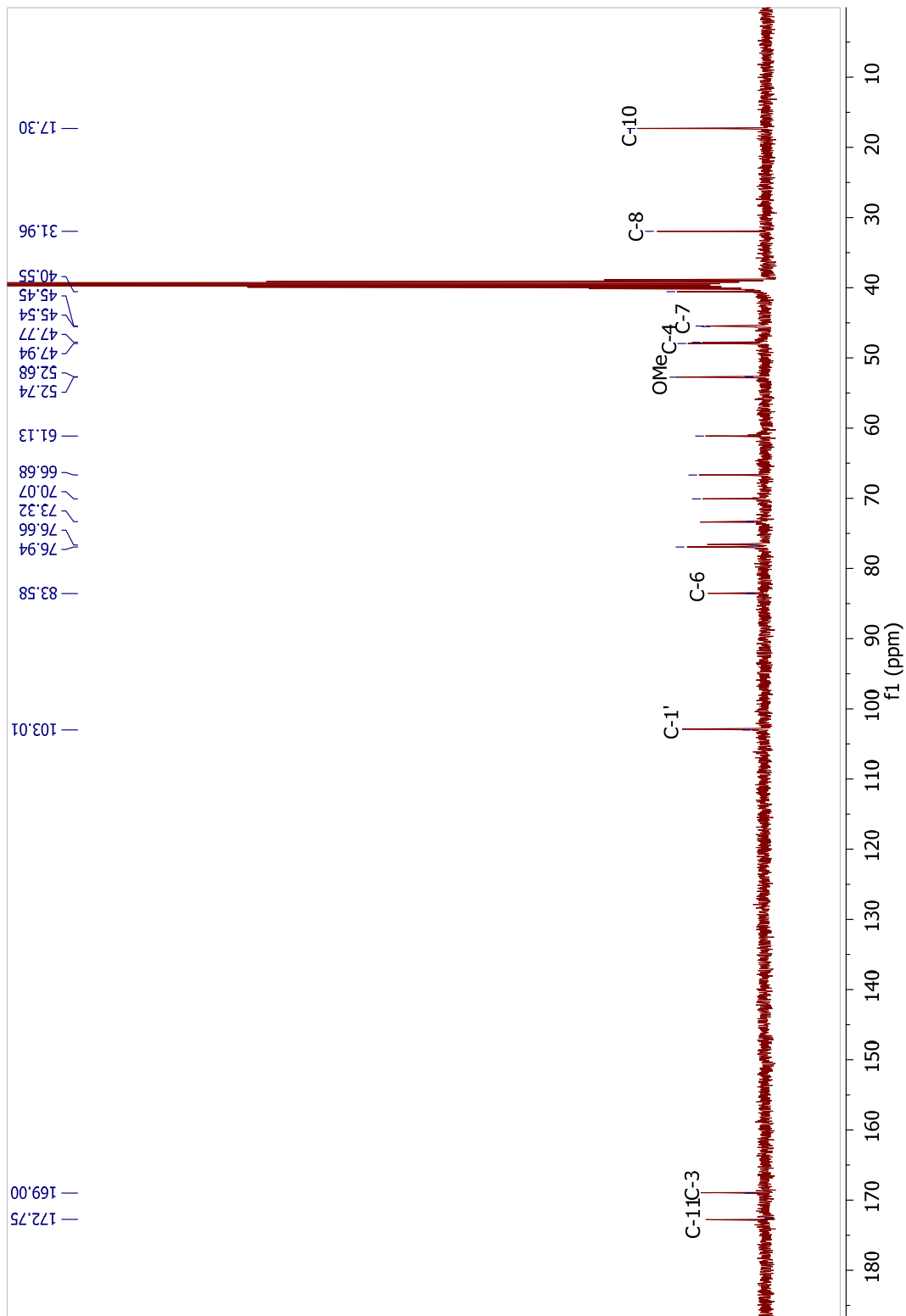


Figure 2.11 ^{13}C NMR spectrum of cornoside A (**59**), 100 MHz, in d_6 -DMSO

Cornolactone A (**60**) was isolated as a colorless gum, showed an $[M + H]^+$ ion at m/z 171.1010 in the HRESIMS consistent with molecular formula $C_9H_{14}O_3$, which requires three degrees of unsaturation. The IR spectrum showed characteristic absorptions for hydroxyl (3423 cm^{-1}), and ester carbonyl ($1752, 1023\text{ cm}^{-1}$) functionality. The ^{13}C NMR and gHSQC spectra revealed 9 carbon signals including four sp^3 methines, three sp^3 methylenes and one quaternary carbon, along with one methyl group. The ^1H , ^{13}C NMR (**Figures 2.15** and **2.16**) and HSQC spectra of **60** showed resonances for an oxymethine [δ_{H} 5.00 (1H, t, $J = 6.0$ Hz, H-6), δ_{C} 85.1 (C-6)]; three additional methines [δ_{H} 3.10 (1H, m, H-5), 1.78 (1H, m, H-9), 1.76 (1H, m, H-8), δ_{C} 50.8 (C-9), 40.3 (C-5), 33.0 (C-8)]; an oxymethylene [δ_{H} 3.83 (1H, dd, $J = 10.8, 4.0$ Hz, H-1a), 3.55 (1H, dd, $J = 10.4, 8.4$ Hz, H-1b), δ_{C} 61.6 (C-1)]; two deoxymethylene groups [δ_{H} 2.63 (1H, dd, $J = 18.8, 4.7$ Hz, H-4 α), 2.59 (1H, dd, $J = 18.8, 9.8$ Hz, H-4 β), 2.16 (1H, dd, $J = 14.0, 5.2$ Hz, H-7 α), 1.40 (1H, ddd, $J = 14.0, 12.0, 5.6$ Hz, H-7 β), δ_{C} 29.9 (C-4), 41.9 (C-7)], and a methyl group [δ_{H} 1.00 (1H, d, $J = 5.6$ Hz), δ_{C} 17.8] (**Table 2.4**).

Table 2.4 NMR Data of compound **60**. Measured at 400 MHz (^1H) and 100 MHz (^{13}C) in CDCl_3 . δ in ppm, J in Hz..

no.	δ_{H}	δ_{C}	HMBC (H \rightarrow C)	NOESY
1a	3.83 (1H, dd, 10.8, 4.0)	61.6	C-5, C-8, C-9	H-1b, H-2, H-8
1b	3.55 (1H, dd, 10.4, 8.4)		C-5, C-8, C-9	H-1a, H-2, H-8
4	2.63 (1H, dd, 18.8, 4.7) 2.59 (1H, dd, 18.8, 9.8)	29.9	C-5, C-6, C-9, C-11	H-1a, H-5
5	3.10 (1H, m)	40.3	C-4, C-8, C-9, C-11	H-2, H-6
6	5.00 (1H, t, 6.0)	85.1	C-8, C-9, C-11	H-5, H-7 β
7 α	2.16 (1H, dd, 14.0, 5.2)	41.9	C-5, C-6, C-8, C-9	H-7 β , H-8
7 β	1.40 (1H, ddd, 14.0, 12.0, 5.6)		C-8, C-10	H-6, H-7 α , H-10
8	1.76 (1H, m)	33.0	C-1, C-9	
9	1.78 (1H, m)	50.8	C-8	
10	1.00 (3H, d, 5.6)	17.8	C-7, C-8, C-9	H-8
11		1785		

The ^1H and ^{13}C NMR data suggested that cornolactone A (**60**) had the same molecular skeleton as cornoside A (**59**), except for the absence of the signals for the methine at C-4, the methyl ester C-3, the glucopyranosyl group and the appearance of signals for a diastereotopic methylene at δ_{H} 2.63 (H-4 α) and δ_{H} 2.59 (H-4 β). This suggested that **60** was a iridoid aglycone that was missing the C-3 methyl ester. This conclusion was further confirmed by the 2D NMR data.

The $^1\text{H} - ^1\text{H}$ COSY and gHSQC experiments allowed the assignment of only one spin system as drawn with bold lines in **Figure 2.12**. Clear COSY correlations observed from H₂-1 (δ_{H} 3.85, 3.55) to H-9 (δ_{H} 1.78), from H-9 to H-5 (δ_{H} 3.10), from H-5 to H-4 (δ_{H} 2.63) and H-6 (δ_{H} 5.00), which in turn coupled to H₂-7 (δ_{H} 2.16, 1.40), from H₂-7 to H-8 (δ_{H} 1.76) which in turn coupled to H₃-10 (δ_{H} 1.00) allowed the formation this linear spin system.

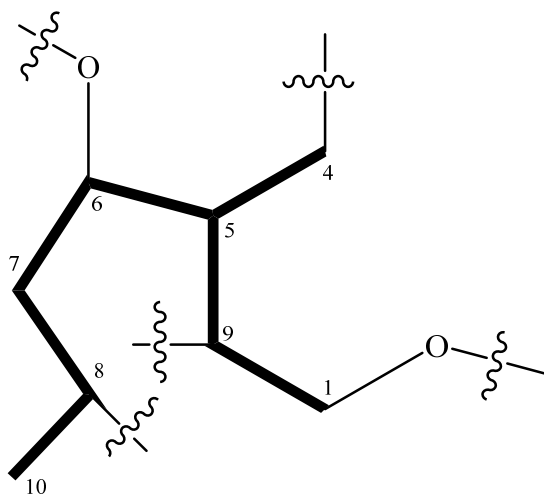


Figure 2.12 Isolated ^1H spin system of cornolactone A (**60**).

This spin system and its connectivity with the remaining carbonyl carbon (C-11) enabled assembly into the final planar structure of **60** based upon extensive analysis of

the HMBC spectrum. Clear HMBC correlations between H₂-1 (δ_{H} 3.85, 3.55) and C-8 (δ_{C} 33.0) confirmed the connectivity between C-8 and C-9 to be a tetra-substituted cyclopentane ring. This was further confirmed by correlations between Me-10 (δ_{H} 1.00) and C-7 (δ_{C} 41.9) and C-9 (δ_{C} 50.8). In addition, HMBC correlations from H₂-4 to C-5, C-6, C-11 and from both H-6 (δ_{H} 5.00) and H-5 (δ_{H} 3.10) to the ester carbon observed at δ_{C} = 178.5 ppm allowed for C-11 to be incorporated into the molecular structure, and for the five-membered lactone ring to be determined. Thus, the planar structure of **60** was established as shown in figure 2.5.

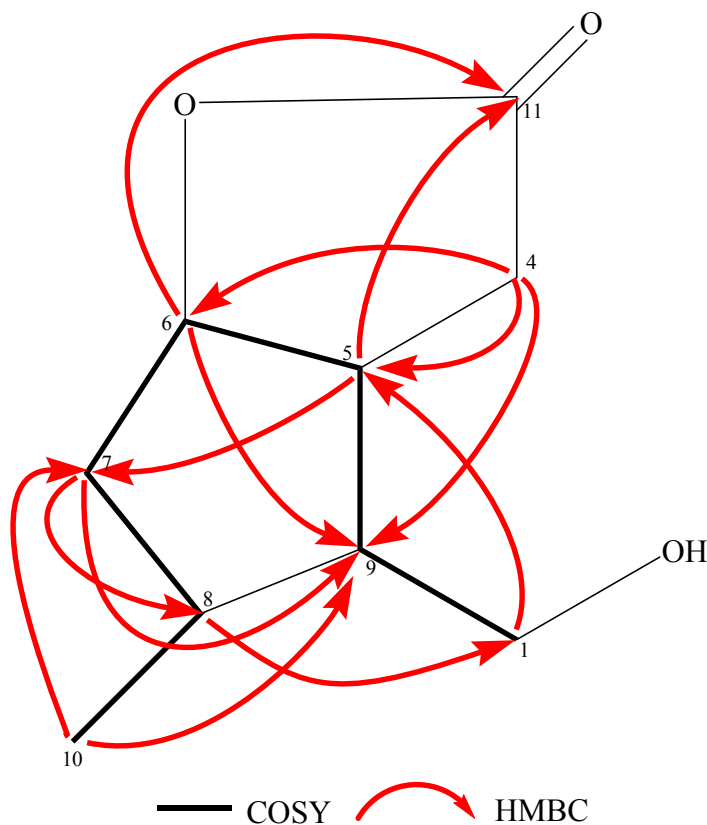


Figure 2.13 Key ¹H–¹H COSY and HMBC correlations of cornolactone A (**60**).

The relative configuration of compound **60** was determined by comparison of coupling constants to the literature data and by analysis of NOESY correlations (**Figure**

2.14). The small coupling constants of $J_{\text{H-6, H-7ax}}$ 6.0 Hz, $J_{\text{H-6, H-7eq}}$ 12.0 Hz allowed H-6 in β -orientation as observed in compound **59**, as well as in previously reported iridoids.²³ In addition, NOE correlations observed from H-6 to H-5 and H-7 β , and from H-5 to H-9 confirmed all of these protons shared β -configuration. The similarity of proton–proton coupling constants and ^1H and ^{13}C NMR chemical shifts together with the NOESY spectrum of **60** showed the same relative configuration as that of **59** for all four chiral centers. This further suggested that compound **60** might to be a product of **59** after decarboxylation and hydrolysis of the glucopyranosyl group. The absolute configuration of **60** was assigned by the identical NMR spectra data and comparable optical rotation values $[[\alpha]_D^{18} + 3.23 (0.2) \text{ lit}[\alpha]_D + 14.73 (0.9)]$ in the literature.⁴³ Thus, compound **60** was determined to be $[3aR,4R,5S,6aS]$ -4-hydroxymethyl-5-methyl-hexahydro-cyclopenta [b] furan-2-one and given the trivial name cornolactone A.

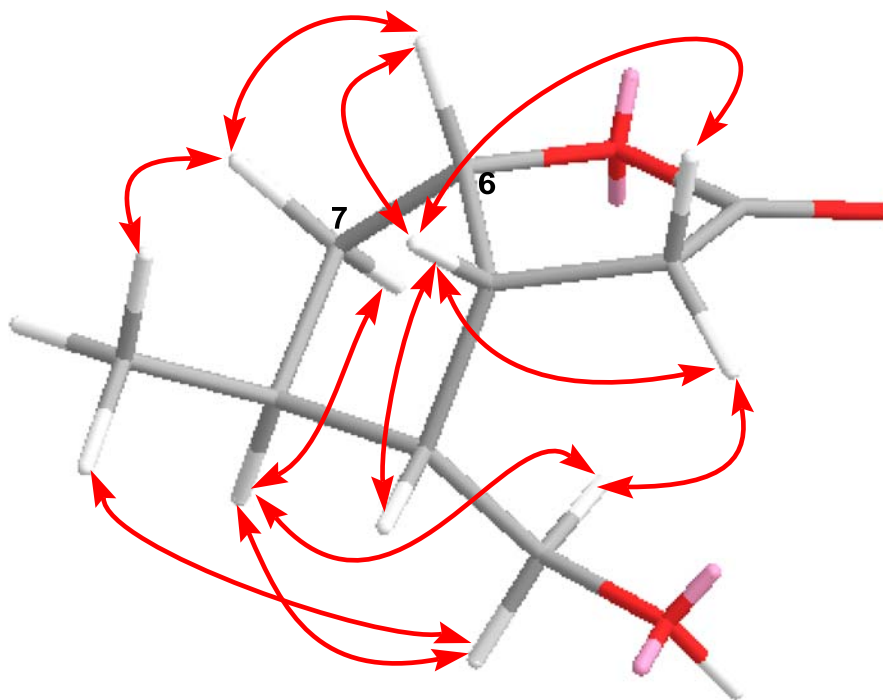


Figure 2.14 Key NOESY correlations of cornolactone A (**60**).

Interestingly, compound **60** was isolated as a natural γ -lactone from *C. controversa*. It has been synthesised by Dr. Giovanni Vidari's group as a key building block for the total synthesis of semperoside A.⁴³ Since this is the first report of **60** from a natural source, the isolation, structure elucidation, and full spectroscopic data are reported.

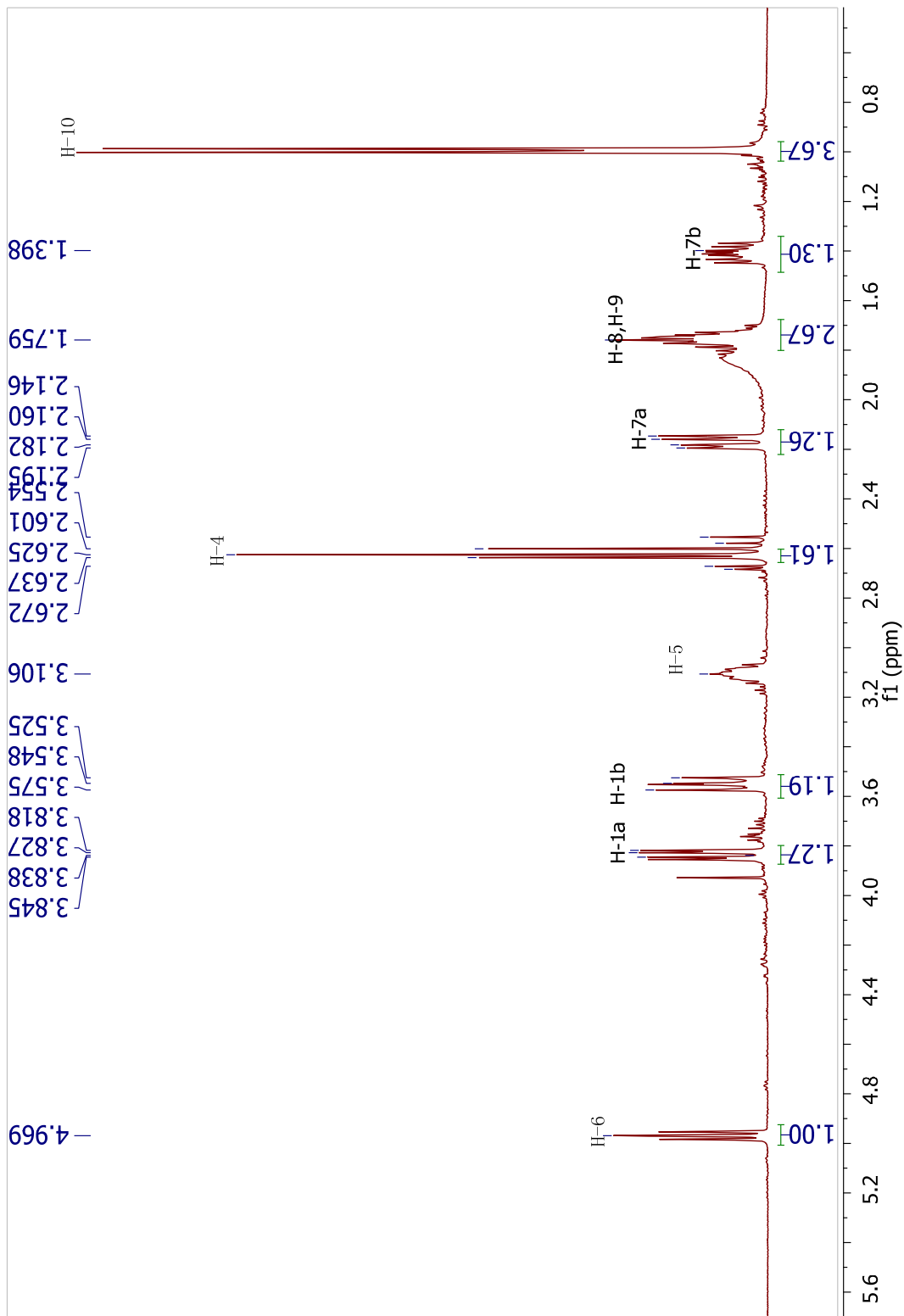


Figure 2.15 ¹H NMR spectrum of cornolactone A (**60**), 400 MHz, in CDCl₃

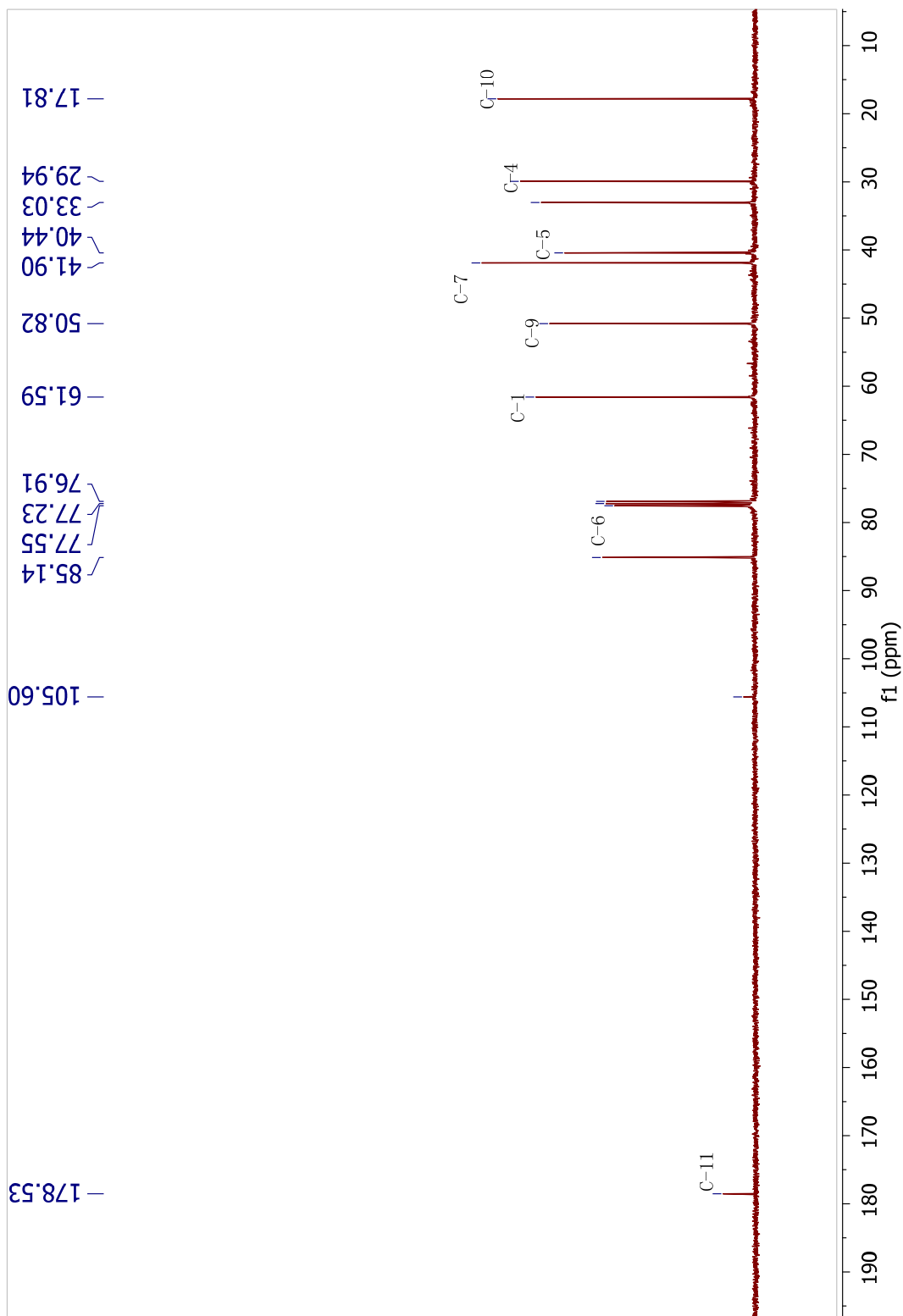


Figure 2.16 ^{13}C NMR spectrum of cornolactone A (**60**), 100 MHz, in CDCl_3

Cornolactone B (**61**) was isolated as a colorless gum. The molecular formula of cornolactone B (**61**), C₁₀H₁₂O₄, was suggested from the HRESIMS of the [M + H]⁺ ion at *m/z* 197.0811 (calcd 197.0808), which requires five degrees of unsaturation. An initial analysis of the ¹³C NMR and DEPT data revealed 10 carbon signals, two of them arising from ester carbonyl groups (δ_C 170.2, 164.8). A signal at δ_C 85.1 ppm was similar to that observed in **59** for a lactone ring, while the signal at δ_C 68.8 ppm was consistent with an oxygenated methylene. The remaining six signals at high field could be attributed to four sp³ methines, one sp³ methylene, and one methyl carbon atom. The ¹H (**Figure 2.20**), ¹³C NMR (**Figure 2.21**) and HSQC spectra of **61** afforded signals at δ_H 5.04 (1H, t, *J* = 5.5 Hz, H-6), δ_C 85.1 (C-6), for an oxymethine, δ_H 3.78 (1H, d, *J* = 9.6 Hz, H-4), 3.35 (1H, dd, *J* = 9.2, 6.4 Hz, H-5), 2.10 (1H, ddd, *J* = 15.6, 8.0, 5.2 Hz, H-9), 2.04 (1H, m, H-8), δ_C 45.7 (C-4), 42.3 (C-5), 43.1 (C-9), 34.2 (C-8), for four other methines, δ_H 4.47 (1H, dd, *J* = 12.2, 4.8 Hz, H-1a), 4.05 (1H, dd, *J* = 12.2, 8.0 Hz, H-1b), δ_C 68.8 (C-1), for an oxymethylene, δ_H 2.36 (1H, dd, *J* = 14.8, 6.8 Hz, H-7α), 1.68 (1H, ddd, *J* = 14.8, 9.4, 5.6 Hz, H-7β), δ_C 41.2 (C-7), for a methylene, and a methyl group at δ_H 1.12 (1H, d, *J* = 6.7 Hz), δ_C 19.4 (**Table 2.5**). All of this evidence, along with careful inspection of the HBMC spectrum indicated that the molecular skeleton of **61** is similar to that of **60** except for the absence of the signals for the methylene group at C-4, and the addition of signals for an ester carbonyl carbon at δ_C 164.7 (C-3) and a methine δ_H 3.78 (H-4). Accounting for the 2 degrees of unsaturation occupied by two carbonyl groups, the remaining 3 degrees of unsaturation indicated that **61** was a tricyclic system. The only

possible connection was between the C-1 oxygen and the ester carbonyl carbon C-3 to form a δ -lactone ring.

Table 2.5 NMR Data of compound **61**. Measured at 400 MHz (^1H) and 100 MHz (^{13}C) in CDCl_3 , δ in ppm, J in Hz..

no.	δ_{H}	δ_{C}	HMBC (H \rightarrow C)	NOESY
1a	4.47(1H, dd, 12.2, 4.8)	68.3	C-3, C-5, C-8, C-9	H-1b, H-9, H-10
1b	4.05 (1H, dd, 12.2, 8.0)		C-3, C-5, C-8	H-1a, H-9
3		164.8		
4	3.78 (1H, d, 9.5)	45.7	C-3, C-5, C-9, C-11	
5	3.35 (1H, dd, 15.4, 9.3)	42.3	C-11	H-6, H-9
6	5.04 (1H, t, 5.5)	85.1	C-8, C-9, C-11	H-5, H-7 α , H-7 β
7 α	2.36 (1H, dd, 14.8, 7.0)	41.2	C-5, C-6, C-8, C-9, C-10	H-5, H-7 β
7 β	1.68 (1H, ddd, 14.8, 9.6, 5.5)		C-8, C-10	H-6, H-7 α
8	2.04 (1H, qddd, 9.6, 7.0, 6.7, 2.6)	34.2	C-1, C-5	H-1a, H-10
9	2.10 (1H, ddd, 15.4, 8.1, 4.9)	43.1	C-4, C-8, C-10	H-1a, H-1b, H-5
10	1.12 (1H, d, 6.7)	19.4	C-7, C-9	H-1a, H-7 α , H-8
11		170.2		

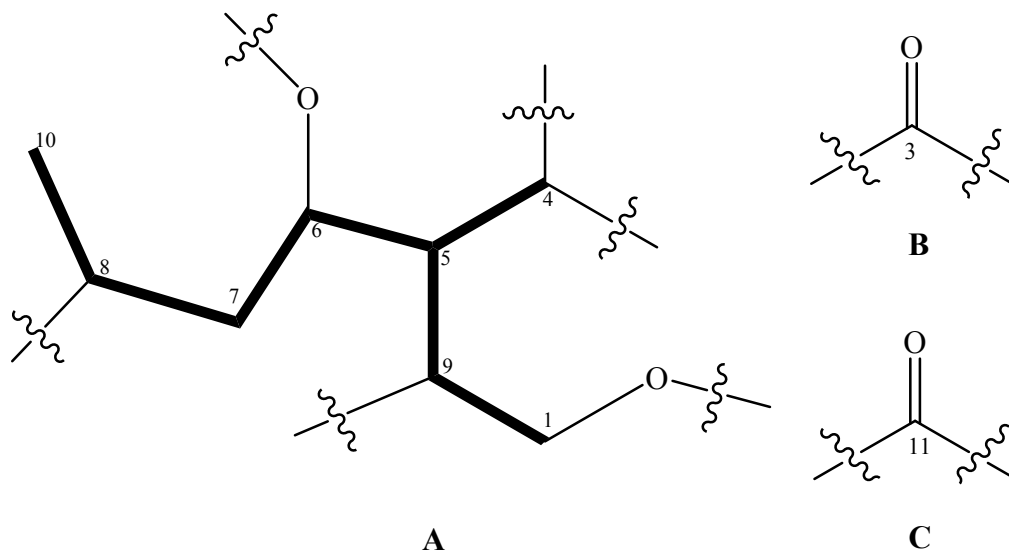


Figure 2.17 Subfragments (A – C) of cornolactone B (**61**).

Detailed analysis of the ^1H , ^{13}C NMR and $^1\text{H} - ^1\text{H}$ COSY spectra coupled with the gHSQC spectrum led to the assignment of only one spin system as drawn with bold lines in **Figure 2.17**. Clear COSY correlations from H-6 (δ_{H} 5.04) to H-5 (δ_{H} 3.35) and H-7 β (δ_{H} 1.68), from H-8 (δ_{H} 2.04) to H₂-7 (δ_{H} 2.36, 1.68) and Me-10 (δ_{H} 1.12), from H-

5 to H-4 (δ_{H} 3.78) and H-9 (δ_{H} 2.10), and from H-9 to H₂-1 (δ_{H} 4.47, 4.05) allowed for the connectivity of the linear fragment A.

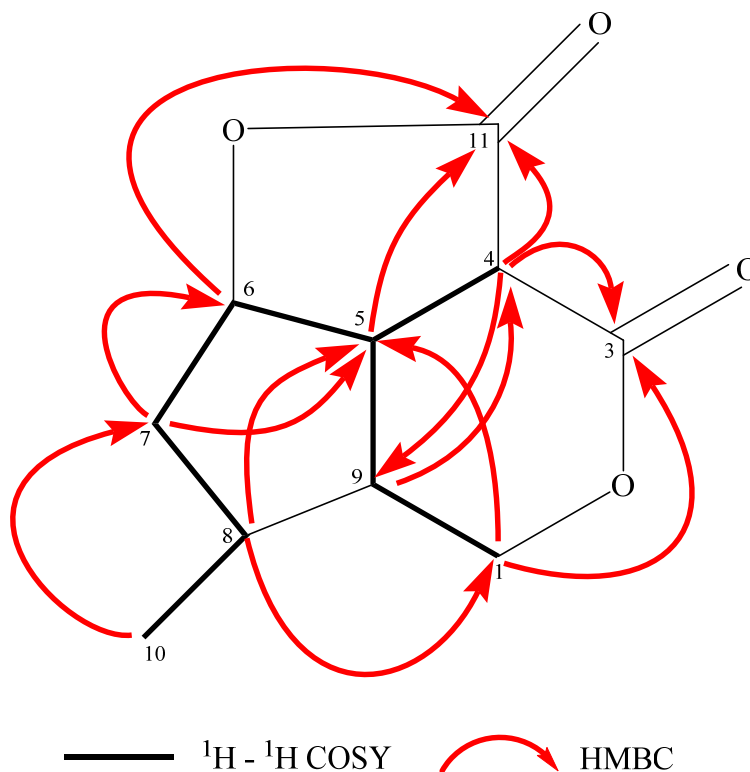


Figure 2.18 Key ¹H – ¹H COSY and HMBC correlations of cornolactone B (**61**).

On the basis of the HMBC experiment, the planar structure of **61** could be completely established by inserting the “loose ends” of the two quaternary carbons of C-3 and C-11. HMBC correlations between H-6 (δ_{H} 5.04) and C-8 (δ_{C} 34.2), C-9 (δ_{C} 43.1) and C-11 (δ_{C} 170.2), between H-4 (δ_{H} 3.78) and C-3 (δ_{C} 164.8), C-9 and C-11, and between H-5 (δ_{H} 3.35) and C-11 allowed for the connectivity between C-11 and C-4 (subfragments C to A) and the linkage between C-11 and C-6 through an oxygen to form the first five-membered lactone ring containing C-4, C-5, C-6, O and C-11. In addition, HMBC correlations between H₂-1 (δ_{H} 4.47, 4.05) and C-3, C-8 and C-9, and between the methyl Me-10 (δ_{H} 1.12) and C-7, C-8 and C-9 established the planar structure of **61**

(**Figure 2.5**) to be a tricyclic dilactone iridoid with a 1*H*-2,6-dioxahexahydrocyclopent [*c*, *d*] indene-1,7 (2*H*)-dione ring system. The more detailed HMBC correlations are shown in **Figure 2.18**.

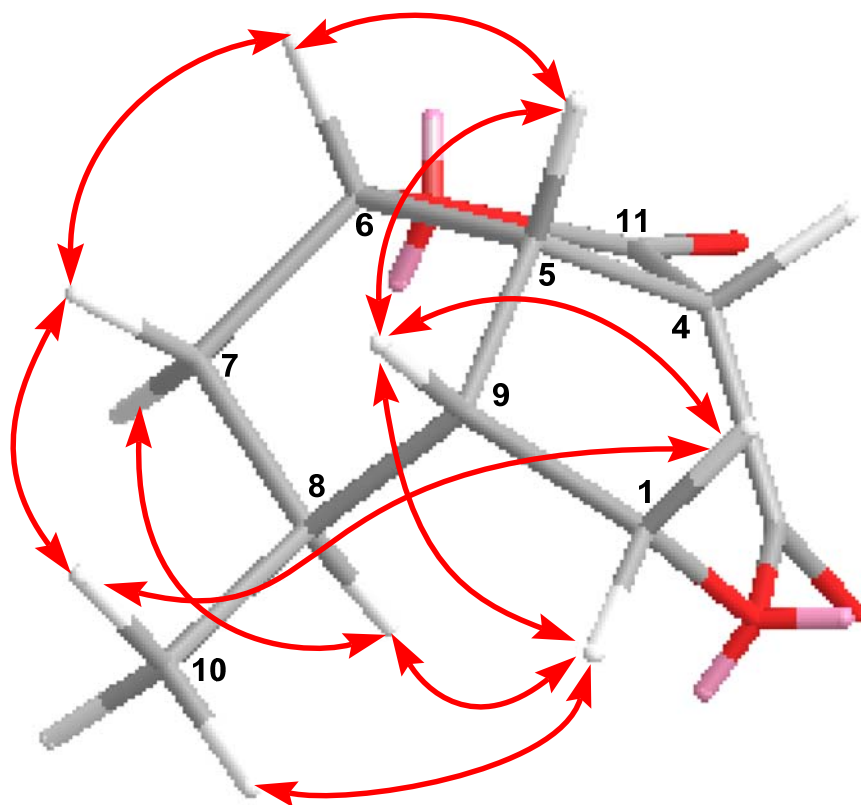


Figure 2.19 Key NOESY correlations of cornolactone B (**61**).

The relative configuration of **61** at C-5, C-6, C-8 and C-9 was determined to be identical to that of **59** and **60** by NOE correlations observed in a NOESY experiment and scalar coupling in the ^1H NMR spectrum. Clear NOE correlations (in **Figure 2.19**) between H-5 and H-6 and H-9, and between H-9 and H-1 β (δ_{H} 4.47) and Me-10 indicated the β -orientation of these protons. The absence of NOE correlations observed to or from H-4 made it difficult to assign the configuration at C-4. However, the presence of a large ^1H coupling constant ($J = 9.6$ Hz) between H-4 and H-5 suggested the *cis*-relationship of these two protons and the β -orientation of H-4. This coupling constant is consistent with

that observed for the *cis*-fused tricyclic iridoids semperoside ($J = 10.5$ Hz), 9-hydroxysemperoside ($J = 11.4$ Hz), and dihydrobrasoside ($J = 10.5$ Hz),⁴⁹ together with the dilactone compounds, asperuloside tetraacetate lactone ($J = 9.8$ Hz) and dihydroasperuloside tetraacetate lactone ($J = 10.0$ Hz), produced from the oxidation of the iridoid glucoside asperuloside.⁵¹ Thus the structure of cornolactone B (**61**) is therefore defined as $4S,5S,6S,8S,9R$.

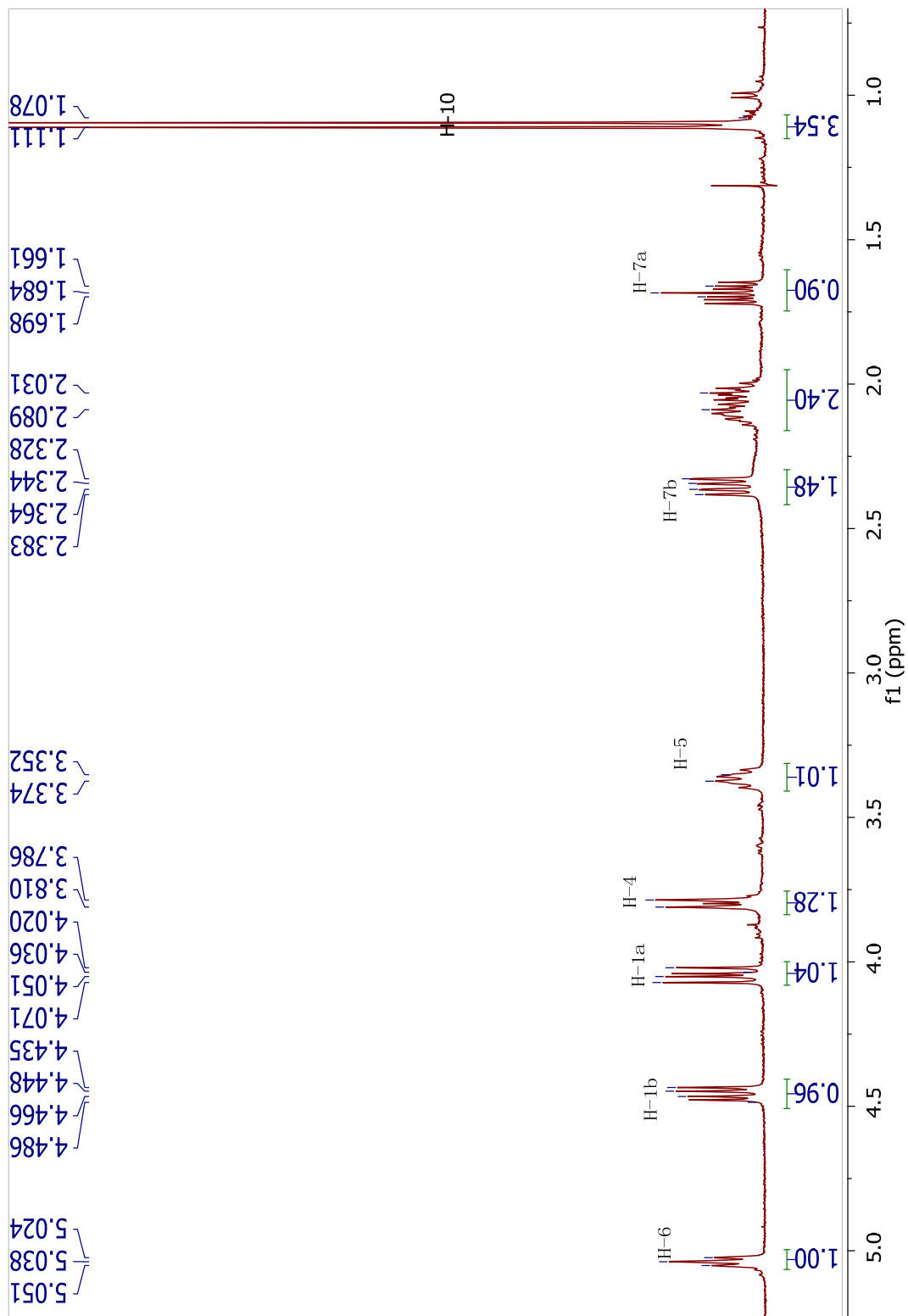


Figure 2.20 ^1H NMR spectrum of cornolactone B (**61**), 400 MHz, in CDCl_3

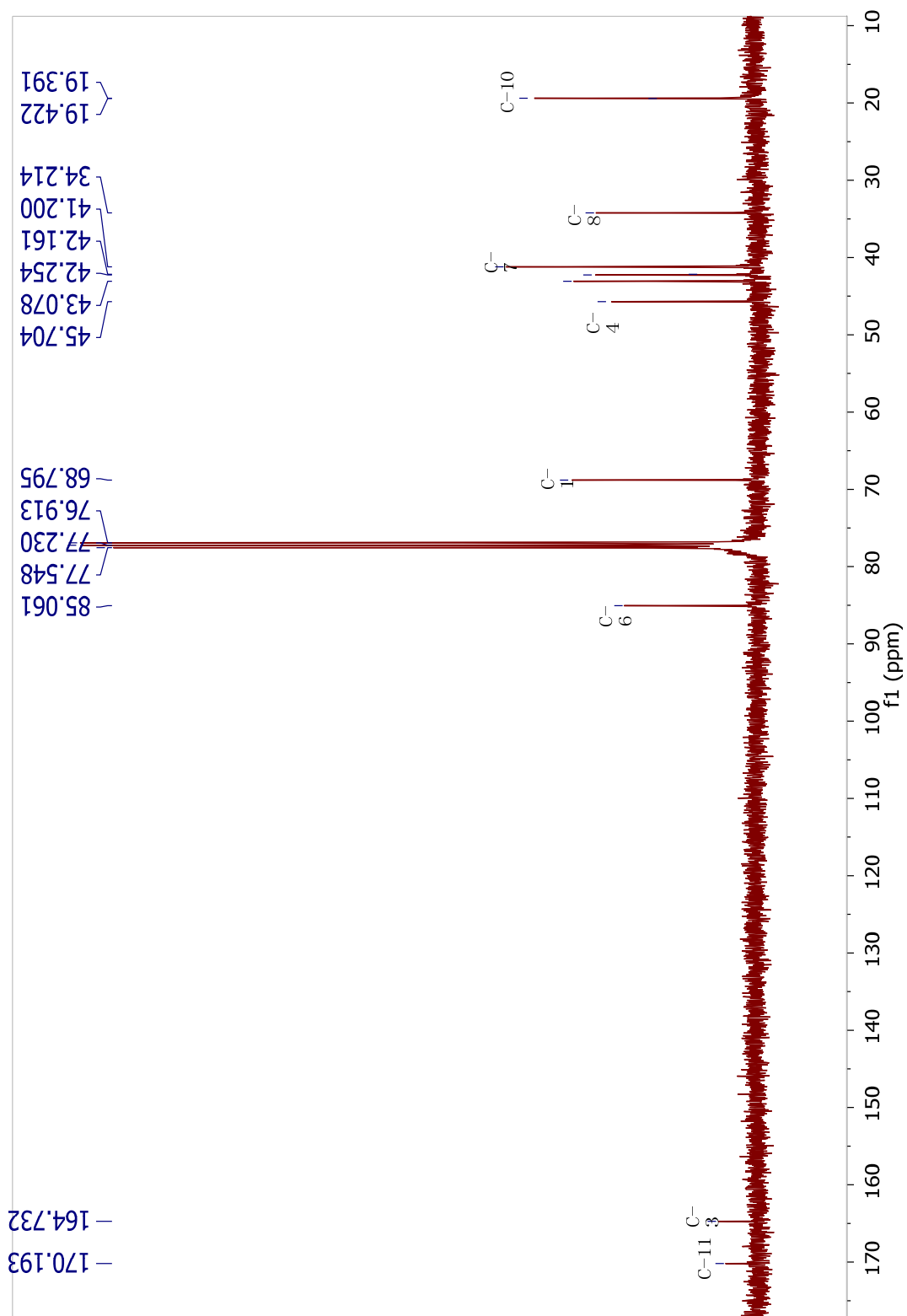


Figure 2.21 ^{13}C NMR spectrum of cornolactone B (**61**), 100 MHz, in CDCl_3

Cornolactone C (**62**) was obtained by allowing **61** to stand in CD₃OD during the NMR experiments. Its molecular formula C₁₀H₁₄O₅ was established on the basis of HRESIMS for the [M – H₂O + D]⁺ at *m/z* 198.0869 (calcd 198.0871), which indicated 4 degrees of unsaturation. An initial analysis of the ¹³C NMR, HSQC and HMBC data revealed 10 carbon signals including five sp³ methines, two sp³ methylenes, one methyl and two carbonyl carbons (δ_C 174.3, 169.9). The ¹H, ¹³C NMR (**Figure 2.22, 2.23**) and HSQC spectra of **62** afforded signals at δ_H 5.08 (1H, t, *J* = 6.4 Hz, H-6), δ_C 86.2 (C-6), for an oxymethine, δ_H 3.42 (1H, t, *J* = 7.4 Hz, H-5), 2.09 (1H, overlapped, H-9), 1.96 (1H, overlapped, H-8), δ_C 47.5 (C-5), 51.6 (C-9), 34.2 (C-8), for three other methines, δ_H 3.78 (1H, dd, *J* = 11.2, 3.6 Hz, H-1a), 3.54 (1H, dd, *J* = 11.2, 8.2 Hz, H-1b), δ_C 61.1 (C-1), for an oxymethylene, δ_H 2.12 (1H, dd, *J* = 14.3, 5.8 Hz, H-7α), 1.52 (1H, ddd, *J* = 14.3, 11.7, 6.0 Hz, H-7β), δ_C 42.3 (C-7), for a methylene, and a methyl group at δ_H 1.04 (1H, d, *J* = 5.9 Hz), δ_C 17.8 (in **Table 2.6**). All of those data suggested that the molecular skeleton of compound **62** was similar to that of the compound **61**. The most significant spectral differences observed between **62** and **61** were the chemical shifts of the two proton signals at δ_H 3.78 (H-1a), 3.54 (H-1b) in ¹H NMR spectrum, both of them shifted upfield by 0.66 and 0.49 ppm compared with that of **61**, respectively. As well as, the chemical shift of C-1 also shifted upfield from 68.3 for **61** to 61.1 ppm in **62**. Interestingly, for the high acidity characterization of the 1,3-dicarbonyl, the signal at δ_H 3.78 (H-4) in compound **61** never showed up in compound **62**, indicating it was deuterated by *d*₄-methanol. Accounting for the 2 degrees of unsaturation occupied by two

carbonyl groups, the remaining 2 degrees of unsaturation indicated that **62** was a bicyclic compound.

Table 2.6 NMR Data of compound **62**. Measured at 400 MHz (^1H) and 100 MHz (^{13}C) in CD_3OD , δ in ppm, J in Hz..

no.	δ_{H}	δ_{C}	COSY	HMBC (H→C)
1a	3.78 (1H, dd, 11.2, 3.6)	61.1	H-1b, H-9	C-5, C-9
1b	3.54 (1H, dd, 11.2, 8.2)		H-1a	C-5, C-8, C-9
3		169.9		
4	deuterated	50.0		
5	3.42 (1H, t, 7.4)	47.5	H-9	C-1, C-3, C-8, C-9, C-11
6	5.08 (1H, t, 6.4)	86.2	H-5, H-7 β	C-8, C-9, C-11
7 α	2.12 (1H, dd, 14.3, 5.8)	42.3	H-8, H-7 β , H-10	C-5, C-6, C-8, C-9
7 β	1.52 (1H, ddd, 14.3, 11.7, 6.0)		H-7 α , H-8	C-8, C-10
8	1.82 (1H, overlapped)	34.2		
9	1.80 (1H, overlapped)	51.6		
10	1.04 (3H, d, 5.9)	17.8	H ₂ -7, H-8	C-7, C-8, C-9
11		174.3		

Combined with the evidence of 18 mass units higher in the mass spectrum and 1 lesser degree of unsaturation than those of **61** suggested that compound **62** might be the product yielded by cleaving the six-membered lactone ring of compound **61**. This conclusion was further confirmed by the proton NMR spectrum (see appendix A1-25) which was obtained from compound **61** after the sample was left in *d*-chloroform for almost three months.

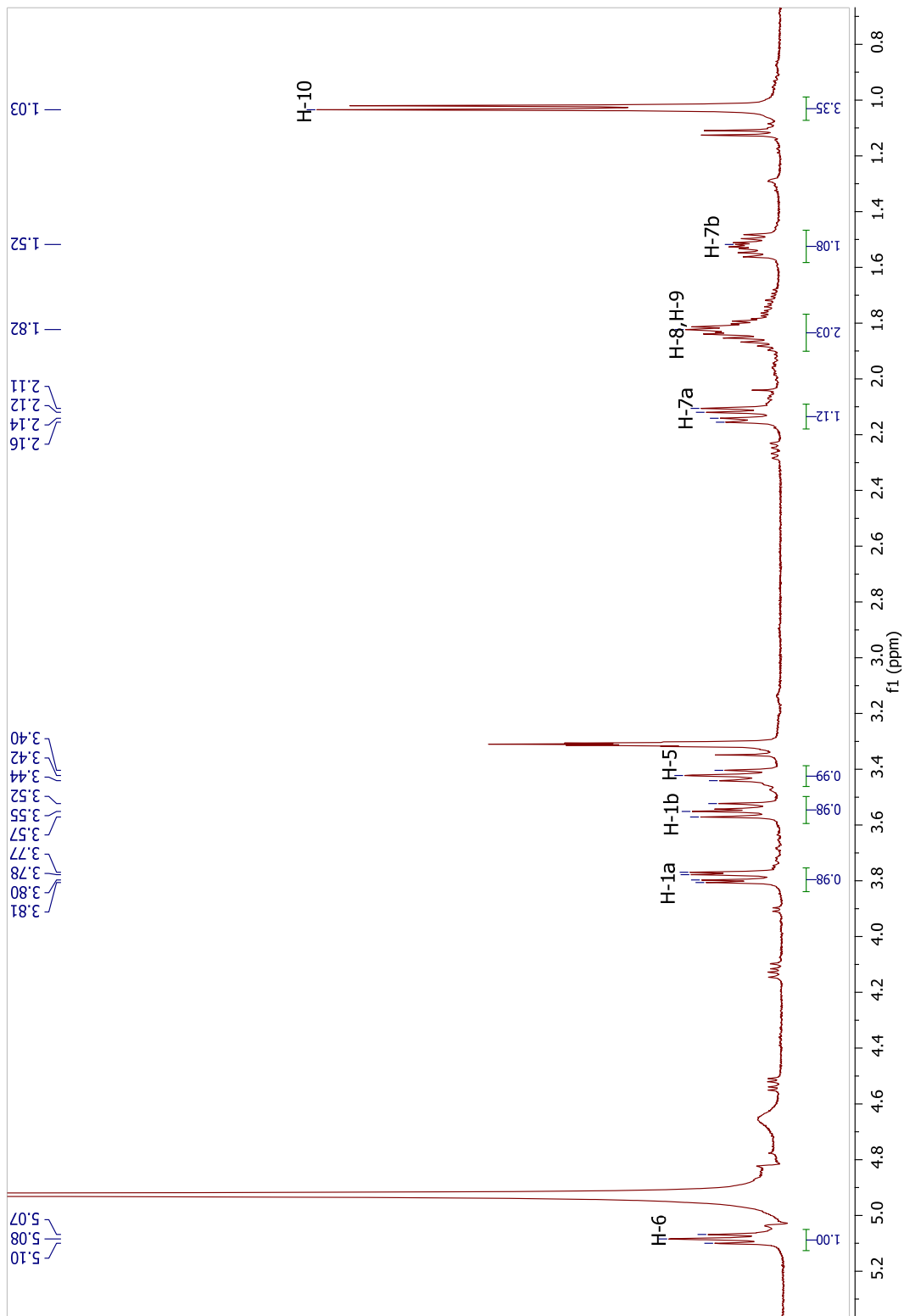


Figure 2.22 ¹H NMR spectrum of cornolactone C (**62**), 400 MHz, in CD₃OD

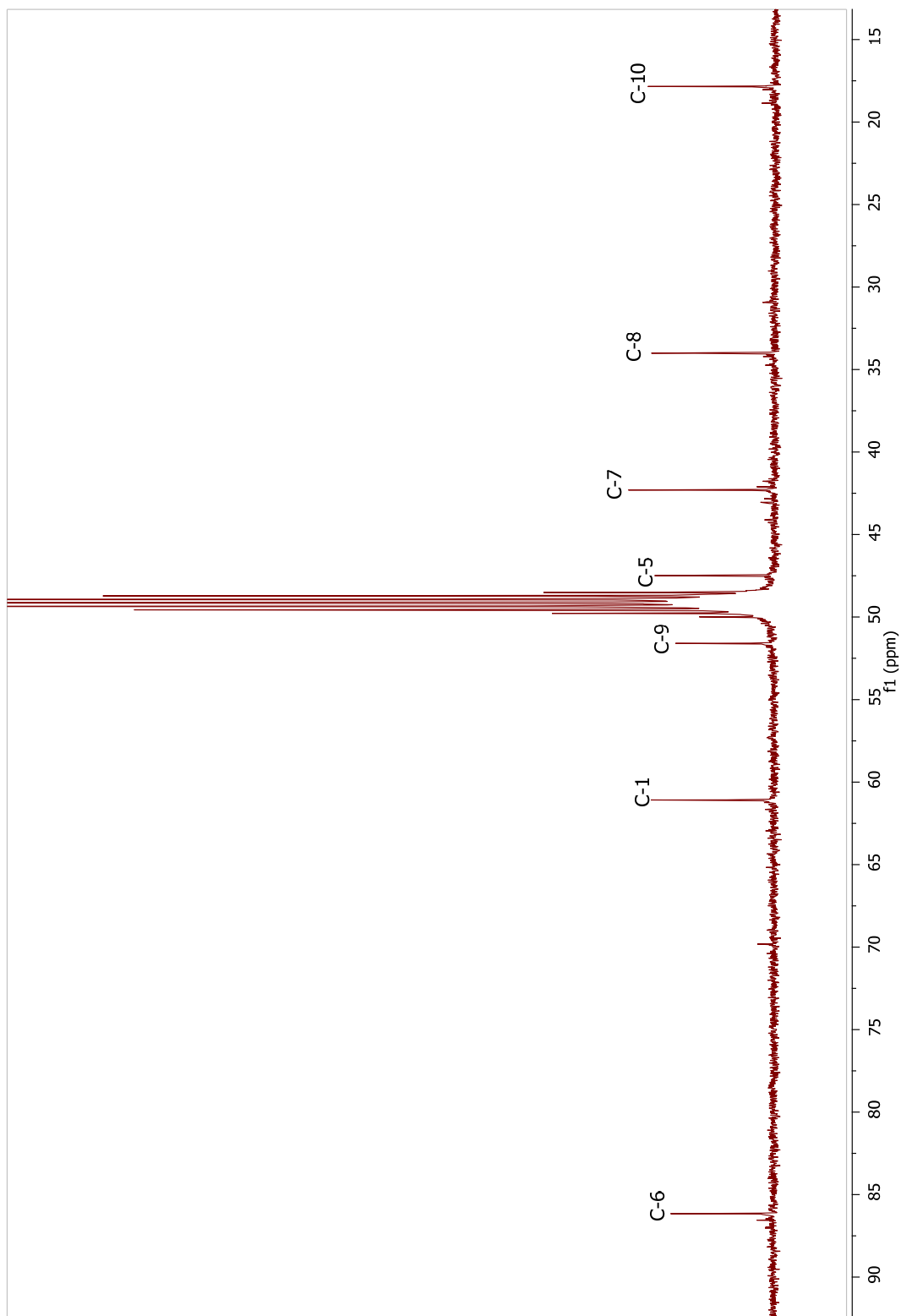


Figure 2.23 ^{13}C NMR spectrum of cornolactone C (**62**), 100 MHz, in CD_3OD

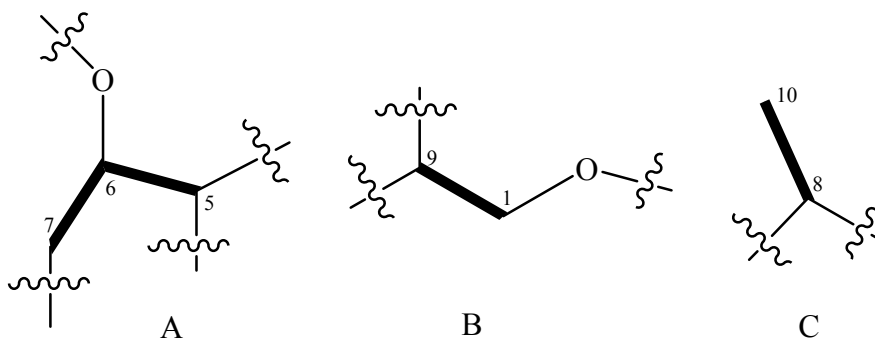


Figure 2.24 Subfragments (A – C) of cornolactone C (**62**).

The structure of **62** was further confirmed by a detailed analysis of the 2D NMR. Interpretation of the $^1\text{H} - ^1\text{H}$ COSY spectrum coupled with the gHSQC spectrum led to the assignment of three isolated spin systems (A – C) as drawn with bold lines in **Figure 2.24**. Clear COSY correlations observed from H-6 (δ_{H} 5.08) to H-5 (δ_{H} 3.42) and H-7 β (δ_{H} 1.52) allowed for the connectivity between C-5 and C-7, which lead to the formation of the linear subfragment A. The connectivity between C-1 and C-9 was confirmed by the COSY correlations from the methylene signals at δ_{H} 3.54, 3.78 for H₂-1 to a methine signal at δ_{H} 2.09 for H-9. And the correlation between Me-10 and H-8 (δ_{H} 1.96) allowed the connectivity of the methyl to C-8 as in subfragment C.

On the basis of an HMBC experiment, those fragments could be fully connected by inserting the remaining the tertiary and quaternary carbon atoms C-8, C-9, C-3 and C-11 (**Figure 2.25**). The diagnostic HMBC correlations are observed from H-5 (δ_{H} 3.78) to C-1 (δ_{C} 61.1), C-3 (δ_{C} 169.9), C-7 (δ_{C} 42.3), C-8 (δ_{C} 34.2) and C-11 (δ_{C} 174.3). These correlations allowed for the establishment of the connectivities of C-5 to C-9 (subfragments A to B), C-7 to C-8 (subfragments A to C) and C-8 to C-9 (subfragments C to B) and established the tetra-substituted cyclopentane ring moiety, as well as

confirming the location of carboxylic acid group at C-4. In addition, the significant HMBC correlations from Me-10 (δ_{H} 1.04) to C-7, C-8, and C-9 (δ_{C} 51.6) further confirmed the methyl group to be linked with the five-membered cyclopentane ring by tertiary carbon C-8. Furthermore, the distinct HMBC correlation from H-1a (δ_{H} 3.78) to C-5, C-8 and C-9 (δ_{C} 51.6) also confirmed the connections of fragments C to A and B by C-9. Finally, HMBC correlations from H-6 (δ_{H} 5.08) to C-8, C-9 and C-11, leading the formation of 2H-hexahydrocyclopenta [b]furan-2-one ring system by the linkage of fragment A to partial structure of the lactone ring through C-6-O-C-11. Thus, the planar structure of **62** was established as shown in figure 2.5.

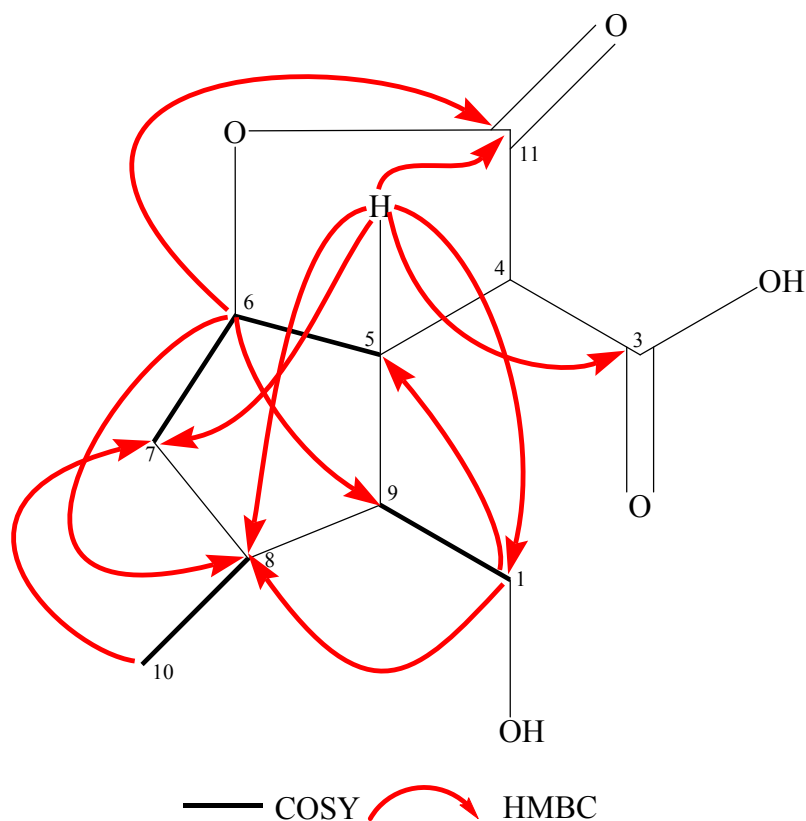


Figure 2.25 Key $^1\text{H} - ^1\text{H}$ COSY and HMBC correlations of cornolactone C (**62**).

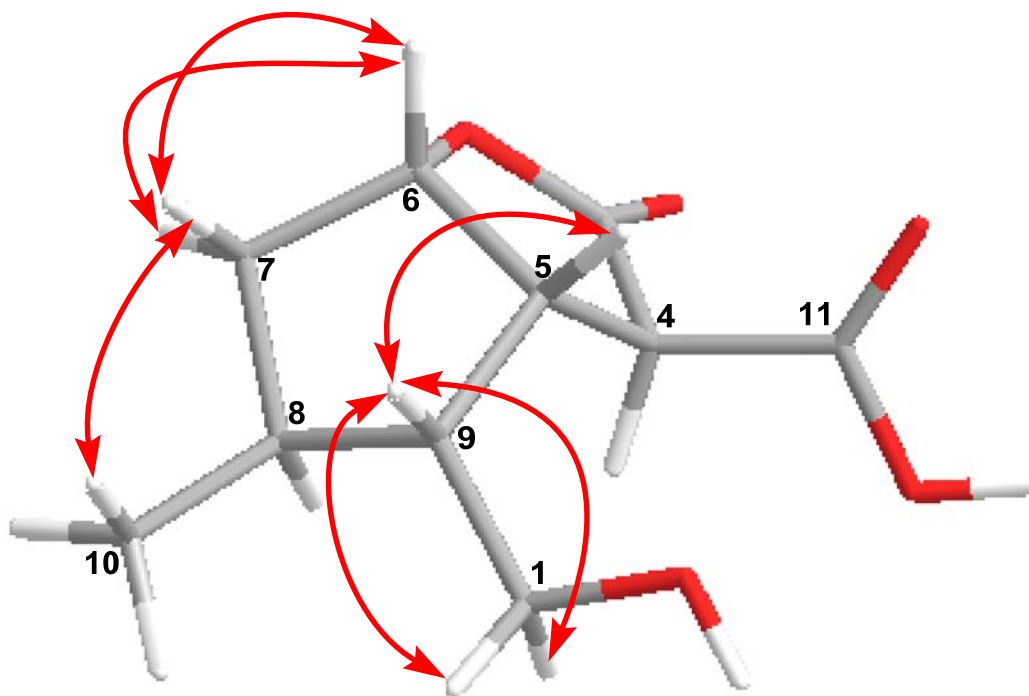


Figure 2.26 Key NOESY correlations of cornolactone C (**62**).

The relative configuration of compound **62** was assigned by comparison of the coupling patterns in the ^1H NMR spectrum with that of compound **61**. The small coupling constant of $J_{\text{H-5, H-9}}$ 7.6 Hz was similar to that of compound **61**, suggesting the *cis* configuration of H-5 and H-9. In the same way, the small coupling constants of $J_{\text{H-6, H-7ax}}$ 5.8 Hz, $J_{\text{H-6, H-7eq}}$ 6.0 Hz indicated that H-6 shared β -orientation with H-5 and H-9. The stereochemistry at C-4 could be determined to be a *trans*-disposition of the involved protons through the small coupling constant observed for H-5 (δ_{H} 3.42, t, 7.4), which was similar with that observed in gelsemiol 1-glucoside (**70**)⁴⁹ and **59** with H-4 in α -orientation. The chemical shift of H-10 (δ_{H} 1.04) indicated the β -configuration of the methyl group at C-8 as observed in all other iridoids.^{27,49} The absolute configuration of **62** was determined based on the nearly identical NMR data and comparable optical

rotation values ($[\alpha]_D^{18} - 11.4$) with those of borrerlagenin ($[\alpha]_D^{18} - 1.3$)⁵⁰ and 59 ($[\alpha]_D^{18} - 13.8$). Thus, the structure of **62** was therefore defined as 4*S*,5*S*,6*S*,8*S*,9*R*.

Cornolactone D (**63**) was isolated as a colorless gum. The molecular formula was deduced to be C₁₁H₁₆O₅, with 4 degrees of unsaturation, on the basis of its HRESIMS data at m/z 251.0884 [M + Na]⁺ (calcd 251.0890), which indicated 31 mass units higher and 1 lesser degree of unsaturation than those of **61**.

The ¹H NMR spectrum (**Figure 2.30**) of **63** was similar to that of cornolactone B (**61**), except that it showed the addition of a methoxyl group (δ_H 3.80; δ_C 53.4) and H-6 [δ_H 5.04, t (5.5)] was shifted upfield by 1.22 ppm (Table 2.7) as compared to that of **61**. This suggested **63** was the product from methanolysis of the γ -lactone ring in **61**. The ¹³C NMR spectrum (**Figure 2.31**) was quite similar to that of cornolactone B (**61**), and the main differences were the appearance of a methyl carboxylate group at δ_C 169.2 and 53 ppm and the resonance of C-6 (δ_C 77.7) was shifted upfield by 8.6 ppm (Table 2.7), in comparison with that of **61**.

Table 2.7 NMR Data of compound **63**. Measured at 400 MHz (¹H) and 100 MHz (¹³C) in CDCl₃, δ in ppm, J in Hz..

no.	δ_H	δ_C	HMBC (H→C)	NOESY
1a	4.27 (1H, dd, 12.0, 5.6)	69.3	C-3, C-5, C-8, C-9	H-1b, H-9
1b	4.00 (1H, dd, 11.6, 6.0)		C-3, C-5, C-8	H-1a, H-4, H-8
3		169.0		
4	3.58 (1H, d, 6.6)	50.4	C-5, C-6, C-9, C-11	H-1a, H-5
5	2.76 (1H, dt, 11.6, 7.2)	46.1	C-1, C-4, C-6, C-9, C-11	H-4, H-9
6	3.82 (1H, overlapped)	77.4	C-4	H-7 α , H-8
7 α	2.12 (1H, dd, 11.7, 5.9)	43.2	C-5, C-6, C-8, C-9, C-10	H-6, H-7 β
7 β	1.38 (1H, dd, 12.1, 10.2)		C-6, C-8, C-10	H-7 α , H-8
8	1.78 (1H, qddd, 12.1, 9.4, 6.3, 2.7)	33.8	C-1	H-1a, H-7 β , H-10
9	2.20 (1H, ddd, 11.7, 9.4, 6.3)	42.8		H-1a, H-1b, H-5, H-10
10	1.07 (3H, d, 6.3)	18.8	C-7, C-8	H-8, H-9
11		169.2		
OMe	3.80 (3H, s)	53.3	C-11	

Detailed analysis of the ^1H , ^{13}C NMR and $^1\text{H} - ^1\text{H}$ COSY, gHSQC spectra coupled with the HMBC spectrum led to the assignment of the similar spin system as cornolactone B (**61**), a tetra-substituted cyclopentane ring as drawn with bold lines in **Figure 2.27**, as well as a methyl carboxylate group (fragment B) and a quaternary carbon (fragment C). Clear COSY correlations from H-6 (δ_{H} 3.82) to H-5 (δ_{H} 2.76) and H₂-7 (δ_{H} 2.12, 1.38), from H-8 (δ_{H} 1.78) to H₂-7 (δ_{H} 2.12, 1.38), Me-10 (δ_{H} 1.07) and H-9 (δ_{H} 2.20), from H-9 to H₂-1 (δ_{H} 4.47, 4.05) and H-5 and from H-5 to H-4 (δ_{H} 3.58) allowed for the establishment of the tetra-substituted cyclopentane ring moiety of subfragment A. HMBC correlation between the methoxyl group at δ_{H} 3.80 and C-11 (δ_{C} 169.2) further confirmed that compound **63** possesses a methyl ester at C-11 (fragment B).

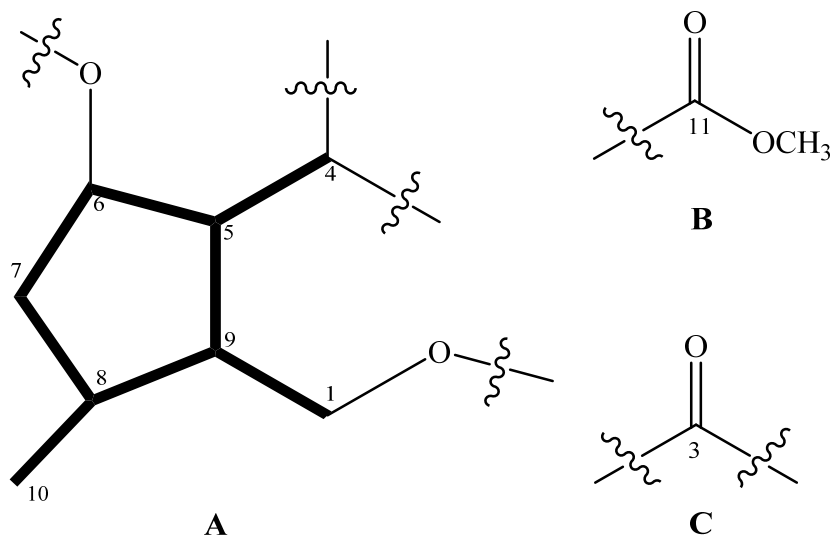


Figure 2.27 Subfragments (A – C) of cornolactone D (**63**).

On the basis of these data and combination of its degrees of unsaturation, compound **63** was initially presumed to be a bicyclic dilactone by cleavage of the five-membered lactone ring of **61**. This was further confirmed by the lack of HMBC correlation between H-6 and C-11. Clear HMBC correlations as shown (in **Figure 2.28**)

between H-5 and C-1 (δ_C 69.3), C-4 (δ_C 50.4), C-6 (δ_C 77.4), C-8 (δ_C 33.8), C-9 (δ_C 42.8) and C-11 confirmed the presence of the tetra-substituted cyclopentane ring and allowed the connectivity between the methyl carboxylate group (subfragment B) and subfragment A through C-4. HMBC correlations between H-4 (δ_H 3.58) and C-3 (δ_C 169.0), C-5 (δ_C 46.1), C-6, C-9 and C-11 further confirmed that methoxycarbonyl group is attached to C-4. Furthermore, distinct HMBC correlations between H₂-1 and C-3 allowed the connectivity between C-3 and C-1 through oxygen to be a six-membered lactone ring. Thus, the planar structure of compound **63** was determined as shown in **Figure 2.5**.

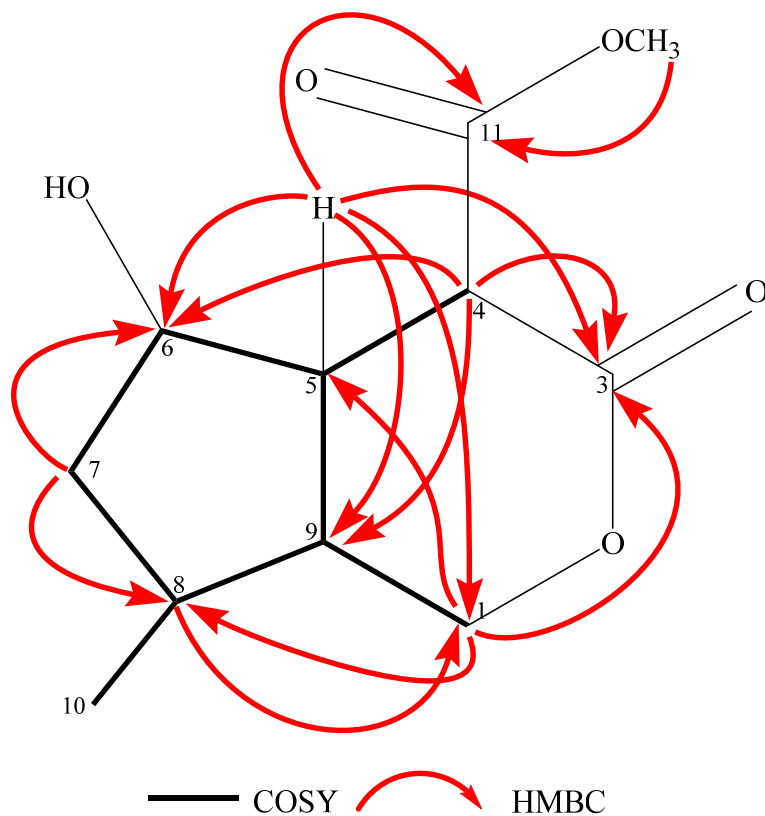


Figure 2.28 Key ^1H - ^1H COSY and HMBC correlations of cornolactone D (**63**).

The relative configuration of compound **63** was readily assigned as shown in Figure 2.5 by 1D and 2D NOE correlations, combined with the coupling patterns in the

^1H NMR spectrum. The NOE correlations (**Figure 2.29**) from H-5 to H-4, H-7 β and H-9, together with correlations from H₃-10 to H-7 β and H-9 established the *cis*-fusion of the cyclopenta[*c*]pyran skeleton with H-4, H-5, H-7 β , H-9 in the β -orientation. The *cis* relationship between H-5 and H-9 was further confirmed by their coupling constant ($^3J = 11.6$ Hz), which is larger in *trans*-fused iridoids (~ 13 Hz). The α -orientation of H-6 was indicated by an NOE correlation observed from H-6 to H-7 α and H-8 on the underside of the cyclopentane ring. This assignment was further supported by the 1D NOESY correlation from H-6 to H-8 as H-8 was irradiated (A1-33). Thus the structure of cornolactone C (**63**) is therefore defined as $4R,5S,6R,8S,9R$.

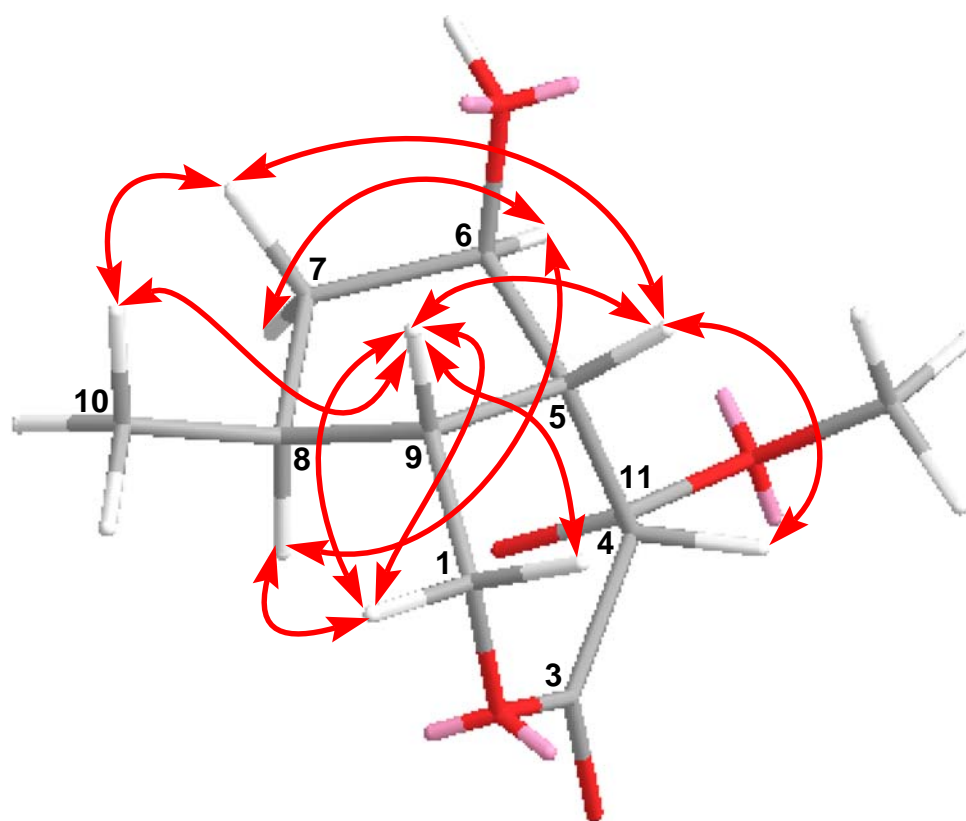


Figure 2.29 Key NOESY correlations of cornolactone D (**63**).

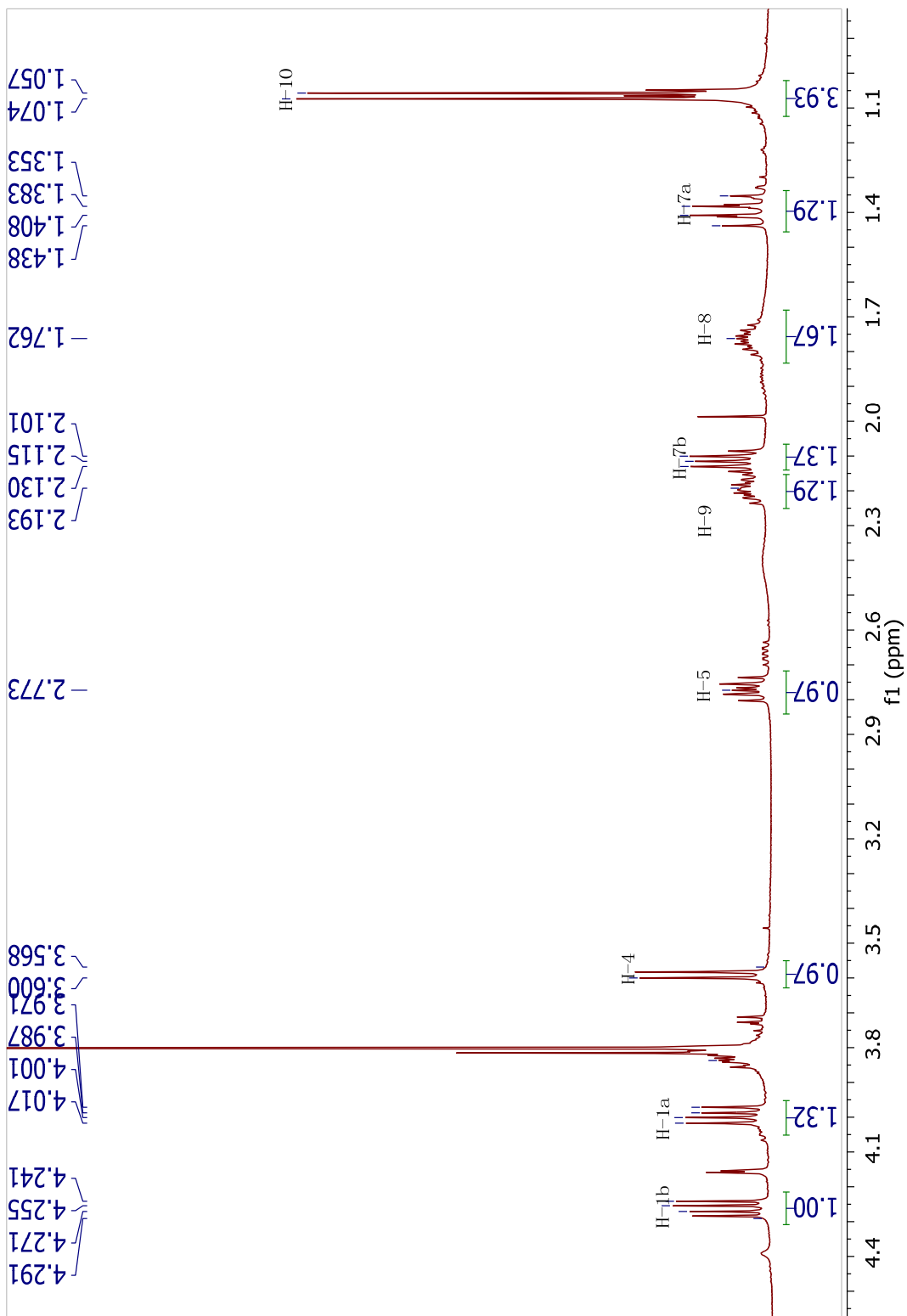


Figure 2.30 ^1H NMR spectrum of cornolactone D (63), 400 MHz, in CDCl_3

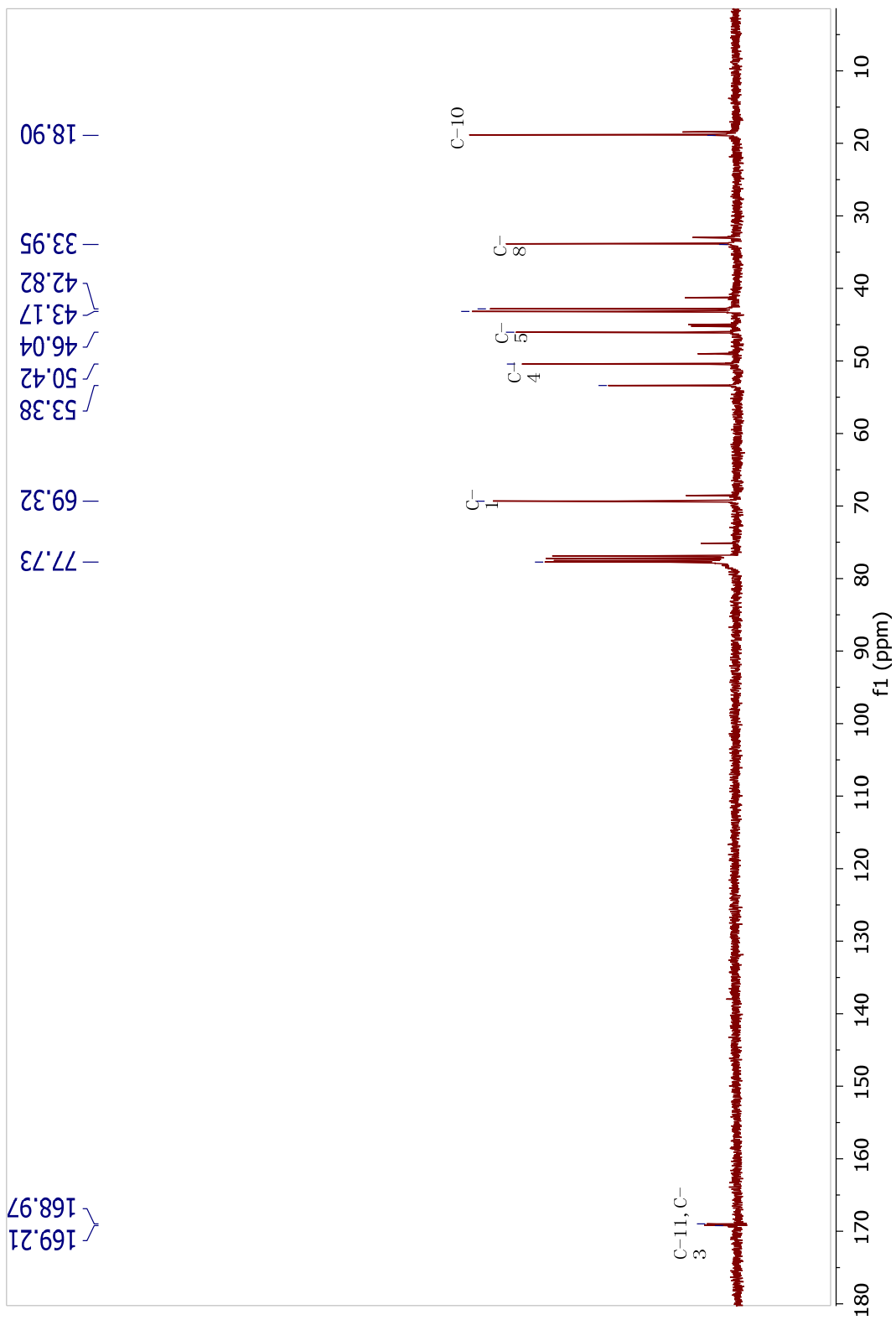


Figure 2.31 ^{13}C NMR spectrum of cornolactone D (**63**), 100 MHz, in CDCl_3

Cornolactone E (**64**) was isolated as a colorless gum. The molecular formula $C_9H_{14}O_3$ was determined from the the HRESIMS of the $[M + H]^+$ ion at m/z 193.0834 (calcd 193.0835) and required 3 degrees of unsaturation. An initial inspection of the ^{13}C NMR, HSQC and HMBC data revealed 9 carbon signals including four sp^3 methines, three sp^3 methylenes, one methyl and one carbonyl carbons (δ_C 174.0). The 1H , ^{13}C NMR and HSQC spectra of **64** afforded signals at δ_H 3.71 (1H, ddd, $J = 10.2, 7.8, 5.5$ Hz, H-6), δ_C 77.8 (C-6), for an oxymethine, δ_H 2.39 (1H, m, H-5), 1.97 (1H, m, H-9), 1.79 (1H, m, H-8), δ_C 42.6 (C-5), 43.2 (C-9), 33.1 (C-8) for three other methines, δ_H 4.18 (1H, dd, $J = 11.6, 4.0$ Hz, H-1a), 4.08 (1H, dd, $J = 12.0, 3.2$ Hz, H-1b), δ_C 68.6 (C-1), for an oxymethylene, δ_H 2.01 (1H, m, H-7 α), 1.27 (1H, dt, $J = 12.1, 11.2$ Hz, H-7 β), δ_C 42.6 (C-7), for a methylene, 2.57 (2H, d, $J = 5.2$ Hz, H-4), δ_C 32.6 (C-4), for another methylene and a methyl group at δ_H 1.03 (1H, d, $J = 6.4$ Hz), δ_C 18.7 (, in **Table 2.8**). All of those data suggested that the molecular skeleton of compound **64** was similar to that of the compound **63**. The most significant differences observed between **64** and **63** were the absence of a methyl carboxylate group at C-4 (δ_C 50.4) in **63** and the presence of a methylene (δ_C 32.6) in **64**, which was further confirmed by the HMBC correlations from H₂-4 (δ_H 2.57) to C-3 (δ_C 174.0), and from H-6 (δ_H 3.71) to C-4 (δ_C 32.6). This suggested that **64** was missing the C-11 methyl ester.

Interpretation of the 1H , ^{13}C NMR and $^1H - ^1H$ COSY spectra coupled with the gHSQC spectrum led to the assignment of three subfragments (A – C) as drawn with bold lines in **Figure 2.32**. Clear COSY correlations observed from H-6 (δ_H 3.71) to H-5 (δ_H 2.39) and H-7 β (δ_H 1.48), from H-5 to H-4 (δ_H 2.57) and H-9 (δ_H 2.01) and from H-9

to H₂-1 (δ_{H} 4.18, 4.08) allowed for the establishment of the linear subfragment A. The connectivity between C-8 and Me-10 (subfragment B) was confirmed by the COSY correlation from the methyl signal at δ_{H} 1.03 to a methine signal at δ_{H} 1.79 for H-8.

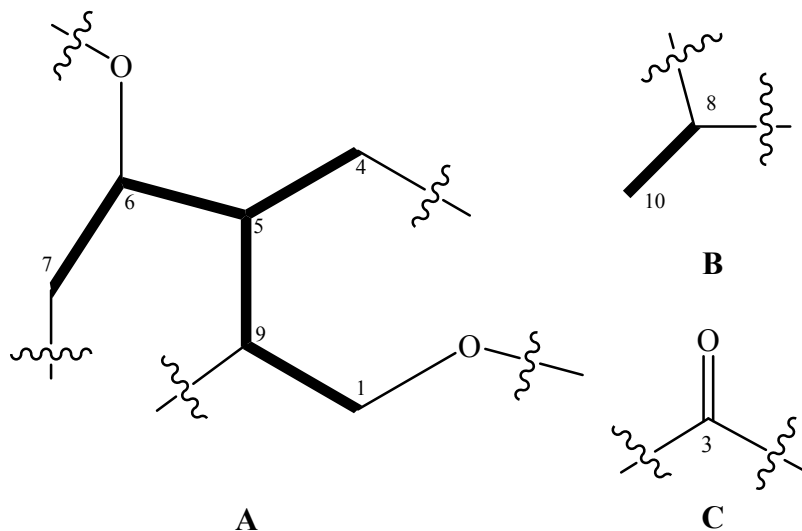


Figure 2.32 Subfragments (A – C) of cornolactone E (**64**).

Table 2.8 NMR Data of compound **64**. Measured at 400 MHz (¹H) and 100 MHz (¹³C) in CDCl₃. δ in ppm, J in Hz..

no.	δ_{H}	δ_{C}	HMBC (H→C)	NOESY
1a	4.18 (1H, dd, 11.6, 4.0)	68.6	C-3, C-5	H-1b, H-4
1b	4.08 (1H, dd, 12.0, 3.2)		C-3, C-5, C-8	H-1a
3		174.0		
4	2.57 (2H, d, 5.2)	32.6	C-3, C-5, C-9	H-6
5	2.39 (1H, m)	42.6	C-1, C-3, C-6, C-8	H-7 β
6	3.71 (1H, ddd, 10.2, 7.8, 5.5)	77.8	C-4, C-8, C-9	H-8
7 α	2.01 (1H, m)	42.6		
7 β	1.27 (1H, dt, 12.1, 11.2)		C-6, C-8, C-10	H-5, H-7 α , H-10
8	1.79 (1H, m)	33.1	C-1, C-10	H-1a, H-6
9	1.97 (1H, m)	43.2		
10	1.03 (3H, d, 6.4)	18.7	C-7, C-8, C-9	H-1a, H-8

Detailed analysis of the HMBC experiment allowed for those fragments to be fully connected and enabled assembly into the final planar structure of **64**. Accordingly, the diagnostic HMBC correlations (see **Figure 2.33**) between H-6 (δ_{H} 3.71) and carbons C-8 (δ_{C} 33.1) and C-9 (δ_{C} 43.2), between Me-10 (δ_{H} 1.03) and C-8 and C-9, and between

H₂-1 (δ_{H} 4.18, 4.08) and C-8 supported the linkage between spin systems A and B through C-8. This assignment was further supported by correlations from H-5 (δ_{H} 2.39) to C-1 (δ_{C} 68.6), C-6 (δ_{C} 77.8), C-8 and C-9. In addition, the significant HMBC correlations between the ester carbon observed at δ_{C} = 174.0 ppm (C-3) and H₂-1 and H-5 allowed for C-3 to be incorporated into the molecular structure creating a six-membered lactone ring system. Thus, the planar structure of **64** was established as shown in figure 2.5.

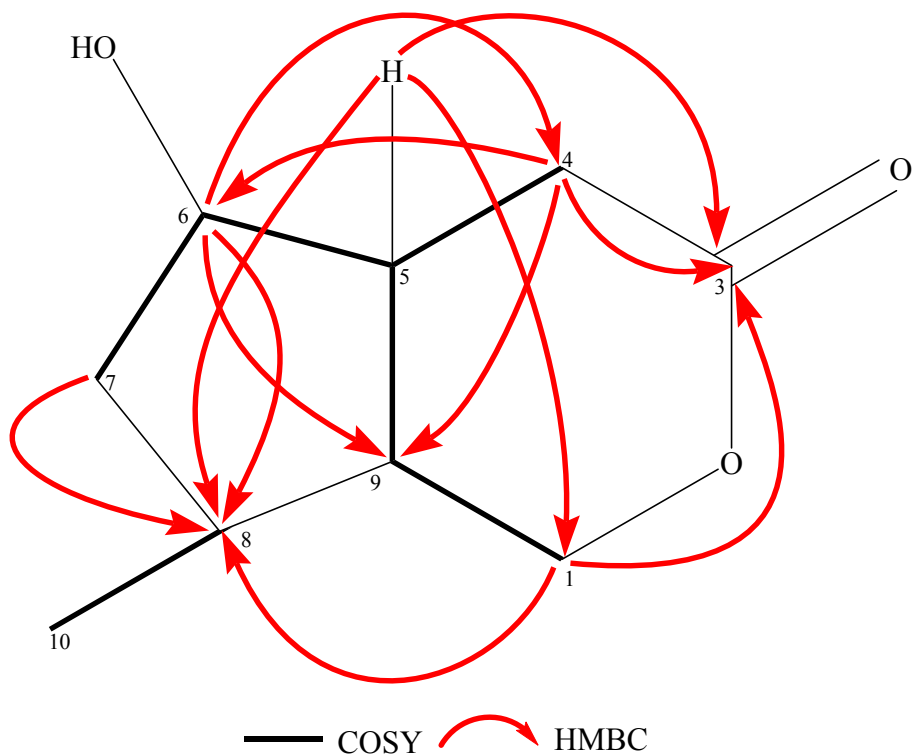


Figure 2.33 Key ¹H – ¹H COSY and HMBC correlations of cornolactone E (**64**).

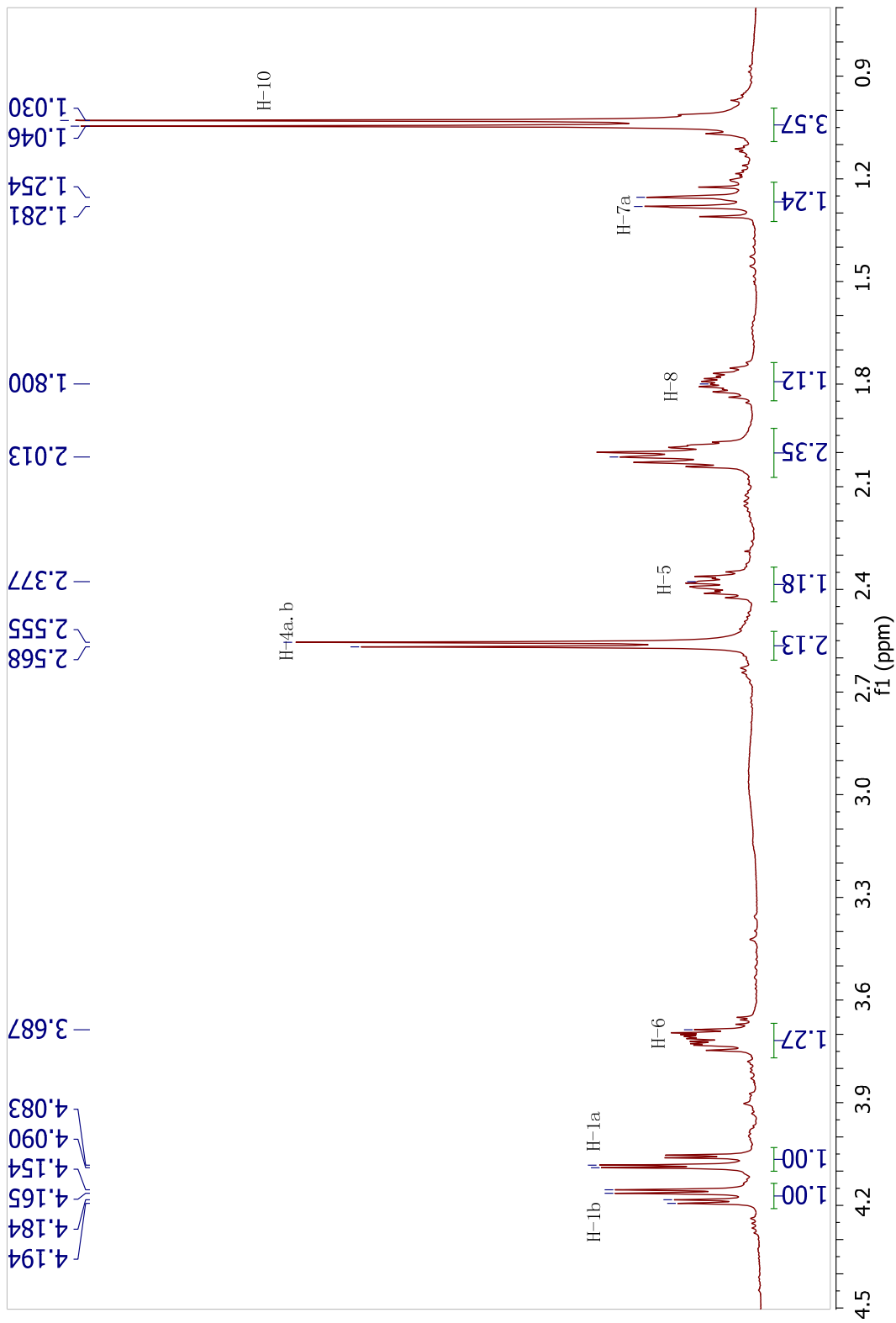


Figure 2.34 ^1H NMR spectrum of cornolactone E (**64**), 400 MHz, in CDCl_3

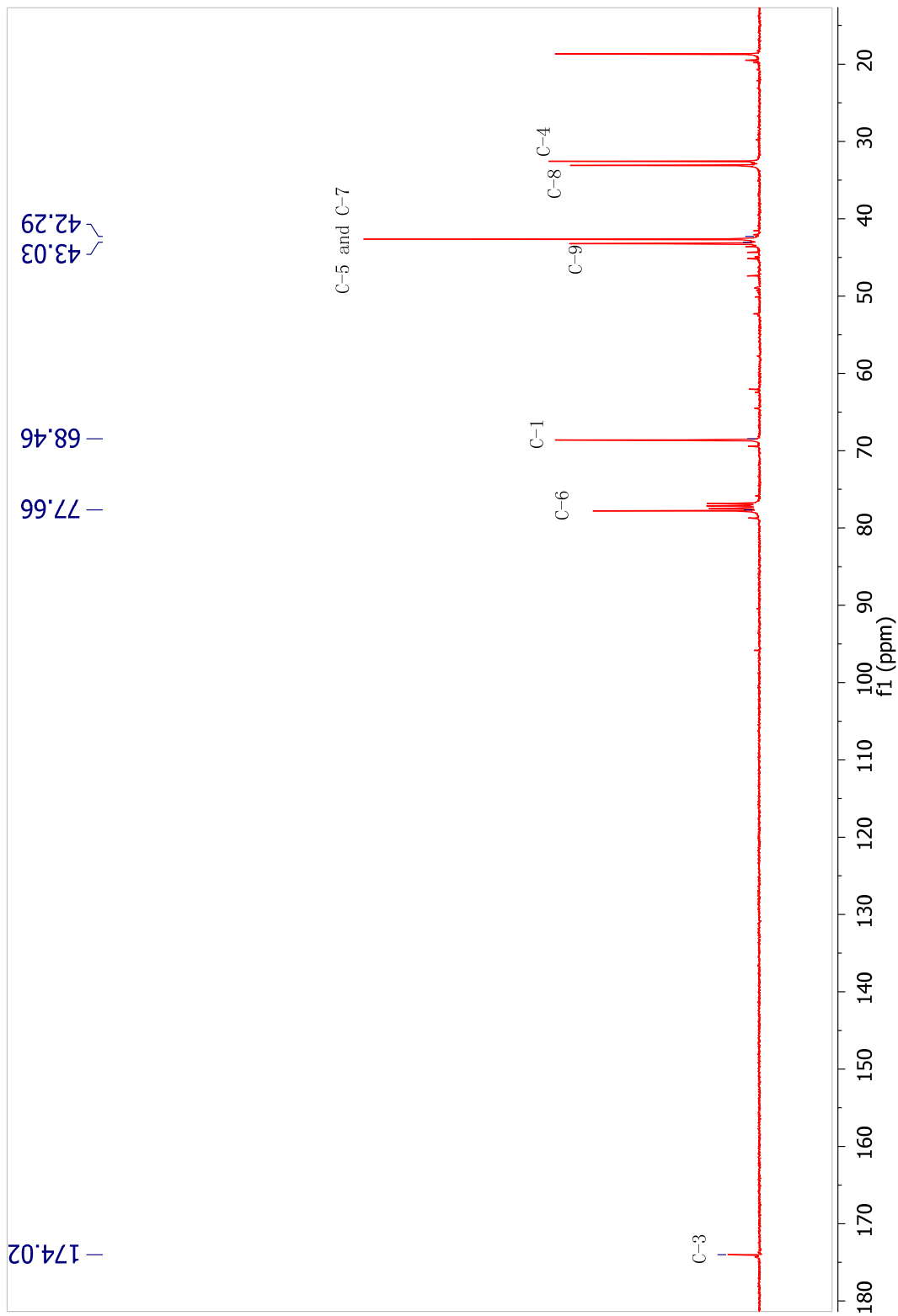


Figure 2.35 ^{13}C NMR spectrum of cornolactone E (**64**), 100 MHz, in CDCl_3

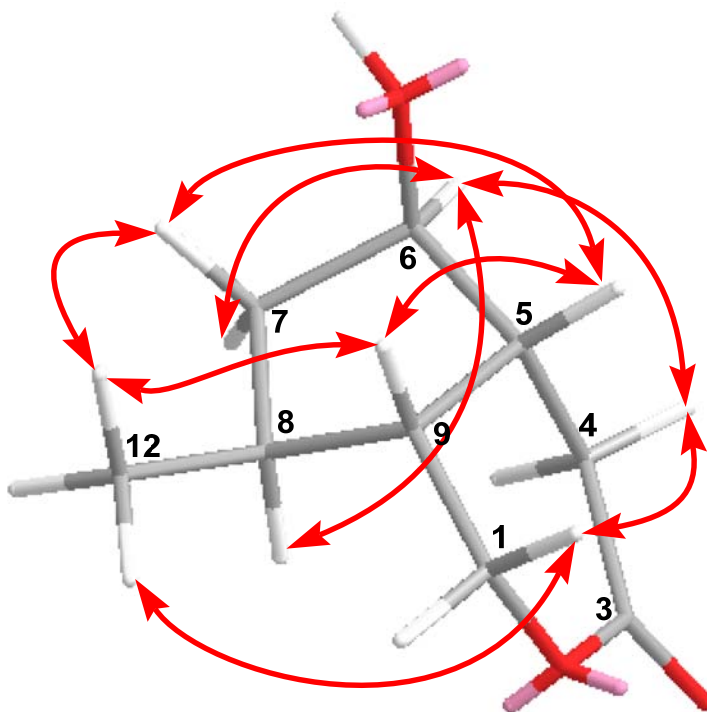


Figure 2.36 Key NOESY correlations of cornolactone E (**64**).

The relative configuration of compound **64** was assigned as shown in Figure 2.5 by interpretation of the 2D NOESY spectrum and the coupling patterns in the ^1H NMR spectrum. The nOe correlations as shown in **Figure 2.36** from H-6 to H-8, and from H-5 to H-7 β indicated that H-5, Me-10 and OH-6 were in β -orientation. This was further confirmed by the large coupling constants of $J_{\text{H-5, H-6}}$ 13.3 Hz, $J_{\text{H-6, H-7ax}}$ 12.1 Hz. And the small coupling constant ($^3J = 7.8$ Hz) between H-5 and H-9 confirmed the *cis*-fusion of the ring system. The similarity of proton–proton coupling constants and ^1H and ^{13}C chemical shifts together with a NOESY spectrum of **64** showed the same relative configuration as **63** at the four chiral centers. Thus the structure of cornolactone D (**64**) is therefore defined as *5R,6R,8S,9R*.

Cornoside B (**65**) was isolated as an orange gum. The HRESIMS of **65** showed an $[\text{M} - \text{H}]^-$ ion at m/z 366.1219 (calcd for $\text{C}_{17}\text{H}_{20}\text{NO}_8$ 366.1220), corresponding to the

molecular formula $C_{17}H_{21}NO_8$ with eight degrees of unsaturation. The IR spectrum showed characteristic absorptions for OH (3305 cm^{-1}), aromatic ring ($1650, 1453, 769\text{ cm}^{-1}$), carboxylic acid (1715 cm^{-1}) and C–O ($1081, 1017\text{ cm}^{-1}$) groups. In the case of the glycoside with the odd mass number at m/z 367 clearly indicating it was a nitrogenous compound. This was further confirmed by the TLC which gave an intense orange color with the Dragendorff reagent.

The ^{13}C NMR and gHSQC spectra revealed 17 carbon signals including five sp^2 methines, six sp^3 methines, two sp^3 methylenes and four quaternary carbons. Among them, the signals at δ_C 103.0, 76.1, 76.0, 73.3, 69.7 and 61.6 were characteristic for a β -glucopyranosyl moiety,⁴⁸ Which was further confirmed by the coupling constant ($J = 8.0$ Hz) of the anomeric proton and the signals observed for the other protons of the sugar moiety were in good agreement with data previously published for β -D-glucopyranosyl moiety.²⁷ The presence of a 3-substituted indole ring system suggested by: **a**) the four aromatic protons's coupling patterns at δ_H 7.49 (1H, d, $J = 7.6$ Hz, H-4), 7.25 (1H, d, $J = 6.7$ Hz, H-7), 7.03, 6.96 (each 1H, t, $J = 7.2$ Hz, H-6, H-5) and six aromatic carbons at δ_C 136.6 (C-8), 127.8 (C-9), 121.9 (C-6), 119.4 (C-5), 118.4 (C-4) and 111.6 (C-7); **b**) a broad signal at δ_H 8.11 (s) for NH measured in CD_3OD , which disappeared in $CDCl_3$ and the signals at δ_H 7.06 (H-2, s, in $CDCl_3$), δ_C 123.8 (C-2); **c**) the absence of a high field aromatic signal near δ_H 6.40 indicated that the indole nucleus was substituted at position 3.⁵² The ^1H , ^{13}C NMR, HSQC and HMBC spectra of **65** also showed: one oxygenated methine [δ_H 4.28 (1H, dd, $J = 7.6, 4.8$ Hz, H-11), δ_C 79.0 (C-11)]; one deoxymethylene

carbon [δ_{H} 3.12 (2H, dd, $J = 15.0, 7.8$ Hz, H-10), δ_{C} 28.8 (C-10)]; one downfield quaternary carbon at δ_{C} 174.4 (C-12, in **Table 2.9**).

Table 2.9 NMR data of compound **65**, measured at 400 MHz (^1H) and 100 MHz (^{13}C) in CDCl_3 , δ in ppm, J in Hz..

no.	δ_{C}	δ_{H}	COSY	HMBC(H \rightarrow C)
1		8.11 (1H, s) ^a		
2	123.8	7.06 (1H, s)		C-3, C-8, C-9
3	109.1			
4	118.4	7.49 (1H, d, 7.6)	H-5	C-8, C-6, C-3
5	119.4	6.96 (1H, t, 7.8)	H-4, H-6	C-7, C-9
6	121.9	7.03 (1H, t, 7.8)	H-5, H-7	C-4, C-8
7	111.6	7.25 (1H, d, 6.7)	H-6	C-5, C-9
8	136.6			
9	127.8			
10	28.8	3.12 (2H, dd, 15.0, 7.8)	H-11	C-12, C-9, C-2, C-3, C-11
11	79.0	4.28 (1H, dd, 7.6, 4.8)	H-10	C-12, C-3, C-1', C-10
12	174.4			
1'	102.9	4.14 (1H, d, 8.0)	H-2'	C-11
2'	73.3	3.18 (1H, overlapped)	H-1'	
3'	76.1	3.19 (1H, overlapped)		
4'	69.7	3.24 (1H, m)	H-5'	
5'	76.1	3.04 (1H, m)	H-4', H-6'b	
6'a	61.6	3.60 (1H, dd, 12.0, 2.8)		
6'b		3.54 (1H, dd, 12.0, 5.2)	H-4',	

^aMeasured in CD_3OD

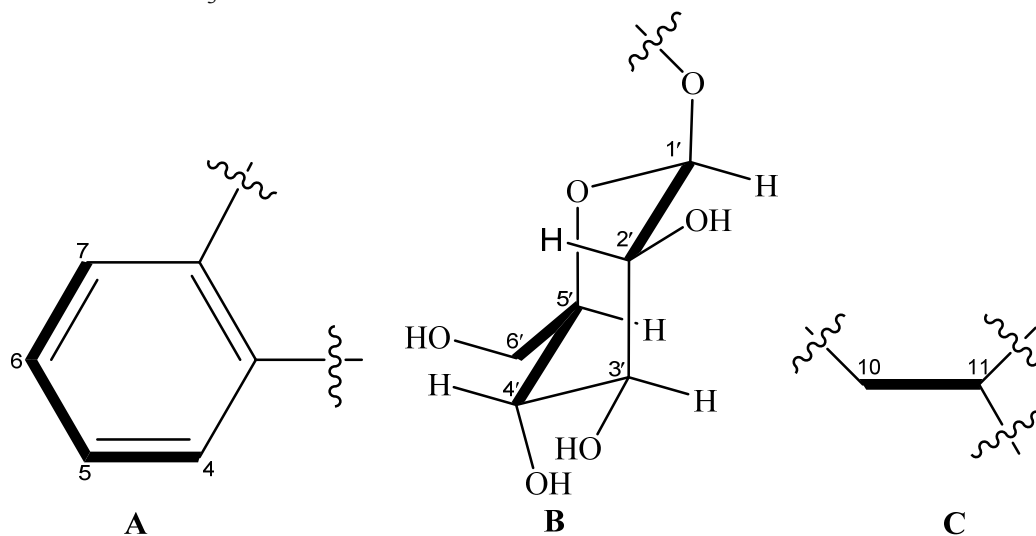


Figure 2.37 Isolated ^1H spin systems (A – C) of cornoside B (**65**).

Interpretation of the $^1\text{H} - ^1\text{H}$ COSY spectrum coupled with the gHSQC spectrum indicated the presence of three isolated spin systems as drawn with bold lines in **Figure 2.37**: **A**) the ortho-disubstituted benzene ring was confirmed by the COSY correlations from H-5 (δ_{H} 6.96) to H-4 (δ_{H} 7.49) and H-6 (δ_{H} 7.03), from H-6 to H-7 (δ_{H} 7.25); **B**) the β -glucopyranosyl moiety was indicated by COSY correlations from H-1' (δ_{H} 4.14) to H-2' (δ_{H} 3.18), from H-6'a (δ_{H} 3.60) to H-5' (δ_{H} 3.04) and from H-5' to H-4' (δ_{H} 3.24); and **C**) H-10 (δ_{H} 3.12) to H-11 (δ_{H} 4.28).

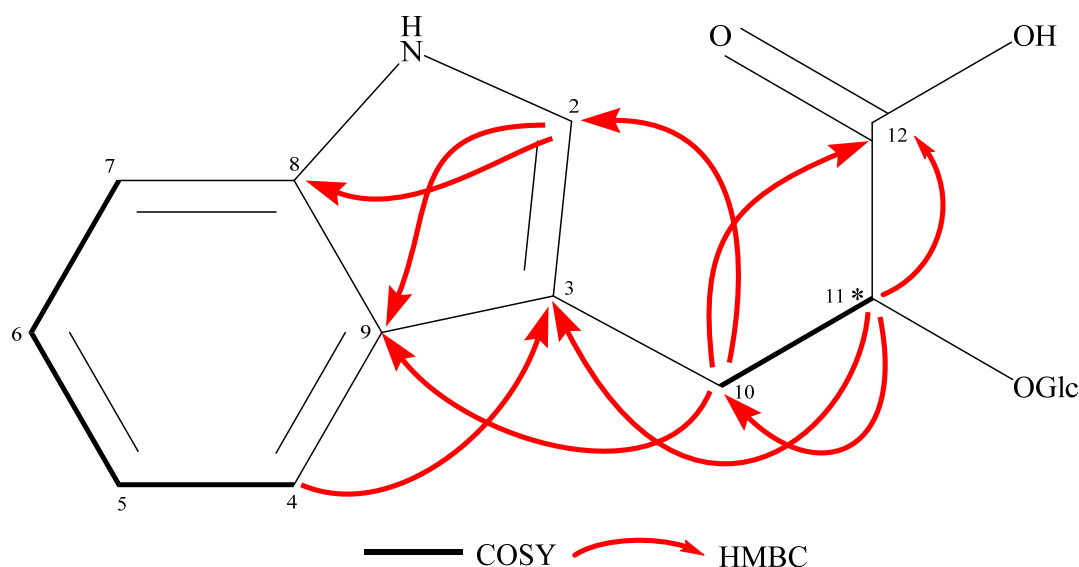


Figure 2.38 Key $^1\text{H} - ^1\text{H}$ COSY and HMBC correlations of cornoside B (**65**).

Further detailed HMBC correlations (in **Figure 2.38**) analysis allowed the full connection of these three fragments and established the gross structure of **65** to be indole-3-lactic acid glucoside bearing a β -D-glucopyranosyl moiety at C-11. The distinct three bonds HMBC correlations from the aromatic proton at δ_{H} 7.49 (H-4) to C-6 (δ_{C} 121.9), C-8 (δ_{C} 136.6) and C-3 (δ_{C} 109.1) was in agreement with those from H-7 (δ_{H} 7.25) to C-9 (δ_{C} 127.8) and C-5 (δ_{C} 119.4), as well as the correlations between H-2 (δ_{H} 7.06) and C-8,

C-9 and C-3 leading to the formation of the indole ring system. In addition, the significant three bond HMBC correlations between H-10 (δ_{H} 3.12) and C-2 (δ_{C} 123.8), C-9, C-12 (δ_{C} 174.4) resulted in the linkage between fragment **C** and **A** through the quaternary carbon C-3 and the placement of a carboxylic acid group at the C-11 (δ_{C} 79.0) position. This was further confirmed by the HMBC correlations between H-11 (δ_{H} 4.28) and C-3 and C-12. Finally, the clear HMBC correlations from H-1' (δ_{H} 4.14) to C-11 and from H-11 to C-1' (δ_{C} 103.2) confirmed the glucosylation at C-11 and established the planar structure of **65** as depicted. The absolute configuration of C-11 was not successfully determined for the limited quantity of sample.

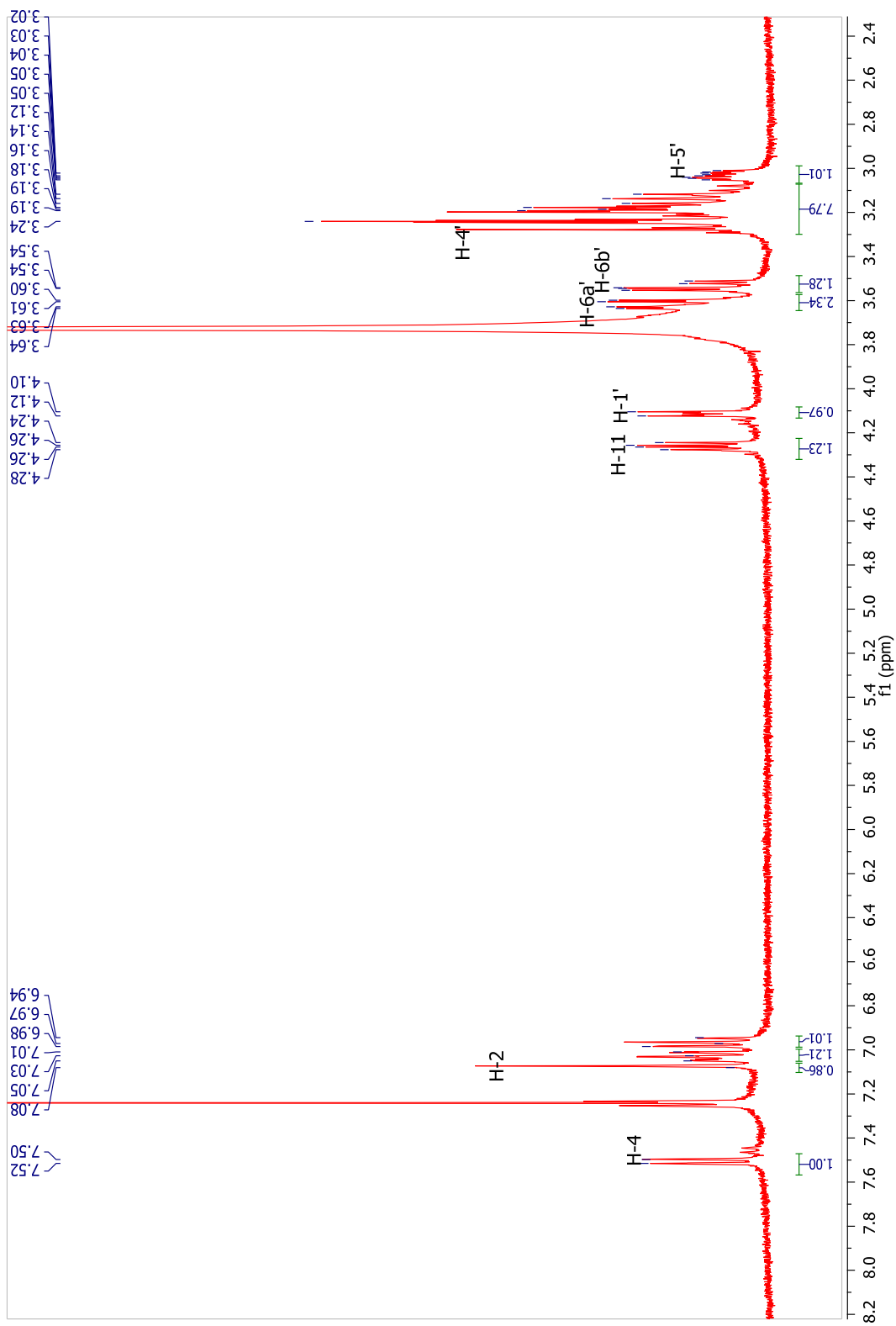


Figure 2.39 ^1H NMR spectrum of cornoside B (**65**), 400 MHz, in CDCl_3 and CD_3OD

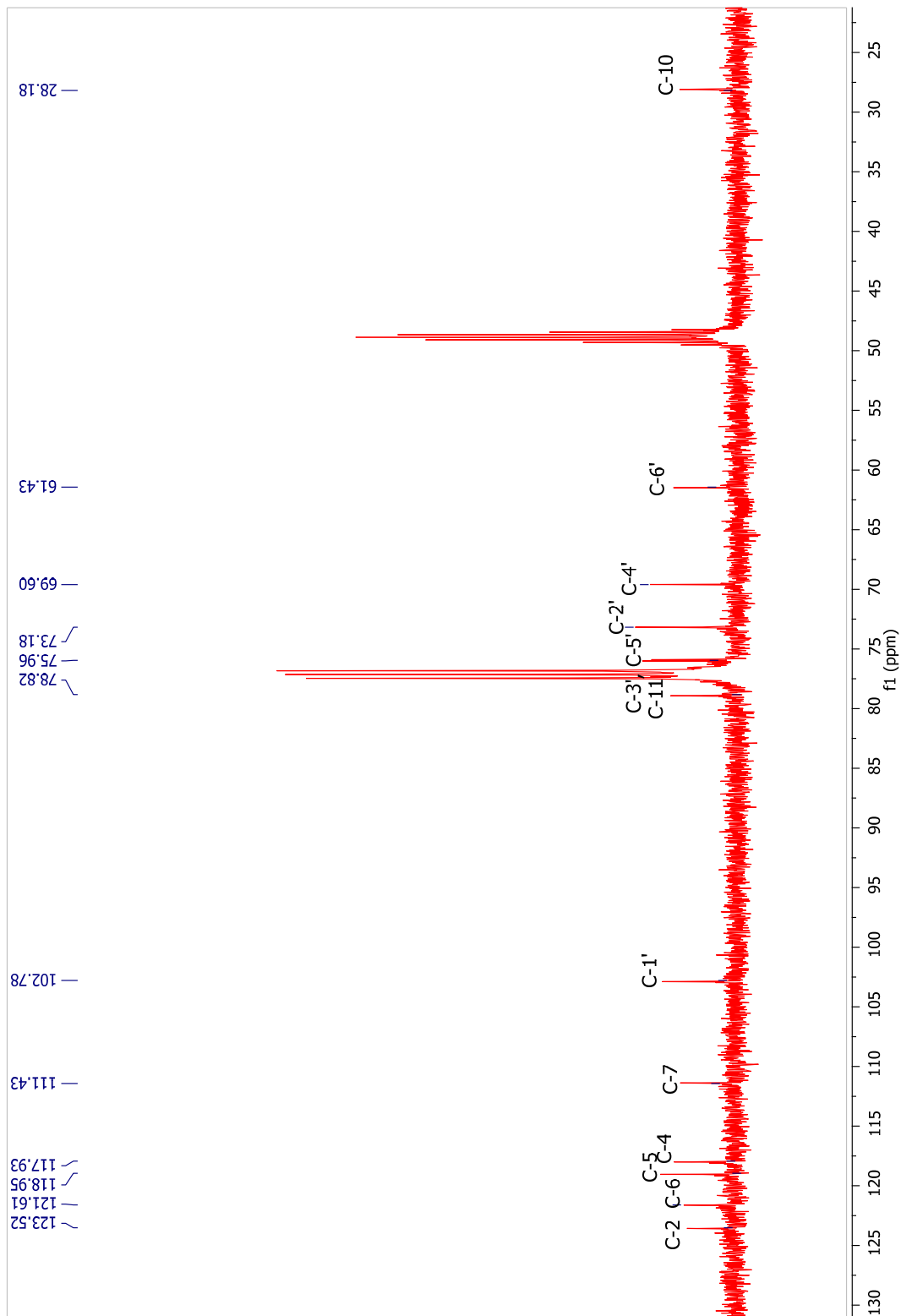


Figure 2.40 ^{13}C NMR spectrum of cornoside B (65), 100 MHz, in CDCl_3 and CD_3OD

2.3 PPAR γ and LXR agonistic activities and cytotoxicity

Compounds **59**, **60**, **63**, **64** and three known compounds cornin (**4**), dihydrocornin (**10**), cornalternoside (**58**) were selected to evaluate for agonistic activity for PPAR- γ and cytotoxicity against the MCF-7 and MDA-MB-231 (breast cancer cell lines). Unfortunately, all the compounds revealed no agonistic activity for PPAR- γ and no cytotoxicity for both MCF-7 and MDA-MB-231 cells lines, except compound **64** exhibiting slight activity at 100 μM against MDA-MB-231, but no EC_{50} could be reached. However, previously in Dr. Mark T. Hamann's laboratory at the University of Mississippi cornoside A (**59**) and cornin (**4**) were tested for their agonistic activity for Liver X receptors (LXR). The results indicated that cornoside A exhibited potent LXR agonistic activity with the EC_{50} value of 0.9 μM . Cornin (**4**) showed moderate LXR agonistic activity with the EC_{50} value of 9.8 μM .

2.4 Conclusions

In a continuing exploration of natural products for nuclear receptor activators as leads with potential anti-diabetic drug candidates from genus *Coruns*, a proton NMR-guided fractionation of the ethanol extract of *Cornus controversa* leaves resulted in the isolation of seven new compounds, including one new iridoid glucoside, cornoside A (**59**), and five new iridoid aglycones, cornolactones A – E (**60** – **64**), and an indole-3-lactic acid glucoside, cornoside B (**65**), together with 10 known compounds. Cornoside A (**59**) is one of a small number of C_{10} iridoid glucosides where the δ -lactone is ring-opened between the C-1 and O-2 position and contains a γ -lactone linkage between C-6 and C-11. Others reported include gelsemiol 3-*O*- β -d-glucoside,⁴⁹ gelsemiol 6'-*trans*-caffeoyl-1-

glucoside⁵³ and verbenabraside A and B.⁵⁴ Cornolactone B (**61**) is the first natural *cis*-fused tricyclic dilactone iridoid containing both a five- and six- membered lactone ring. Interestingly, cornolactone D (**63**) and E (**64**) have opposite configuration at C-6 compared to that of compounds **59–61**. This suggests that rather than cleavage of the γ -lactone in **61** by methanolysis at C-11, to give the C-6 epimer of **63** (*6-epi-63*) with retention of configuration, an alternative biosynthetic pathway is necessary (**Figure 2.41**). A possible pathway leading to inversion of configuration at C-6 could occur through the S_N2 hydrolysis of **61** at C-6, followed by either methylation to give cornolactone D (**63**) or decarboxylation to give cornolactone E (**64**). Considering the broad fascinating bioactivities of iridoids and the pharmaceutical values of genus *Cornus* used as Chinese traditional medicine to treat diabetes, further study and more attention are needed from the related scientific communities.

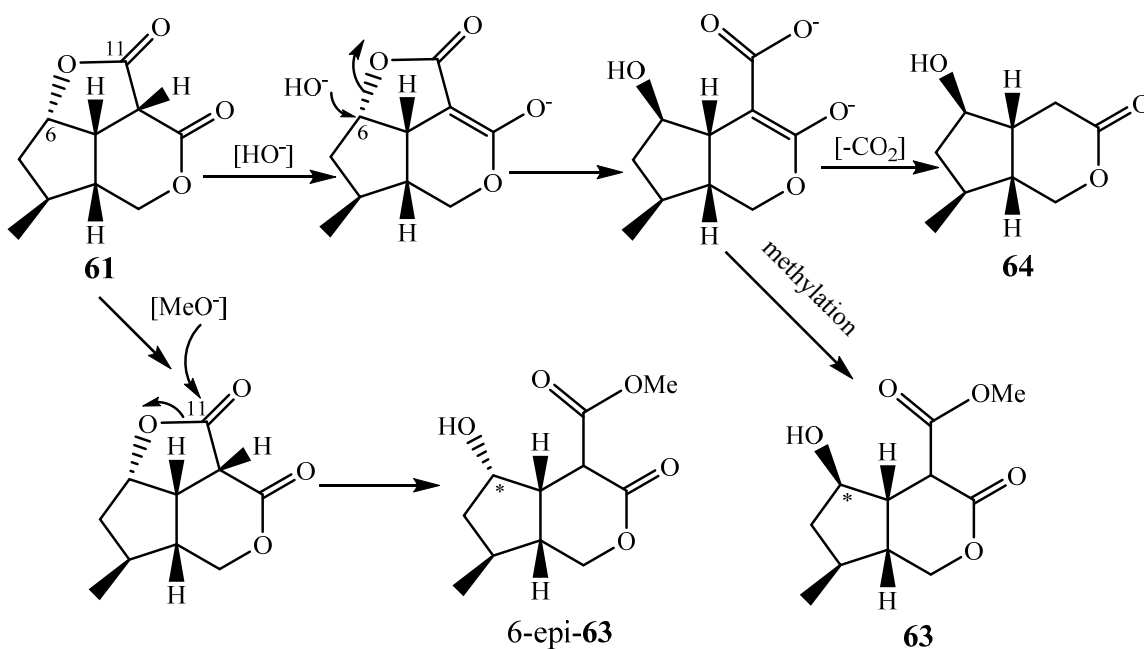


Figure 2.41. Possible biosynthetic route to inversion of configuration at C-6 in **63** and **64**.

3. DELPHATISINE D AND CHRYSOTRICHUMINES A – B, THREE NEW DITERPENOID ALKALOIDS FROM *DELPHINIUM CHRYSOTRICHUM*

3.1 Background

The genus *Delphinium*, like the genus *Aconium* and *Consolida*, is a rich source of diterpenoid alkaloids. They exhibit complex structures and a broad range of bioactivities including anti-inflammatory, analgesics, anti-arrhythmic, curariform, arrhythmogenic, hypotensive, neurotropic, local anesthetic, spasmolytic, and psychotropic. Diterpenoid alkaloids have attracted considerable interest of medicinal chemists for decades.⁵⁵⁻⁵⁸ Crude preparations from *Delphinium* plants have been widely used as cardiotonics, febrifuges, sedatives, and anodynes in folklore and traditional medicine.⁵⁷ There are about 350 species of *Delphinium* distributed mainly in the northern hemisphere, of which 173 are endemic to mainland China.⁵⁹

Delphinium chrysotrichum Finet et Gagnepain, mainly distributed in northwest of Sichuan and the eastern district of the Tibetan region of mainland China, has been used in Tibetan folk medicine for the treatments of rheumatism and neuralgia for a long time.^{59,60} Our previous chemical investigation on this plant has resulted in the isolation of three diterpene alkaloids delphatisine A – C (**71–73**)^{61,62} together with delpheline (**74**),⁶² delbrunine (**75**),⁶³ and delectinine (**76**)⁶⁴ as shown in **Figure 3.1**. As part of an ongoing phytochemical investigation of the chemistry and anticancer activities of diterpenoid alkaloids from *Aconitum* and *Delphinium* plants, we have investigated the whole plant of

D. chrysotrichum, which led to the isolation of three novel compounds, including a new C₂₀-diterpenoid alkaloid, delphatisine D (**77**), and two new C₁₉-diterpenoid alkaloids, chrysotrichumines A and B (**78** and **79**), as well as 11 known compounds: isodelpheline (**80**),⁶⁰ delphatisine A (**81**),⁶¹ delpheline (**74**),⁶² 3 β ,6 α -dlphydroxysclareollda (**82**),⁶⁵ lycoctonine (**83**),⁶⁶ davidisine B (**84**),⁶⁷ delsemine A (**85**),⁶⁸ delavaine A (**86**),⁶⁹ delcorine (**87**),⁷⁰ delbrusine (**88**)⁶³ and sharwuphinine A (**89**),⁷¹ as shown in **Figure 3.2**. Delphatisine D (**77**) is a rare atisine-type alkaloid from genus *Delphinium* and is the C-15 epimer of spiramine C (**90**) which bears an internal carbinolamine ether linkage (N–C–O–C) between C-7 and C-20. Chrysotrichumine A (**78**) is a rare natural C₁₉-diterpenoid alkaloid possessing a nitrone group between C-17 and C-19. We present herein the isolation and structural elucidation of these new diterpenoid alkaloids.

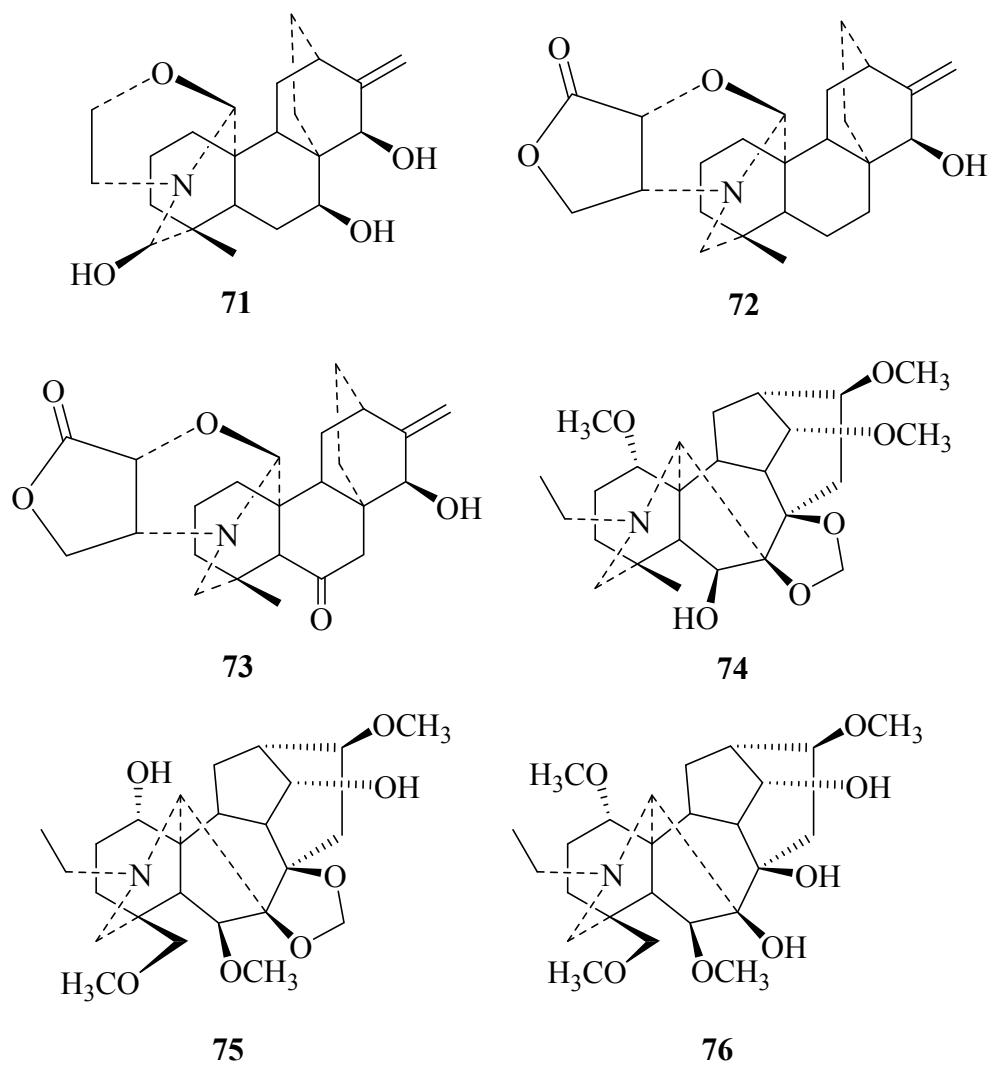


Figure 3.1 Compounds previously isolated from *Delphinium chrysotrichum*.

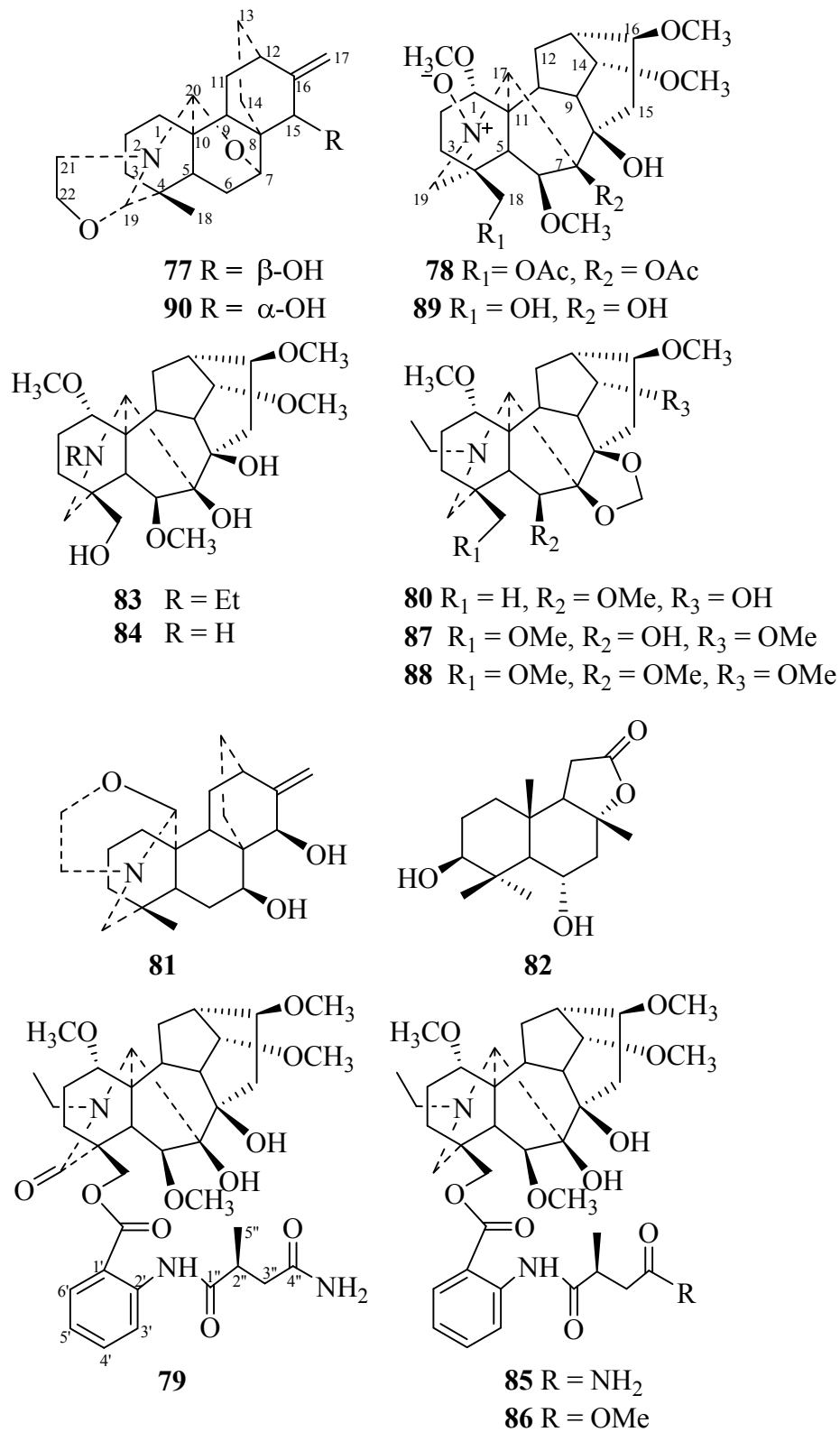


Figure 3.2 Chemical structures isolated from *Delphinium chrysotrichum*.

3.2 Structure Elucidation of Delphatisine D, Chrysotrichumines A and B

A 90% ethanol extract of the dried whole plants of *D. chrysotrichum* (10 kg) was extracted with CHCl_3 at pH 10 to give 210 g of a crude alkaloids fraction. This residue was sequentially separated on silica gel eluted by a gradient of petroleum ether (PE)-acetone-diethylamine (100:10:2, 80:20:5, 60:40:5, 50:50:5, 40:60:5, 20:80:5 and 10:90:5) to afford seven fractions (A – G). Bioassay-guided fractionation of fractions F and G were further chromatographed over a silica gel column and then a series of HPLC separations (prep. and semi-prep.) with columns supported on C18, C8 and PRP-1 to yield compounds (**77** – **79**) and other known compounds (see **Figure 3.3** and **3.4**).

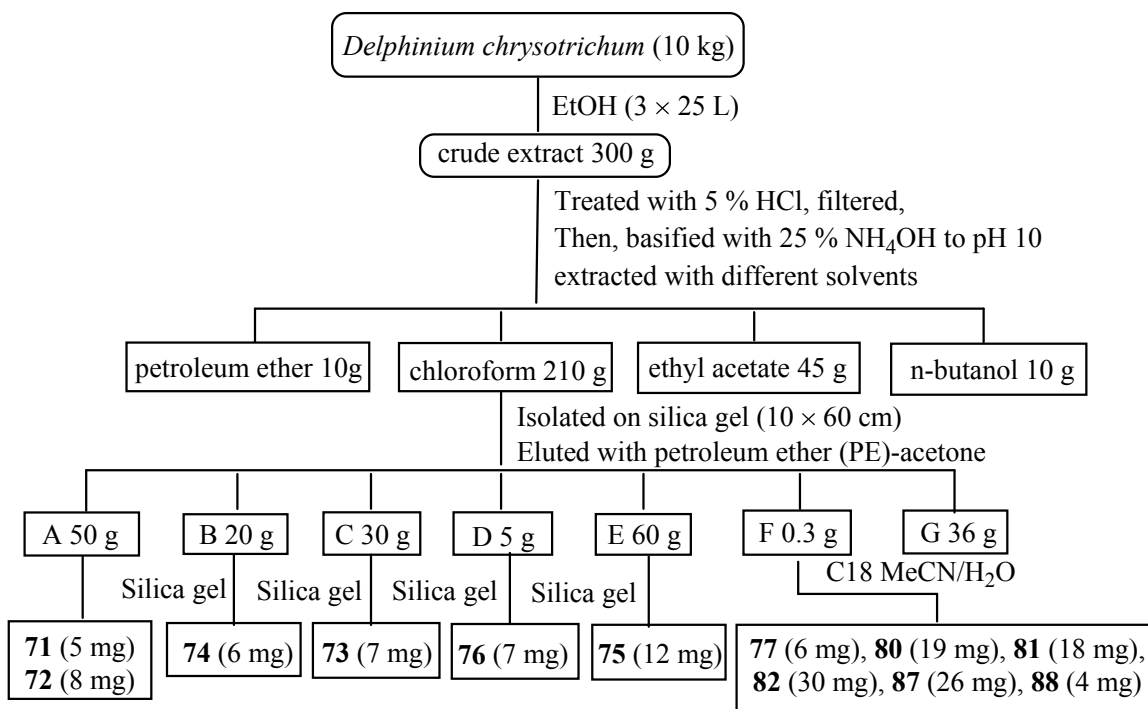


Figure 3.3 Isolation scheme for Delphatisine D (**77**).

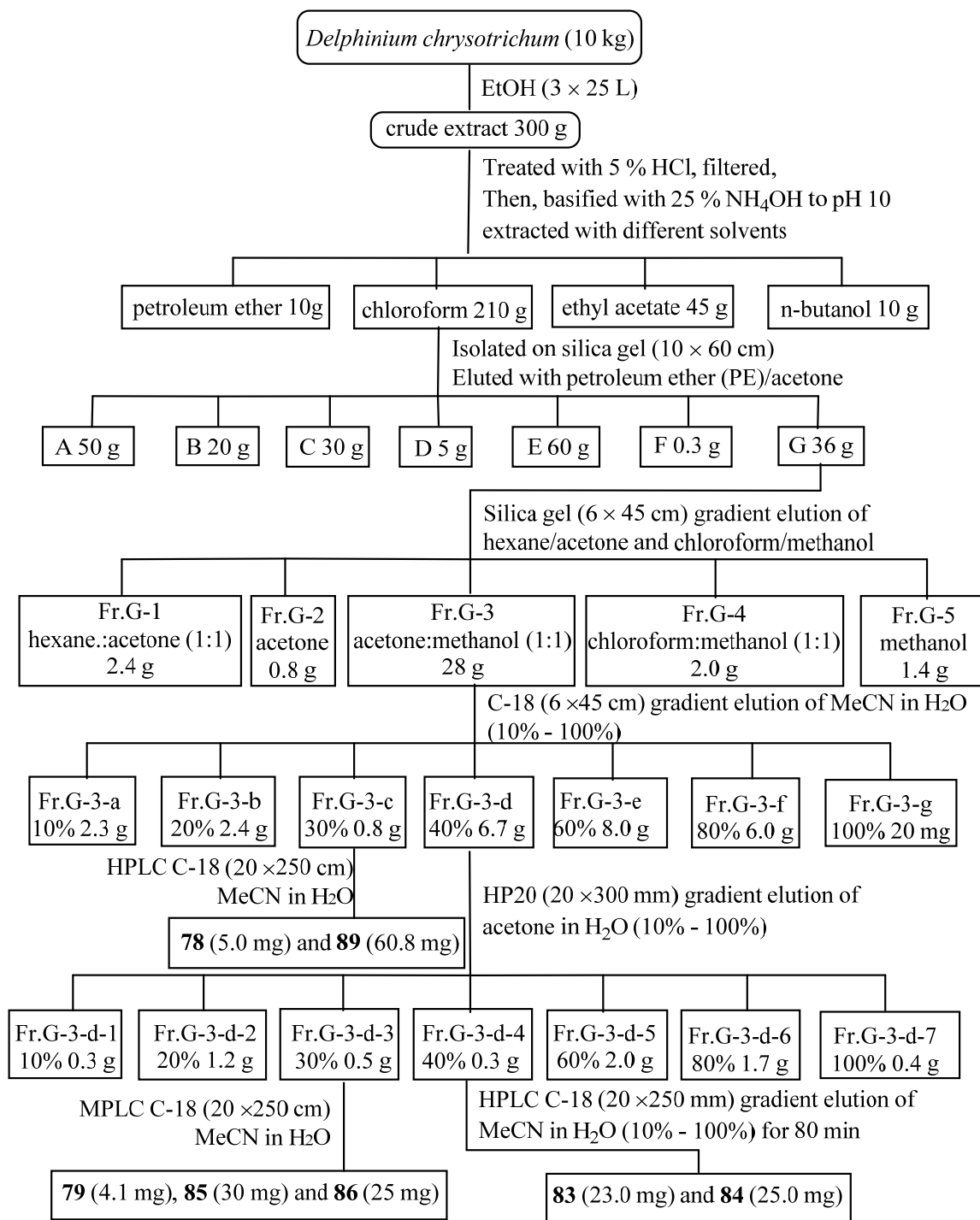


Figure 3.4 Isolation scheme for compounds **78** and **79**.

Delphatisine D (**77**) was obtained as a white amorphous powder, and the molecular formula $C_{22}H_{31}NO_3$ was suggested on the basis of HRESIMS for the $[M + H]^+$ at m/z 358.2377 (calcd 358.2377), which indicated 8 degrees of unsaturation. The IR spectrum showed characteristic absorptions for hydroxyl (3443 cm^{-1}), exomethylene ($1640, 911\text{ cm}^{-1}$) and simple ether (1031 cm^{-1}) groups. The ^{13}C NMR and DEPT revealed 22 carbon signals including one sp^3 methyl, nine sp^3 and one sp^2 methylenes, seven sp^3 methines and four quaternary carbons. The 1H , ^{13}C NMR (**Figures 3.7** and **3.8**) and HSQC (Appendix 2.2) spectra of **77** indicated signals at δ_H 1.05 (3H, s, H-18), δ_C 23.1 for a tertiary methyl group; four methine signals at δ_H 4.61 (1H, s, H-20), 4.15 (1H, s, H-15), 3.90 (1H, s, H-19), 3.51 (1H, d, $J = 4.4\text{ Hz}$, H-7), δ_C 86.3, 75.6, 95.6, 71.6, respectively; an oxygenated methylene signal at δ_H 3.68 (1H, dd, $J = 14.4, 8.4\text{ Hz}$, H-22 α), 3.45 (1H, ddd, $J = 9.2, 6.4, 2.8\text{ Hz}$, H-22 β), δ_C 63.3, one nitrogen-substituted methylene δ_H 3.34 (1H, ddd, $J = 10.8, 7.6, 2.4\text{ Hz}$, H-21 α), 3.21 (1H, dt, $J = 11.6, 8.8\text{ Hz}$, H-21 β), δ_C 51.3, and two broad singlets at δ_H 5.09, 4.98, each 1H; δ_C 157.4, 108.2 (see **Table 3.2**) indicated the presence of an exocyclic methylene group.

Interpretation of the $^1H - ^1H$ COSY spectrum coupled with the g-HSQC and HMBC spectra led to the assignment of six isolated spin systems (**A – F**, in **Figure 3.6**). The connectivity of the linear fragment **A** was determined through COSY correlations observed between the methylene signals at δ_H 2.02 (H-2 α) to H-1 α (δ_H 1.55) and H-3 α (δ_H 1.40). HMBC correlations from H-2 α to C-1 (δ_C 30.1) and C-3 (δ_C 41.0) and from H-1 α to C-2 and C-3 confirmed the connectivity of C-1 to C-3 and the establishment of substructure **A**.

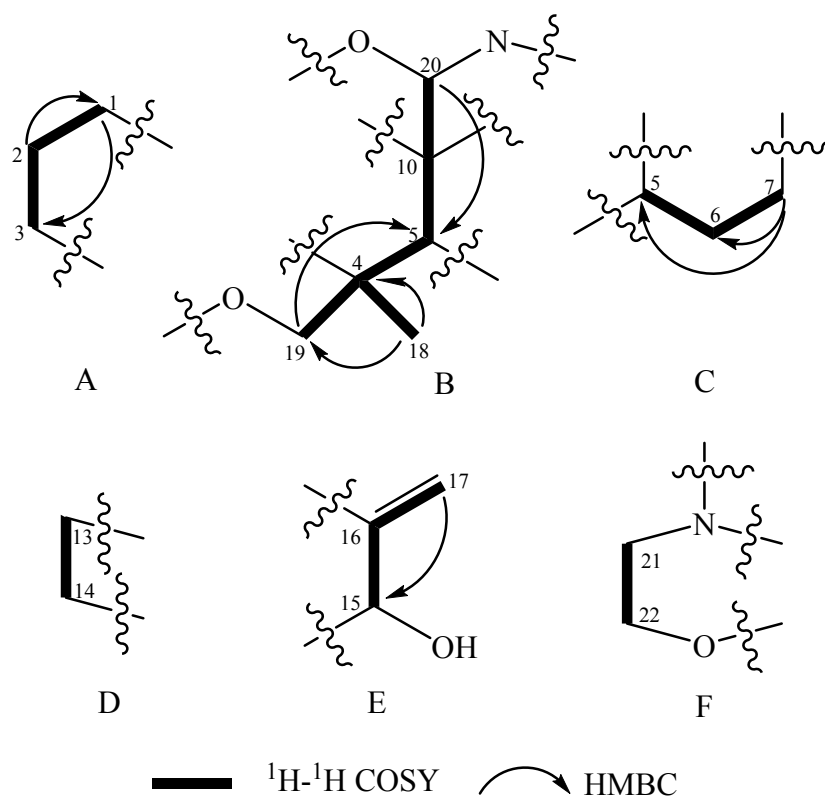


Figure 3.5 Substructures (**A – F**) of delphatisine D (**77**).

A linear fragment comprised of two methines one substituted by oxygen and another by nitrogen (C-19, δ_C 95.6 and C-20, δ_C 86.3), two quaternary carbons (C-4 and C-10), a methine and a tertiary methyl group (fragment **B**) was determined through COSY correlations. The obviously long range W-COSY correlations observed from the methine, H-5 (δ_H 1.12) to both methines H-19 (δ_H 3.90) and H-20 (δ_H 4.61) as well as H-19 to Me-18 (δ_H 1.05) allowed the establishment of the linear spin system of **B**. In addition, three bond HMBC correlations between C-5 and both H-19 and H-20 allowed the connectivity between C-10–C-5–C-4, which provided further evidence for the existence of the linear substructure **B**. HMBC correlations between a tertiary methyl resonance (δ_H 1.04, s, H-18) and carbons C-3, C-4, and C-19 served to place it on C-4.

Substructure **C** was established by COSY correlations observed from a methylene signal at δ_{H} 2.41 (H-6 α) to H-5 (δ_{H} 1.12) and H-7 (δ_{H} 3.51), and it was further confirmed by the HMBC correlations between H-6 α and C-7 and between H-7 and C-5. The COSY correlation between a methylene signal at (δ_{H} 2.10) of H-14 and the signal at δ_{H} 1.58 (H-13) along with comparison of the chemical shifts with those isoatisine (**91**)⁷² allowed for the establishment of the fragment **D** (see **Table 3.1**). The connectivity of the substructure **E** was readily determined through long range COSY correlations observed between both singlets of the exocyclic methylene group (H₂-17) at δ_{H} 5.09, 4.98 and H-15 (δ_{H} 4.14) along with the HMBC correlations from H₂-17 to C-15 (δ_{C} 75.6). The substructure of **F** was established through COSY correlations observed between the methylene signal of H-22 α at δ_{H} 3.66 to H₂-21 (δ_{H} 3.32, 3.21).

Table 3.1 Comparison of ¹³C NMR data of compounds **77**^a and **90**^b.

compounds	77	90	77	90
position	δ_{C}	δ_{C}	position	δ_{C}
1	30.1	40.8	12	37.0
2	26.5	23.0	13	25.4
3	41.0	29.9	14	26.7
4	35.6	35.4	15	75.6
5	43.1	45.5	16	157.4
6	20.6	25.2	17	108.2
7	71.6	69.0	18	23.1
8	35.1	41.5	19	95.6
9	40.8	43.1	20	86.3
10	42.0	34.1	21	51.3
11	27.1	23.5	22	63.3

^aMeasured in CDCl₃; ^bMeasured in C₆D₆, δ in ppm.

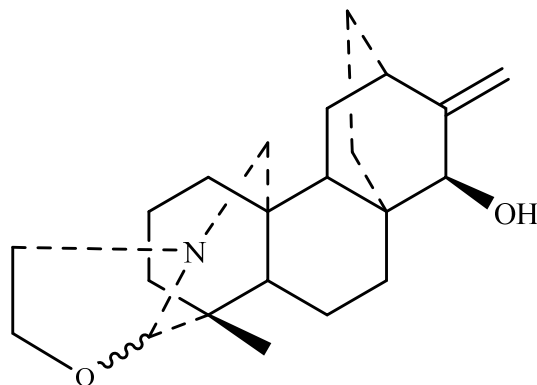


Figure 3.6 The chemical structure of isoatisine (**91**)

Table 3.2 NMR Data of compound **77**. Measured in CDCl₃ at 400 MHz (¹H) and 100 MHz (¹³C), δ in ppm, *J* in Hz.

no.	δ_H	δ_C	HMBC (H→C)	NOESY
1 α	1.55 (1H, overlapped)	30.1	C-20	H-20
1 β	1.09 (1H, overlapped)			
2 α	2.02 (1H, m)	20.6	C-1, C-3	H-3 α , H-19
2 β	1.33 (1H, overlapped)			
3 α	1.40 (1H, m)	41.0	C-1, C-2, C-5, C-18, C-19	H-19
3 β	1.10 (1H, overlapped)			
4		35.7		
5	1.12 (1H, m)	43.1	C-7, C-9, C-19, C-20	H-9
6 α	2.12 (1H, t, 12.4)	26.5	C-4, C-5	H-7
6 β	2.41 (1H, dt, 13.6, 4.4)		C-7, C-8, C-10	H-7
7	3.51 (1H, d, 4.4)	71.6	C-5, C-9, C-15, C-20	H-7
8		42.0		
9	1.46 (1H, dd, 12.0, 8.0)	40.8	C-5, C-15, C-20	H-5
10		35.1		
11a	1.58 (1H, overlapped)	27.0		
11b	1.30 (1H, overlapped)			
12	2.36 (1H, dt, 4.3, 8.6)	37.0	C-9, C-14, C-15, C-17	H-17b
13a	1.58 (1H, overlapped)	25.4		
13b	1.33 (1H, overlapped)			
14a	2.10 (1H, m)	26.7	C-15	
14b	1.32 (1H, overlapped)			
15	4.14 (1H, br s)	75.6	C-9, C-14, C-16	H-7, H-17a
16		157.4		
17a	5.09 (1H, br s)	108.2	C-12, C-15, C-16	H-15
17b	4.98 (1H, br s)		C-12, C-15	H-12
18	1.08 (3H, s)	22.8	C-3, C-4, C-19	
19	3.90 (1H, s)	95.6	C-3, C-5, C-20	H-2 α , H-3 α , H-21 β , H-22 β
20	4.61 (1H, s)	86.3	C-1, C-5, C-7, C-9, C-10, C-19, C-21	H-1 α , H-14 α , H-21 α
21 α	3.34 (1H, ddd, 2.7, 7.8, 11.0)	51.3	C-20	H-21 β
21 β	3.21 (1H, dt, 8.6, 11.4)		C-19, C-20	H-19, H-21 α
22 α	3.68 (1H, dd, 7.0, 14.1)	63.3	C-19, C-21	H-21 α , H-22 β
22 β	3.45 (1H, ddd, 3.1, 6.3, 9.0)			H-19, H-22 α

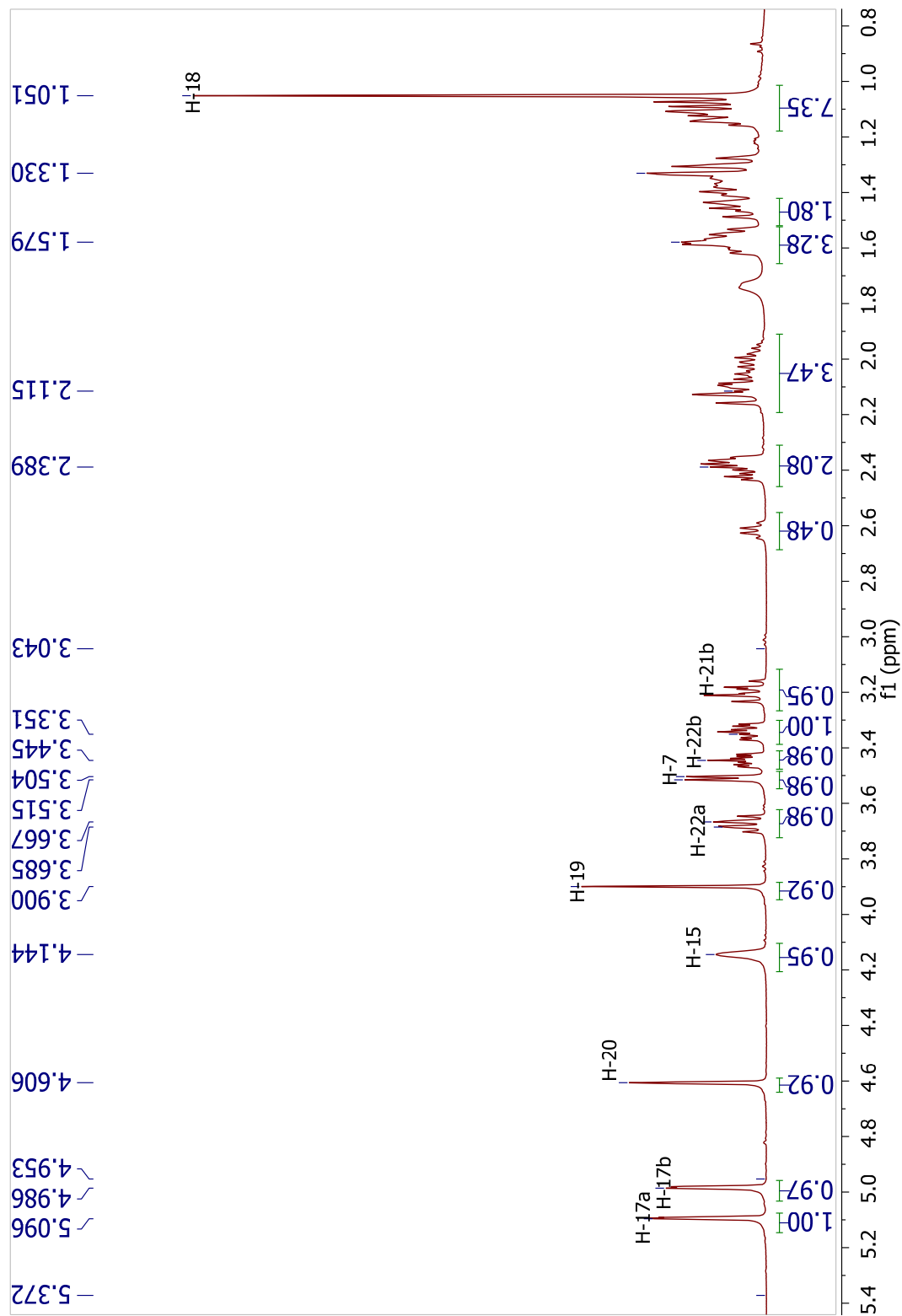


Figure 3.7 ^1H NMR spectrum of delphatisine D (77), 400 MHz, in CDCl_3

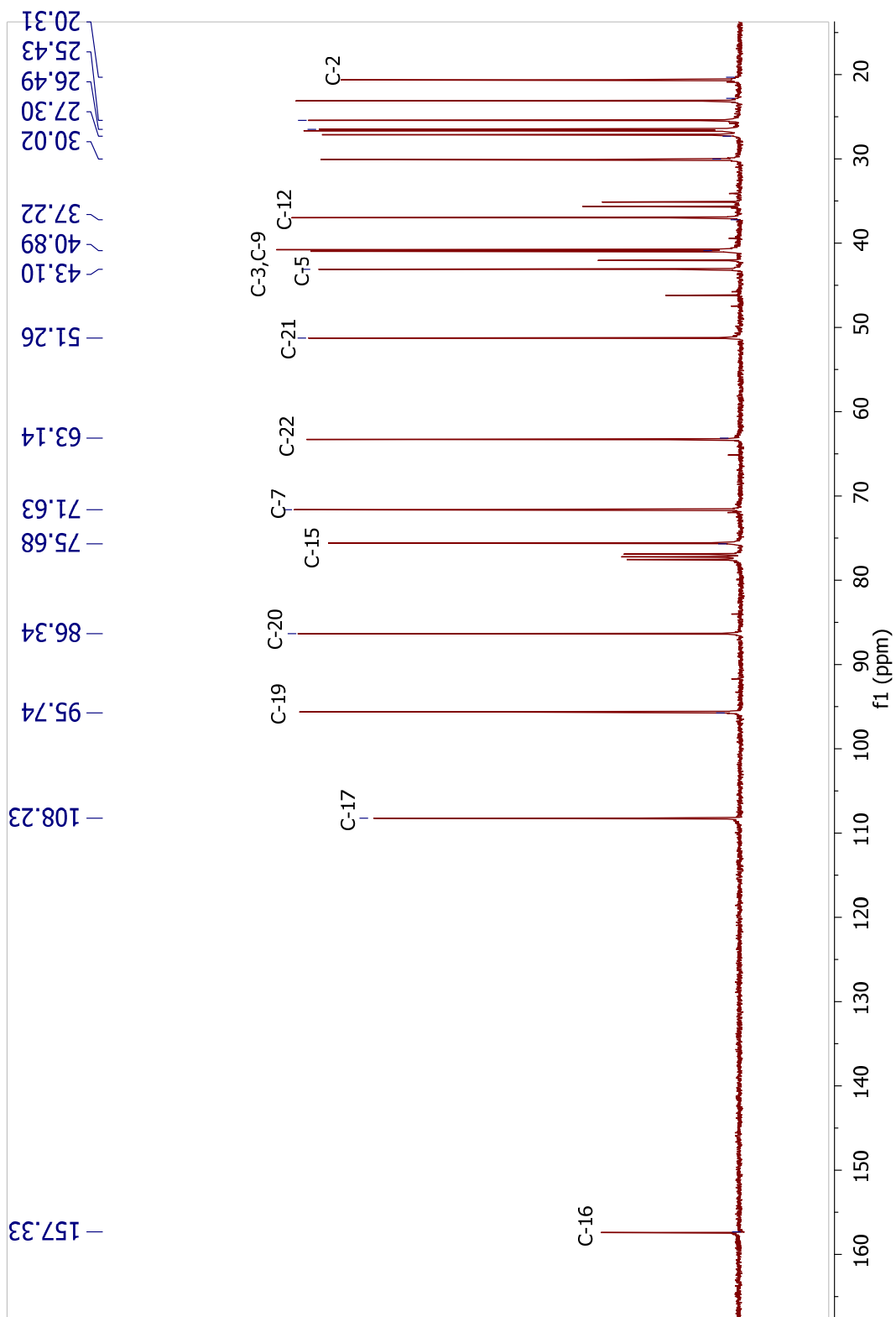


Figure 3.8 ^{13}C NMR spectrum of delphatisine D (77), 100 MHz, in CDCl_3

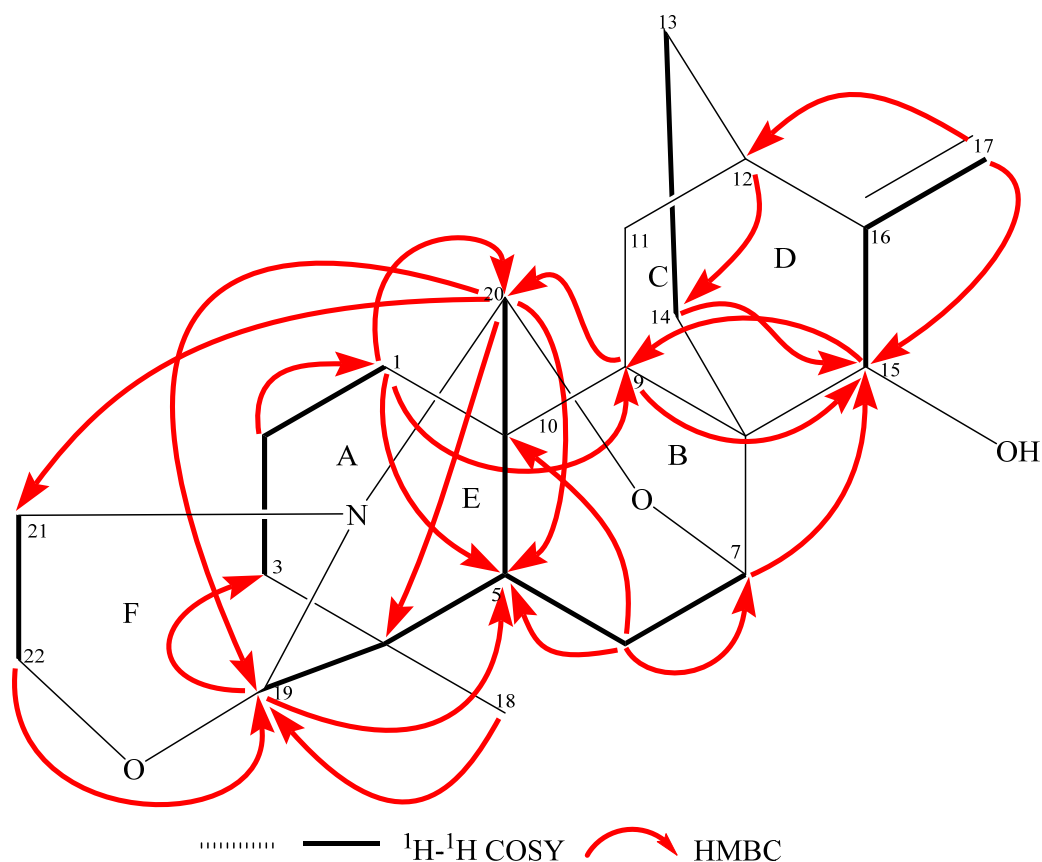


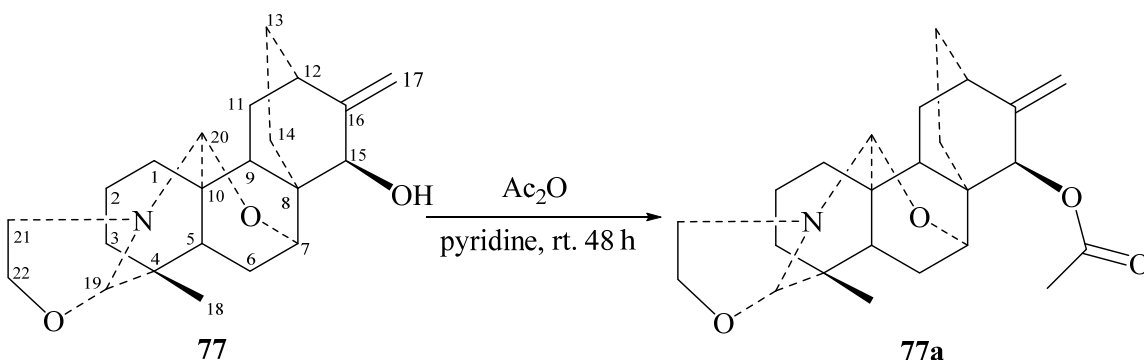
Figure 3.9 Key $^1\text{H}-^1\text{H}$ COSY and HMBC correlations of delphatisine D (**77**).

The connectivities of all these substructures with the remaining carbons were established by 2J , 3J $^1\text{H}-^{13}\text{C}$ coupling observed in the HMBC spectrum (**Figure 3.9** and Appendix 2.5) and by the comparison of NMR data with that of the known compound spiramine C (**90**) as shown in **Table 3.1**.⁷³ Accordingly, the obvious HMBC correlations observed from H-1 α at δ_{H} 1.55 to C-5 and from H-3 α at δ_{H} 1.41 to C-1 and C-5 allowed for the connectivity between fragments **A** and **B** through quaternary carbons C-4 and C-10 to form the first six-membered ring **A** containing C-1, C-2, C-3, C-4, C-5 and C-10 (**Figure 3.9**). Further correlations from both H-22 α and H-21 α to C-19 (δ_{C} 95.6) established the connectivity of substructures **F** to **B** through oxygen and nitrogen and confirmed the presence of an oxazolidine ring **F**, which could be linked to C-20 and

confirmed by further correlations between H₂-21 and C-20. Thus a six-membered piperidine E ring containing C-4, C-5, C-10, C-20, N, C-19 was confirmed through HMBC correlations from H-20 to C-5 and C-19 and from H-19 to C-5 and C-20. Clearly three bond correlations from H-7 to C-5, C-9 and C-20 and from H-9 to C-5 and C-20 served to link subfragments **C** to **B** and to support the establishment of a six-membered ring B (from C-5 to C-10) and an ether linkage between C-7 and C-20 in delphatisine D (**77**) similar to that in spiramine C, which was further supported by the correlation between H-20 and C-7. In addition, HMBC correlations from H-12 to C-14, C-15, C-16 and C-17 established C-12–C-13 and C-12–C-16 bonds, together with the correlations from H-15 to C-14 and C-16 determined the connectivity of subfragments **D** and **E**, thus, allowing the six-membered ring D containing C-9, C-14, C-13, C-12, C-16 and C-15 to be formed. Finally, the unification of rings D to B was assigned on the basis of HMBC correlations from both H-12 and H-15 to C-9, thus allowing for the remaining methylene signal at δ_C 27.0 to be incorporated into the molecular structure to complete the six-membered ring C containing C-8, C-9, C-11, C-12, C-16 and C-15. This assignment was further supported by the HMBC correlations between both H-9 and H-7 and C-15, carrying a hydroxyl group. This was further confirmed by acetylation carried out with acetic anhydride in pyridine for 48 h at room temperature as shown in **Scheme 3.1**.

The proton NMR spectrum of the acetate ester (**77a**) is consistent with that of the delphatisine D (**77**) except that the chemical shifts of H-15 (δ_H 4.79) and H-17a (δ_H 5.41) were shifted downfield by 0.64 and 0.32 ppm (see **Figure 3.10**), respectively, as compared with that of delphatisine D (**77**). Furthermore, there is only one acetyl group at δ_H 2.12 (3H, s) in ¹H NMR spectrum further confirmed that only one hydroxyl group at

C-15 was esterified. In addition, the ESIMS peak at m/z 400.2 of the ester ($[M + H]^+$) was consistent with the above conclusion (see **Appendix 2-8**). Thus, the planar structure of delphatisine D (**77**) with a highly fused heptacyclic system bearing an ether linkage between C-7 and C-20 was established.



Scheme 3.1 Esterification reaction of delphatisine **77**.

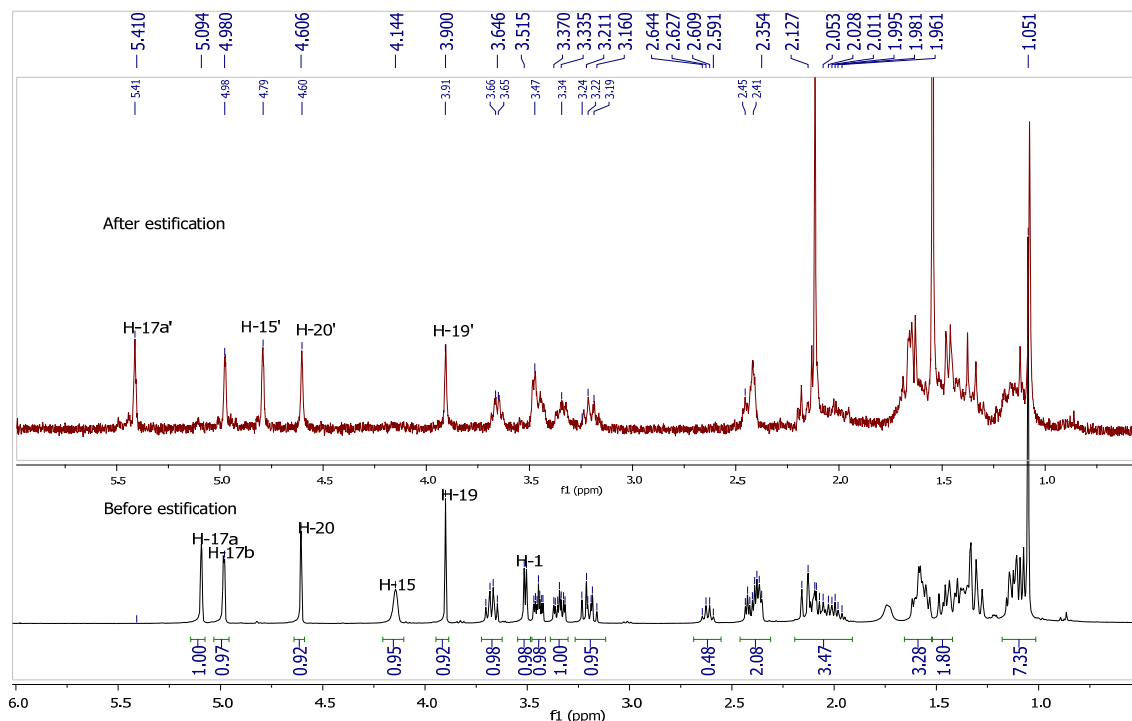


Figure 3.10 ^1H NMR spectra of delphatisine D (**77**) and its acetic ester (**77a**).

The relative configuration of compound **77** was determined by analysis of NOESY correlations (in **Figure 3.11**), and by comparison of chemical shifts to the literature data. In the NOESY spectrum, the cross-peak between H-9 and H-20 was not observed, indicating that the H-20 was in α -orientation, assuming the usual β -H stereochemistry at C-9 as observed in all previously reported atisine-type diterpene alkaloids.^{73,74} In addition, the resonances for the exocyclic methylene group observed at δ_{H} 5.09 and 4.98 were shifted downfield by 0.16 and 0.08 ppm, respectively, as compared with that of spiramine C, indicating the presence of a β -hydroxy group at C-15.⁷⁵ This assignment was further supported by the upfield shifts of C-7 (9.6 ppm) and C-15 (2.2 ppm) as compared with that of 15-epi-dihydroajaconine which exhibited the 1,3-diaxial-like interaction between H-7 β and H-15.⁷³ Moreover, the chemical shift at δ_{C} 95.6 confirmed the *S*-form of C-19 (δ_{C} 96.3 for 19*S* epimer and δ_{C} 91.5 for 19*R* epimer as observed in spiramines C and D.⁷³ Therefore, the structure of **77** was determined as 15-epi-spiramine C and a trivial name delphatisine D was given to **77**.

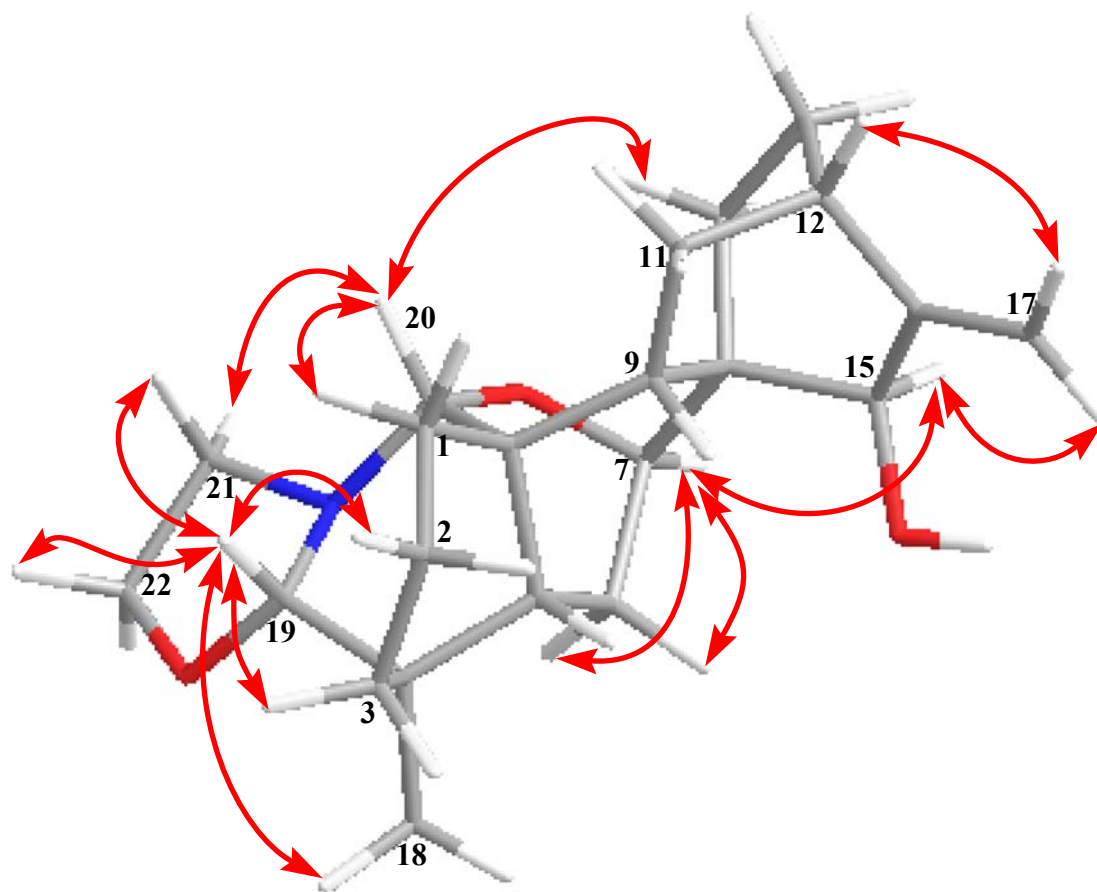


Figure 3.11 Key NOESY correlations of delphatisine D (**77**).

Chrysotrichumine A (**78**) was isolated as colorless gum and its molecular formula $C_{27}H_{39}NO_{10}$ was established on the basis of HRESIMS for the $[M + H]^+$ at m/z 538.2665 (calcd 538.2647), which indicated 9 degrees of unsaturation. The IR spectrum showed characteristic absorptions for OH (3412 cm^{-1}), C=N (1643 cm^{-1}), carbonyl (1733 cm^{-1}) and simple ether (1044 cm^{-1}) groups.

The ^{13}C NMR and gHSQC revealed 27 carbon signals including one sp^2 azomethine, nine sp^3 methines, five sp^3 methylenes and four quaternary carbons, two acetyl groups, along with four methoxyl groups. The ^1H (in **Figure 3.14**), ^{13}C NMR (in **Figure 3.15**) and gHSQC spectra of **78** afforded signals at δ_{H} 4.16 (2H, d, $J = 6.0\text{ Hz}$), δ_{C}

66.7, for an oxymethylene, δ_{H} 3.26 (1H, overlapped), 3.42 (1H, overlapped), 3.65 (1H, t, $J = 4.8$ Hz), 3.80 (1H, s), 4.54 (1H, s), δ_{C} 80.2, 82.0, 84.1, 78.1, 83.1, for five oxymethines, δ_{H} 6.79 (1H, s), δ_{C} 137.1, for an imino group, δ_{H} 3.25, 3.35, 3.42, 3.44 (each 3H, s), δ_{C} 56.7, 57.2, 58.1, 58.2 four methoxyl groups, two quaternary oxygenated carbon signals at δ_{C} 92.8, 79.3, two acetyl groups at δ_{H} 2.08, 2.16 (each 3H, s), δ_{C} 20.9, 170.5, 22.8, 171.5 (**Table 3.3**). However, the NMR spectra did not show signals for the angular methyl and *N*-ethyl groups. Since three of the degrees of unsaturation were occupied by two carbonyls and an imino group, the remaining 7 degrees of unsaturation indicated that **78** possesses a hexacyclic skeleton.

All of this evidence, along with a careful inspection of the HMBC spectrum indicated that the structure of **78** is similar to that of the sharwuphinine A (**89**)⁷¹ except for the presence of the two acetyl groups described above (**Table 3.4**). An acetyl group was attached to C-18 to account for its chemical shift ($\delta_{\text{C}} = 66.7$ ppm), and based on HMBC correlations between H₂-18 and a carbonyl carbon observed at $\delta_{\text{C}} = 170.5$ ppm. This was further supported by the signal at δ_{H} 4.16 in the ¹H NMR spectrum which appeared to move downfield 0.38 ppm, when compared with the analogous signal of sharwuphinine A [δ_{H} 3.78 (H₂-18)]. In addition, the assignment of the second acetyl group (δ_{H} 2.16; δ_{C} 22.8, 171.5) was initially hampered by the lack of protons at C-7 and C-8. However, the resonances of C-7 (δ_{C} 92.6) and C-6 (δ_{C} 83.0) were shifted downfield and upfield by 5.7 and 8.0 ppm, respectively, in comparison with those of sharwuphinine A [δ_{C} 86.9 (C-7) and δ_{C} 91.0 (C-6)] suggesting that the hydroxyl group at C-7 in

sharwuphinine A (**89**) was also esterified by an acetyl group in **78**. The structure of compound **78** was further confirmed by extensive analysis of the 2D NMR data.

Table 3.3 NMR Data of compound **78**. Measured in CDCl₃ at 400 MHz (¹H) and 100 MHz (¹³C), δ in ppm, *J* in Hz..

no.	δ_H	δ_C	HMBC (H→C)	NOESY
1	3.42 (1H, overlapped)	80.2		H-9, H-1 β , H-10
2a	1.92 (1H, m)	20.8		
2b	1.43 (1H, overlapped)			
3	1.70 (2H, m)	26.6		
4		42.1		H-10
5	2.03 (1H, d, 4.8)	47.0	C-6, C-7, C-11, C-17, C-19	H-6, H-9
6	4.54 (1H, br s)	83.0	C-4, C-5, C-8, C-11	H-5, H-18
7		92.6		
8		79.2		
9	3.03 (1H,t, 4.7)	43.2	C-8, C-10, C-12, C-13,	H-10, H-14
10	2.12 (1H, overlapped)	42.8		H-1 α , H-4, H-7 β , H9
11		50.6		
12a	2.10 (1H, overlapped)	30.8		
12b	1.39 (1H, overlapped)			
13	2.38 (1H, t, 3.5)	38.7	C-10, C-16	H-14
14	3.65 (1H, t, 4.8)	84.1	14-OMe, C-8, C-16	H-9, H-10, H-13
15a	2.80 (1H, dd, 15.2, 8.4)	33.1	C-7, C-8, C-9, C-13, C-16	H-15b, H-17
15b	1.82 (1H, dd, 15.6, 8.0)		C-7, C-8, C-16	H-15a
16	3.26 (1H, overlapped)	82.0		
17	3.80 (1H, s)	78.1	C-5, C-6, C-7	H-5, H-15a, H-16
18	4.15 (1H, d, 6.0)	66.7	C-3, C-4, C-5 C-19, OAc	H-3, H-5
19	6.74 (1H, s)	137.2	C-4, C-5, C-17, C-18	H-3, H-18
7-COCH ₃		171.5		
7-COCH ₃	2.16 (3H, s)	22.8		
18-COCH ₃		170.5		
18-COCH ₃	2.08 (3H, s)	20.8		
OMe-1	3.25 (3H, s)	56.7		
OMe-6	3.44 (3H, s)	58.0		
OMe-14	3.42 (3H, s)	58.2		
OMe-16	3.38 (3H, s)	57.2		

Table 3.4 Comparison of ^{13}C NMR data of compounds **78**^a and **89**^b.

position	78	89	position	78	89
1	80.2	82.1	14	84.1	85.6
2	20.8	21.0	15	33.0	34.3
3	26.6	26.3	16	82.0	84.1
4	42.1	45.7	17	78.1	79.0
5	47.0	46.1	18	66.7	65.0
6	83.1	91.0	19	137.2	144.1
7	92.6	86.9	1-OCH ₃	56.7	57.0
8	79.2	78.8	6-OCH ₃	58.0	59.3
9	43.2	44.4	14-OCH ₃	58.2	58.1
10	42.8	43.7	16-OCH ₃	57.2	56.6
11	50.6	53.0	7-COCH ₃	171.5	
12	30.8	32.0	18-COCH ₃	170.5	
13	38.7	39.4			

^aMeasured in CDCl₃ at 100 MHz (^{13}C), δ in ppm.

^bMeasured in CD₃OD at 125 MHz (^{13}C), δ in ppm.

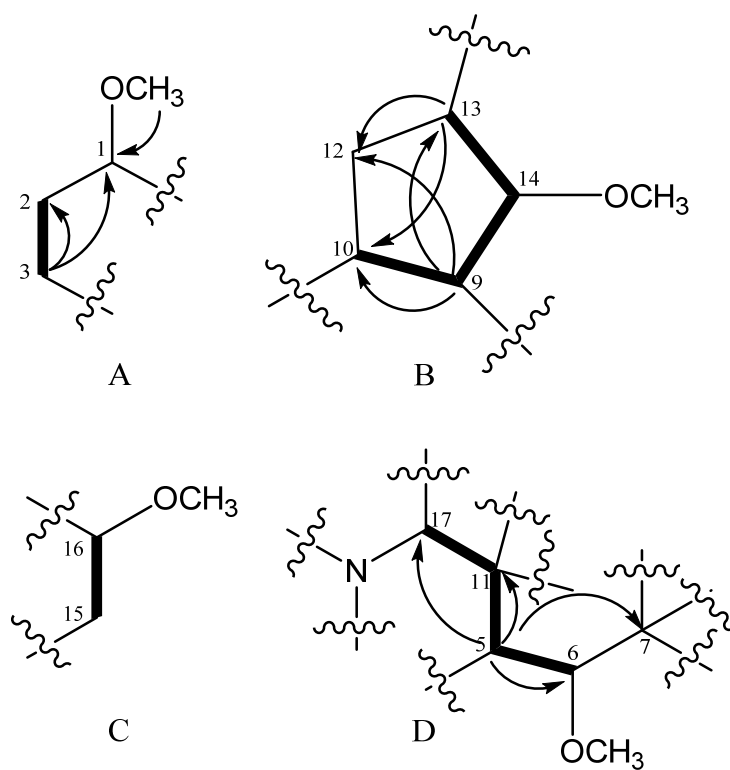


Figure 3.12 Substructures (A – D) of chrysotrichumine A (**78**).

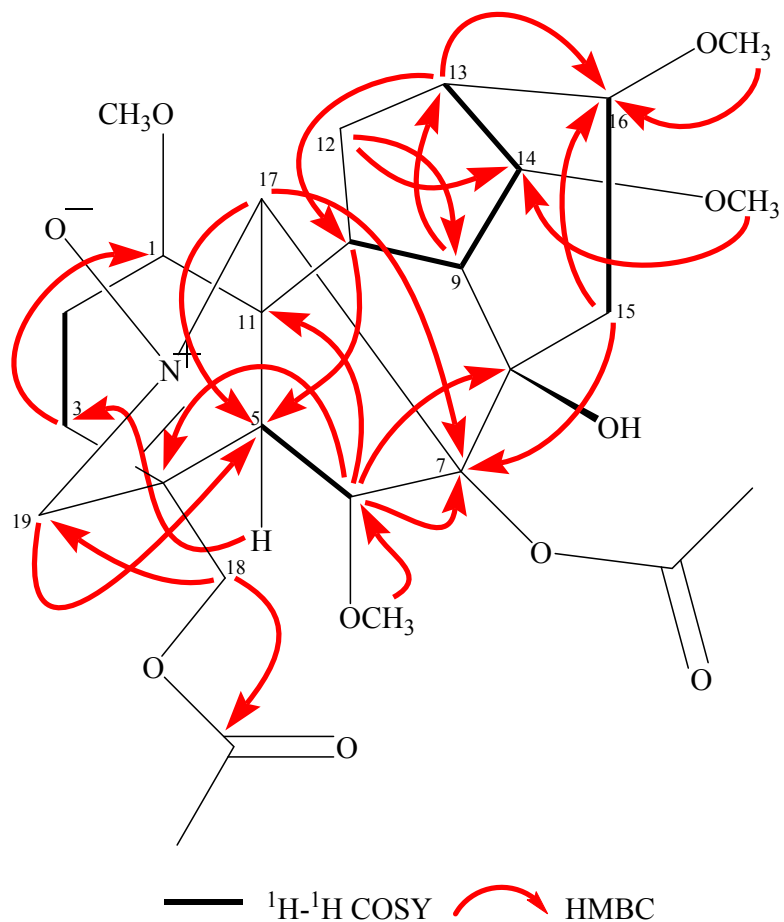


Figure 3.13 Key $^1\text{H} - ^1\text{H}$ COSY and HMBC correlations of chrysostrichumines A (**78**).

Detailed analysis of the $^1\text{H} - ^1\text{H}$ COSY spectrum combined with the gHSQC and HMBC spectra of **78** led to the formation of four substructures (**A – D**) as seen in **Figure 3.12**. The connectivity of the linear fragment **A** was determined on the basis of a COSY correlation between methylene H-2 α (δ_{H} 1.92) and H₂-3 (δ_{H} 1.70). HMBC correlations (in **Figure 3.13**) between H-3 and C-2 (δ_{C} 20.8) and C-1 (δ_{C} 80.2) further confirmed the connectivity of C-1 to C-3 and the establishment of substructure **A**. The connectivity of the tetra-substituted cyclopentane group (substructure **B**) was determined by COSY and HMBC correlations. The COSY correlation from H-9 (δ_{H} 3.03) to H-14 (δ_{H} 3.64) and from H-14 to H-13 (δ_{H} 2.37), along with the HMBC correlations from H-9 to C-10 (δ_{C}

42.9), C-12 (δ_C 30.8) and C-13 (δ_C 38.7), and from H-13 to C-10 and C-12 allowed for the establishment of substructure **B**. The fragment **C** was readily determined through COSY correlations observed from both signals of the methylene group (H₂-15) at δ_H 2.80, 1.82 to H-16 (δ_H 3.23). The linear fragment **D** was determined by a weak COSY correlation between H-5 (δ_H 2.03) and H-6 (δ_H 4.52) and a long-range W interaction between H-17 (δ_H 3.80) and H-5. This was further confirmed by HMBC correlations from H-5 to C-6 (δ_C 83.0) and C-11 (δ_C 50.6) and from H-17 to C-5 and C-6 (δ_C 92.6).

On the basis of the HMBC experiment, those four fragments could be completely connected by inserting the remaining tertiary and quaternary carbon atoms of C-4, C-8 and C-10. Firstly, the presence of an imino group at C-19 was verified by the IR absorption (1650 cm^{-1}) and its chemical shift at δ_C 137.2 ppm. In addition, the HMBC correlations from H-19 (δ_H 6.74) to C-3 (δ_C 26.6, a weak signal), C-4 (δ_C 42.1), C-5 (δ_C 47.0), C-17 (δ_C 78.1) and C-18 (δ_C 66.7) was in agreement with those from H₂-3 (δ_H 1.70), H-5, H-17 and H₂-18 to C-19 (δ_C 137.2) further confirming the imino group to be located at C (19)=N. The HMBC correlations from H-19 to C-17 and from H-18 to C-4, along with the UV absorption ($\lambda_{\text{max}} = 250\text{ nm}$) corroborated the presence of a nitron group⁷¹ located between C-17 and C-19 and an oxymethylene at C-4. The HMBC cross-peaks from H-6 and H₂-3 (δ_H 1.70) to C-4, and from H-1, H-5 and H-6 to C-11 allowed the connectivity of substructures of **A** and **D** through the quaternary carbons C-4 and C-11. Furthermore, HMBC correlations from H-5 to C-10, from H-6 to C-7 and C-8, from H-15 α (δ_H 2.80) to C-7, C-8, C-9 and C-13, from H-9 to C-15 and from H-13 to C-16 lead to the linkage of the cyclopentane ring (fragment **B**) to **D** through C-7, C-8 and C-11, and

lead to the connectivity of fragments **C** to **B** through quaternary carbon C-8 and tertiary carbon C-13 to form a cyclohexane ring containing C-9, C-10, C-14, C-13, C-16 and C-15. Finally, the location of four methoxyl groups at C-1, C-6, C-14 and C-16 was confirmed by the HMBC correlations between OCH₃-1 (δ_{H} 3.25) and C-1 (δ_{C} 80.2), OCH₃-6 (δ_{H} 3.44) and C-6 (δ_{C} 83.0), OCH₃-14 (δ_{H} 3.42) and C-14 (δ_{C} 84.1), and between OCH₃-16 (δ_{H} 3.26) and C-16 (δ_{C} 82.0), respectively.

The relative configuration of **78** was deduced as shown in **Figure 3.16** by ROESY correlations combined with the analysis of the coupling patterns in the ¹H NMR spectrum. Clear ROE correlations between H-5 and H-9, and between H-19 and H₂-3 indicated that there is no doubt that one relative stereochemistry existed for the fused-tetracyclic ring system (from C-1 to C-11, C-17-N-C-19) without strain.⁷¹ The twisted boat conformation of the cyclohexane ring from C-1 to C-11 was confirmed by the ROESY correlation between H-2 β (δ_{H} = 1.92 ppm) and H-5. In addition, ROESY correlations between H-1 and H-5 suggested that proton H-1 shared a β -configuration with H-5. The correlation between H-6 and H₂-18 and H-19 indicated H-6 was α -oriented. Moreover, the relative configuration of H-14 was determined to be in β -orientation based on the ROESY correlation between H-14 and H-13 and H-9, along with its small coupling constant at J = 4.4 Hz.⁷⁵ The relative configuration of H-16 was not able to be determined due to overlapping signals observed around δ_{H} = 3.26 ppm, however, the similarity of the chemical shifts of C-15 and C-16 (in **Table 3.2**) with that of sharwuphinine A, as well as the comparable optical rotation values ($[\alpha]_{\text{D}}^{18}$ + 5.9 (c 0.008, MeOH) for **78**, $[\alpha]_{\text{D}}^{18}$ + 10.9 (c 0.018, MeOH) for **89**) indicated that compound **78** has the same pattern of

stereochemistry as **89**, having a H-16 in α -orientation. Therefore, the structure of **78** was determined as shown and given the trivial name chrysotrichumines A.

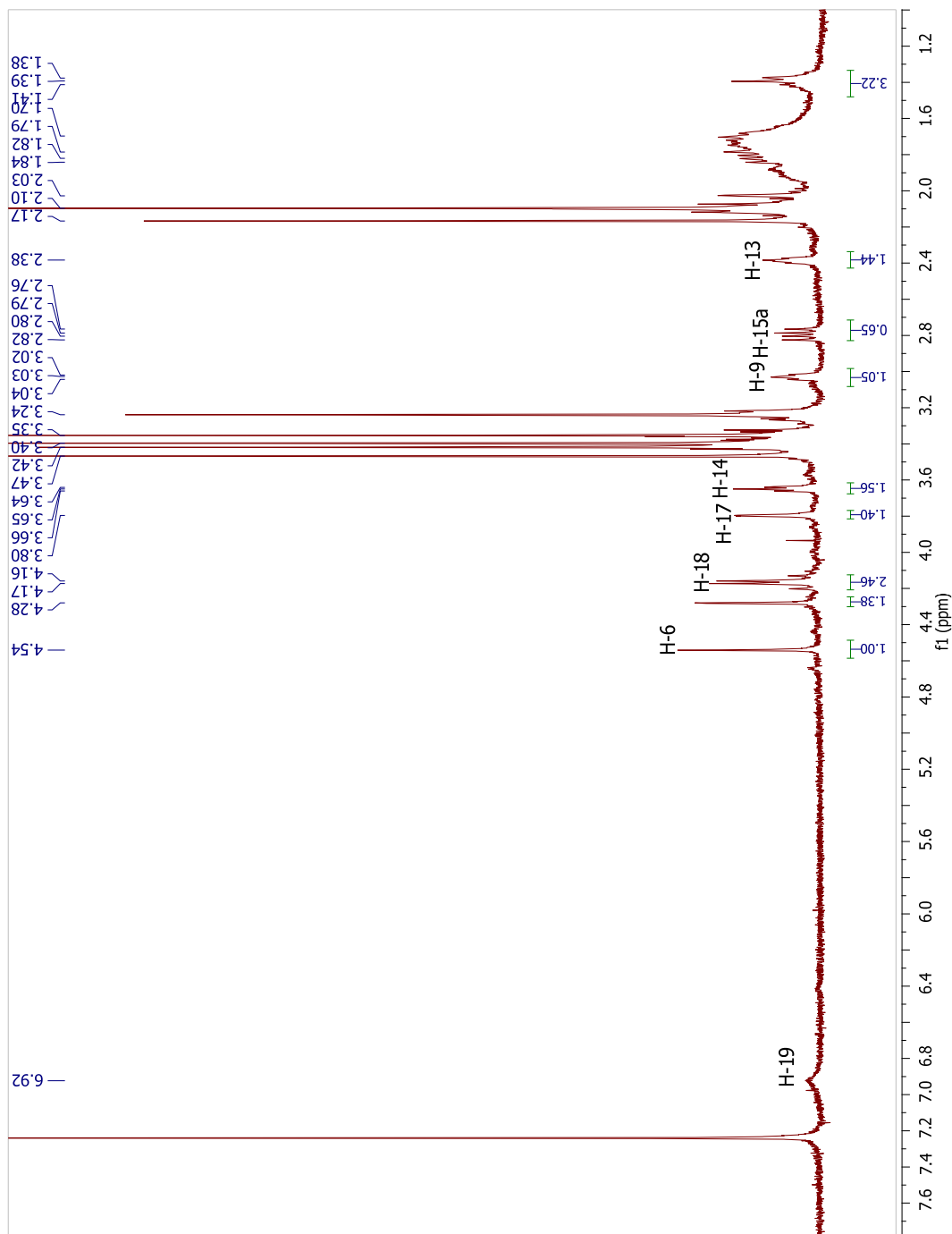


Figure 3.14 ^1H NMR spectrum of chrysotrichumine A (**78**), 400 MHz, in CDCl_3

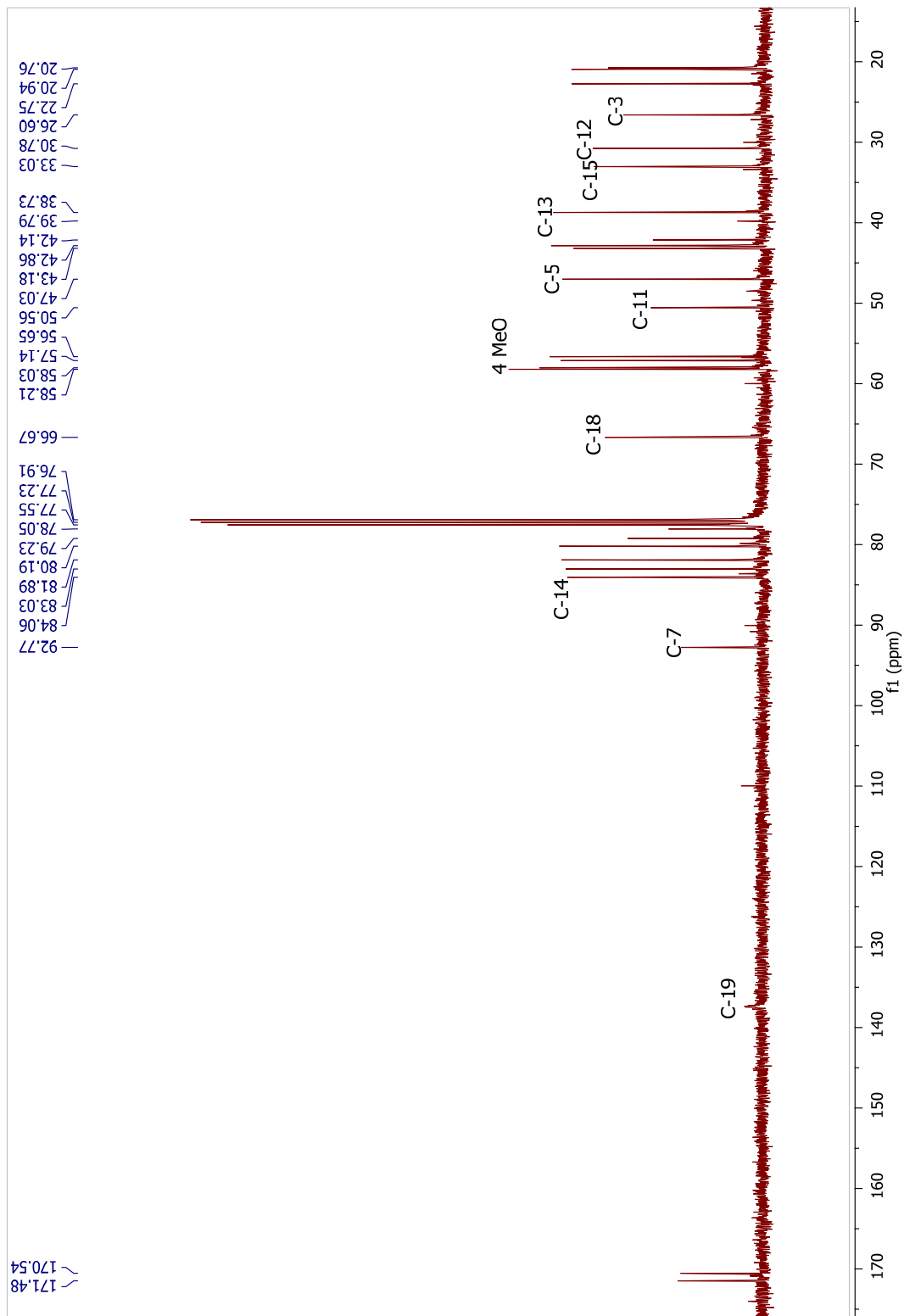


Figure 3.15 ^{13}C NMR spectrum of chrysotrichumine A (**78**), 100 MHz, in CDCl_3

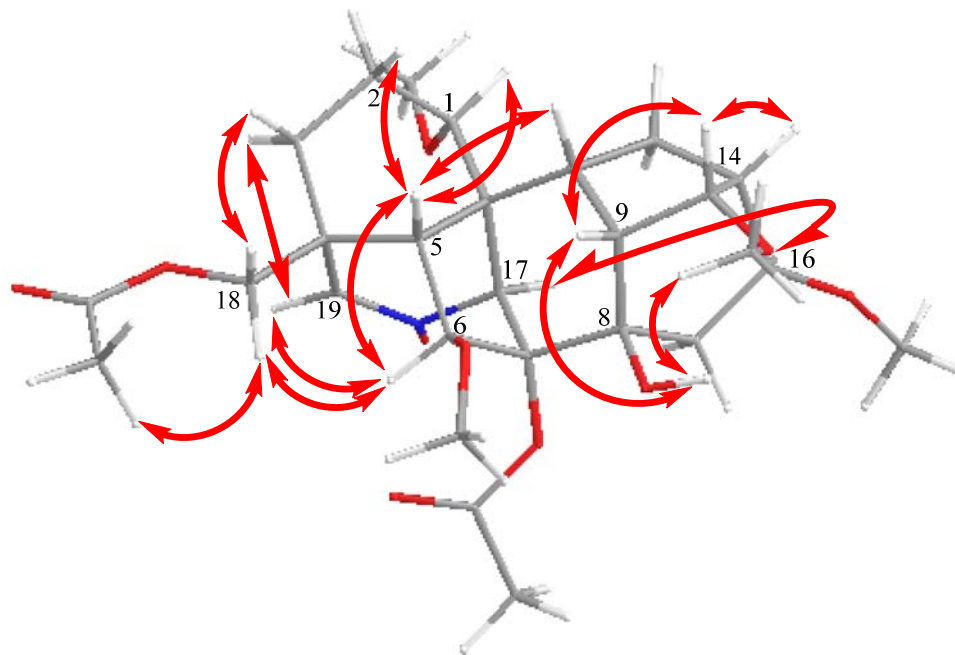


Figure 3.16 Key ROESY correlations of chrysotrichumines A (**78**).

Compound **79** was obtained as an amorphous powder. Its molecular formula $C_{37}H_{51}N_3O_{11}$ was assigned from the HRESIMS of 737.3268 for $[M + Na]^+$ (calcd 737.3256), which indicated 14 degrees of unsaturation. The IR spectrum showed characteristic absorptions for OH (3337 cm^{-1}), carbonyl ($1733, 1710\text{ cm}^{-1}$), aromatic ring ($1643, 764\text{ cm}^{-1}$) and simple ether (1075 cm^{-1}) groups. The ^1H , ^{13}C NMR and gHSQC spectra of chrysotrichumine B (**79**) showed the presence of a *N*-ethyl group [δ_{H} 4.05 (1H, qd, $J = 16.0, 8.0\text{ Hz}$), 3.00 (1H, qd, $J = 16.0, 8.0\text{ Hz}$), 1.08 (3H, t, $J = 8.0\text{ Hz}$); δ_{C} 44.4, 12.8], four methoxyl groups [δ_{H} 3.19, 3.30, 3.41, 3.35 (each 3H, s); δ_{C} 55.9, 59.1, 58.6, 56.9], four oxygenated methine [δ_{H} 3.24 (1H, overlapped), 3.83 (1H, br s), 3.65 (1H, t, $J = 4.0\text{ Hz}$), 3.17 (1H, d, $J = 2.0\text{ Hz}$), δ_{C} 81.4, 92.1, 84.0, 82.2], an oxymethylene [δ_{H} 4.80 (1H, d, $J = 12.0\text{ Hz}$), 4.49 (1H, d, $J = 12.0\text{ Hz}$), δ_{C} 67.4] and a substituted anthranoyl group [δ_{H} 11.1 (1H, s, NH), 7.06, 7.52 (each 1H, t, $J = 8.0\text{ Hz}$), 7.90, 8.67 (each 1H, d, J

= 8.4 Hz, Ar-H), 1.29 (3H, d, $J = 8.0$ Hz); δ_C see **Table 3.5**]. The data summarized above suggested that **79** is a lycoctonine-type C₁₉-diterpenoid alkaloid.⁵⁷

Table 3.5 NMR Data of compound **79**. Measured in CDCl₃ at 400 MHz (¹H) and 100 MHz (¹³C), δ in ppm, J in Hz..

no.	δ_H	δ_C	HMBC (H→C)	NOESY
1	3.24 (1H, overlapped)	81.4		
2a	2.00 (1H, overlapped)	25.3		
2b	1.55 (1H, m)			
3a	2.02 (1H, overlapped)	29.7		
3b	1.70 (1H, m)			
4		47.8		
5	1.99 (1H, overlapped)	50.1		
6	3.83 (1H, br s)	92.1	C-7, C-8, C-11, OCH ₃ -6	H-17, H-18b
7		86.2		
8		77.2		
9	2.94 (1H, overlapped)	42.9		H-14
10	2.13 (1H, overlapped)	45.2		H-14
11		49.2		
12	1.95 (2H, overlapped)	28.6		
13	2.42 (1H, t, 8.0)	37.7	C-15	H-14
14	3.65 (1H, t, 4.0)	84.0		H-9, H-10, H-13
15a	2.57 (1H, dd, 16.0, 8.0)	33.5	C-7, C-8, C-13	
15b	1.75 (1H, dd, 16.0, 4.0)		C-8, C-16	
16	3.17 (1H, overlapped)	82.2	C-12, C-14	
17	3.29 (1H, s)	63.8	C-5, C-19	
18a	4.80 (1H, d, 12.0)	67.4	C-5	H-18b
18b	4.49 (1H, d, 12.0)		C-3	H-6, H-17
19		170.3		
21a	4.05 (1H, qd, 16.0, 8.0)	44.4	C-22	
21b	3.00 (1H, qd, 16.0, 8.0)		C-17, C-19	
22	1.08 (3H, t, 8.0)	12.8	C-21	
OMe-1	3.19 (3H, s)	55.9		
OMe-6	3.30 (3H, s)	59.1		
OMe-14	3.41 (3H, s)	58.6		
OMe-16	3.35 (3H, s)	56.9		
OCO-18		167.8		
1'		115.1		
2'		141.8		
3'	8.66 (1H, d, 8.0)	121.0	C-1', C-5'	
4'	7.53 (1H, dt, 8.0, 4.0)	134.6		
5'	7.09 (1H, dt, 8.0, 4.0)	122.9		
6'	7.93 (1H, d, 8.0)	130.3		
1''		175.0		
2''	2.95 (1H, overlapped)	39.0	C-4''	
3''a	2.83 (1H, dd, 16.8, 8.4)	37.8	C-1'', C-2''	
3''b	2.48 (1H, dd, 16.8, 5.2)		C-1''	
4''		174.5		
5''	1.31 (3H, d, 8.0)	18.3	C-1'', C-3''	
NH-C-2'	11.2 (1H, s)		C-1'', C-3''	

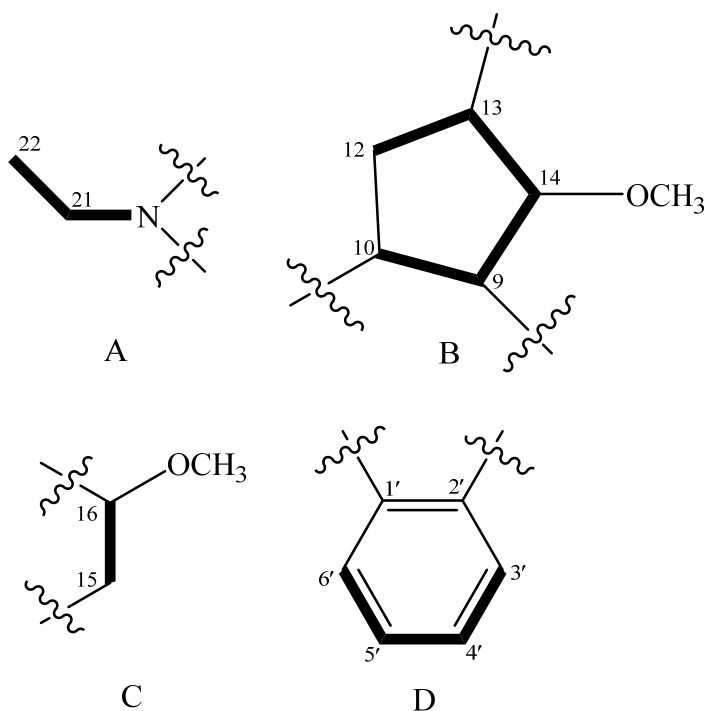


Figure 3.17 Substructures (**A – D**) of chrysotrichumine B (**79**).

Interpretation of the $^1\text{H} - ^1\text{H}$ COSY spectrum coupled with the gHSQC spectrum led to the assignment of five isolated spin systems (**A – D**, in **Figure 3.17**). The linear fragment **A** was determined on the basis of COSY correlations from a nitrogen-substituted methylene H_2 -21 (δ_{H} 4.05, 3.00) to a methyl group at δ_{H} 1.02 (H_3 -22). The clear correlations from H-9 (δ_{H} 2.94) to H-10 (δ_{H} 2.13) and H-14 (δ_{H} 3.65) and from H-13 (δ_{H} 2.41) to H-12 (δ_{H} 1.95) and H-14 in the COSY spectrum along with comparison of the NMR data with that of delsemine A (**85**) allowed for establishment of the substructure **B**. The fragment **C** was determined on the basis of COSY correlations observed from both singlets of the methylene group (H_2 -15) at δ_{H} 2.57, 1.75 to H-16 (δ_{H} 3.17). The COSY correlations from H-5' (δ_{H} 7.09) to H-4' (δ_{H} 7.53) and H-6' (δ_{H} 7.93) and from H-4' to H-3' (δ_{H} 8.66) confirmed the presence of the ortho-substituted aromatic fragment **D**.

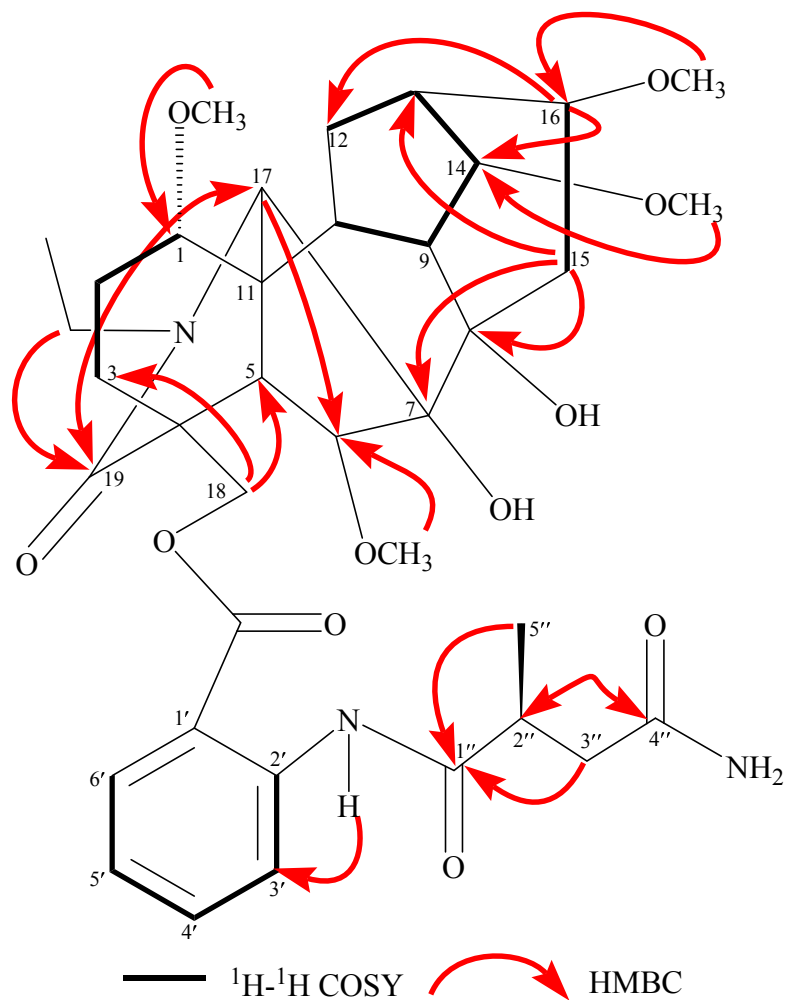


Figure 3.18 Key $^1\text{H}-^1\text{H}$ COSY and HMBC correlations of chrysotrichumines B (**79**).

The planar structure of **79** was determined by extensive analysis of HMBC correlations as well as the comparison of its NMR data with that of the similar known compound delsemine A (**85**).⁶⁸ The HMBC correlations between H-15 β (δ_{H} 2.57) to C-7 (δ_{C} 86.2), C-8 (δ_{C} 77.2) and C-13 (δ_{C} 37.7) and between H-16 (δ_{H} 3.17) to C-12 (δ_{C} 28.6) and C-14 (δ_{C} 84.0) allowed for the connectivity between substructures **C** and **B**. Further HMBC correlations from H-6 (δ_{H} 3.83) to C-4 (δ_{C} 47.8), C-5 (δ_{C} 50.1), C-7 and C-8 were similar to that observed in compound **78**, indicating that **79** had the same carbon skeleton as that of **78**. HMBC correlation from a methylene signal at δ_{H} 2.97 (H-21b) to C-17

allowed for the subfragment **A** to be incorporated into the molecular structure. In addition, HMBC correlations from H-5" (δ_{H} 1.31) to C-1" (δ_{C} 175.0) and C-3" (δ_{C} 37.8), from the methylene signals of H₂-3" at δ_{H} 2.83, 2.48 to C-1", from a methine signal of H-2" (δ_{H} 2.96) to C-4" (δ_{C} 174.5) and from the imino (-NH-) at δ_{H} 11.1 to C-1" and C-3' (δ_{C} 121.0), along with the comparison of the similarity of the chemical shifts of C-18 (δ_{C} 67.4) and the carbonyl group at δ_{C} 167.8 with those of delsemine A (**85**) (see **Table 3.6**) confirmed the presence of an ortho-substituted anthranoyl group at C-18.⁶⁷ This was further confirmed by the weak HMBC correlations from both H₂-18 at δ_{H} 4.80, 4.49 to C-3 (δ_{C} 29.7) and C-5 (δ_{C} 50.1), respectively.

Table 3.6 Comparison of ¹³C NMR data of compounds **79**^a and **85**^a.

position	79	85	position	79	85
1	81.4	83.9	21	44.4	50.9
2	25.3	26.1	22	12.8	14.0
3	29.7	32.2	1-OCH ₃	55.9	55.7
4	47.8	37.6	6-OCH ₃	59.1	57.8
5	50.1	50.5	14-OCH ₃	58.6	58.1
6	92.1	91.0	16-OCH ₃	56.9	56.3
7	86.2	88.6	OCO-18	167.8	168.1
8	77.2	77.5	1'	115.1	114.7
9	42.9	43.3	2'	141.8	141.9
10	45.2	46.1	3'	121.0	120.7
11	49.2	49.1	4'	134.6	134.9
12	28.6	28.7	5'	122.9	122.5
13	37.7	38.2	6'	130.3	130.3
14	84.0	83.9	1"	175.0	174.1
15	33.5	33.7	2"	39.0	39.3
16	82.2	82.6	3"	37.8	39.0
17	63.8	64.5	4"	174.5	172.4
18	67.4	69.8	5"	18.3	18.0
19	170.3	52.4			

^aMeasured in CDCl₃ at 100 MHz (¹³C), δ in ppm.

The molecular formula of C₃₇H₅₁N₃O₁₁ suggested that **79** has one more oxygen than delsemine A. In comparison with their ¹³C NMR data, the absence of the chemical

shift of C-19 at δ_C 52.6 in delsemine A (**85**) and the presence of a carbonyl group at δ_C 170.3 in **79** indicated that this carbonyl group is located at C-19. This was further supported by the HMBC correlation between H-17 (δ_H 3.27) and C-19. The other 1H and ^{13}C NMR data for **79** are similar to those of delsemine A (**85**).

The relative configuration of **79** was assigned as shown in **Figure 3.2** by the coupling patterns in the 1H NMR spectrum and the key NOE correlations observed in the NOESY spectrum as shown in **Figure 3.18**, and by comparing the NMR data with that of delsemine A (**85**). First of all, a triplet signal at δ_H 3.65 ($J = 4.0$ Hz) indicated the β -orientation of H-14.⁷⁵ This assignment was further supported by the NOE correlations from H-14 (δ_H 3.65) to H-9 (δ_H 2.94), H-10 (δ_H 2.13) and H-13 (δ_H 2.41), which indicated that all of those protons shared β -orientation. The $J_{H-5,H-6}$ value of 0 Hz suggested that H-6 was in α -orientation.⁷⁶ The similarly small coupling constants of $J_{H-16,H-15ax} = 8.8$ Hz and $J_{H-16,H-15eq} = 6.4$ Hz observed in **79** with that of the known compounds shawurensine⁷⁷ allowed to assign H-16 in α -orientation. The relative configuration of H-1 could not be definitively determined due to the limited NOE data and the overlapping signals around $\delta_H = 3.25$ ppm. However, the chemical shift of C-1 (δ_C 81.4) is consistent with the assignment of the MeO-1 being α -orientated as observed in all previously reported C₁₉-diterpene alkaloids with a methylsuccinimide moiety at C-18.^{68,78,79} In addition, the stereochemistry of the methylsuccinimide moiety in methyllycaconitine has been assigned to be “S” by Bladbrough.⁸⁰ Therefore, the chemical shift at δ_C 39.0 confirmed the S-form of C-2” in **79**.^{75,80} Thus, the structure of chrysotrichumine B was determined as 19-carbonlydelsemine A (**79**).

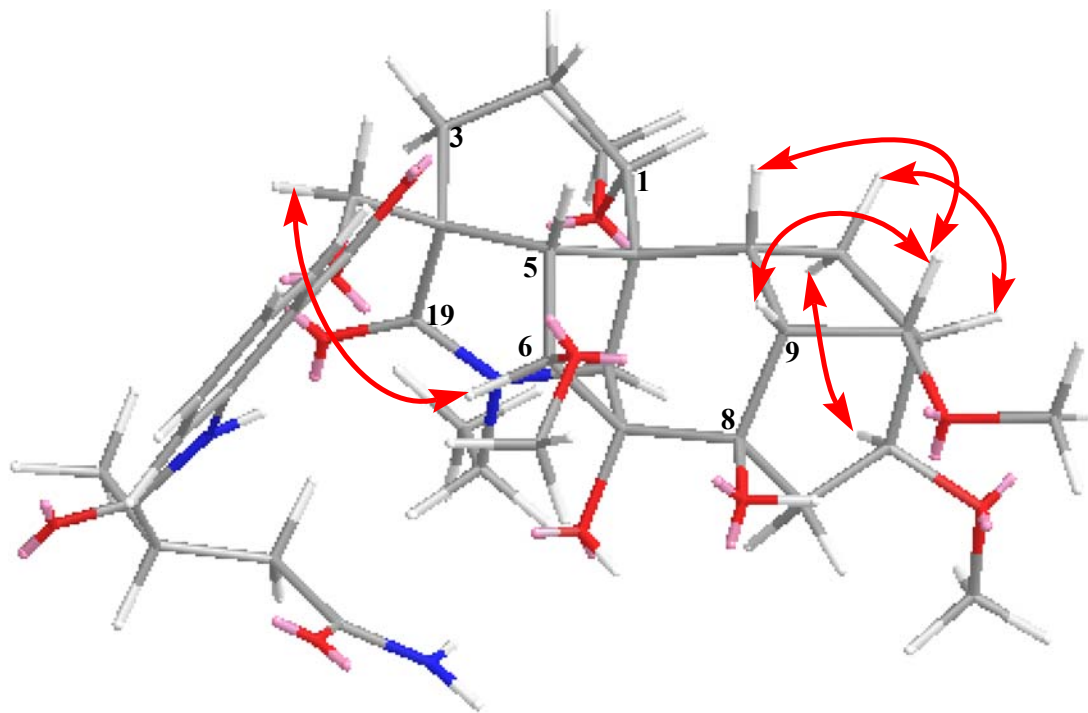


Figure 3.19 Key NOESY correlations of chrysotrichumines B (**79**).

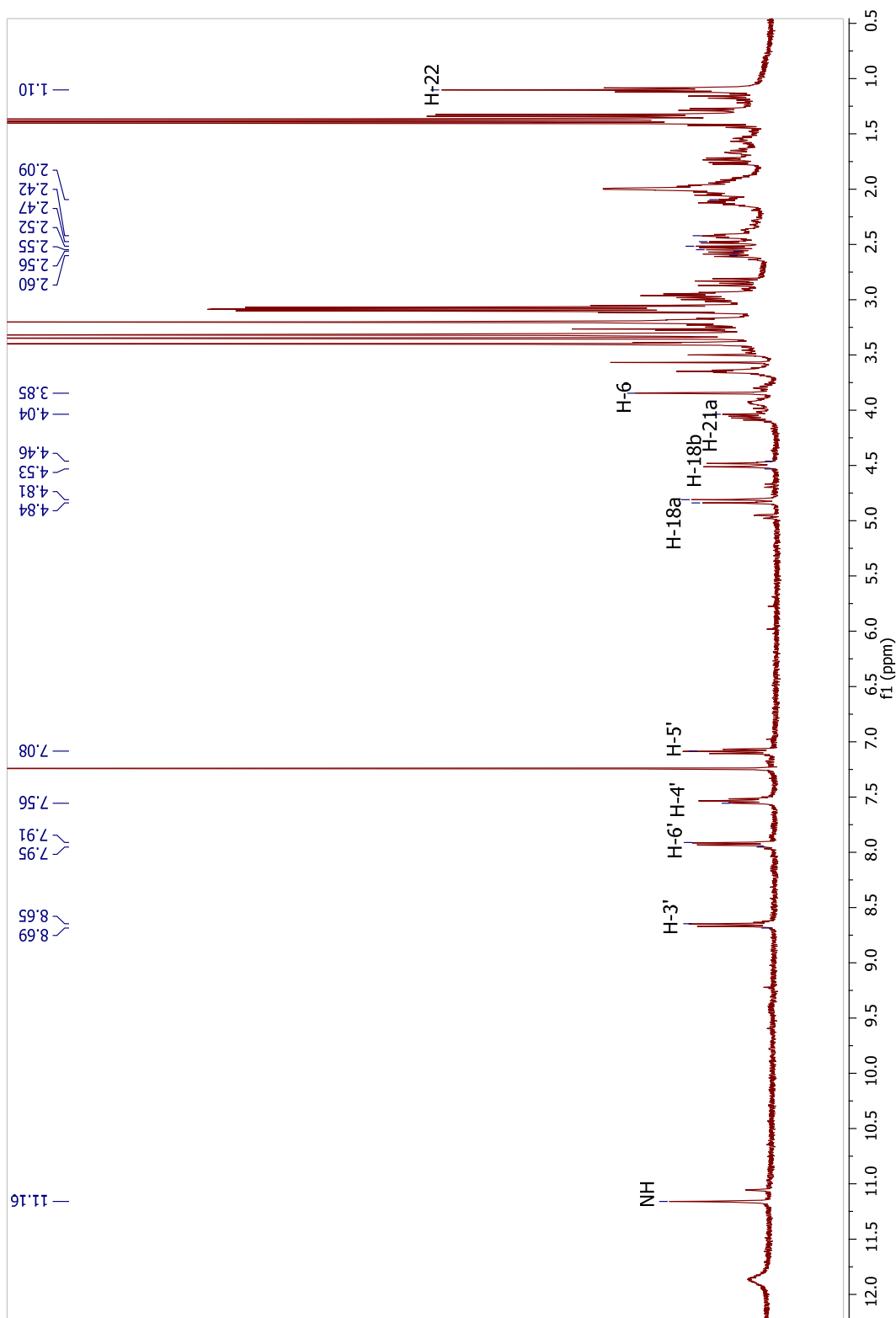


Figure 3.20 ^1H NMR spectrum of chrysotrichumine B (**79**), 400 MHz, in CDCl_3

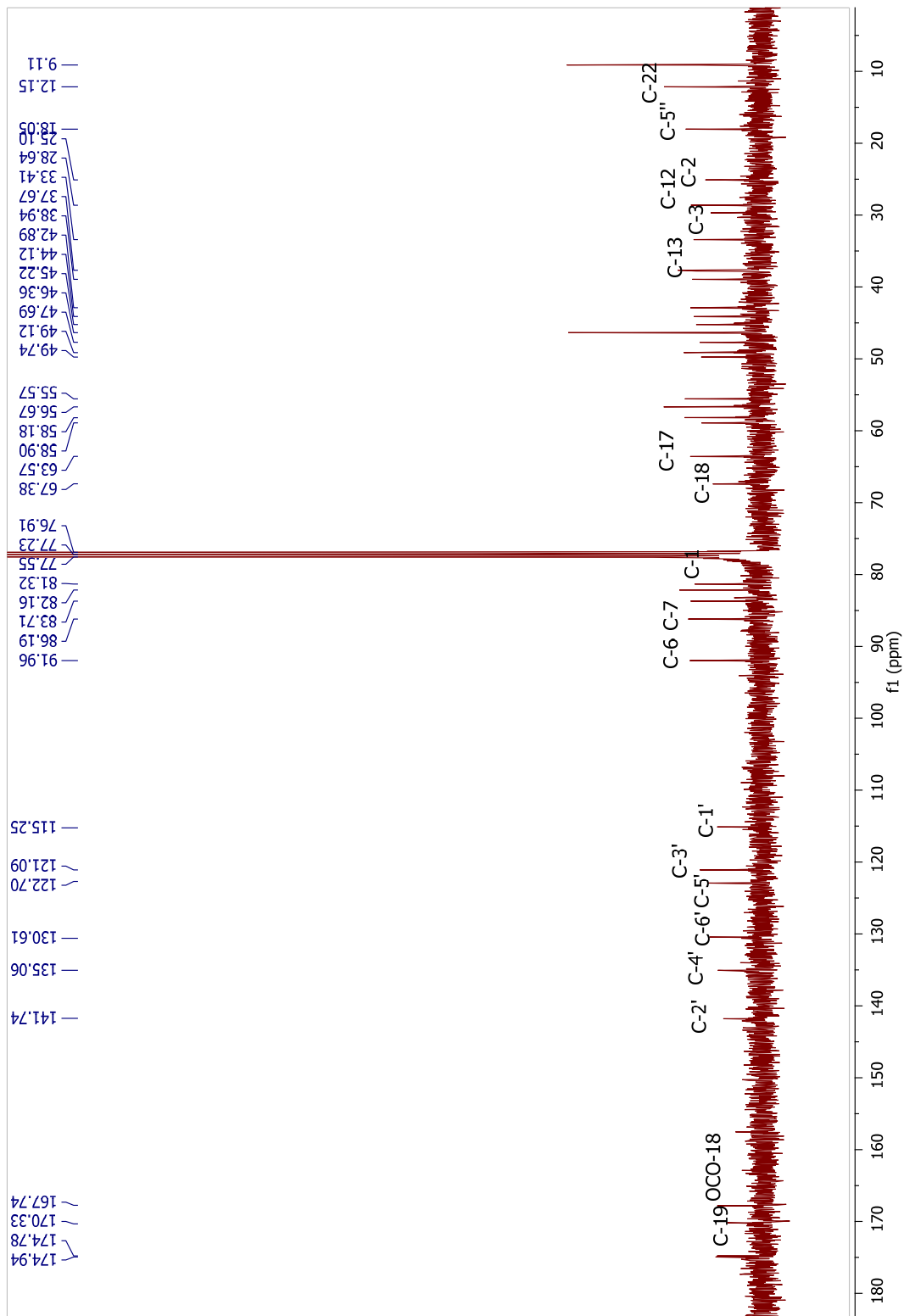


Figure 3.21 ^{13}C NMR spectrum of chrysotrichumine B (**79**), 100 MHz, in CDCl_3

3.3 Cytotoxic Activity

The new compound **77**, and the known compounds delpheline (**74**), isodelphatisine (**80**), delphatisine A (**81**), $3\beta,6\alpha$ -dlphydroxysclareollda (**83**), delsemine A (**85**), delavaine A (**87**) and delcorine (**88**) were evaluated for their cytotoxic activities against the MCF-7 and MDA-MB-231 (breast cancer cell lines). Unfortunately, all of the compounds revealed no cytotoxicity for either MCF-7 or MDA-MB-231 cell lines, except compound **87** which exhibited slight activity at 100 μM against MDA-MB-231, but had not reached the EC_{50} .

3.4 Conclusions

In a continuing exploration of natural products as the potential anti-cancer drug candidates from the genus *Delphinium*, the ethanol extract of *Delphinium chrysotrichum* resulted in the isolation of delphatisine D (**77**), a rare atisine-type alkaloid from genus *Delphinium*. It is the C-15 epimer of spiramine C (**90**) which bears an internal carbinolamine ether linkage (N–C–O–C) between C-7 and C-20. Also found with two new C₁₉-diterpenoid alkaloids, chrysotrichumines A and B (**78** and **79**), together with 11 known compounds. Among them, $3\beta,6\alpha$ -dlphydroxysclareollda (**82**) is a sesquiterpenoid first isolated from the genus *Delphinium*. The new compounds were identified and assigned by extensive spectroscopic analysis using NMR and high resolution mass spectrometry. The known compounds were identified by comparison of their ¹H, ¹³C NMR and MS data with those reported in the literature.

4. EXPERIMENTAL PROCEDURES

4.1 General Experimental Procedures

Optical rotations were measured on a JASCO P-1010 polarimeter (*c* g/100 mL) equipped with a halogen lamp (589 nm) and a 10 mm microcell. CD spectra were recorded with a JASCO J-810 spectropolarimeter by using a 2 mm cuvette with methanol and acetone as the solvent. IR spectra were recorded on a Nicolet Magna-IR 750 spectrophotometer. All NMR spectra were recorded on a Varian Unity-INOVA 400 spectrometer. All chemical shifts (δ) were referenced internally to the residual solvent peak (CD₃OD: ¹H, δ_{H} 3.31 ppm; ¹³C, δ_{C} 49.15 ppm; CDCl₃: ¹H δ_{H} 7.24 ppm; ¹³C δ_{C} 77.23 ppm; *d*₆-DMSO: ¹H δ_{H} 2.50 ppm; ¹³C δ_{C} 39.50 ppm). Short- and long-range ¹H – ¹³C correlations were determined with gradient-enhanced inverse-detected HSQC and HMBC experiments, respectively. NOE correlations were detected by 2D NOESY experiments with a 0.5 s mixing time. ESIMS data were recorded on a Bruker Esquire 3000 plus spectrometer, and HRESIMS data were obtained using Bruker APEX III 7.0T and APEXII FT-ICR spectrometers, respectively. Preparative HPLC was carried out using Shimadzu-20A with Shim-park RP-C18 column (20 × 200 mm), hemi-RP-C18 column (10 × 200 mm), RP-C8 (20 × 200 mm), RP-PRP-1 (20 × 200 mm) and SPD-M20A and ELSD-LTII detectors.

4.2 Plant Material Collections

4.2.1 Collection for *Cornus controversa*

The leaves of *Cornus controversa* were collected in Oxford, Mississippi, in 2011 by Dr. Mark. T. Hamann of the University of Mississippi. The voucher specimens are kept in the Department of Pharmacognosy at the University of Mississippi.

4.2.2 Collection for *Delphinium chrysotrichum*

The aerial part of the plants *Delphinium chrysotrichum* were collected in the Lhasa area, Tibet Autonomous Region, People's Republic of China, in August 2009. Voucher specimens (2009D026) were deposited at the Department of Applied Chemistry, Xi'an University of Technology, Xi'an, China and were identified by Prof. Ping Tian.

4.3 Extraction and Isolation of Cornosides A, B and Cornolactones A –E

The leaves of *C. controversa* (15.0 kg, dry weight) were extracted with 95% ethanol (3 × 25 L, 48 h each), and dried in *vacuo* to give the crude extract (900 g). The crude extract (400 g) was first separated on a silica gel column (20 × 70 cm) eluted by step gradients of hexanes-EtOAc (100:0, 80:20, 50:50 and 0:100, v/v, each 3 L) and EtOAc-CH₃OH mixtures (80:20, 60:40, 50:50 and 0:100, v/v, each 3 L) to afford eight fractions. Fraction E (20% CH₃OH in EtOAc) has been initially found to exhibit moderate anti-fungal activity. Fr. E (90 g) was eluted on HP-20 (8 × 50 cm) with a gradient of acetone in water (90:10, 80:20, 50:50, 40:60, 20:80 and 0:100, v/v, each 2 L) to give six sub-fractions (Fr. E₁- E₆). Then, Fr. E₂ (44.0 g) was repeatedly separated on preparative **RP MPLC** (packed with C18 column; 20 × 250 mm; step gradient from 20% CH₃OH in H₂O to 35% CH₃OH in H₂O for 40 min, and followed by 35-65% CH₃OH in

H₂O for 20 min, 12 mL/min) to afford eight sub-fractions (Fr. E_{2a}–E_{2i}). Fraction Fr. E_{2d} (4.0 g) was further repeatedly chromatographed over **RP MPLC** (C18 column; 20 × 250 mm with gradient elution from 8% to 45% of CH₃CN in H₂O in 120 min to yield eight sub-fractions (Fr. E_{2d-1} to Fr. E_{2d-8}). Fraction Fr. E_{2d-2} (50.0 mg) was separated on **RP HPLC** (Shim-park RP-C18; 5 μm; 10 × 250 mm; 10-40% CH₃OH in H₂O for 90 min, 7 mL/min) to yield compounds **4** (9.7 mg, *t_R* 31.62 min) and **10** (2.0 mg, *t_R* 34.38). Compound **17** (3.5 mg, *t_R* 34.26) was purified from fraction Fr. E_{2d-3} (30.0 mg) by **RP HPLC** C18 column with gradient eluted with 15-45% CH₃OH in H₂O for 50 min, 7 mL/min. Sub-fraction Fr. E_{2d-4} (500 mg) was further purified by **RP HPLC** (Shim-park RP-C18; 5 μm; 20 × 250 mm; 15-45% CH₃OH in H₂O for 90 min, 7 mL/min) to produce two interesting fractions with *t_R* at 35.35 and 37.14 min, based on their ¹H NMR spectra. The first fraction was purified by **RP HPLC** (Polar- C8; 5 μm; 20 × 250 mm; 15-45% CH₃OH in H₂O for 130 min, 5 mL/min) to yield **59** (5.0 mg *t_R* 76.2` min) and **58** (10.2 mg, *t_R* 80.4 min). The second fraction was further separated on **RP HPLC** (Shim-park RP-PRP; 5 μm; 20 × 250 mm; 15-45% CH₃CN in H₂O for 70 min, 7 mL/min) to yield compound **65** (2.2 mg, *t_R* 36.20). Then, Fr. E_{2d-6} (832 mg) was subjected to silica gel column (6 × 70 cm) chromatography using CH₂Cl₂-MeOH (90:10 to 0:100, v/v, each 500 mL) to afford nine fractions (Fr. E_{2d-6-a} to Fr. E_{2d-6-h}). Then, fraction Fr. F_{2d-6-a} (320 mg) was further purified by **RP HPLC** (Polar- C8; 5 μm; 20 × 250 mm; 20-65% CH₃OH in H₂O for 70 min, 5 mL/min) to yield three interesting fractions based on their ¹H NMR spectra with *t_R* at 36.15, 41.79 and 52.25 min. The first fraction was further purified on **PRP-1**; 5 μm; 10× 250 mm; 5-25% CH₃CN in H₂O for 50 min, 4 mL/min) to yield **62**

(2.0 mg, t_R 38.18 min). The second fraction was purified on PRP-1 column; 5 μm ; 20 \times 250 mm; 10-40% CH_3CN in H_2O for 50 min, 7 mL/min) to yield **63** (8.0 mg, t_R 41.52 min). The third fraction was separated on PRP-1; 5 μm ; 20 \times 250 mm; 15-45% CH_3CN in H_2O for 70 min, 7 mL/min) to yield **61** (4.0 mg, t_R 37.89 min).

In order to collect more of compound **59**, using the same procedures mentioned above, the rest of the crude extract (500 g) was loaded on a silica gel column (20 \times 70 cm) again, and eluted by step gradients of hexanes-EtOAc (100:0, 80:20, 50:50 and 0:100, v/v, each 4 L) and EtOAc- CH_3OH mixtures (80:20, 60:40, 50:50 and 0:100, v/v, each 4 L) to afford eight fractions. Fraction E (320 g) was fractionated on HP-20 (20 \times 70 cm) with a gradient of acetone in water (95:5, 90:10, 85:15, 80:20, 70:30, 60:40, 50:50, 40:60, 20:80 and 0:100, v/v, each 3 L) to give ten sub-fractions (Fr. E₁- E₁₀). Then, Fr. E₂ and Fr. E₃, combined together (40 g), was sequentially separated on HP20SS (10 \times 70 cm) by a gradient elution of acetone in water (95:5, 90:10, 85:15, 80:20, 75:25, 70:30, 60:40, 40:60, 20:80 and 0:100, v/v, each 1 L) to give ten sub-fractions (Fr. E_{3a}- Fr. E_{3j}). Compounds **68** (3.0 mg) and **69** (2.5 mg) were directly purified from fraction Fr. E_{3e} (120 mg) by loading on a silica gel column (6 \times 60 cm) and eluted by step gradients of 10% MeOH in CH_2Cl_2 to 100% MeOH. Then, sub-fraction Fr. E_{3b} (9.9 g) was further separated under regular pressure on a C18 column (4 \times 60 cm) and eluted by step gradients of MeOH in H_2O (95:5, 90:10, 85:15, 80:20, 70:30, 60:40, 50:50, 40:60, 20:80 and 0:100, v/v, each 500 mL) to afford ten fractions (Fr. E_{3b-A} to Fr. E_{3b-I}). The first two fractions had similar ¹H NMR spectra and combined together to form Fr. E_{3b-A+B} (1.2 g). This fraction was further separated on Lipophilic Sephadex column (4 \times 60 cm) and eluted by methanol to give four sub-fractions (Fr. E_{3b-A+B-1} to Fr. E_{3b-A+B-4}). Fraction Fr.

$E_{3b-A+B-2}$ (960 mg) was repeatedly separated by **RP HPLC** (Shim-park RP-C18 column; 5 μm ; 20 \times 250 mm; step gradient from 5% to 50% of CH_3CN in H_2O for 50 min, and followed from 50% to 100% for 10 min, 7 mL/min) to yield five fractions (Fr. $E_{3b-A+B-2-a}$ to Fr. $E_{3b-A+B-2-e}$) with t_R at 33.91, 35.98, 36.84, 38.66 and 39.60 min, respectively. Fr. $E_{3b-A+B-2-a}$ (97.5 mg) was sequentially purified by **RP HPLC** (Shim-park RP-C18 column; 5 μm ; 20 \times 250 mm; step gradient from 5% to 40% of CH_3CN in H_2O for 70 min, and then from 50% to 100% for 10 min, 7 mL/min) to yield compound **64** (12 mg, t_R 51.7 min). $E_{3b-A+B-2-b}$ (71.4 mg) was first purified by **RP HPLC** (RP-C18, 5 μm ; 20 \times 250 mm) column, followed by Polar- C8 column (5 μm ; 20 \times 250 mm) with the same gradient from 10% to 40% of CH_3CN in H_2O for 70 min, and then from 50% to 100% for 10 min, 7 mL/min) to yield compound **55** (5.0 mg, t_R 11.8 min). Compounds **60** (15.0 mg, t_R 51.1 min) and **66** (5.6 mg, t_R 63.8 min) were obtained from fraction $E_{3b-A+B-2-c}$ (51.0 mg) with gradient elution of 20-60% CH_3OH in H_2O for 70 min, 5 mL/min by **RP HPLC** (Polar- C8; 5 μm ; 20 \times 250 mm). From the fraction $E_{3b-A+B-2-d}$ (632 mg) we obtained compound **59** (60.0 mg, t_R 44.0 min) again and compound **67** (20.0 mg, t_R 55.1 min), by **RP HPLC** (Polar- C8; 5 μm ; 10 \times 250 mm; 10-20% CH_3OH in H_2O for 70 min, 5 mL/min). Compound **37** (5.2 mg) was yielded from fraction Fr. E_3 (20 g), after it was fractionated on a silica gel column (5 \times 60 cm) eluted by step gradients of CH_2Cl_2 -MeOH (90:10 to 0:100, v/v, each 500 mL) to afford nine fractions (Fr. E_{3-a} to Fr. E_{3-h}). Then Fr. E_{3-b} (30 mg) was further purified by **RP HPLC** (Polar- C8; 5 μm ; 10 \times 250 mm; 10-65% CH_3CN in H_2O for 70 min, 5 mL/min) to yield **37** (t_R 60.6 min).

Cornoside A (59): colorless gum; $[\alpha]_D^{18} - 13.8$ (*c* 0.013, CH₃OH); UV (CH₃OH) λ_{\max} (log ϵ) 230 (3.4) nm; IR (KBr) ν_{\max} : 3355, 2922, 1730, 1073, 1020 cm⁻¹; ¹H and ¹³C NMR data (Table 2.1). HRESIMS *m/z* 413.1417 [M + Na]⁺ (calcd for [M + Na]⁺ 413.1418).

Cornolactone A (60): colorless gum; $[\alpha]_D^{18} + 3.27$ (*c* 0.2, CH₃OH); UV (CH₃OH) λ_{\max} (log ϵ) 237 (3.2) nm; IR (KBr) ν_{\max} : 3355, 2922, 1730, 1073, 1020 cm⁻¹; ¹H and ¹³C NMR data (Table 2.6). HRESIMS *m/z* 171.1010 [M + H]⁺ (calcd for [M + H]⁺ 171.1016).

Cornolactone B (61): colorless gum; $[\alpha]_D^{18} - 7.46$ (*c* 0.015, CH₃OH); UV (CH₃OH) λ_{\max} (log ϵ) 243 (3.1) nm; IR (KBr) ν_{\max} : 2944, 1658, 1023 cm⁻¹; ¹H and ¹³C NMR data (Table 2.2). HRESIMS *m/z* 197.0811 [M + H]⁺ (calcd for [M + H]⁺ 197.0808).

Cornolactone C (62): colorless gum; $[\alpha]_D^{18} - 11.4$ (*c* 0.002, CH₃OH); UV (CH₃OH) λ_{\max} (log ϵ) 201 (3.1) nm; IR (KBr) ν_{\max} : 2960, 1774, 1733, 1086, 886 cm⁻¹; ¹H and ¹³C NMR data (Table 2.3). HRESIMS *m/z* 198.0869 [M - H₂O + H]⁺ (calcd for [M - H₂O + H]⁺ 198.0871).

Cornolactone D (63): colorless gum; $[\alpha]_D^{19} + 13.3$ (*c* 0.027, CH₃OH); UV (CH₃OH) λ_{\max} (log ϵ) 241 (3.1) nm; IR (KBr) ν_{\max} : 3337, 2952, 2937, 1733, 1650, 1017 cm⁻¹; ¹H and ¹³C NMR data (Table 2.4). HRESIMS *m/z* 215.0884 [M + Na]⁺ (calcd for [M + Na]⁺ 215.0890).

Cornolactone E (64): colorless gum; $[\alpha]_D^{18} + 18.5$ (*c* 0.021, CH₃OH); UV (CH₃OH) λ_{\max} (log ϵ) 240 (2.8) nm; IR (KBr) ν_{\max} : 3401, 2952, 1733, 1089, 1068 cm⁻¹; ¹H and ¹³C NMR data (Table 2.5). HRESIMS *m/z* 193.0834 [M + Na]⁺ (calcd for [M + Na]⁺ 193.0835).

Cornoside B (65): colorless gum; $[\alpha]_D^{18}$ - 29.2 (*c* 0.2, CH₃OH); UV (CH₃OH) λ_{\max} (log ϵ) 254 (2.7) nm; IR (KBr) ν_{\max} : 3305, 2970, 1715, 1650, 1453, 1081, 1017 cm⁻¹; ¹H and ¹³C NMR data (Table 2.7). HRESIMS *m/z* 366.1219 [M – H]⁻ (calcd for [M – H]⁻ 366.1220).

4.4 Extraction and Isolation of Delphatisine D (77), Chrysotrichumine A (78) and B (79)

The dried aerial part of *Delphinium chrysotrichum* (10.0 kg) were extracted with 90% ethanol (3 × 20 L, 48 h each), and dried in *vacuo* to give the crude extract. The EtOH extract was treated with 5 % HCl, and then the acidic solution was basified with 26 % NH₄OH to pH 10 and extracted with CHCl₃ (3 × 2 L) to give crude alkaloids (210 g) after removing the solvent. This residue was fractionated on a column packed with silica gel (100-200 μ m, 12 × 90 cm) and eluted by a step gradients of petroleum ether (PE)-acetone-diethylamine (100:10:2, 80:20:5, 60:40:5, 50:50:5, 40:60:5, 20:80:5 and 10:90:5, each 3 L) to afford 7 fractions (A – G). Fractions F and G exhibited moderate inhibitory effects on growth of human tongue cancer Tb cells. Fraction F (320 mg) was repeatedly separated by RP HPLC [Shim-park RP-C18 column; 5 μ m; 20 × 250 mm; step gradient from 20% MeCN in H₂O (0.02% diethylamine) to 40% MeCN in H₂O (0.02% diethylamine) for 40 min, and followed by 40-100% MeCN in H₂O for 50 min, 8 mL/min] to give compounds **83** (29.6 mg, *t_R* 41.4 min), **88** (18.7 mg, *t_R* 54.3 min), **82** (26.0 mg, *t_R* 60.9 min), **80** (19.0 mg, *t_R* 68.2 min), **74** (4 mg, *t_R* 77.4 min) and a major sub-fraction (90 mg) between the *t_R* from 62.2 to 66.7 minute. The major sub-fraction was further purified by RP HPLC (C18 column; 5 μ m; 20 × 250 mm; 25-100% MeCN in H₂O for 80 min, 8 mL/min) to give compounds **77** (6.6 mg, *t_R* 32.8 min) and **81** (18.0 mg,

t_R 38.6 min). Fraction G (36 g) was chromatographed over a silica gel column (100-200 μm , 6×50 cm) by eluting with chloroform/methanol (5:1, 4:1, 3:1, 2:1 and 1:2, v/v, each 2L) to give five sub-fractions (Fr. G₁-G₅). Sub-fraction G₃ (28 g) was further chromatographed on reversed-phase C₁₈ silica gel (6×50 cm) eluted with a gradient of H₂O/MeCN (100% H₂O, 80:20, 60:40, 50:50, 40:60, 20:80 and 100% MeCN, each 2L) to obtain seven sub-fractions (Fr. G_{3a}-G_{3g}). Fraction G_{3d} (6.7 g) was further separated on a 5×60 cm column packed with HP-20 and eluted by a step gradients of acetone-water (100:10, 80:20, 60:40, 50:50, 40:60, 20:80 and 100%, each 500 mL) to give 7 fractions (G_{3d-1} to G_{3d-7}). Sub-fraction G_{3d-4} (320 mg) was separated by reversed-phase HPLC [Shim-park RP-C18 column; 5 μm ; 20×250 mm; step gradient from 10% MeCN in H₂O (0.02% diethylamine) to 40% MeCN in H₂O (0.02% diethylamine) for 40 min, followed by 40-100% MeCN in H₂O (0.02% diethylamine) for 25 min, 8 mL/min] to give compounds **85** (25.0 mg, t_R 38.6 min) and **84** (24.0 mg, t_R 55.3 min). Sub-fraction G_{3d-3} (2.7 g) was repeatedly chromatographed over **RP MPLC** (C18 column; 20×250 mm with gradient elution from 10% to 100% of CH₃CN in H₂O in 120 min) to yield seven sub-fractions (Fr. F_{3d-3-A} to Fr. F_{3d-3-G}). Fractions F_{3d-3-C} and F_{3d-3-D} were combined together (1.1 g) and separated over a silica gel column (100-200 μm , 3×60 cm) by gradient elution with methylene chloride /methanol (5:1, 4:1, 3:1, 2:1 to 1:2, each 400 mL) to give 100 sub-fractions (Fr. F_{3d-3-C 1}- F_{3d-3-C100}, each collected around 20 mL). Fraction Fr. F_{3d-3-C 45} and Fr. F_{3d-3-C 55} were already pure and elucidated as compounds **86** (30 mg) and **87** (25 mg). Fraction Fr. F_{3d-3-C 57} (120 mg) was repeatedly purified by RP HPLC [(PRP-1 column; 5 μm ; 20×250 mm; from 15% MeCN in H₂O (0.02% diethylamine) to 40% MeCN in H₂O (0.02% diethylamine) for 40 min, and followed by

40-100% MeCN in H₂O (0.02% diethylamine) for 20 min, 8 mL/min)] to give compound **79** (4.1 mg, *t_R* 41.8 min). Fraction Fr. G_{3c} was repeatedly separated by reversed-phase HPLC [Shim-park RP-C18 column; 5 μm; 20 × 250 mm; step gradient from 20% MeCN in H₂O (0.02% diethylamine) to 40% MeCN in H₂O (0.02% diethylamine) for 60 min, and followed by 40-100% MeCN in H₂O for 10 min, 7 mL/min] to give **89** (60.8 mg, *t_R* 48.8 min) and a major sub-fraction (70 mg) from *t_R* 70.2 to 72.5 min. This major fraction was further purified by RP HPLC (C18 column; 5 μm; 20 × 250 mm; 15-50% MeCN in H₂O for 80 min, and followed by 50-100% MeCN in H₂O for 10 min, 7 mL/min) to give compound **78** (5.0 mg, *t_R* 71.6 min).

Delphatisine D (77): white amorphous powder; $[\alpha]_D^{18} - 50.0$ (*c* 0.37, MeOH); UV (CH₃OH) λ_{\max} (log ϵ) 242 (3.1) nm; IR (KBr) ν_{\max} : 3443, 2919, 1640, 1031, 911 cm⁻¹; ¹H and ¹³C NMR data (**Table 3.1**). ESI-HRMS *m/z* 358.2377 [M + H]⁺ (calcd for C₂₂H₃₂NO₃, 358.2377).

Chrysotrichumines A (78): colorless gum; $[\alpha]_D^{18} + 5.9$ (*c* 0.008, MeOH); UV (CH₃OH) λ_{\max} (log ϵ) 250 (4.1) nm; IR (KBr) ν_{\max} : 3412, 2941, 1643, 1116, 1044 cm⁻¹; ¹H and ¹³C NMR data (**Table 3.4**). ESI-HRMS *m/z* 538.2665 [M + H]⁺ (calcd for C₂₅H₄₀NO₆, 538.2647).

Chrysotrichumines B (79): colorless amorphous powder; $[\alpha]_D^{18} + 12.0$ (*c* 0.02, MeOH); UV (CH₃OH) λ_{\max} (log ϵ): 321 (3.4), 268 (3.4), 252 (3.6) and 220 (3.6) nm; IR (KBr) ν_{\max} : 3337, 1631, 1173, 1075, 764 cm⁻¹; ¹H and ¹³C NMR data (**Table 3.5**). ESI-HRMS *m/z* 737.3271 [M + Na]⁺ (calcd for C₃₇H₅₁N₃O₁₁Na, 737.3256).

2.5.4 Acid Hydrolysis and Determination of the Sugar Configuration

Cornoside A (**59**) (2 mg) was hydrolyzed by using 1 M HCl (0.4 mL) at 100 °C for 2 h under the argon and neutralized with Amberlite IR 400. After drying in *vacuo*, the residue was dissolved in pyridine (0.4 mL) containing L-cysteine ethyl ester hydrochloride (2 mg) and heated at 60 °C for 1 h. A 0.4 mL solution of 3, 5-dichlorophenyl isothiocyanate (2 mg) in pyridine was added to the mixture, which was heated to and held at 60 °C for 1 h. The reaction mixture was directly analyzed by analytical HPLC on a Shim-park RP-C18 column; 5 μ m; 4.6 \times 250 mm column by eluting with a gradient of 30-80% CH₃CN in H₂O with 0.02% HCOOH for 40 min and subsequent washing of the column with 100% CH₃CN at a flow rate 0.8 mL/min. In the acid hydrolysate of **59**, D-glucose was confirmed by comparison of the retention times of their derivatives with those of D-glucose and L-glucose derivatives prepared in the same way, which showed retention times of 34.8 and 34.0 min, respectively.

4.5 Determination of PPAR γ and LXR Agonistic Activities

Cell-based luciferase reporter gene assay was used to evaluate PPAR γ and LXR agonistic activities of compounds. Human hepatoma (HepG2) cells and Chinese hamster ovary cells (CHO) cells were cultured in DMEM/ Ham's F12 medium which was supplemented with FBS (10%) and antibiotics (penicillin G sodium 100 U/mL and streptomycin 100 lg/mL) at 37 °C in an atmosphere of 95% humidity and 5% CO₂. At about 75% confluence, cells were harvested by trypsinization and transfected with firefly Luc reporter gene constructs containing PPAR γ and peroxisome proliferator response element (PPARE) in HepG2 cells and CHO cells, respectively. Briefly, 25 μ g of DNA was added to 500 μ L cell suspension (5×10^6 cells) and incubated for 5 min at room

temperature in BTX disposable cuvettes. The cells were electroporated at 150 V and a single 70 ms pulse in a BTX Electro Square Porator T 820 (BTX I, San Diego, CA (4 mm)). Transfected cells were plated in 96-well plate at a density of 5×10^4 cells/well and grown for 24 h. The cells were treated with different concentrations of test compounds for 24 h, followed by addition of 40 μ L 1:1 mixture of Luc-Lite reagent and PBS containing 1 mM calcium and magnesium. Luciferase activity was determined in terms of light output measured on a TopCount microplate reader (Packard Instrument Co. Meriden, CT) in a single photon counting mode.

For LXR agonistic activity, 5×10^6 of CHO cells were harvested and transiently transfected with the reporter gene constructs LXR and LXRE using electroporation (155 V, 70 mV, 1 pulse). After transfection, cells were transferred into 96 well microtiter plates and cultured for 24 h. Cells were washed once with Ham's F12 basic medium and cultured in Ham's F12 medium with 5% NCLDS serum and 20 μ g/mL of LDL or without LDL. Drug treatment and luciferase assay were the same as PPAR assay. The ciglitazone and 25-hydroxyl-cholesterol were used as positive control for PPAR γ and LXR, respectively.

4.6 MTT Cytotoxicity Assay

Cell viability was assessed using Human breast cancer cell lines MCF-7 and MDA-MB-231 were cultured in DMEM medium, supplemented with 10% fetal bovine serum, 100 units/mL penicillin, and 100 μ g/mL streptomycin. The cell cultures were incubated at 95% relative humidity, 5% CO₂, and 37°C. Cytotoxicity was measured by a 3-(4,5-dimethylthiazol-2-yl)-2,5-diphenyltetrazolium bromide (MTT) colorimetric

assay with minor modification as described in the reference procedure.⁵² In short, cells were seeded in 96-well microculture plates at 2×10^4 cells per well and allowed to adhere for 24 h before drug addition. Then, each tumor cell was treated with various concentrations of compounds **4**, **10**, **58**, **59**, **62 – 64** and **74**, **80**, **81**, **83** and **86 – 88** for 48 h at 37°C. After the incubation, 20 μ L 5 mg/mL MTT was added to each well and incubation was continued for 4h at 37°C. After 4 h, the culture medium supernatant was removed from wells by slow aspiration using a multichannel pipet and replaced with 150 μ L DMSO. Cell viability was measured using a microculture plate reader (Dynatech MR600, Alexandria, VA) at 540 nm (single wavelength, calibration factor = 1.00). Assays were run in duplicate and vincristine (Sigma) was used as a positive control.

APPENDIX 1

ISOLATION AND STRUCTURAL ELUCIDATION OF SEVEN NEW COMPOUNDS FROM *CORNUS CONTROVERSA*

A1-1 HRESIMS spectrum of cornoside A (**59**)

A1-2 $^1\text{H} - ^1\text{H}$ COSY spectrum of cornoside A (**59**), 400 MHz, in d_6 -DMSO

A1-3 HSQC spectrum of cornoside A (**59**), 400 MHz, in d_6 -DMSO

A1-4 HMBC spectrum of cornoside A (**59**), 400 MHz, in d_6 -DMSO

A1-5 NOESY spectrum of cornoside A (**59**), 400 MHz, in d_6 -DMSO

A1-6 1DNOESY spectrum of Cornoside A (**59**) in d_6 -DMSO (irradiated H-6)

A1-7 1DNOESY spectrum of Cornoside A (**59**) in d_6 -DMSO (irradiated H-4)

A1-8 1DNOESY spectrum of Cornoside A (**59**) in d_6 -DMSO (irradiated H-7 α)

A1-9 1DNOESY spectrum of Cornoside A (**59**) in d_6 -DMSO (irradiated H-8)

A1-10 HRESIMS spectrum of cornolactone A (**60**)

A1-11 $^1\text{H} - ^1\text{H}$ COSY spectrum of cornolactone A (**60**), 400 MHz, in CDCl_3

A1-12 HSQC spectrum of cornolactone A (**60**), 400 MHz, in CDCl_3

A1-13 HMBC spectrum of cornolactone A (**60**), 400 MHz, in CDCl_3

A1-14 NOESY spectrum of cornolactone A (**60**), 400 MHz, in CDCl_3

A1-15 HRESIMS spectrum of cornolactone B (**61**)

A1-16 $^1\text{H} - ^1\text{H}$ COSY spectrum of cornolactone B (**61**), 400 MHz, in CDCl_3

A1-17 HSQC spectrum of cornolactone B (**61**), 400 MHz, in CDCl_3

A1-18 HMBC spectrum of cornolactone B (**61**), 400 MHz, in CDCl₃

A1-19 NOESY spectrum of cornolactone B (**61**), 400 MHz, in CDCl₃

A1-20 HRESIMS spectrum of cornolactone C (**62**)

A1-21 ¹H – ¹H COSY spectrum of cornolactone C (**62**), 400 MHz, in CD₃OD

A1-22 HSQC spectrum of cornolactone C (**62**), 400 MHz, in CD₃OD

A1-23 HMBC spectrum of cornolactone C (**62**), 400 MHz, in CD₃OD

A1-24 NOESY spectrum of cornolactone C (**62**) after estification, 400 MHz, in CD₃OD

A1-25 ¹H NMR spectrum of cornolactone C (**62**) after estification, 400 MHz, in CDCl₃

A1-26 HRESIMS spectrum of cornolactone D (**63**)

A1-27 ¹H – ¹H COSY spectrum of cornolactone D (**63**), 400 MHz, in CDCl₃

A1-28 HSQC spectrum of cornolactone D (**63**), 400 MHz, in CDCl₃

A1-29 HMBC spectrum of cornolactone D (**63**), 400 MHz, in CDCl₃

A1-30 NOESY spectrum of cornolactone D (**63**), 400 MHz, in CDCl₃

A1-31 1DNOESY spectrum of Cornolactone D (**63**) in CDCl₃ (irridated H-1α)

A1-32 1DNOESY spectrum of Cornolactone D (**63**) in CDCl₃ (irridated H-4)

A1-33 1DNOESY spectrum of Cornolactone D (**63**) in CDCl₃ (irridated H-8)

A1-34 HRESIMS spectrum of cornolactone E (**64**)

A1-35 ¹H – ¹H COSY spectrum of cornolactone E (**64**), 400 MHz, in CDCl₃

A1-36 HSQC spectrum of cornolactone E (**64**), 400 MHz, in CDCl₃

A1-37 HMBC spectrum of cornolactone E (**64**), 400 MHz, in CDCl₃

A1-38 NOESY spectrum of cornolactone E (**64**), 400 MHz, in CDCl₃

A1-39 HRESIMS spectrum of cornoside B (**65**)

A1-40 ¹H NMR spectrum of cornoside B (**65**), 400 MHz, in CD₃OD

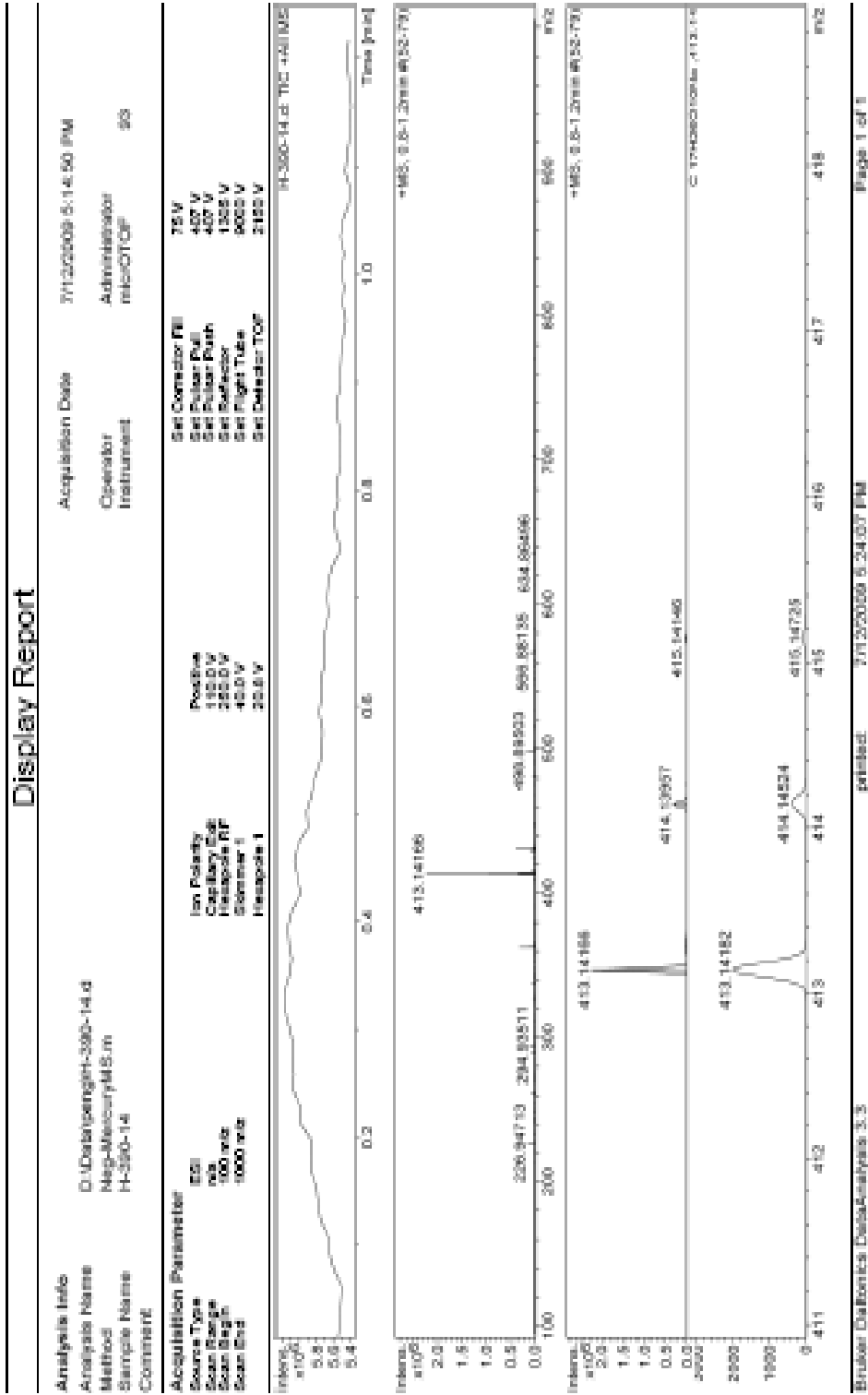
A1-41 ^{13}C NMR spectrum of cornoside B (**65**), 100 MHz, in CD_3OD

A1-42 $^1\text{H} - ^1\text{H}$ COSY spectrum of cornoside B (**65**), 400 MHz, in CDCl_3

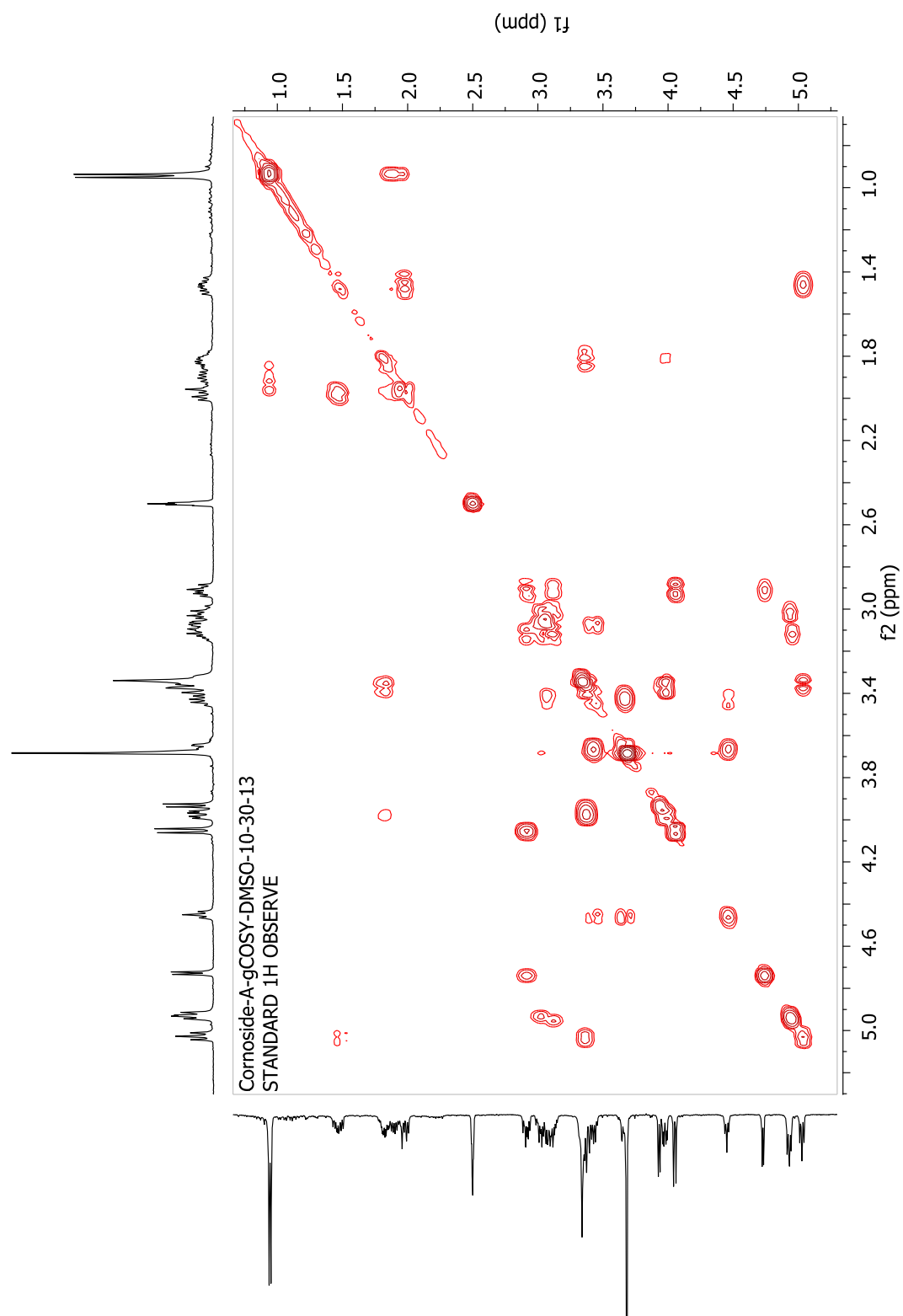
A1-43 HSQC spectrum of cornoside B (**65**), 400 MHz, in CDCl_3

A1-44 HMBC spectrum of cornoside B (**65**), 400 MHz, in CDCl_3

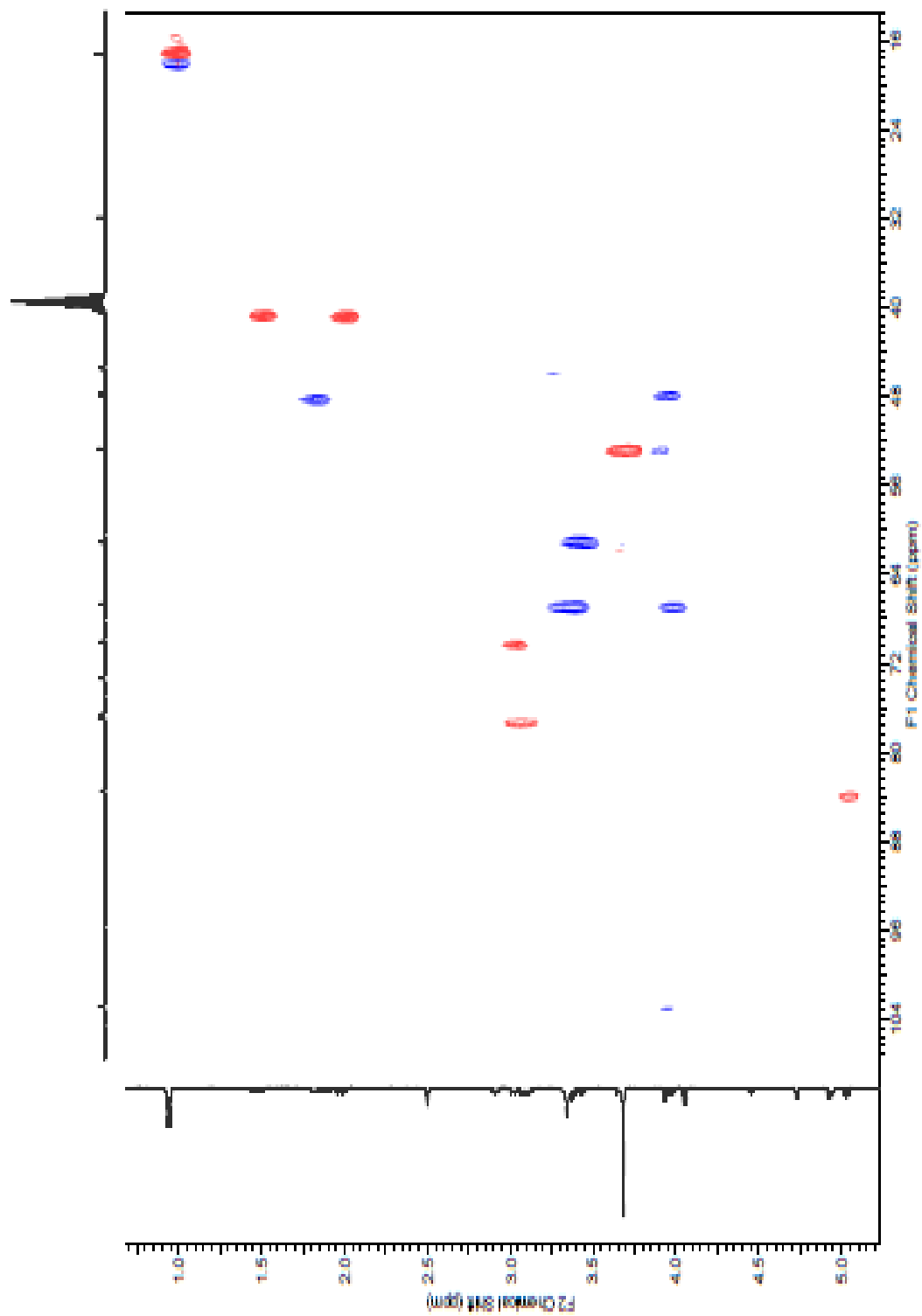
A1-1 HRESIMS spectrum of cornoside A (59)



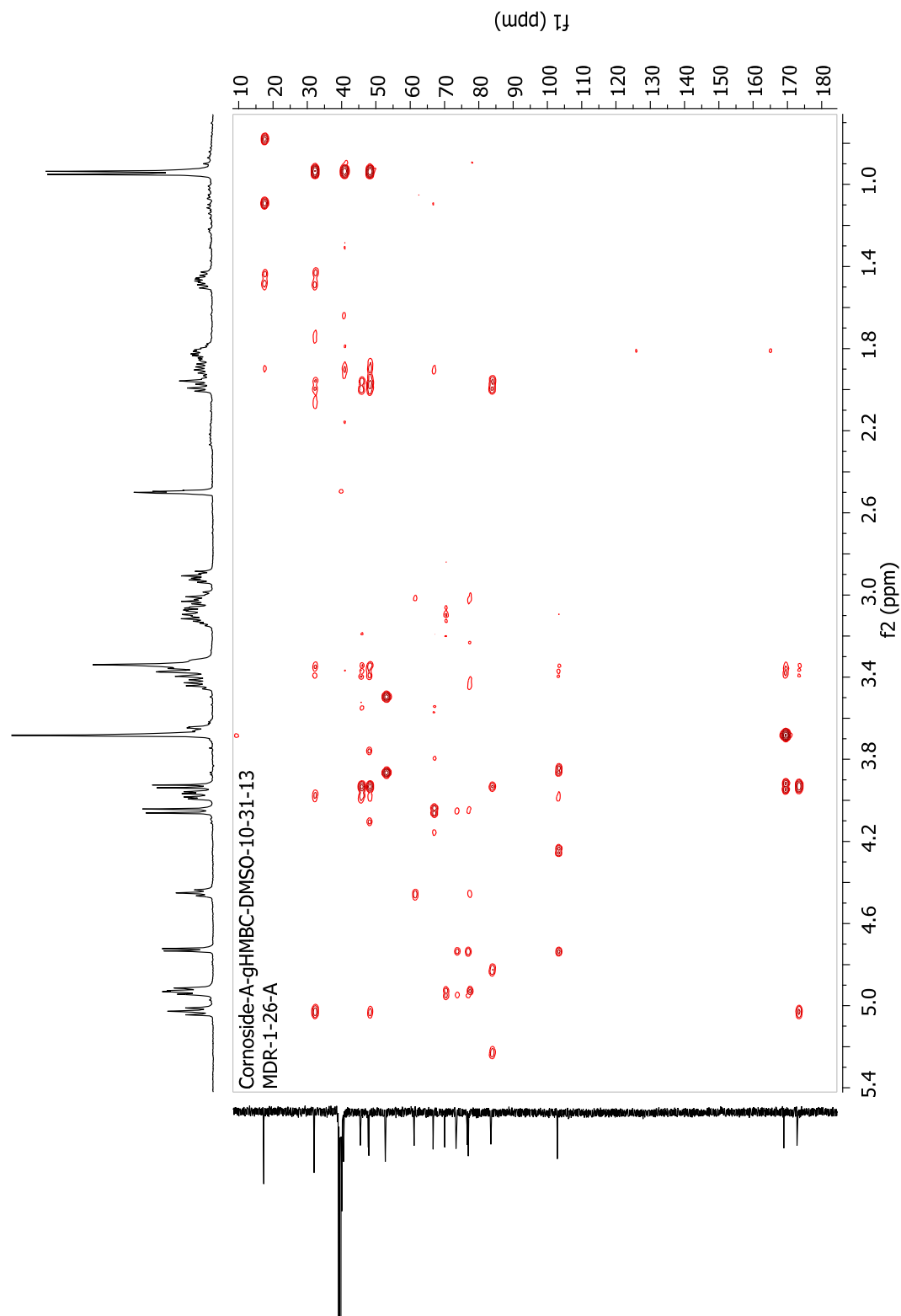
A1-2 $^1\text{H} - ^1\text{H}$ COSY spectrum of cornoside A (**59**), 400 MHz, in d_6 -DMSO



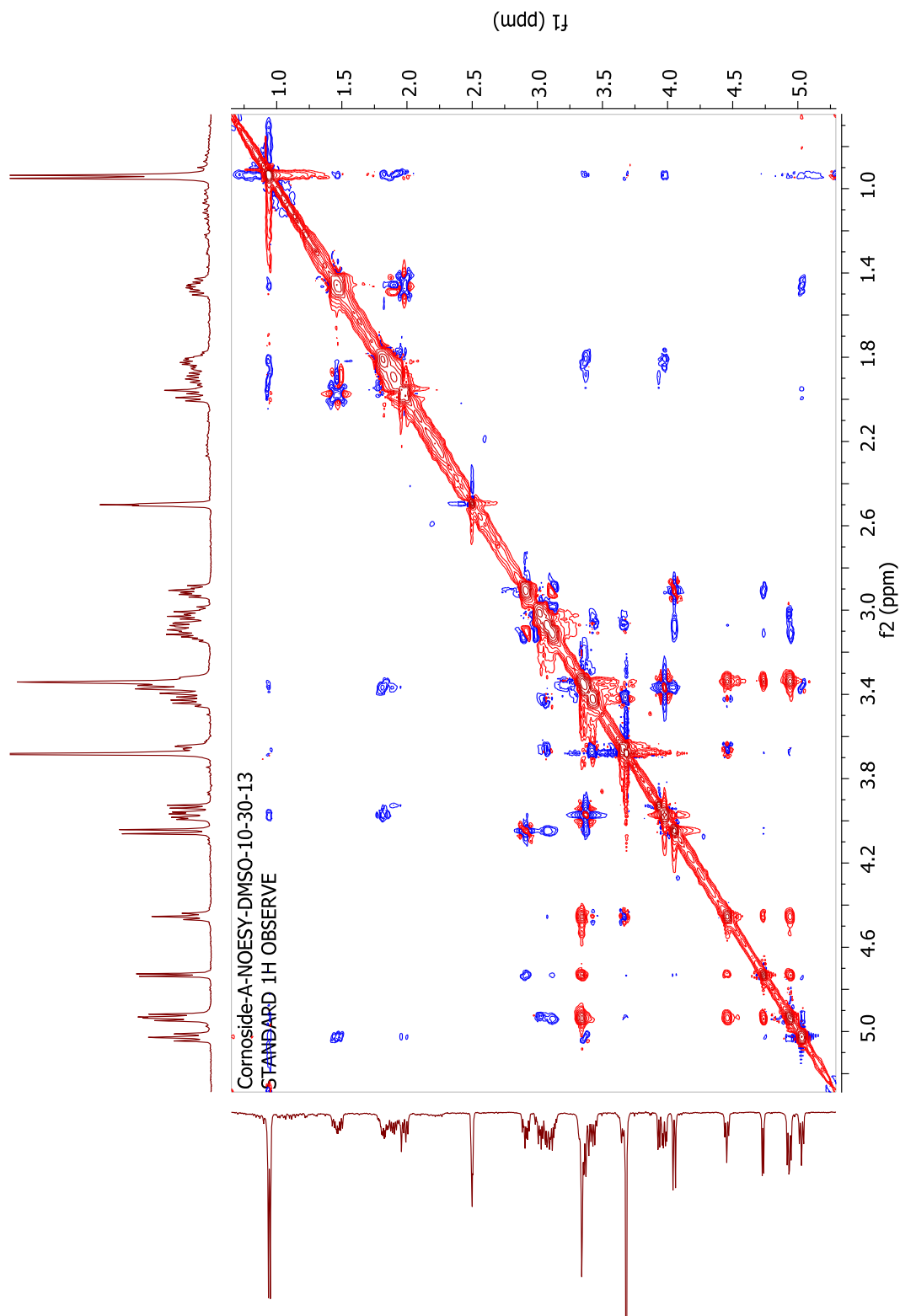
A1-3 HMQC spectrum of cornoside A (**59**), 400 MHz, in d_6 -DMSO



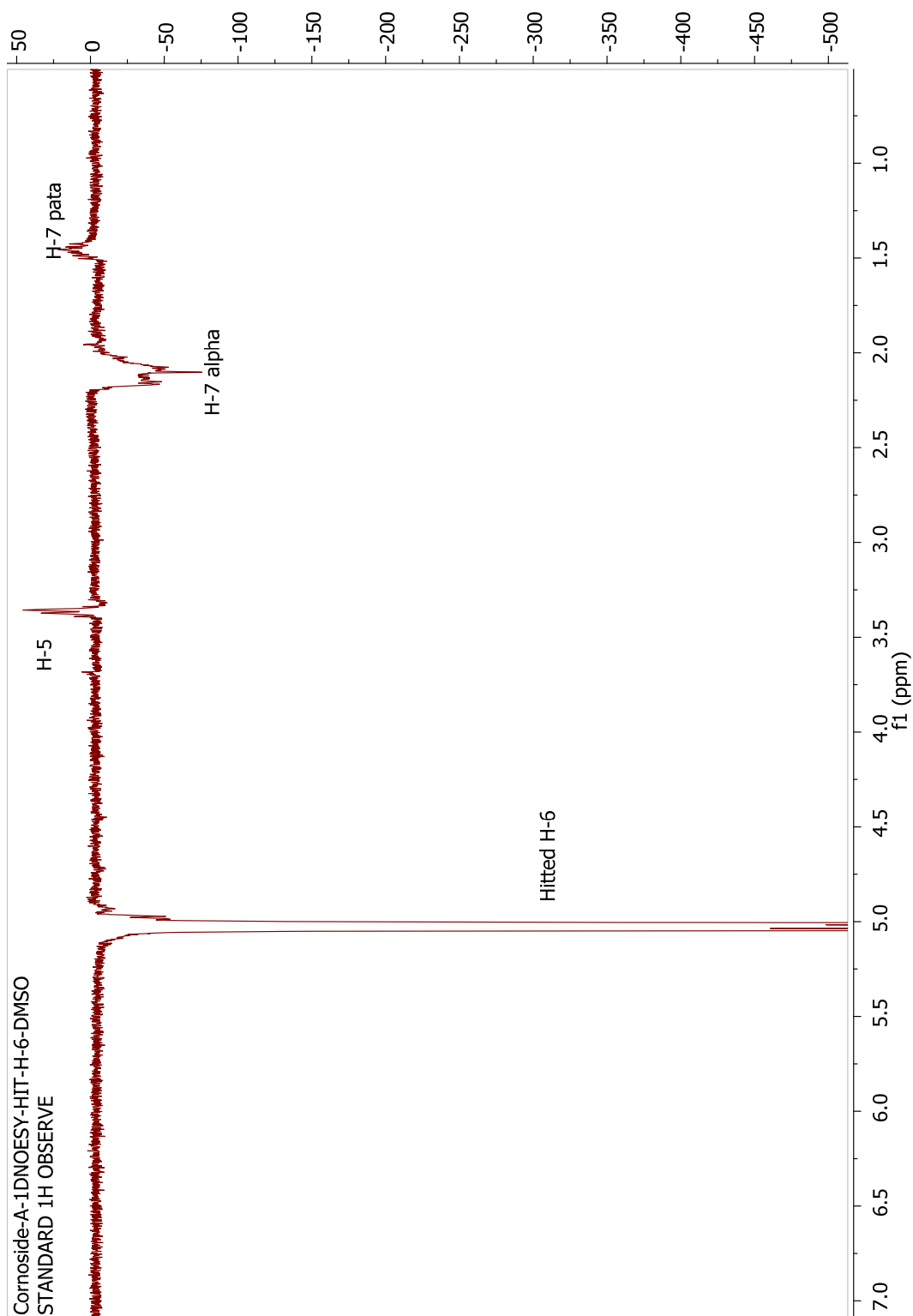
A1-4 HMBC spectrum of cornoside A (59), 400 MHz, in d_6 -DMSO



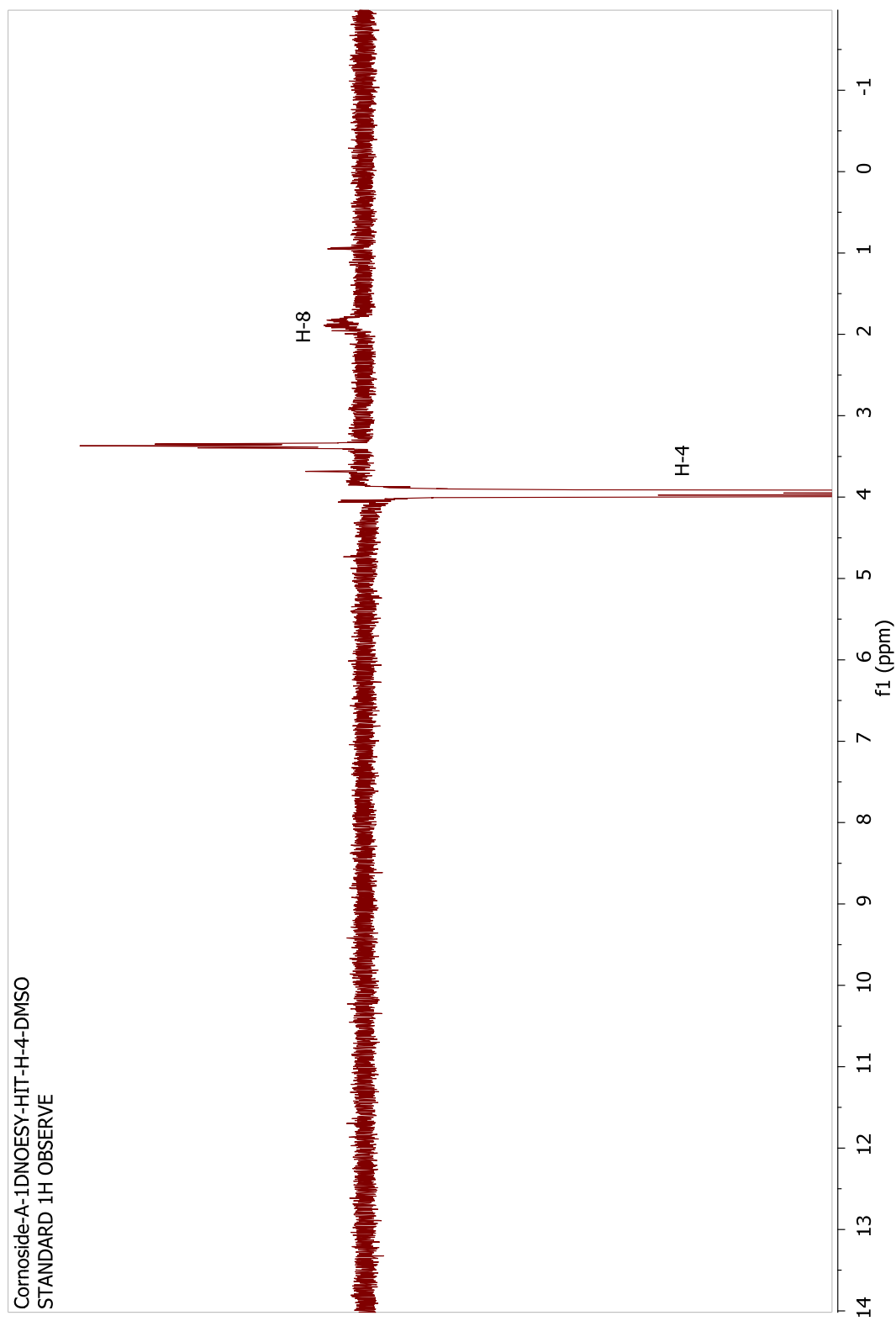
A1-5 NOESY spectrum of cornoside A (**59**), 400 MHz, in d_6 -DMSO



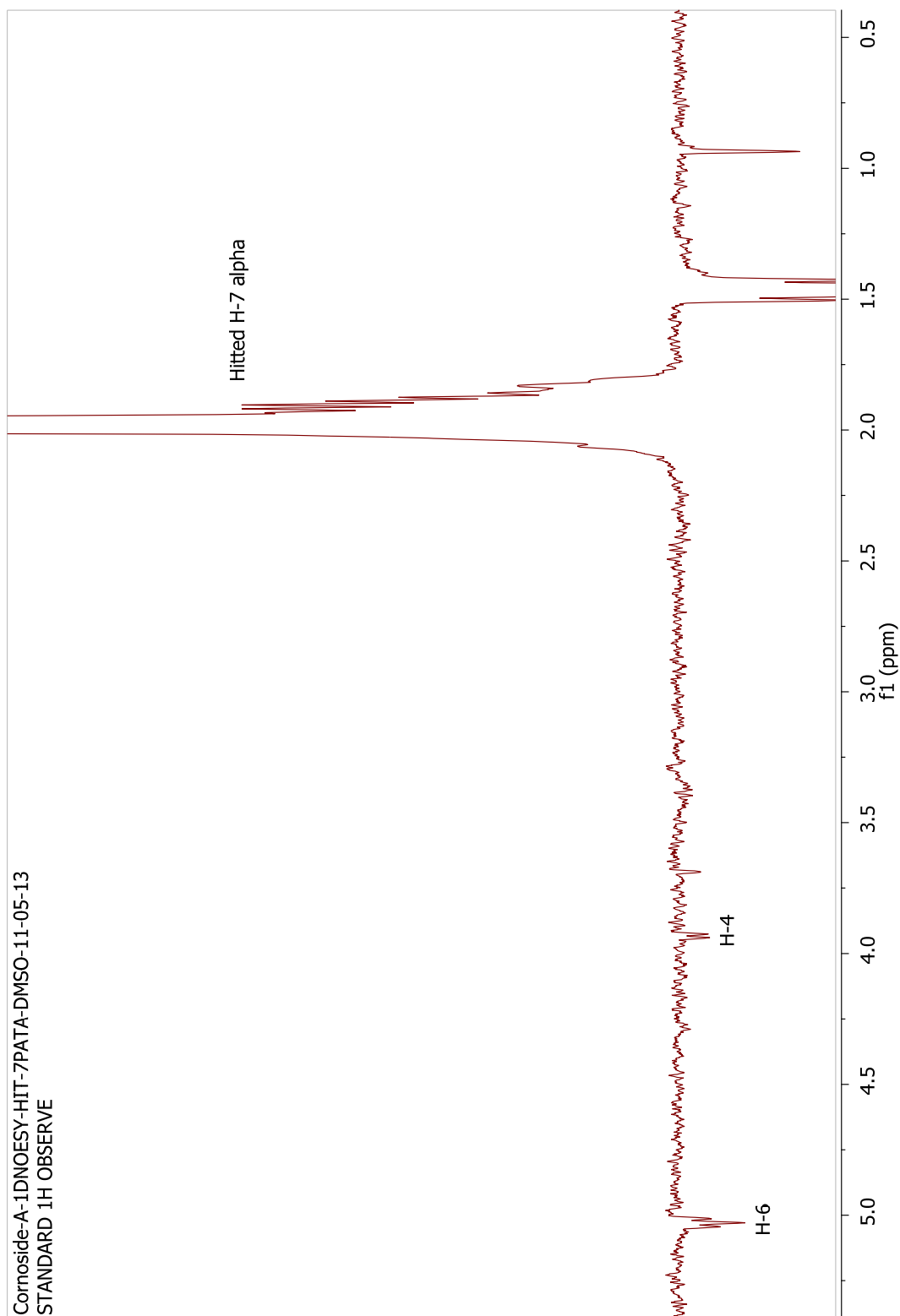
A1-6 1D NOESY spectrum of Cornoside A (**59**) in d_6 -DMSO (irradiated H-6)



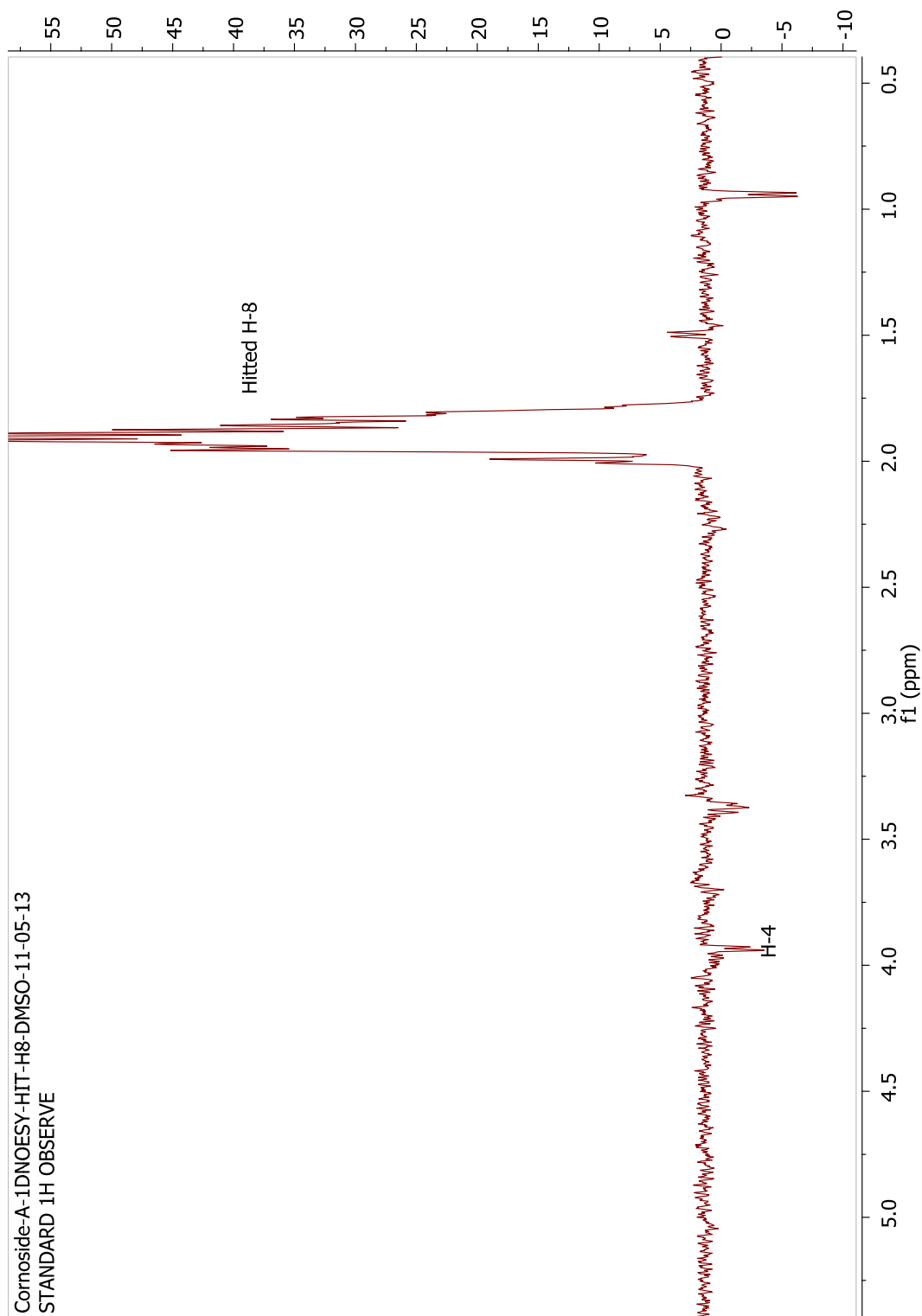
A1-7 1D NOESY spectrum of Cornoside A (**59**) in d_6 -DMSO (irradiated H-4)



A1-8 1D NOESY spectrum of Cornoside A (**59**) in d_6 -DMSO (irradiated H-7 α)

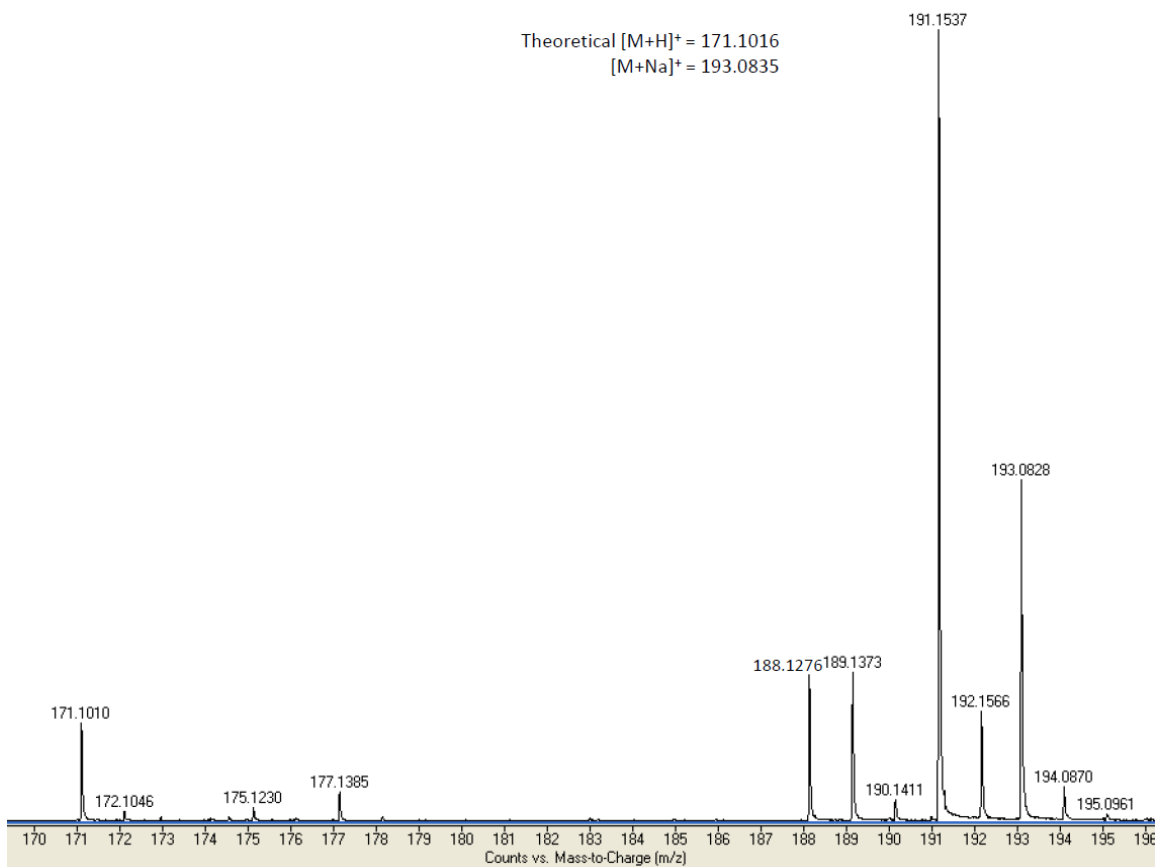


A1-9 1D NOESY spectrum of Cornoside A (59) in d_6 -DMSO (irradiated H-8)

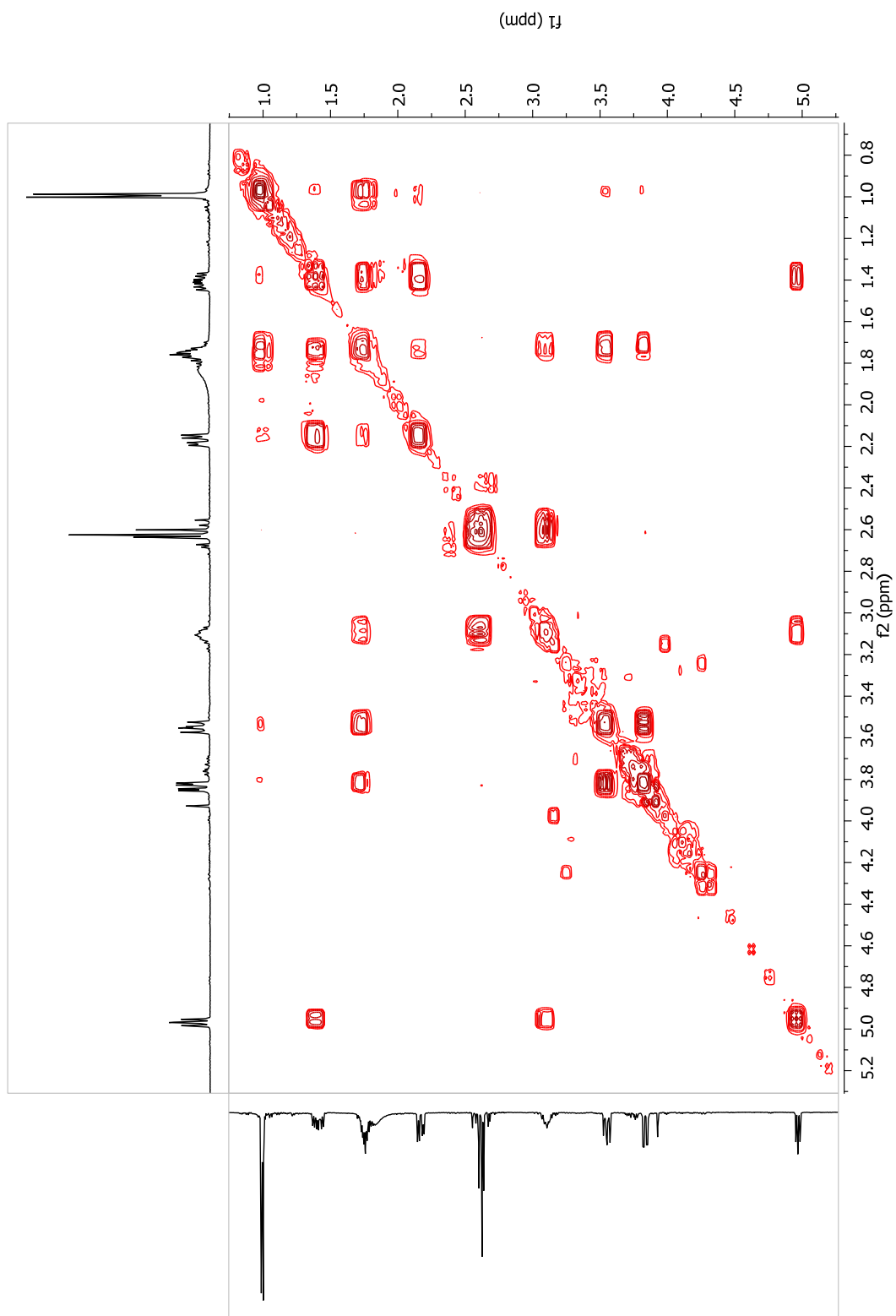


A1-10 HRESIMS spectrum of cornolactone A (60)

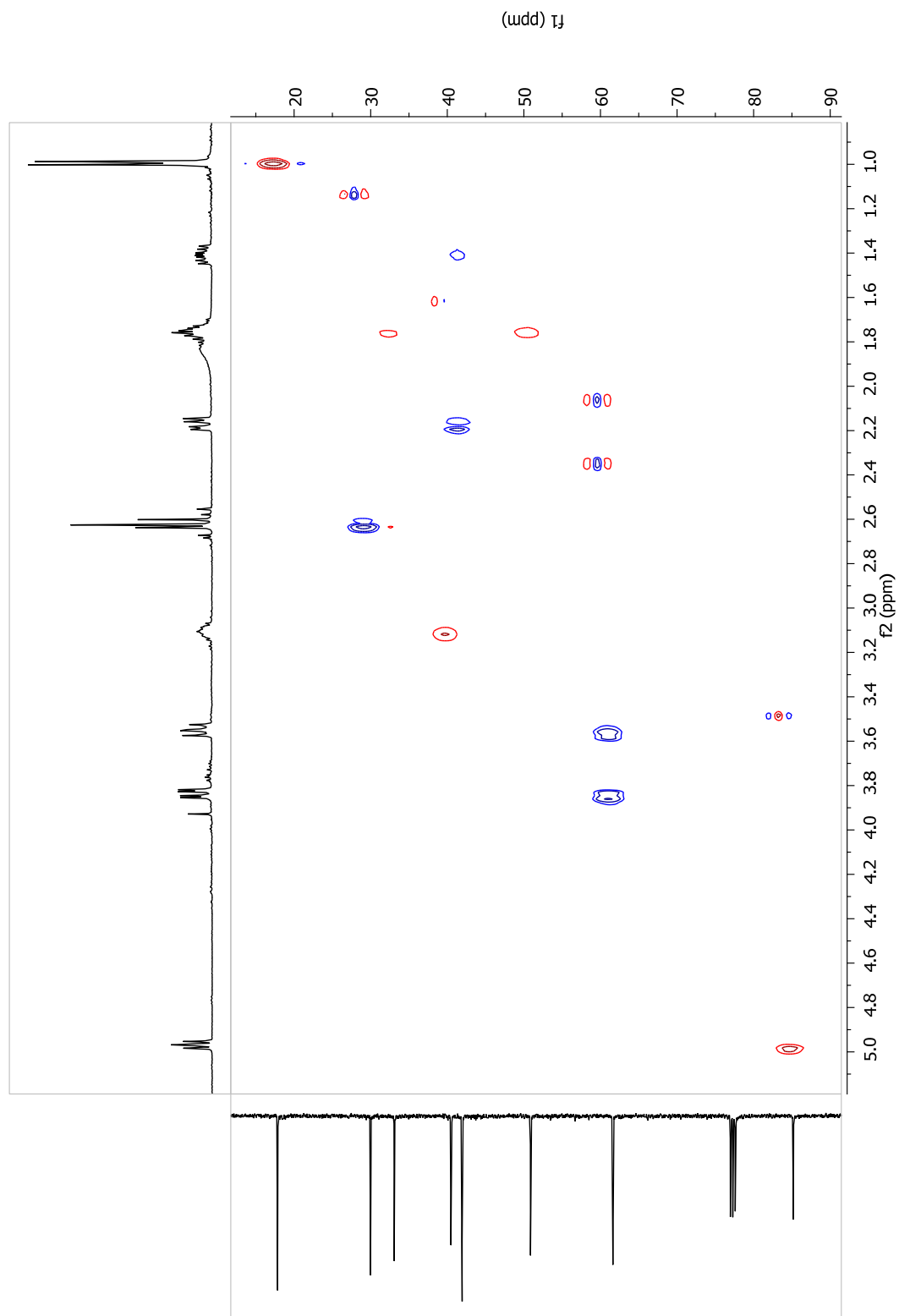
+ESI Scan (0.135-0.185 min, 4 scans) Frag=120.0V 19803_Cornoside F_ESI.d Subtract



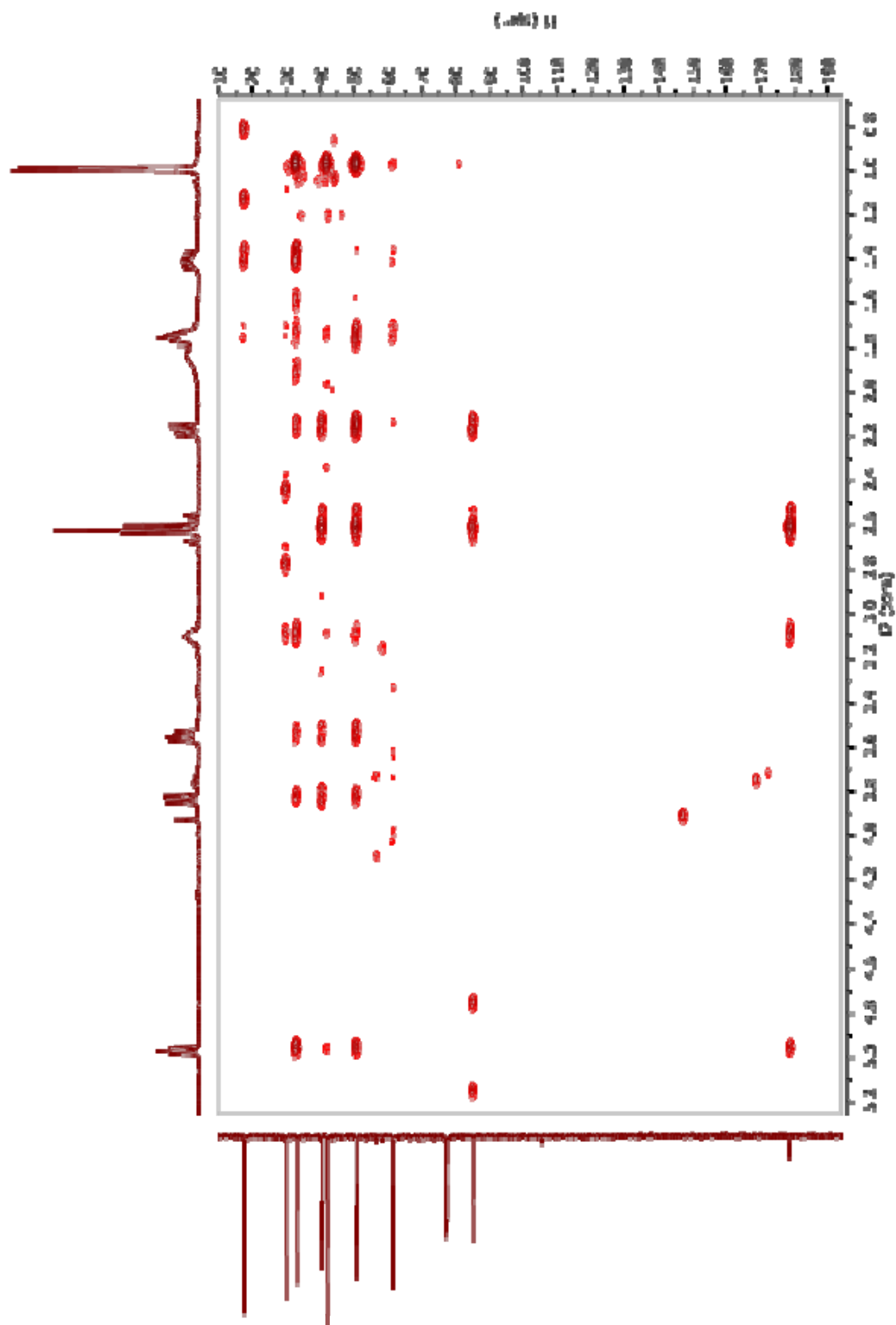
A1-11 $^1\text{H} - ^1\text{H}$ COSY spectrum of cornolactone A (**60**), 400 MHz, in CDCl_3



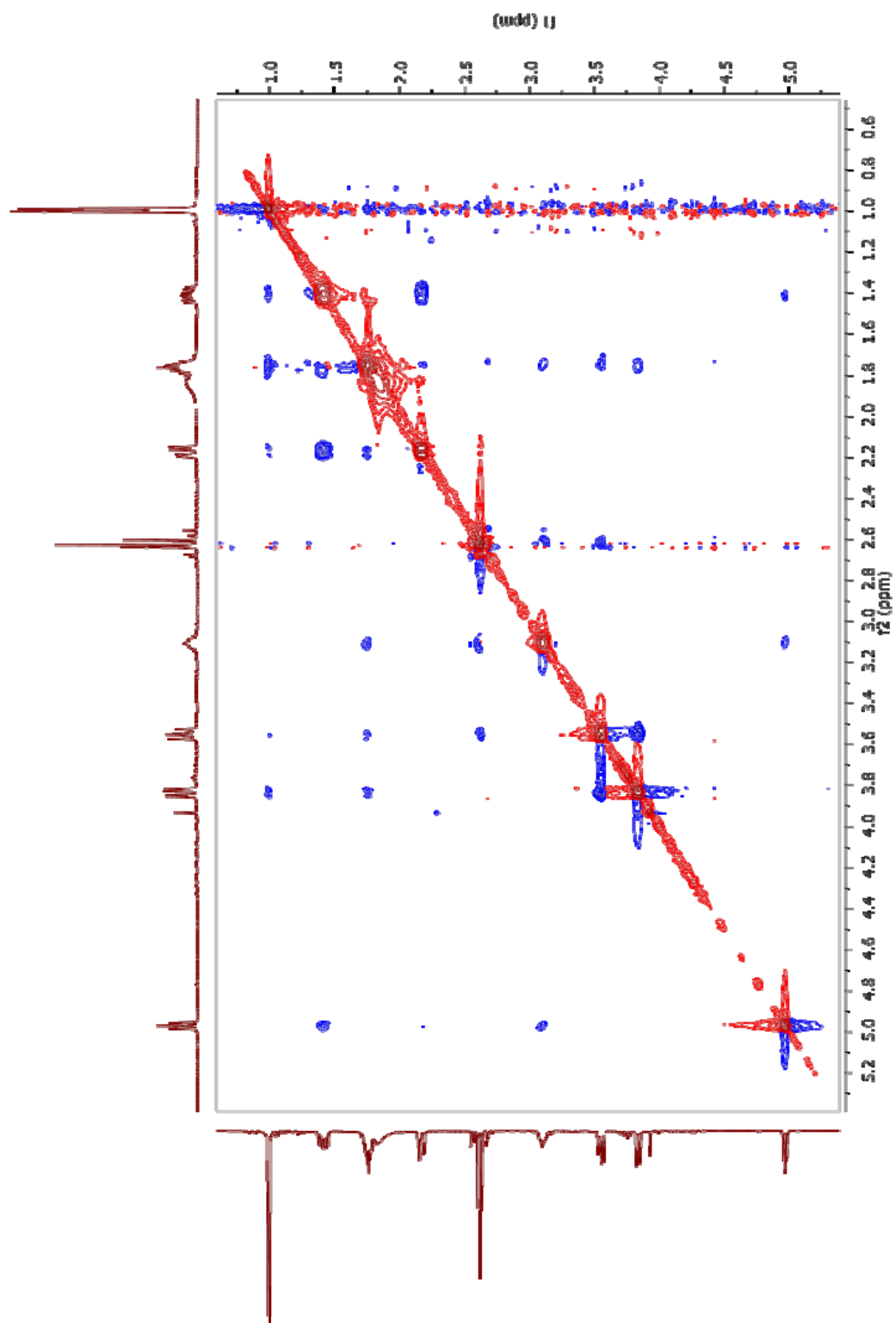
A1-12 HSQC spectrum of cornolactone A (**60**), 400 MHz, in CDCl₃



A1-13 HMBC spectrum of cornolactone A (**60**), 400 MHz, in CDCl₃

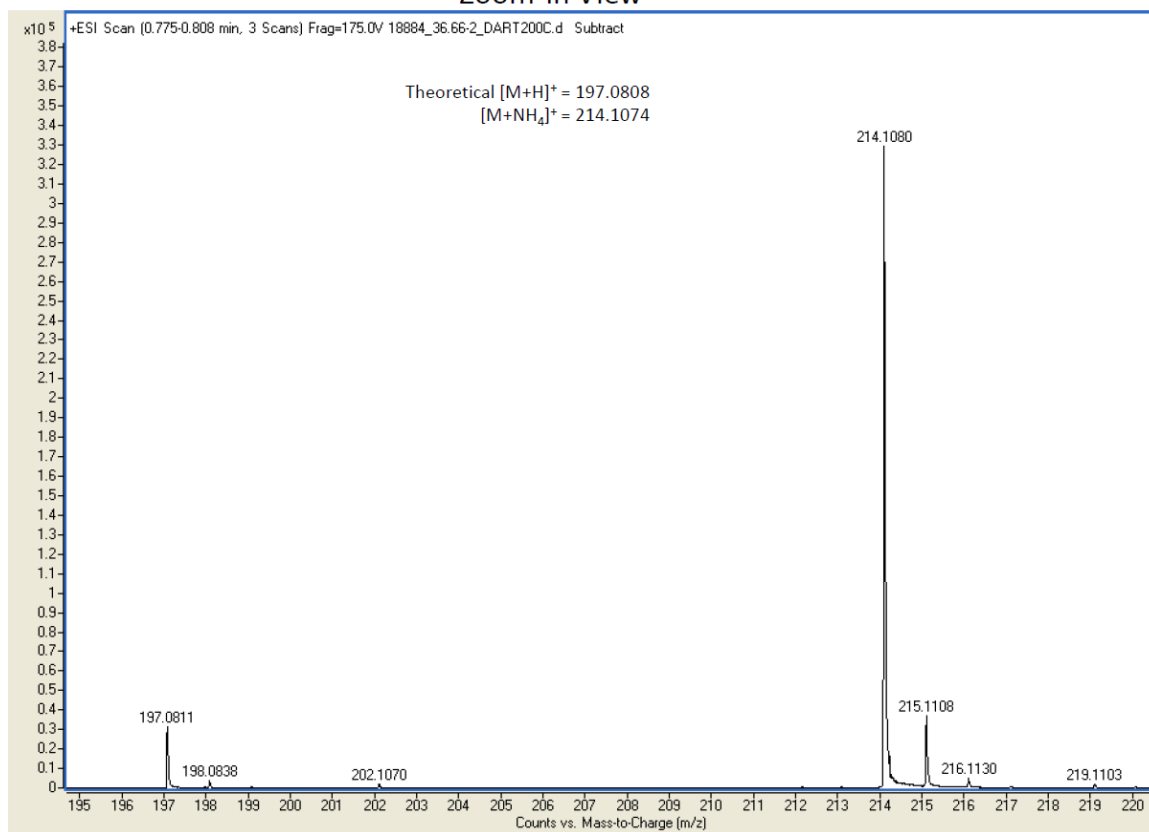


A1-14 NOESY spectrum of cornolactone A (**60**), 400 MHz, in CDCl₃

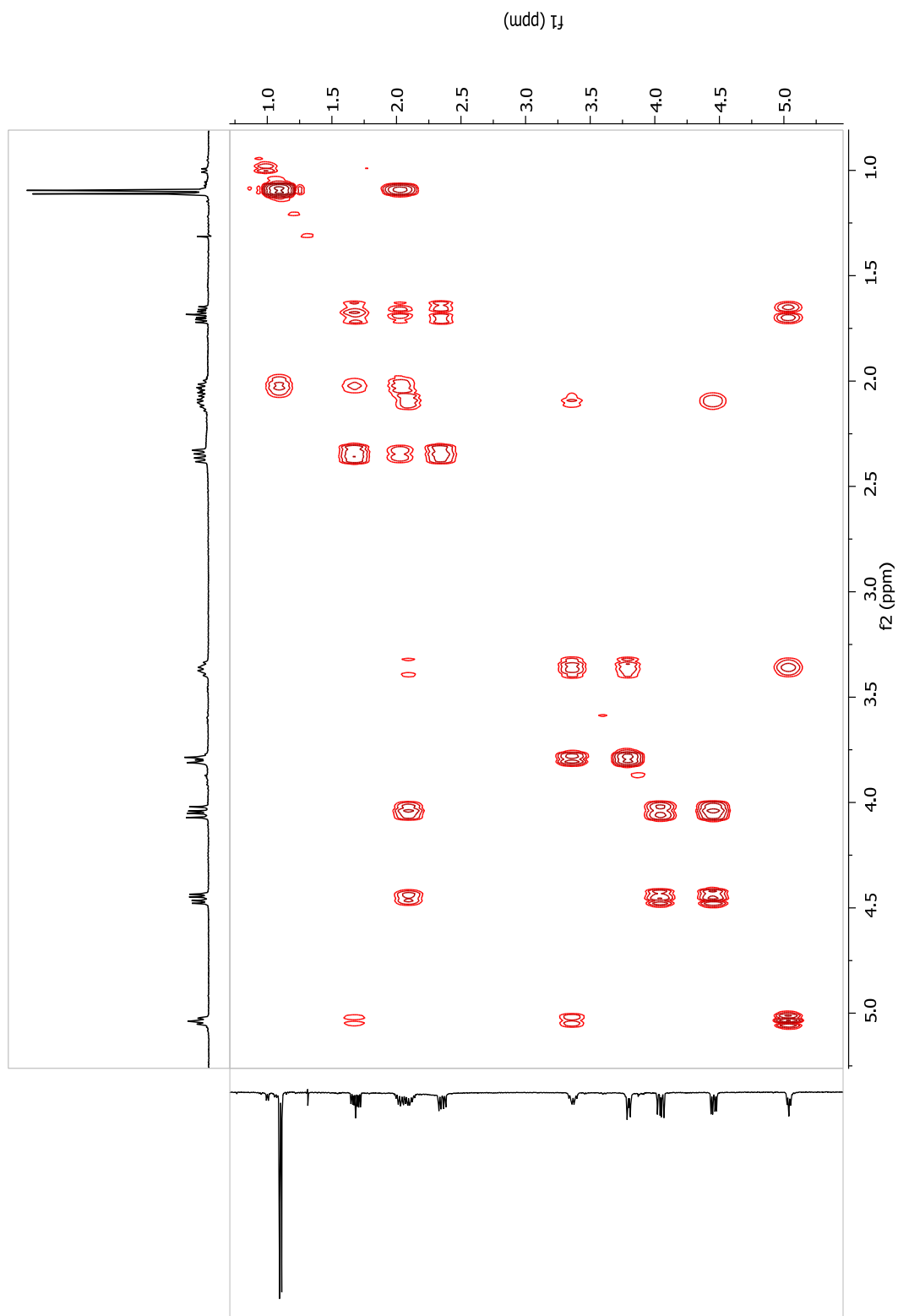


A1-15 HRESIMS spectrum of cornolactone B (61)

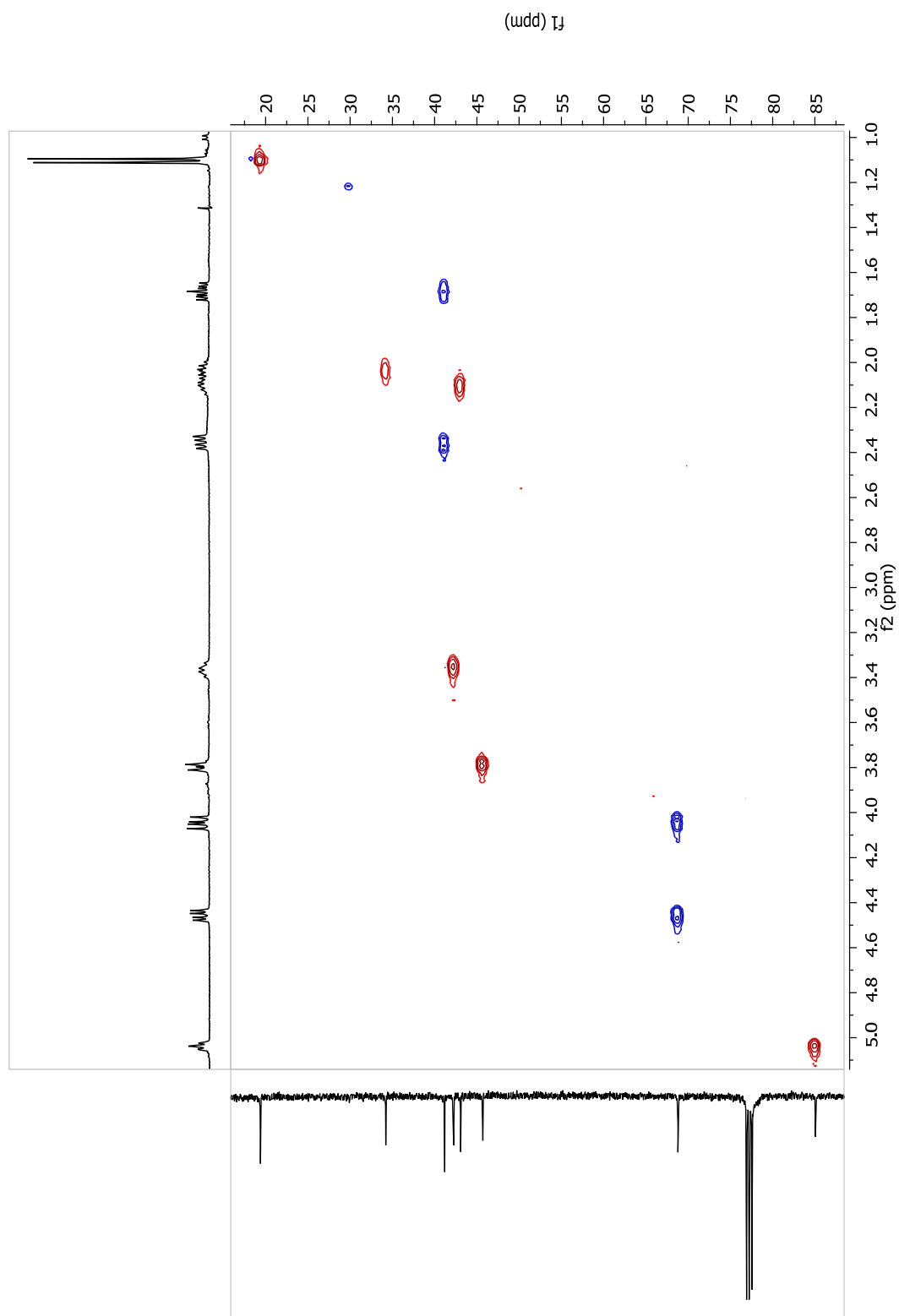
Zoom-In View



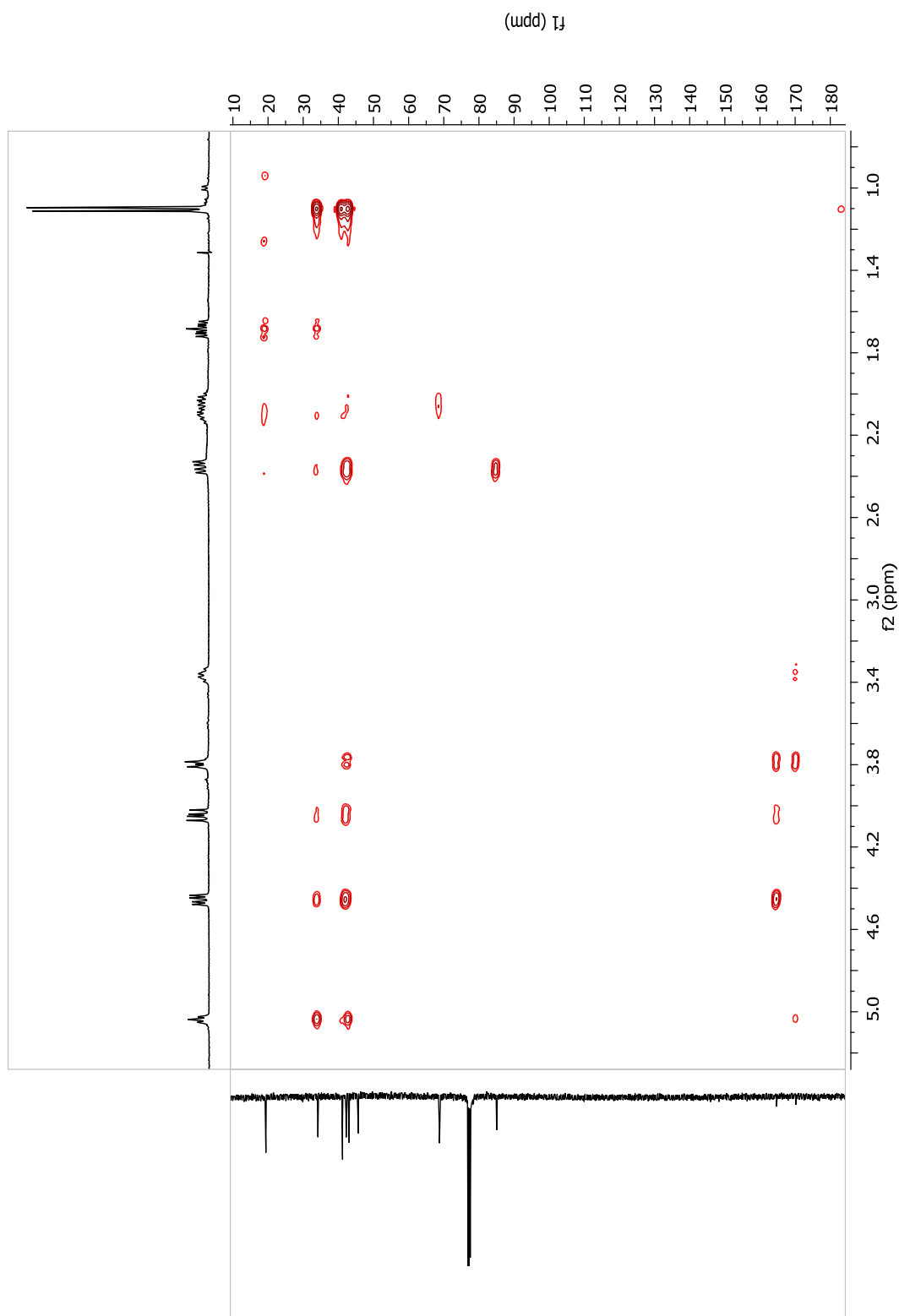
A1-16 $^1\text{H} - ^1\text{H}$ COSY spectrum of cornolactone B (61), 400 MHz, in CDCl_3



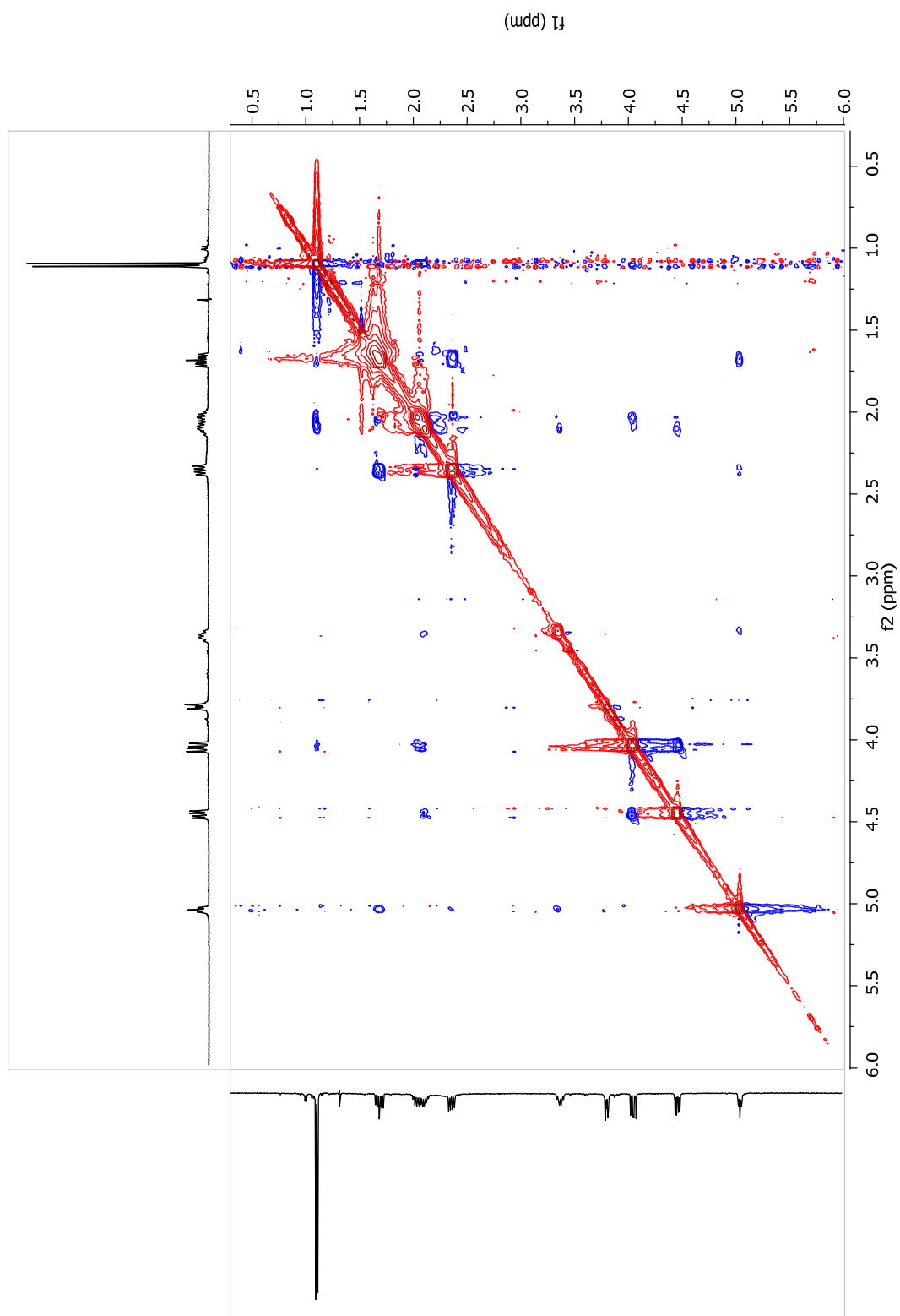
A1-17 HSQC spectrum of cornolactone B (**61**), 400 MHz, in CDCl₃



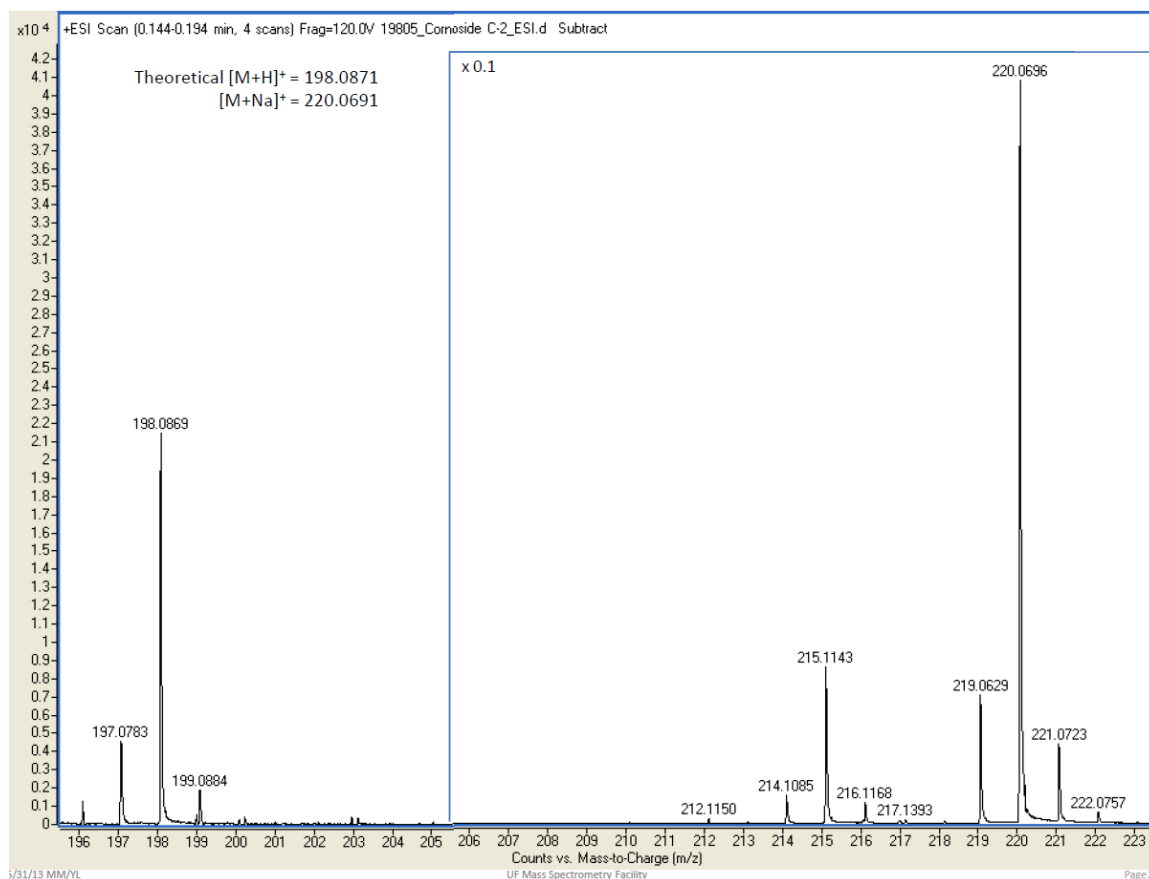
A1-18 HMBC spectrum of cornolactone B (**61**), 400 MHz, in CDCl₃



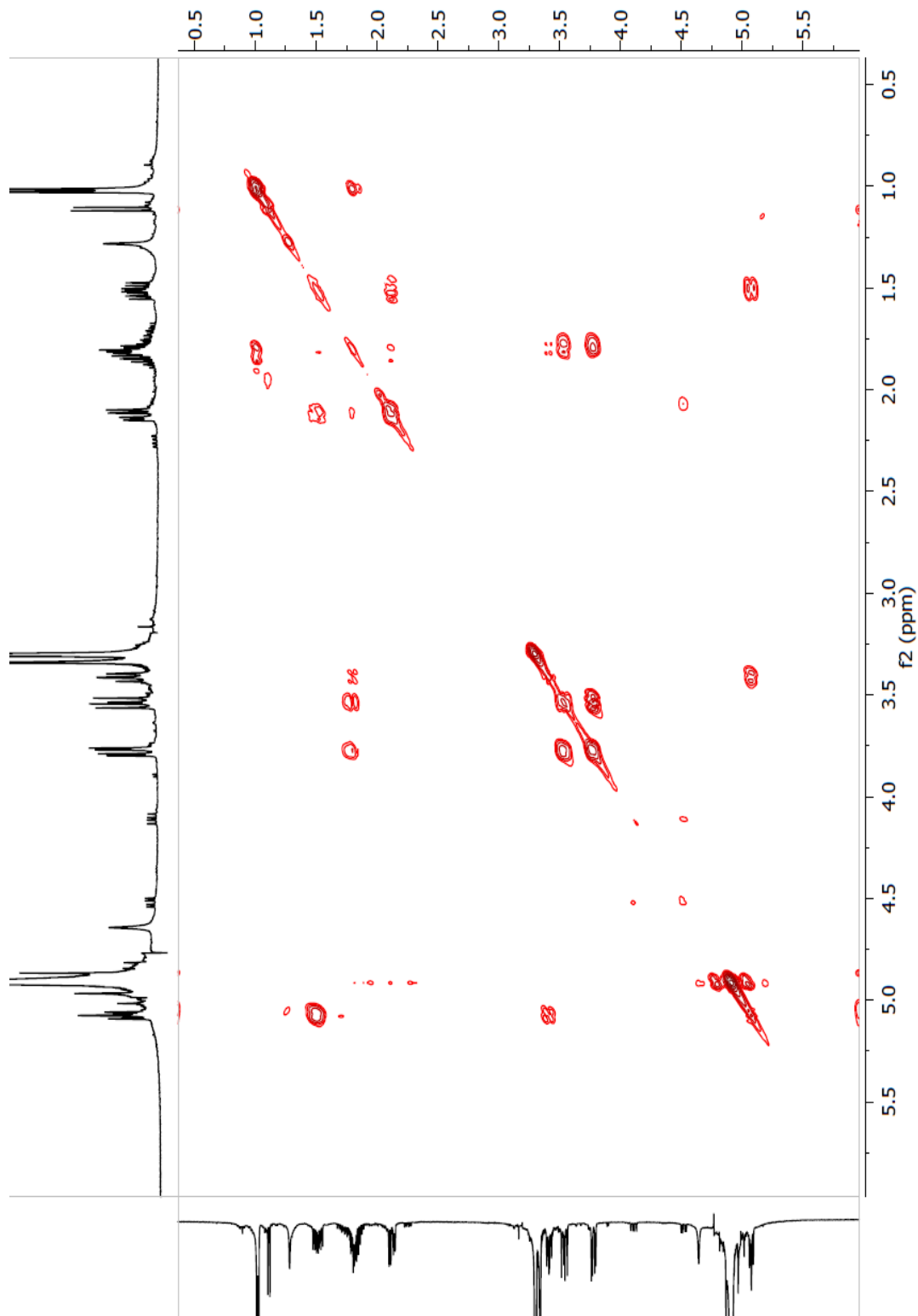
A1-19 NOESY spectrum of cornolactone B (**61**), 400 MHz, in CDCl₃



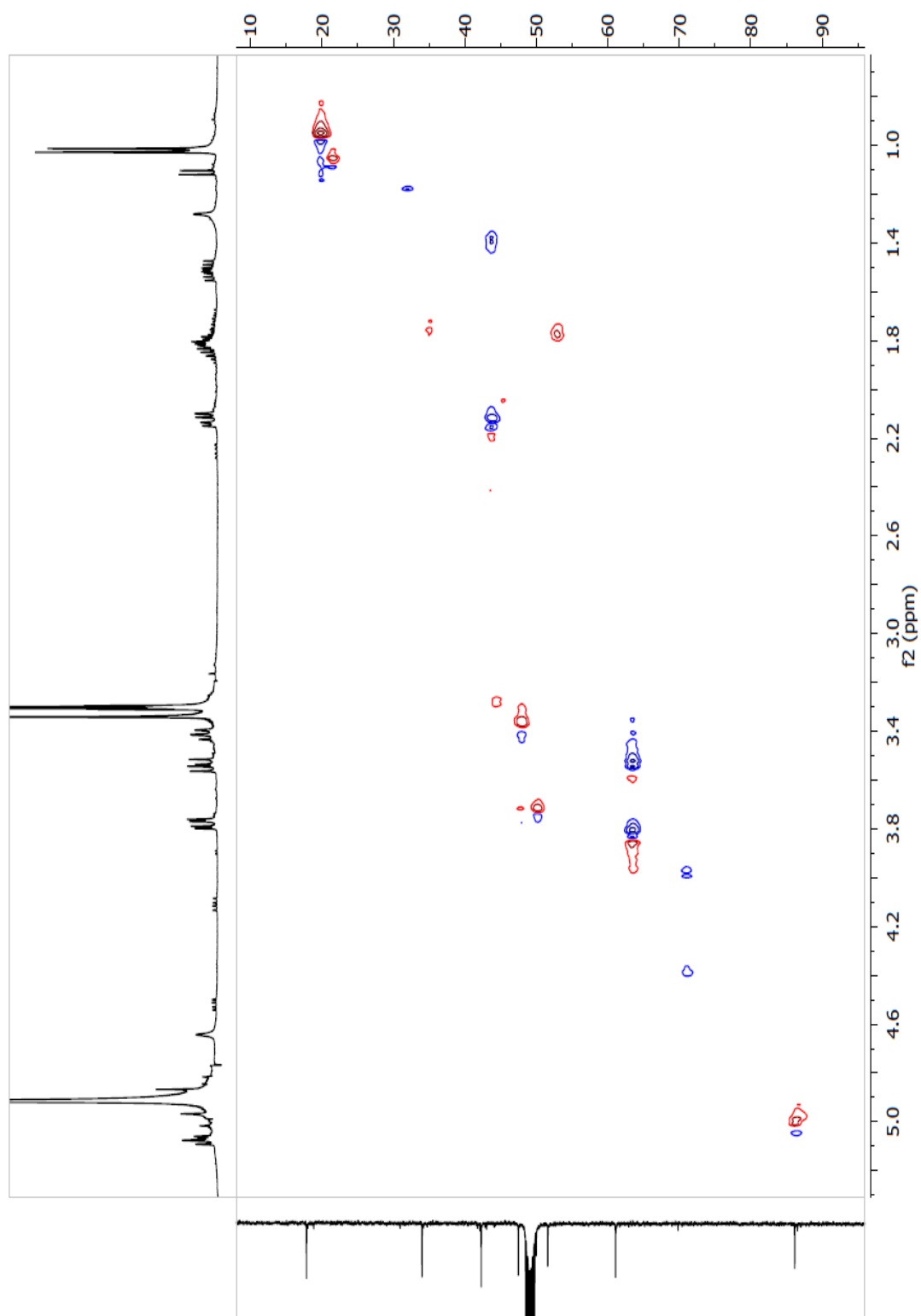
A1-20 HRESIMS spectrum of cornolactone C (62)



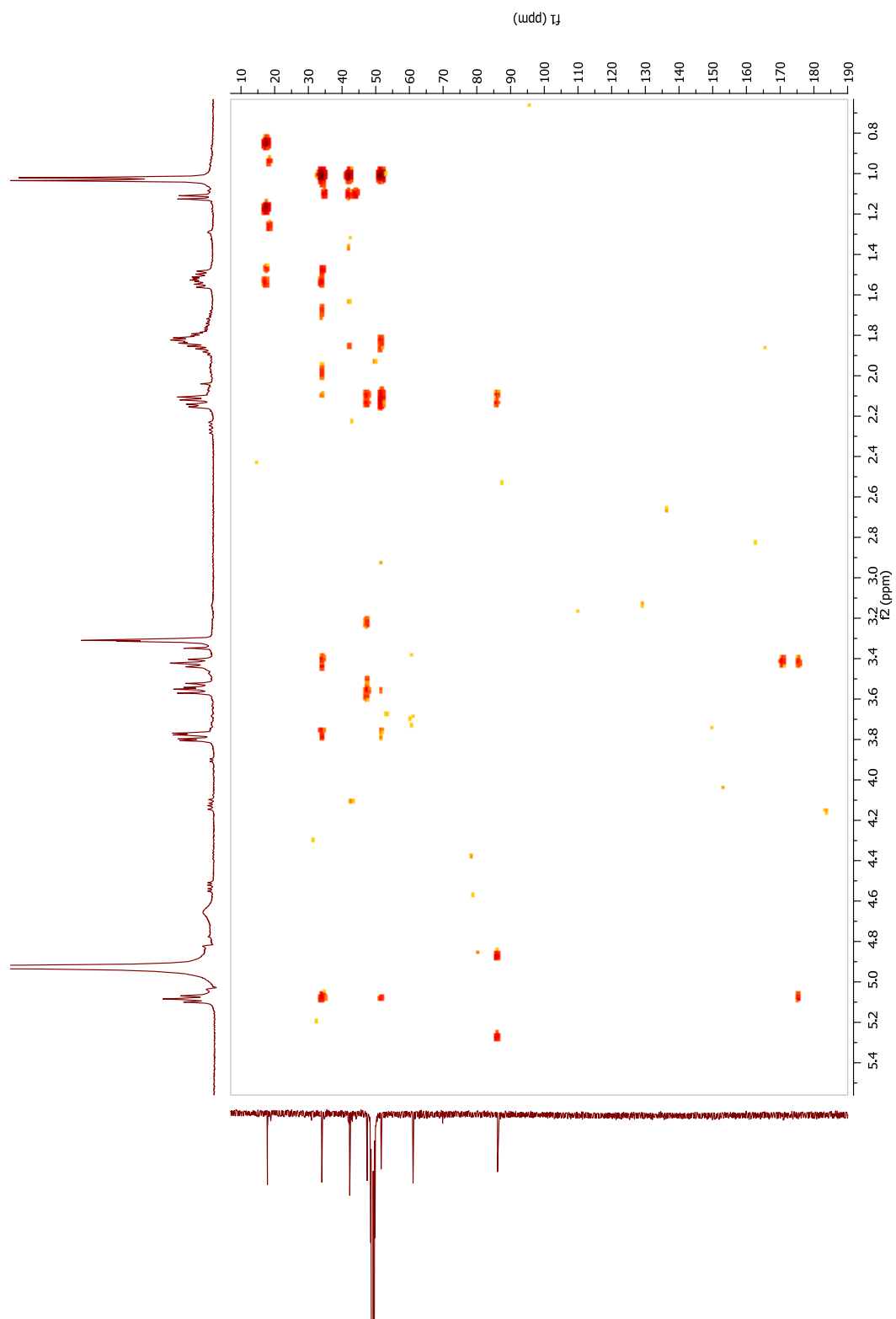
A1-21 $^1\text{H} - ^1\text{H}$ COSY spectrum of cornolactone C (**62**), 400 MHz, in CD_3OD



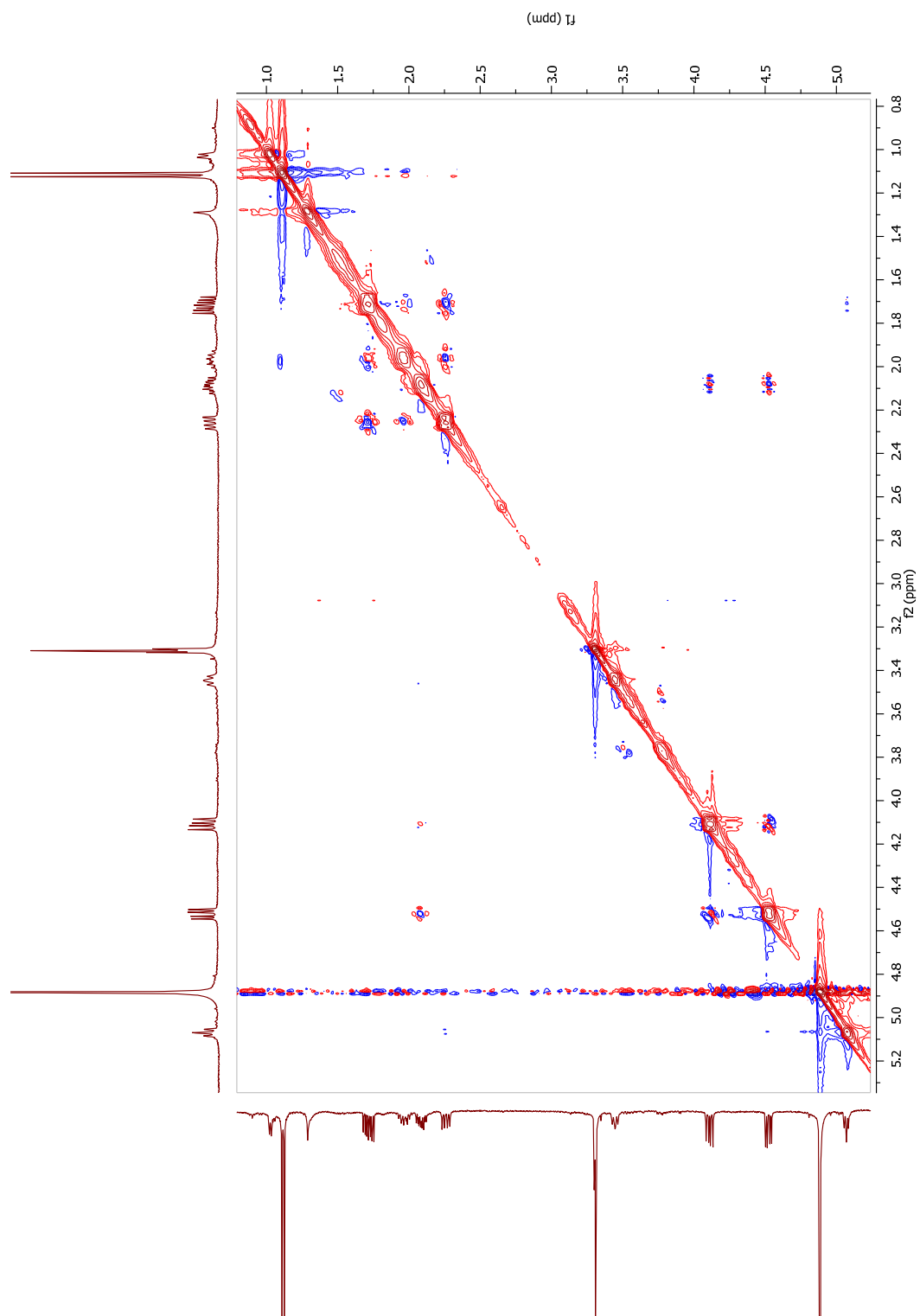
A1-22 HSQC spectrum of cornolactone C (**62**), 400 MHz, in CD₃OD



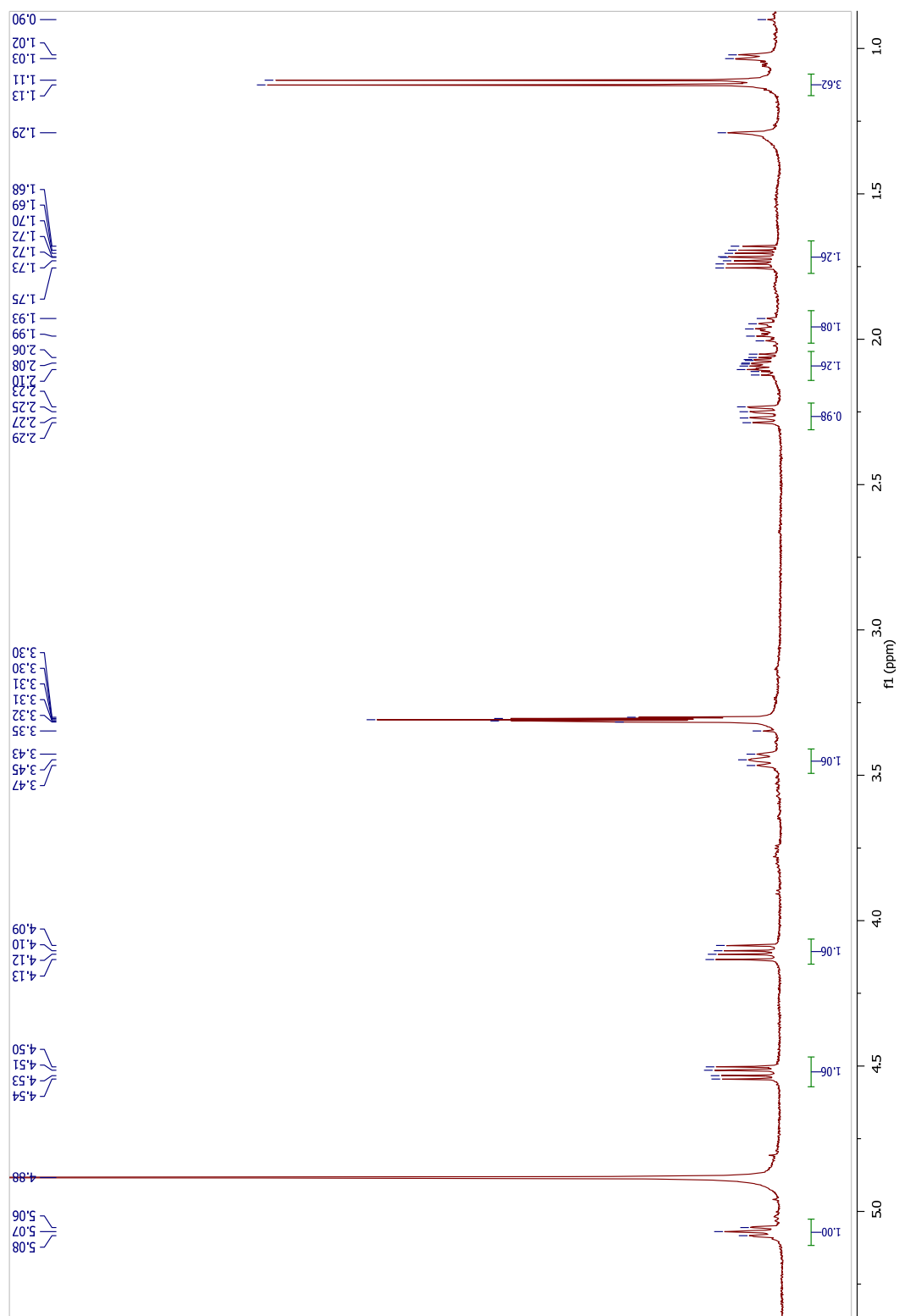
A1-23 HMBC spectrum of cornolactone C (**62**), 400 MHz, in CD₃OD



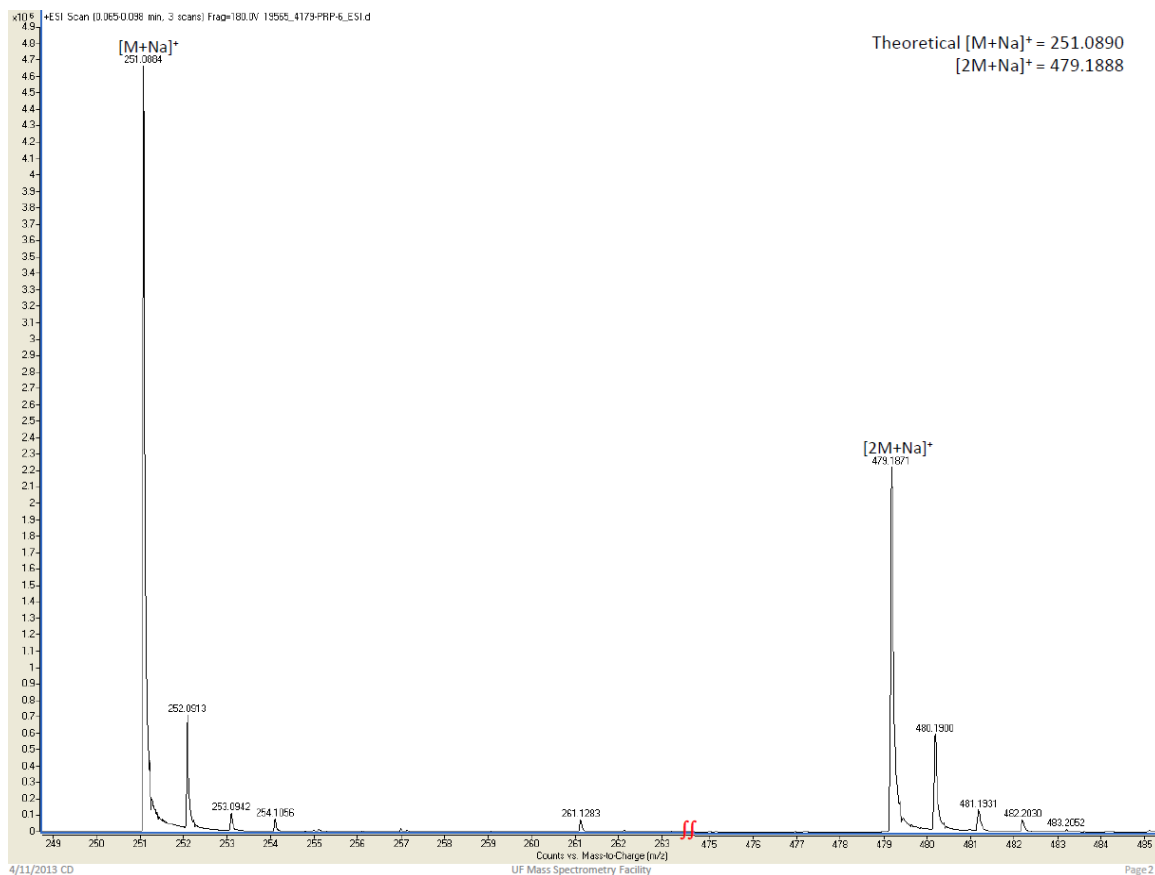
A1-24 NOESY spectrum of cornolactone C (**62**) after estification, 400 MHz, in CD₃OD



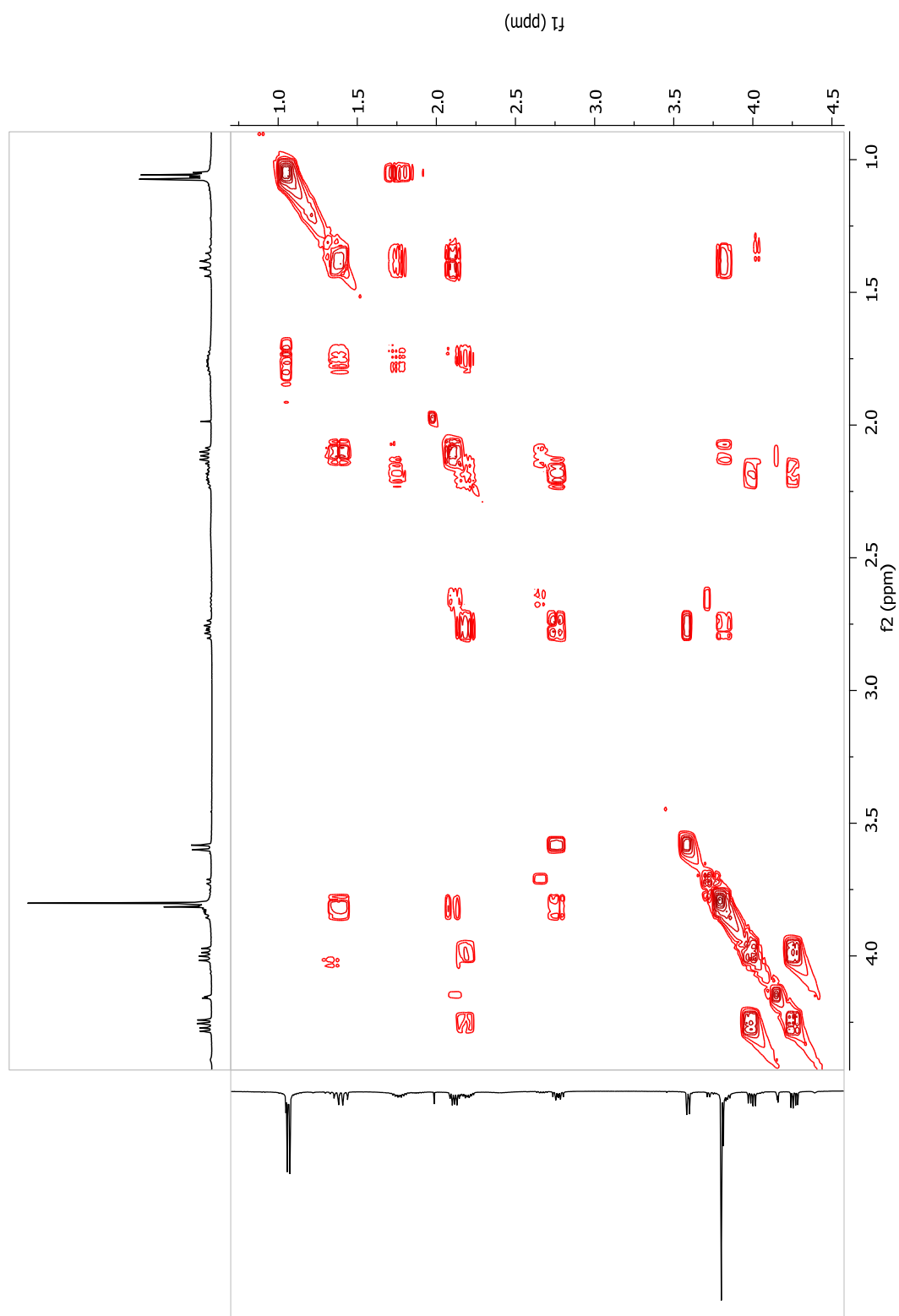
A1-25 ^1H NMR spectrum of cornolactone C (**62**) after estification, 400 MHz, in CD_3OD



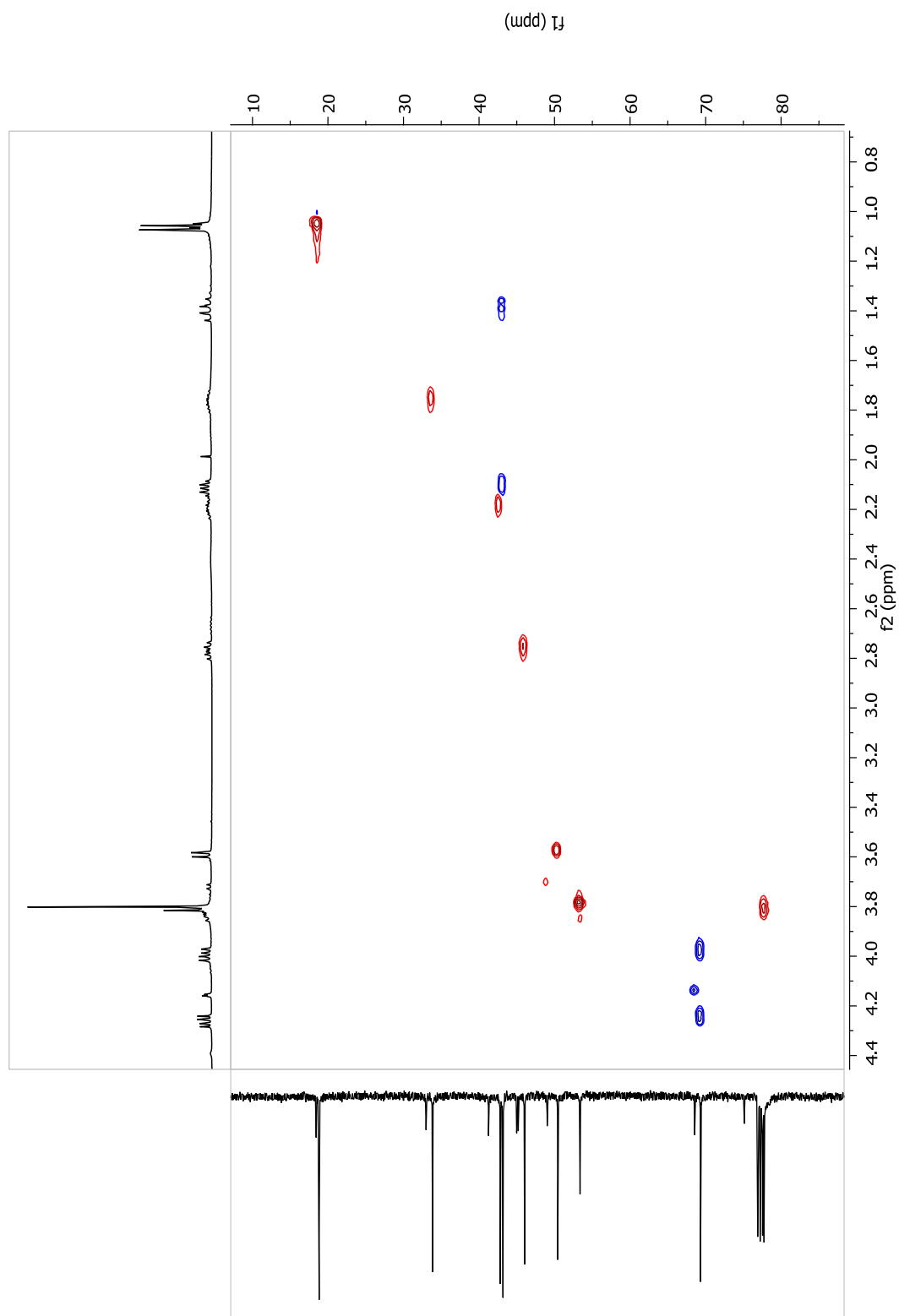
A1-26 HRESIMS spectrum of cornolactone D (63)



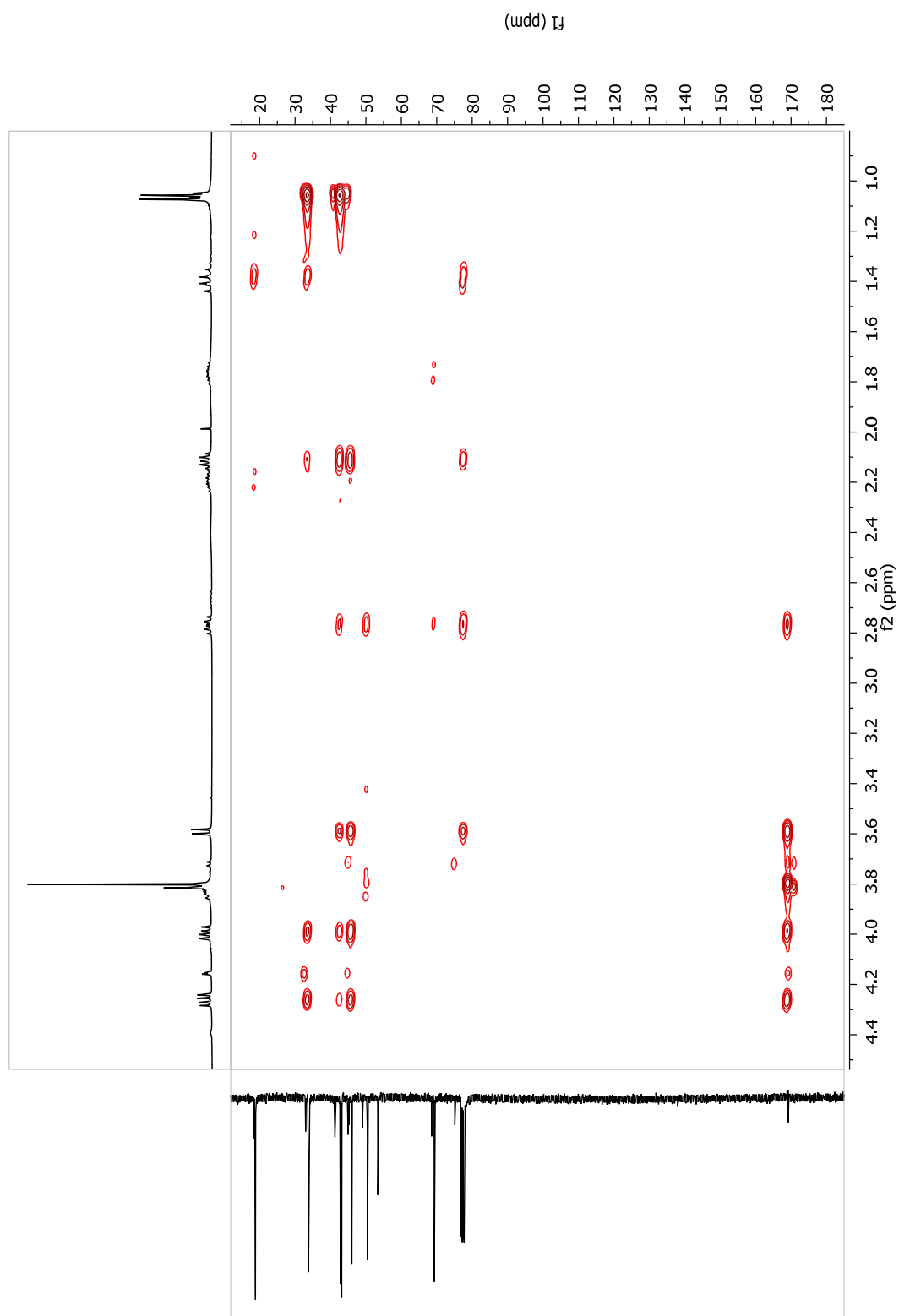
A1-27 $^1\text{H} - ^1\text{H}$ COSY spectrum of cornolactone D (**63**), 400 MHz, in CDCl_3



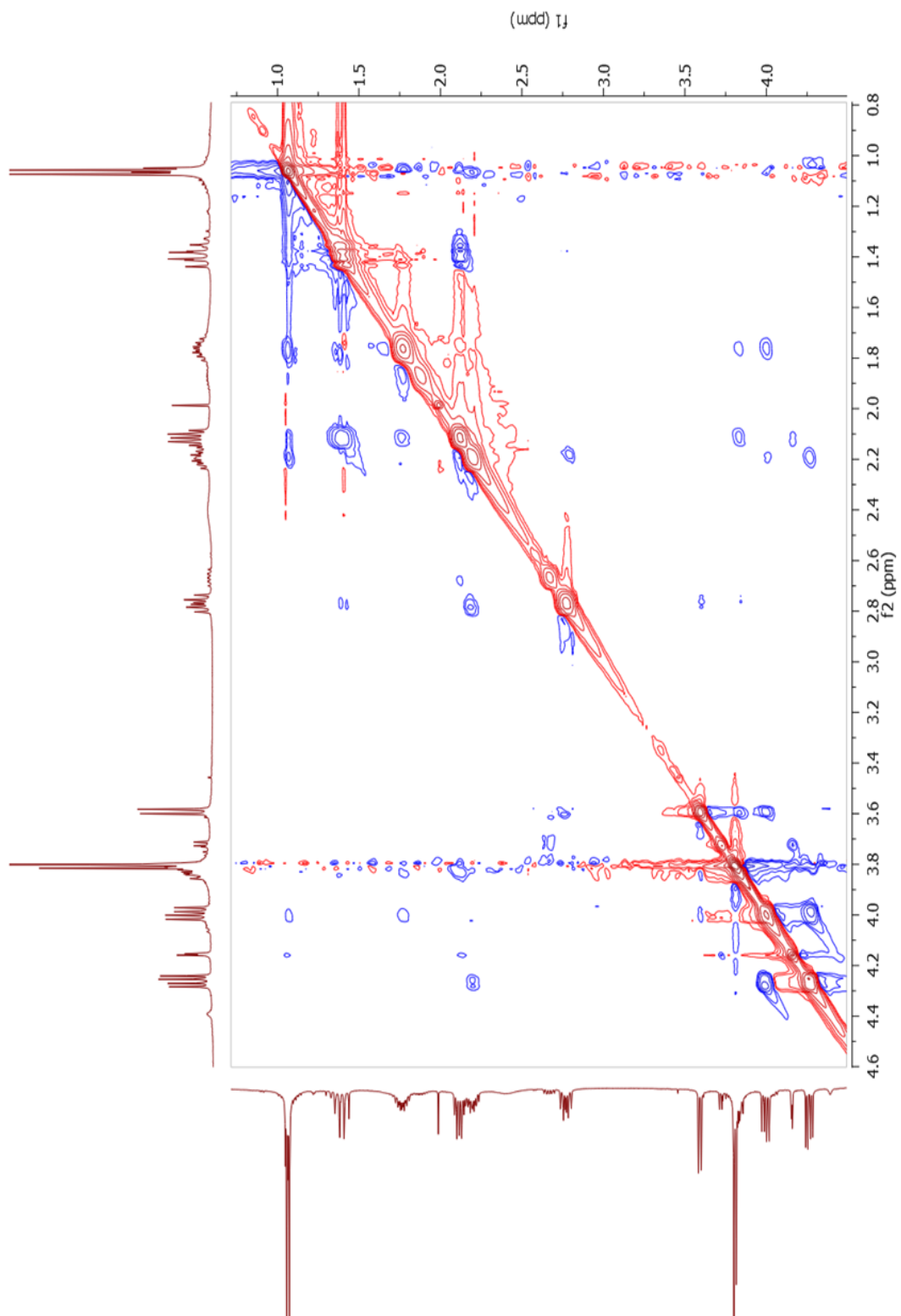
A1-28 HSQC spectrum of cornolactone D (**63**), 400 MHz, in CDCl₃



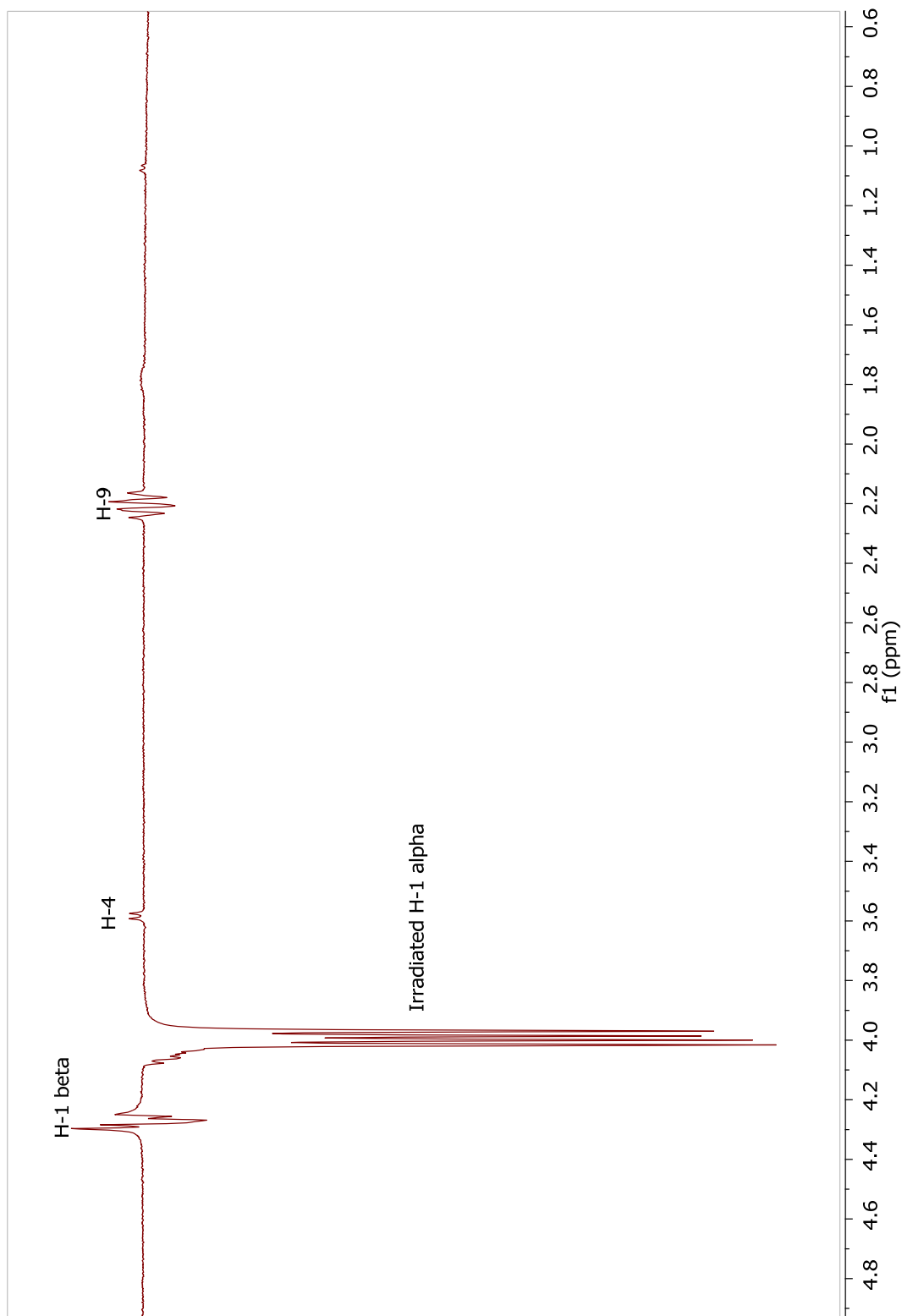
A1-29 HMBC spectrum of cornolactone D (**63**), 400 MHz, in CDCl₃



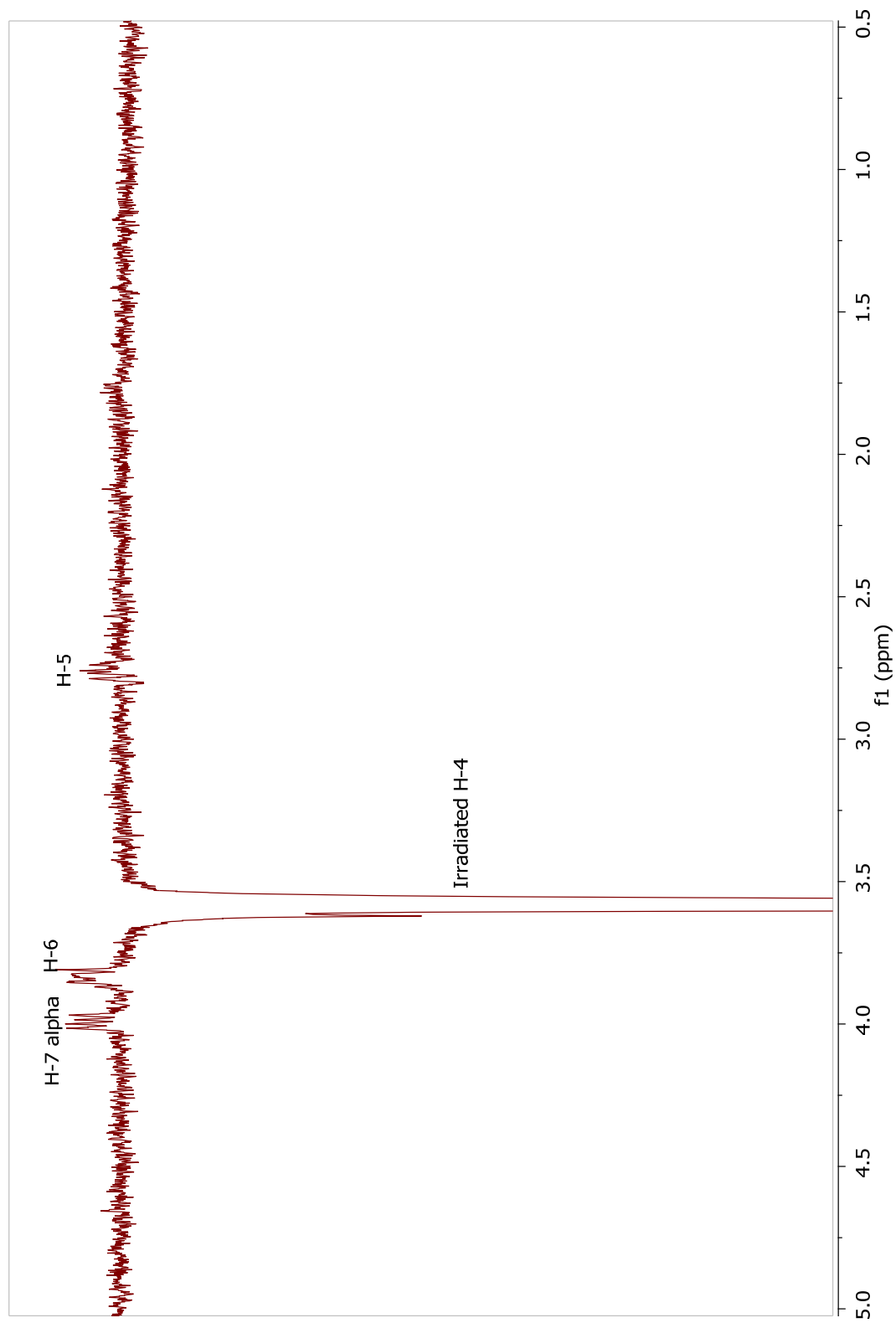
A1-30 NOESY spectrum of cornolactone D (**63**), 400 MHz, in CDCl₃



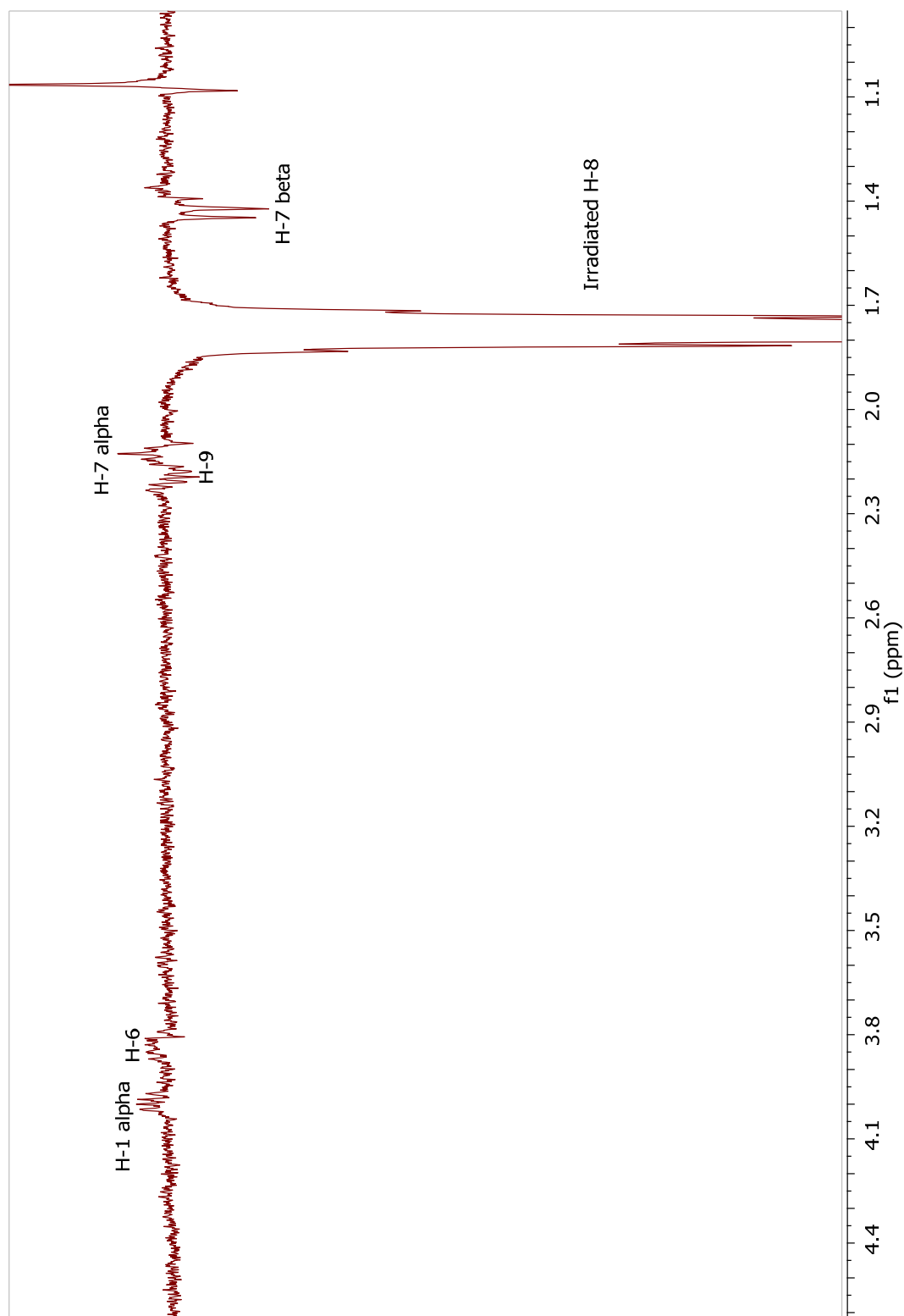
A1-31 1D NOESY spectrum of Cornolactone D (**63**) in CDCl₃ (irradiated H-1 α)



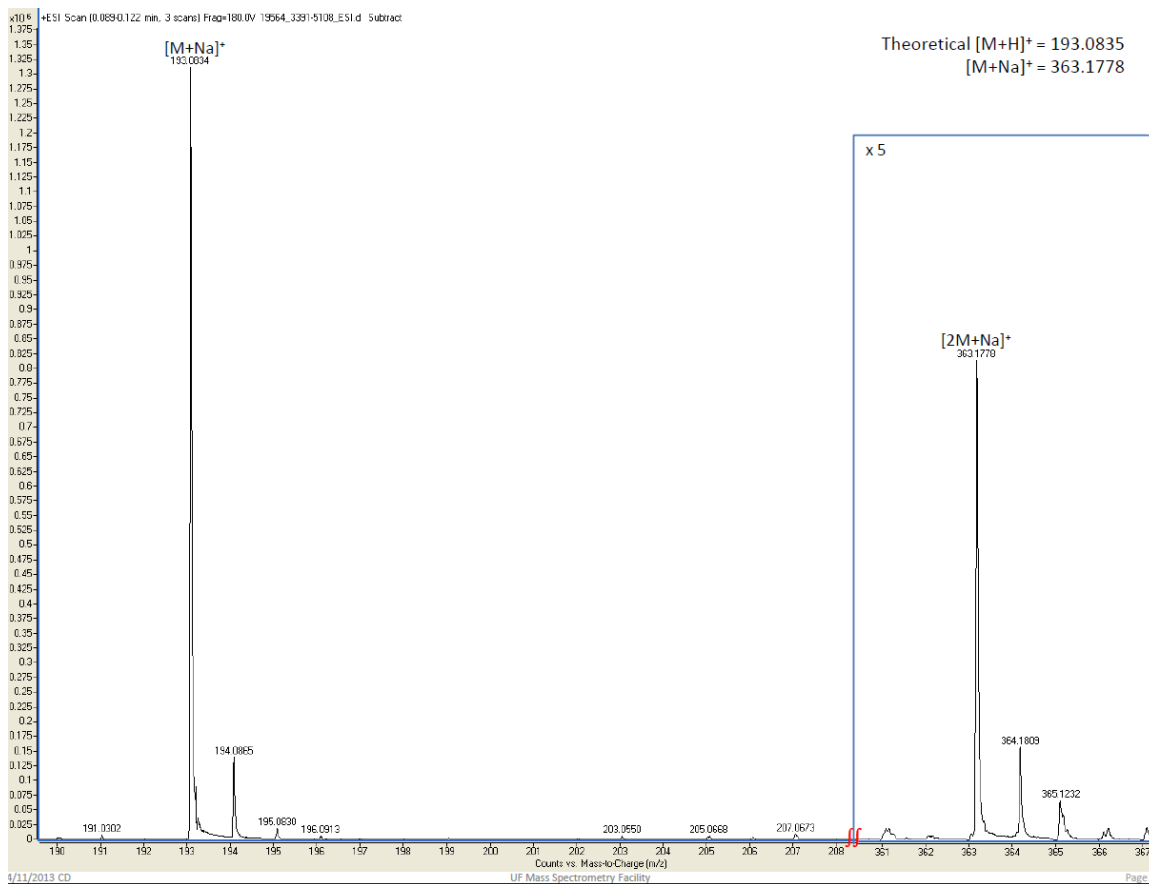
A1-32 1D NOESY spectrum of Cornolactone D (**63**) in CDCl₃ (irradiated H-4)



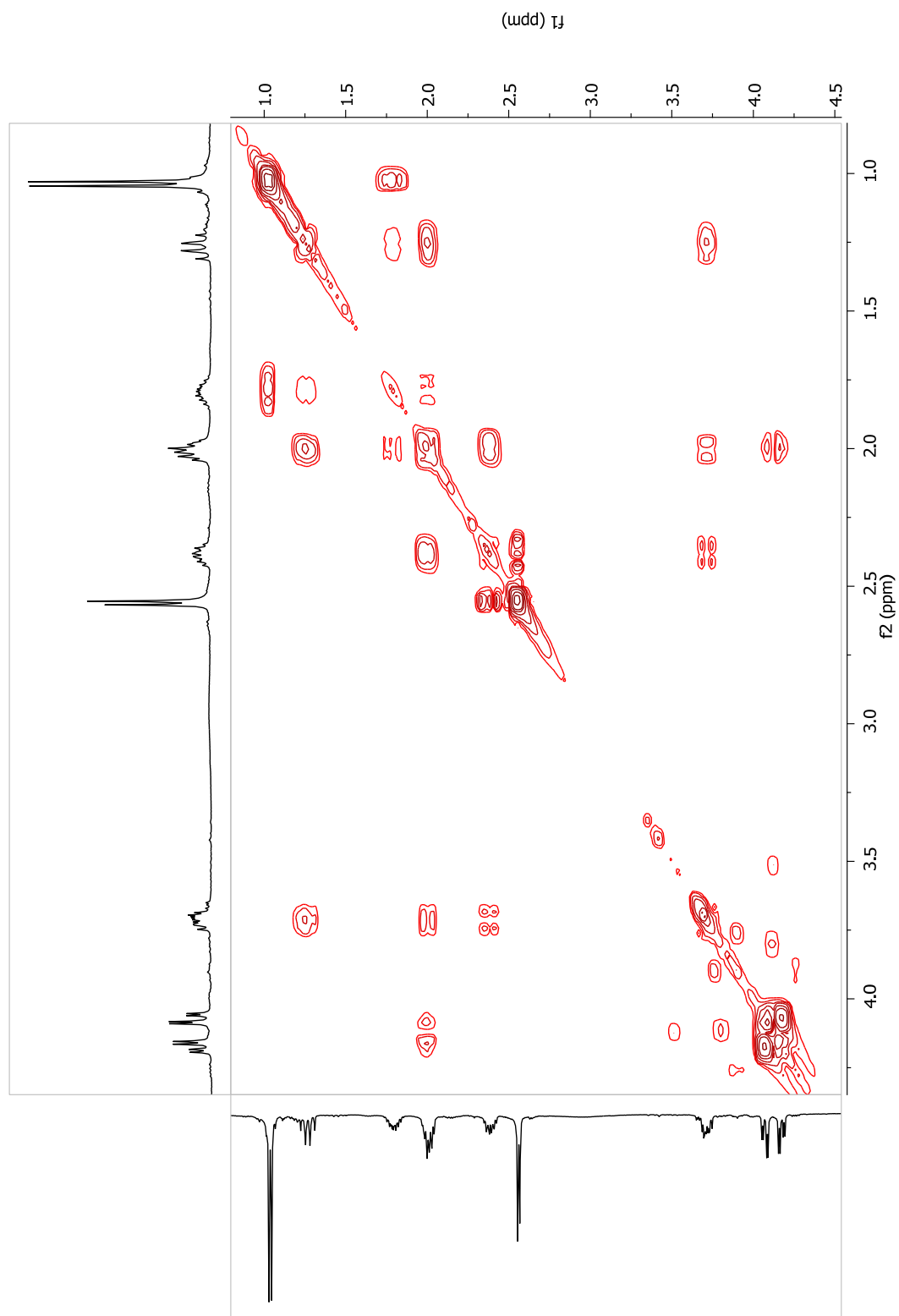
A1-33 1D NOESY spectrum of Cornolactone D (**63**) in CDCl₃ (irradiated H-8)



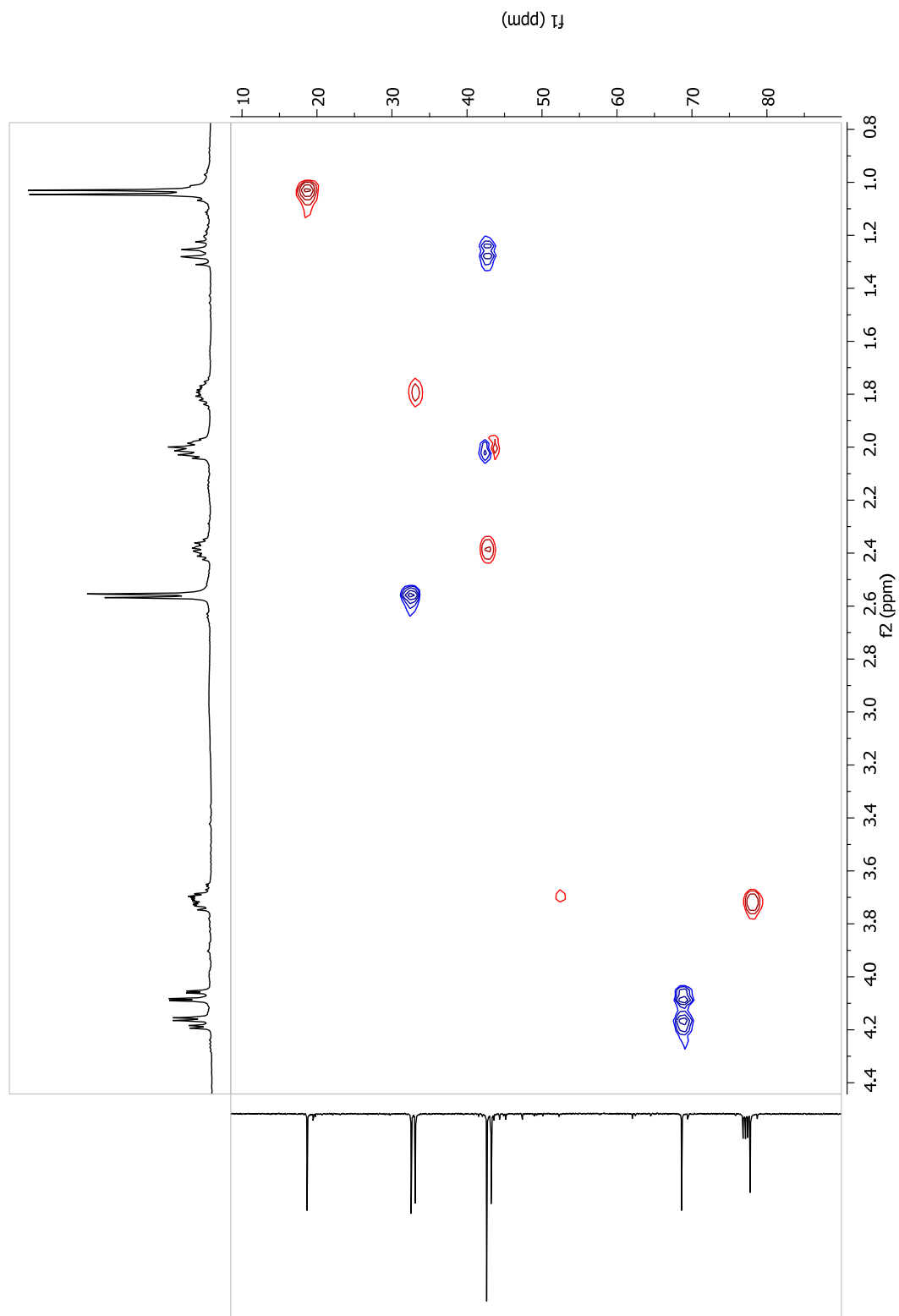
A1-34 HRESIMS spectrum of cornolactone E (64)



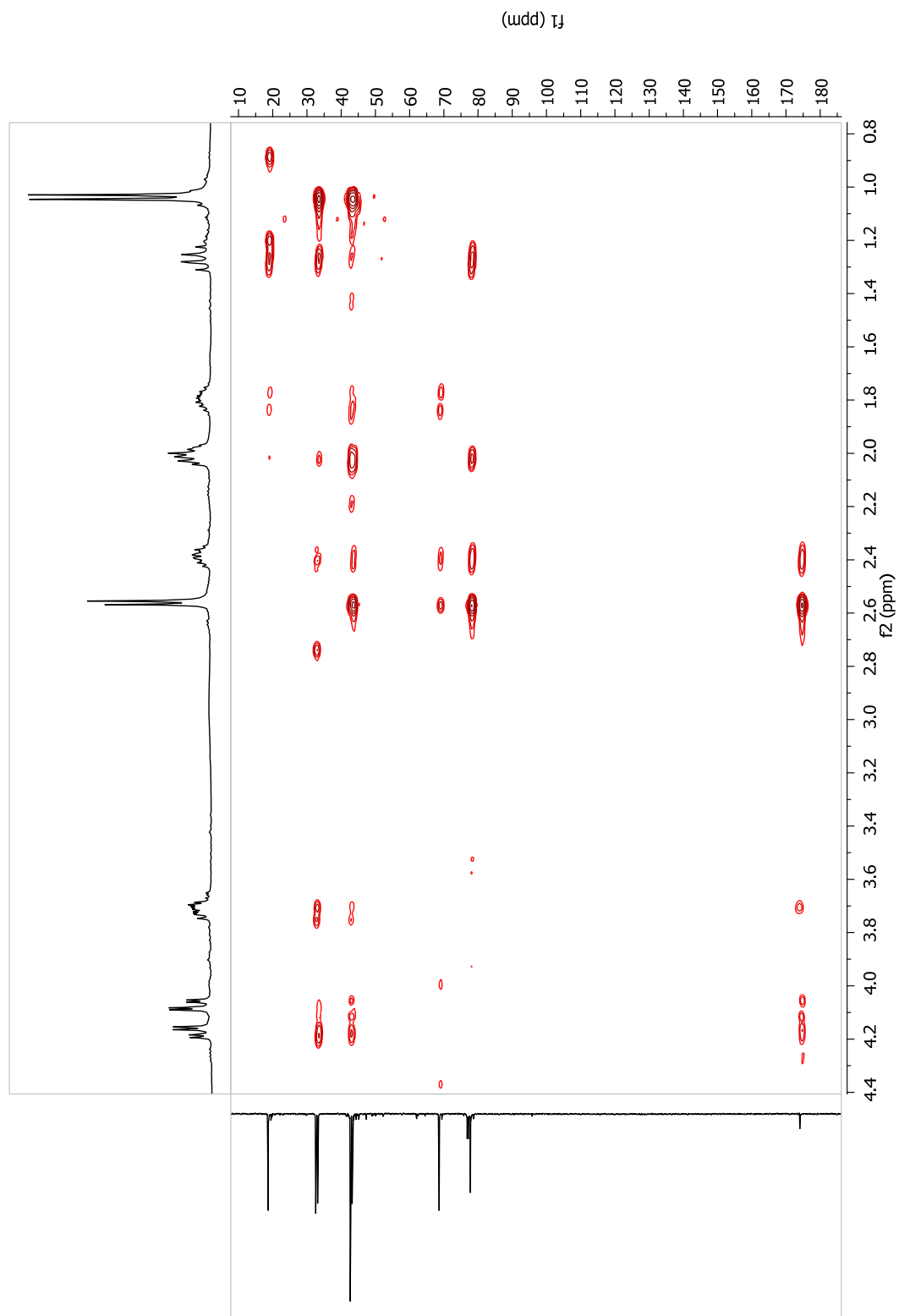
A1-35 $^1\text{H} - ^1\text{H}$ COSY spectrum of cornolactone E (64), 400 MHz, in CDCl_3



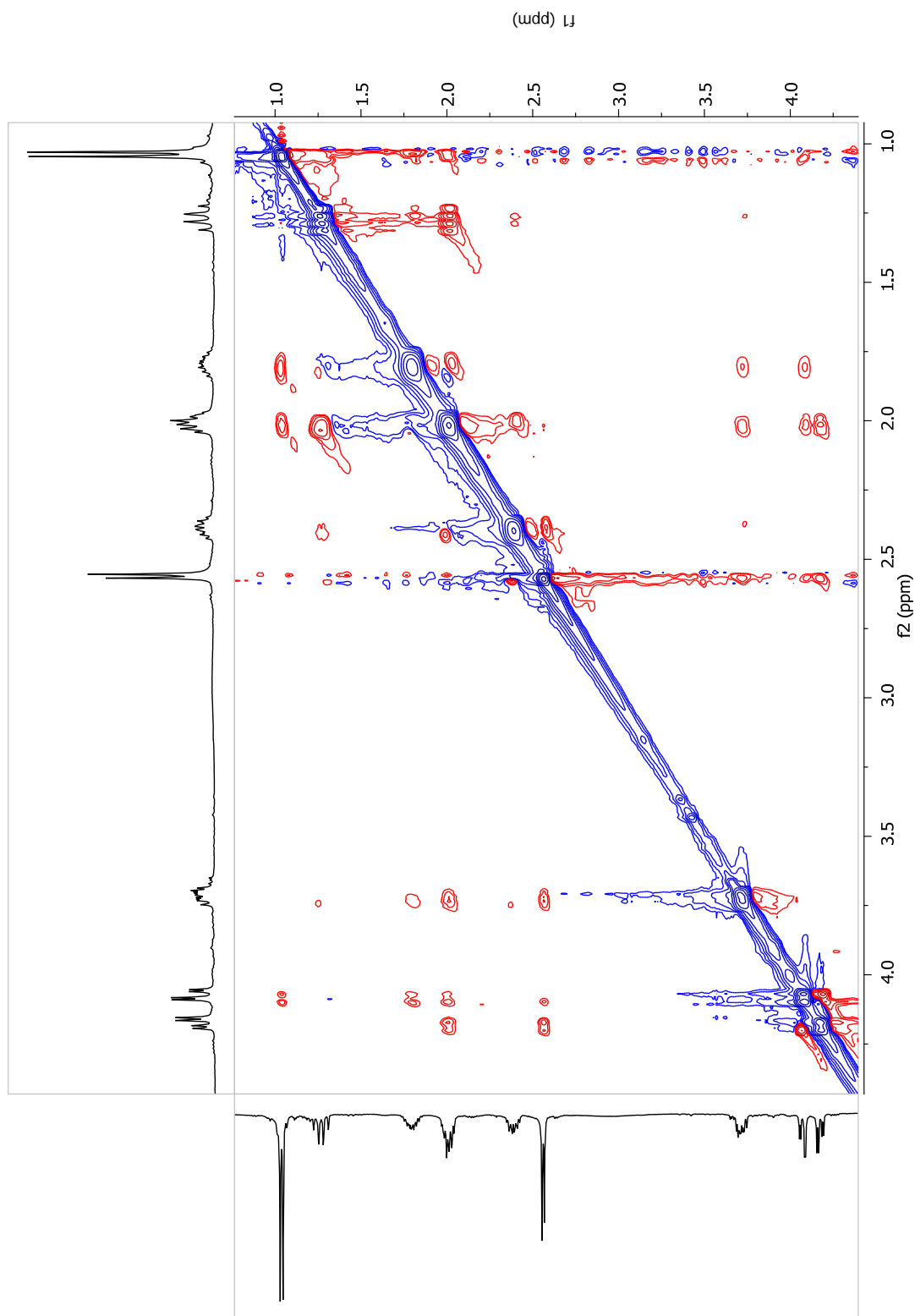
A1-36 HSQC spectrum of cornolactone E (**64**), 400 MHz, in CDCl₃



A1-37 HMBC spectrum of cornolactone E (**64**), 400 MHz, in CDCl₃



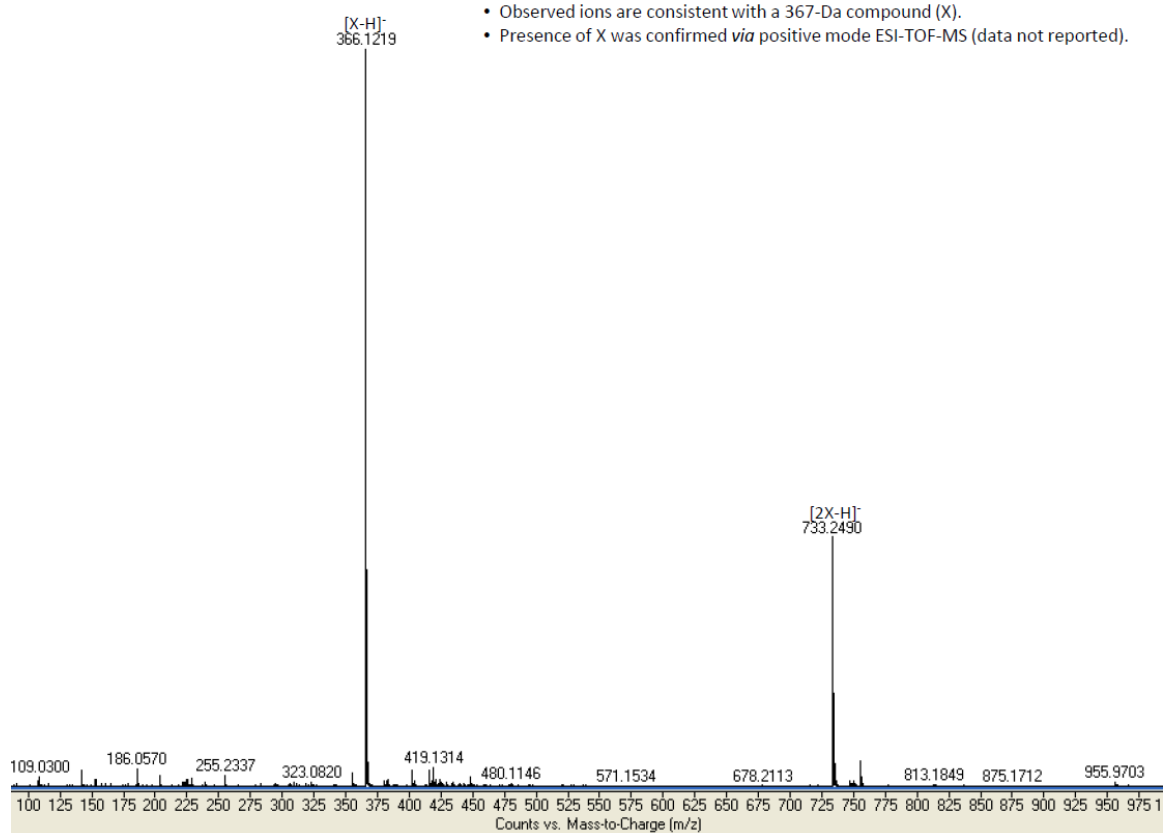
A1-38 NOESY spectrum of cornolactone E (**64**), 400 MHz, in CDCl₃



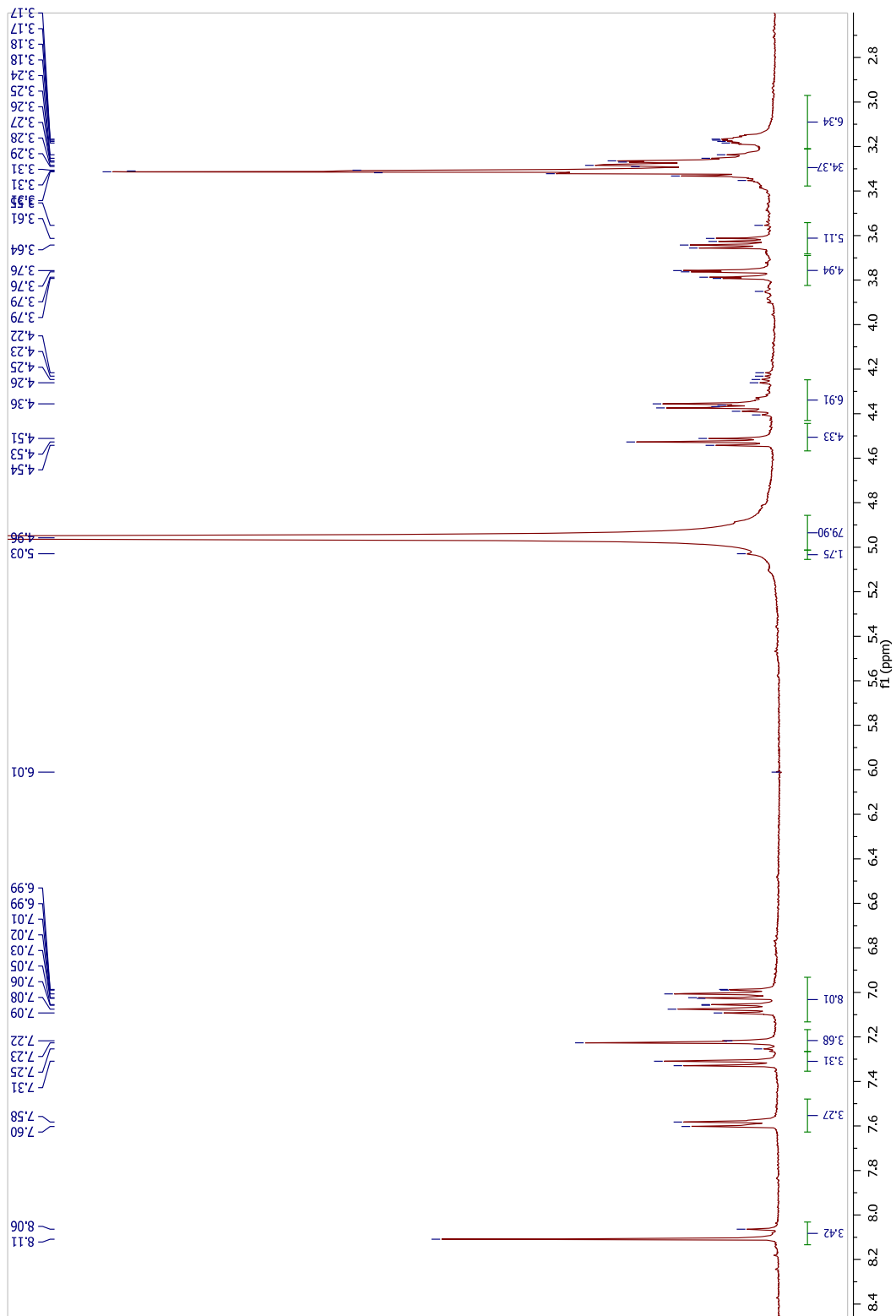
A1-39 HRESIMS spectrum of cornoside B (65)

Full spectrum:

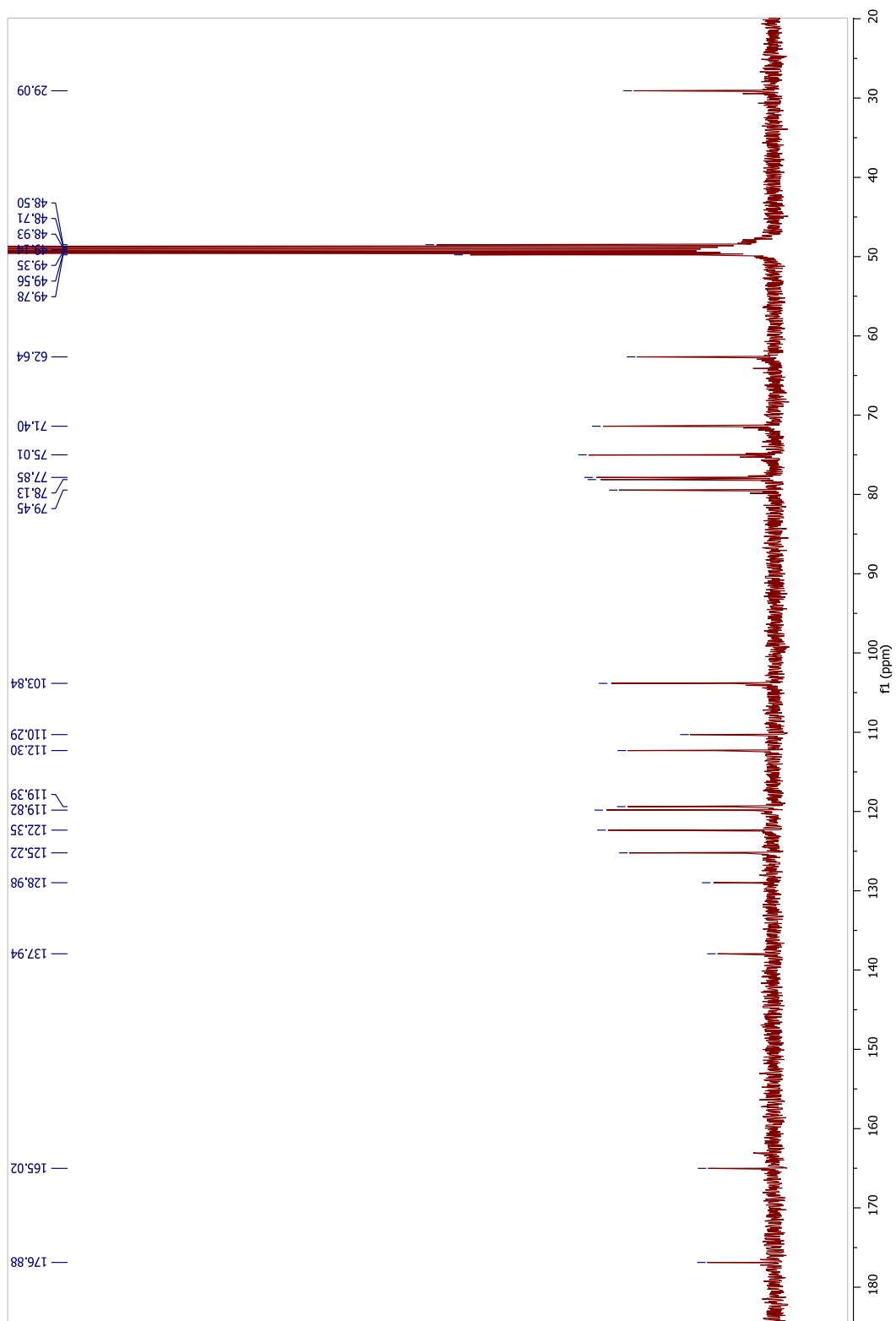
- Expected ions for 380-Da compound were not found *via* (+/-)ESI-TOF-MS.
- Observed ions are consistent with a 367-Da compound (X).
- Presence of X was confirmed *via* positive mode ESI-TOF-MS (data not reported).



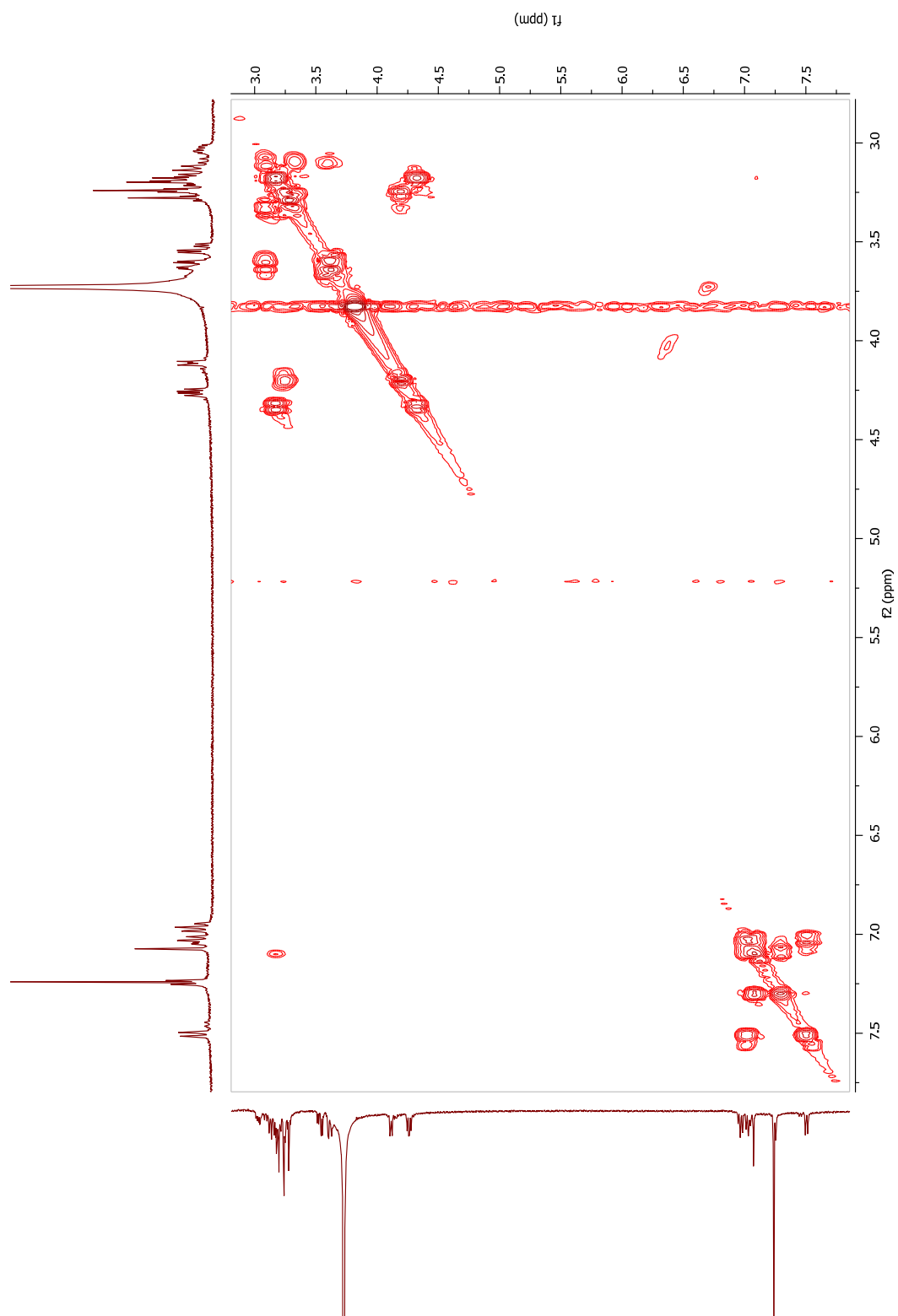
A1-40 ^1H NMR spectrum of cornoside B (**65**), 400 MHz, in CD_3OD



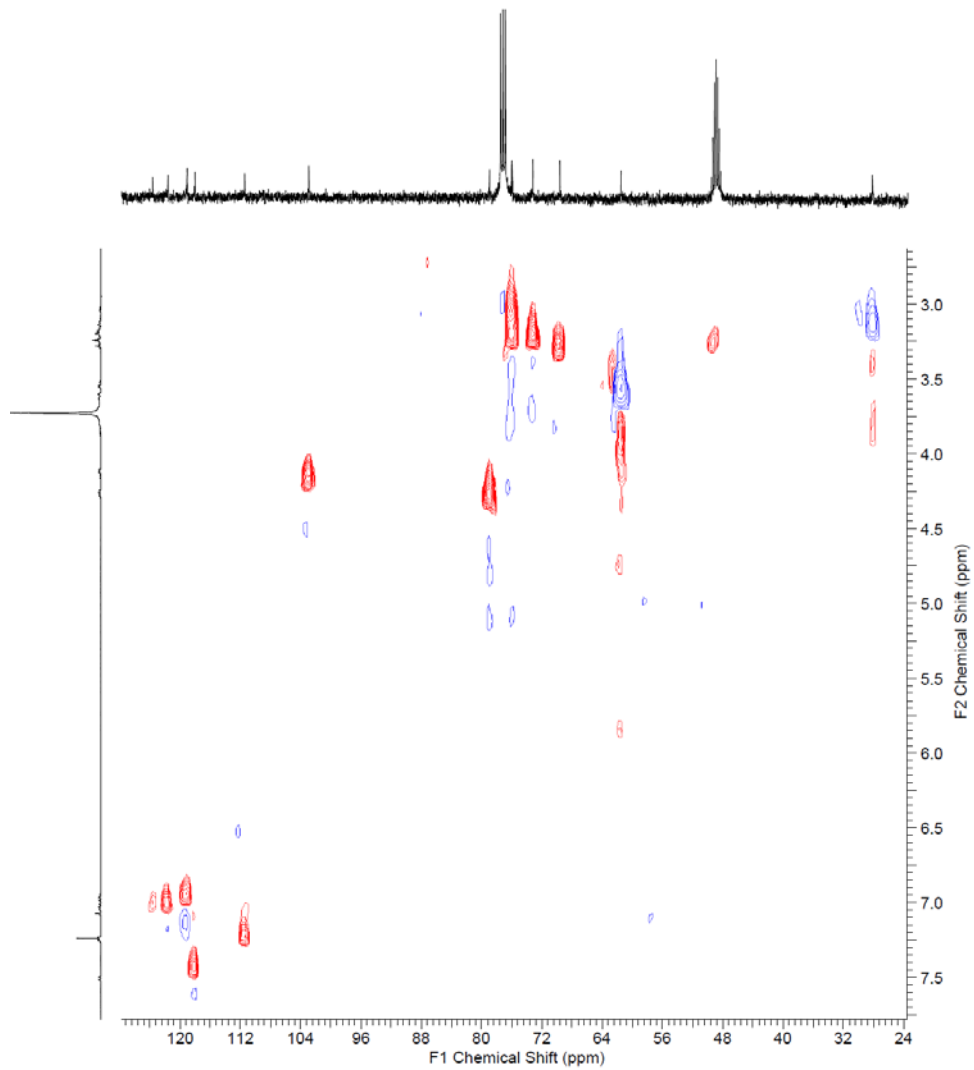
A1-41 ^{13}C NMR spectrum of cornoside B (**65**), 100 MHz, in CD_3OD



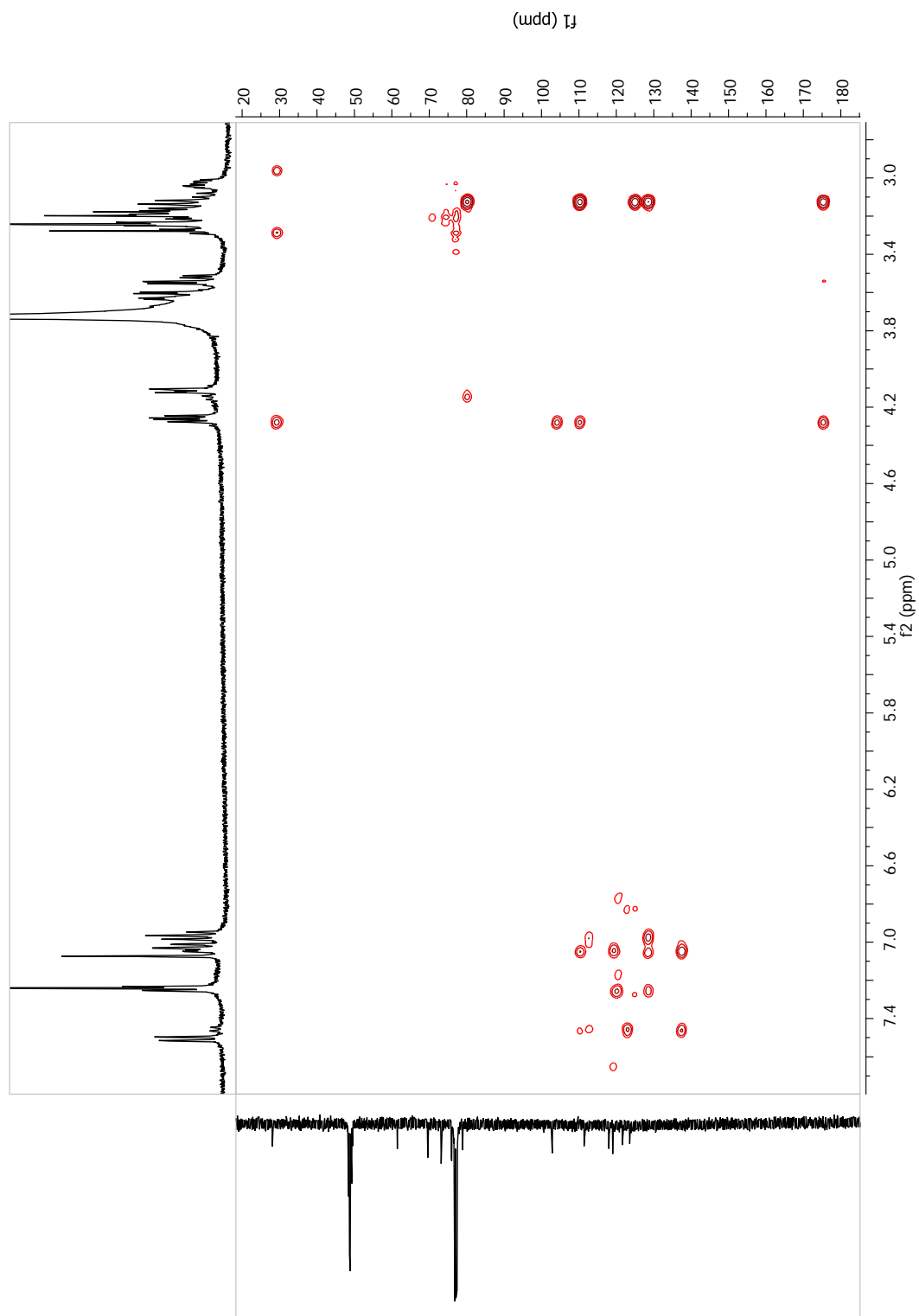
A1-42 $^1\text{H} - ^1\text{H}$ COSY spectrum of cornoside B (**65**), 400 MHz, in CDCl_3



A1-43 HSQC spectrum of cornoside B (**65**), 400 MHz, in CDCl₃



A1-44 HMBC spectrum of cornoside B (65), 400 MHz, in CDCl₃



APPENDIX 2

DELPHATISINE D AND CHRYSOTRICHUMINES A – B, THREE NEW DITERPENOID ALKALOIDS FROM *DELPHINIUM CHRYSOTRICHUM*

A2-1 HRESIMS spectrum of delphatisine D (**77**)

A2-2 DEPT spectrum of delphatisine D (**77**)

A2-3 $^1\text{H} - ^1\text{H}$ COSY spectrum of delphatisine D (**77**), 400 MHz, in CDCl_3

A2-4 HSQC spectrum of delphatisine D (**77**), 400 MHz, in CDCl_3

A2-5 HMBC spectrum of delphatisine D (**77**), 400 MHz, in CDCl_3

A2-6 NOESY spectrum of delphatisine D (**77**), 400 MHz, in CDCl_3

A2-7 ^1H NMR spectrum of **77** after estification, 400 MHz, in CDCl_3

A2-8 ESIMS spectrum of **77** after estification

A2-9 HRESIMS spectrum of chrysotrichumine A (**78**)

A2-10 $^1\text{H} - ^1\text{H}$ COSY spectrum of chrysotrichumine A (**78**), 400 MHz, in CD_3OD

A2-11 HSQC spectrum of chrysotrichumine A (**78**), 400 MHz, in CD_3OD

A2-12 HMBC spectrum of chrysotrichumine A (**78**), 400 MHz, in CD_3OD

A2-13 EXPENDED NOESY spectrum of chrysotrichumine A (**78**) in CD_3OD

A2-14 NOESY spectrum of chrysotrichumine A (**78**), 400 MHz, in CD_3OD

A2-15 HRESIMS spectrum of chrysotrichumine B (**79**)

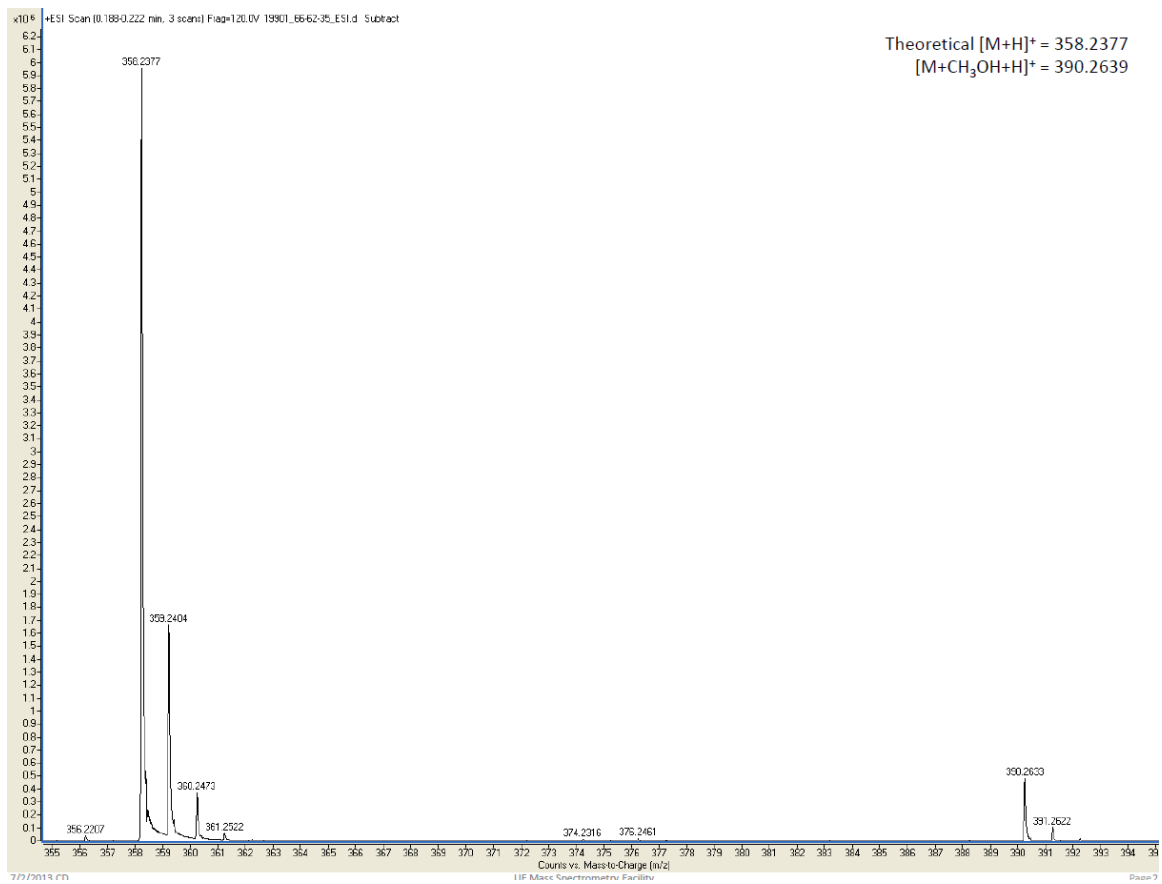
A2-16 $^1\text{H} - ^1\text{H}$ COSY spectrum of chrysotrichumine B (**79**), 400 MHz, in CDCl_3

A2-17 HSQC spectrum of chrysotrichumine B (**79**), 400 MHz, in CDCl_3

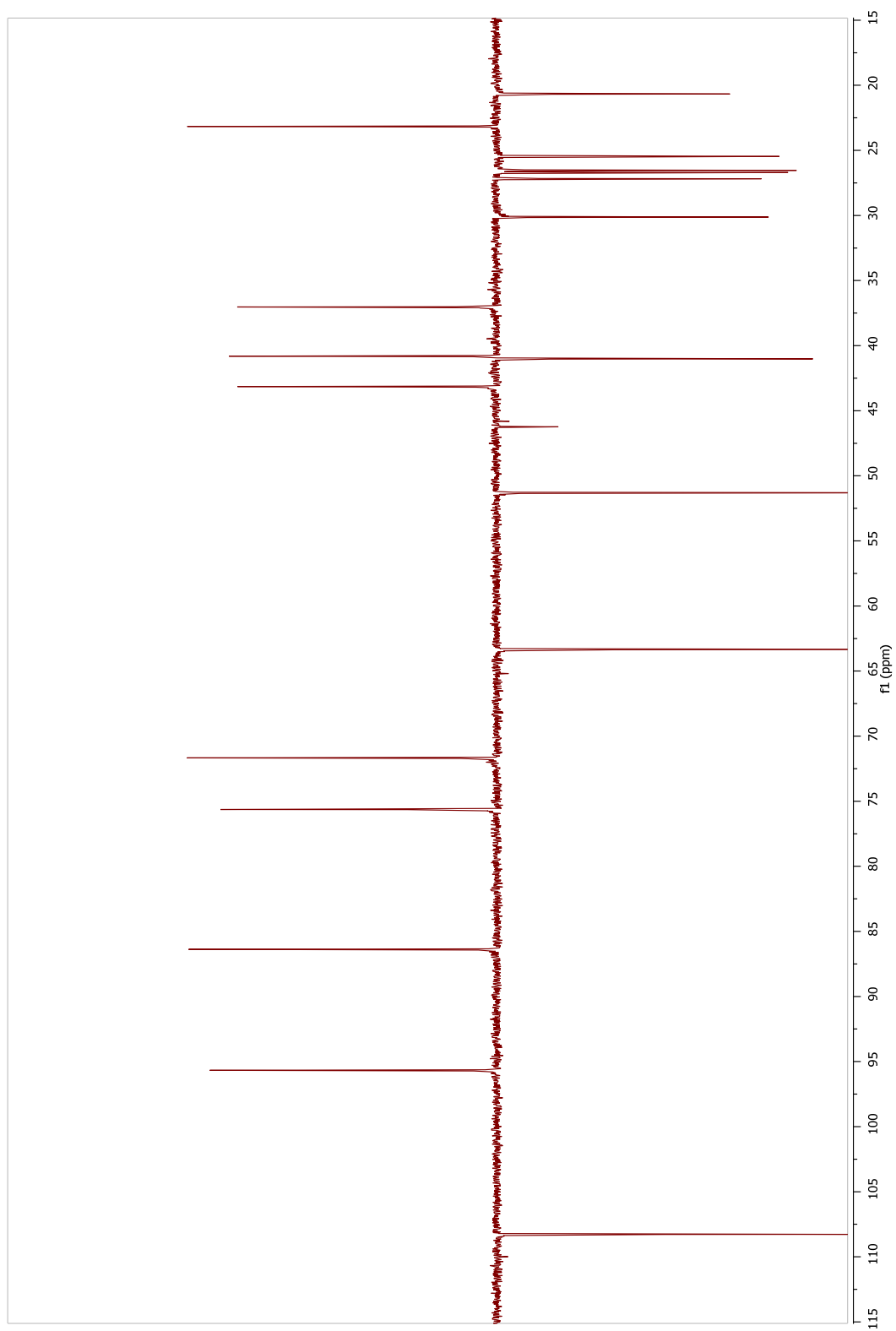
A2-18 HMBC spectrum of chrysotrichumine B (**79**), 400 MHz, in CDCl₃

A2-19 NOESY spectrum of chrysotrichumine B (**79**), 400 MHz, in CDCl₃

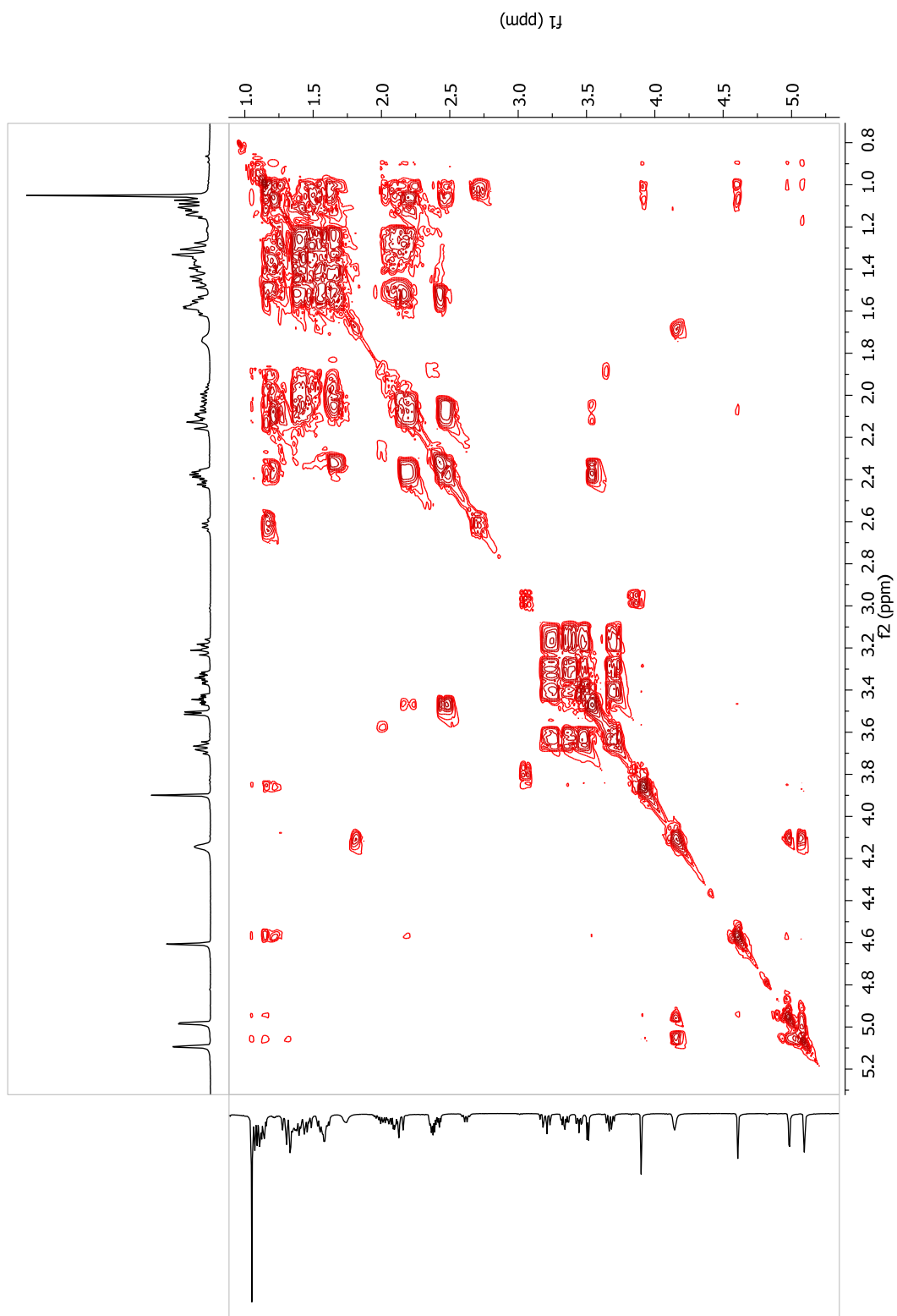
A2-1 HRESIMS spectrum of delphatisine D (77)



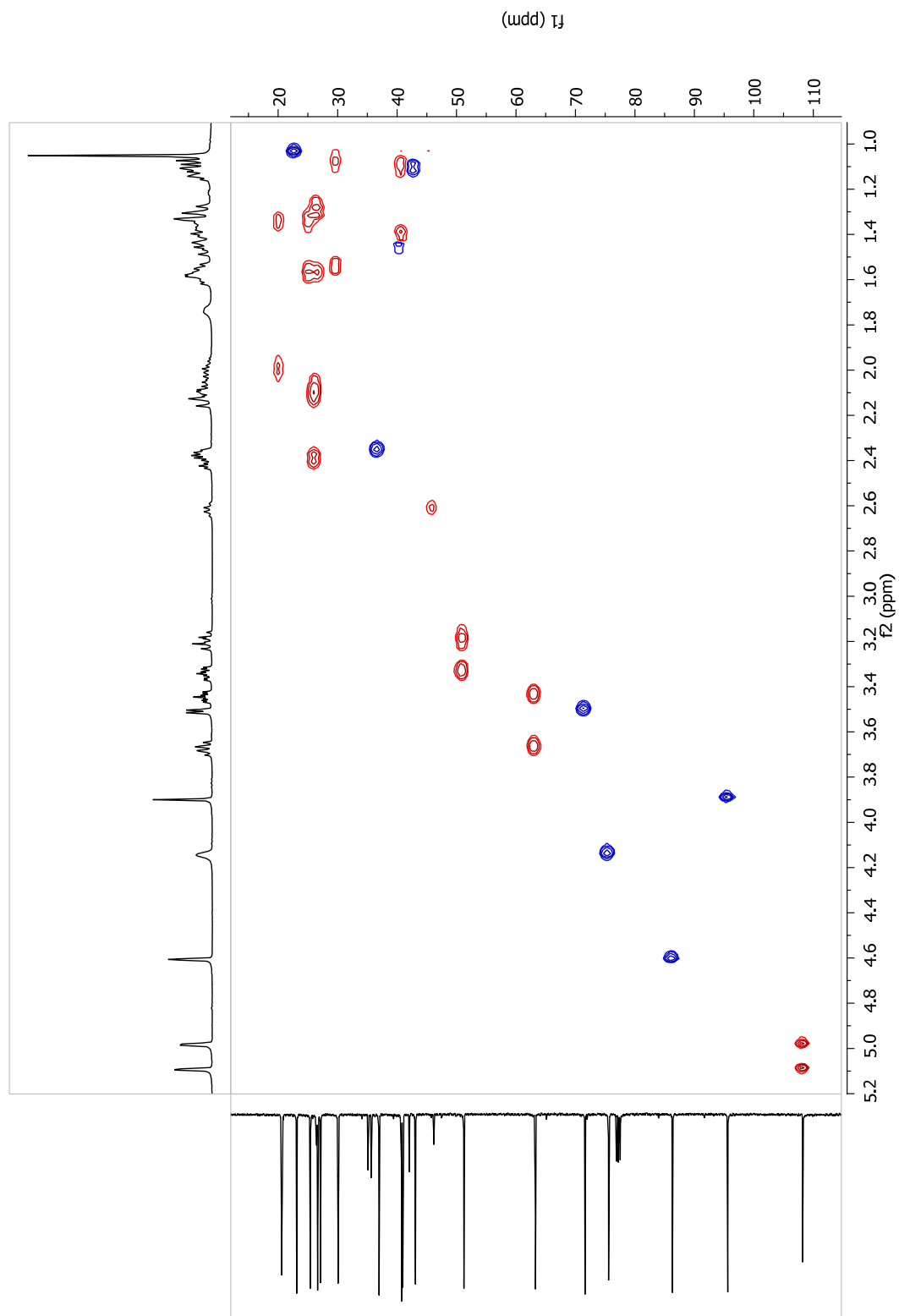
A2-2 DEPT spectrum of delphatisine D (77)



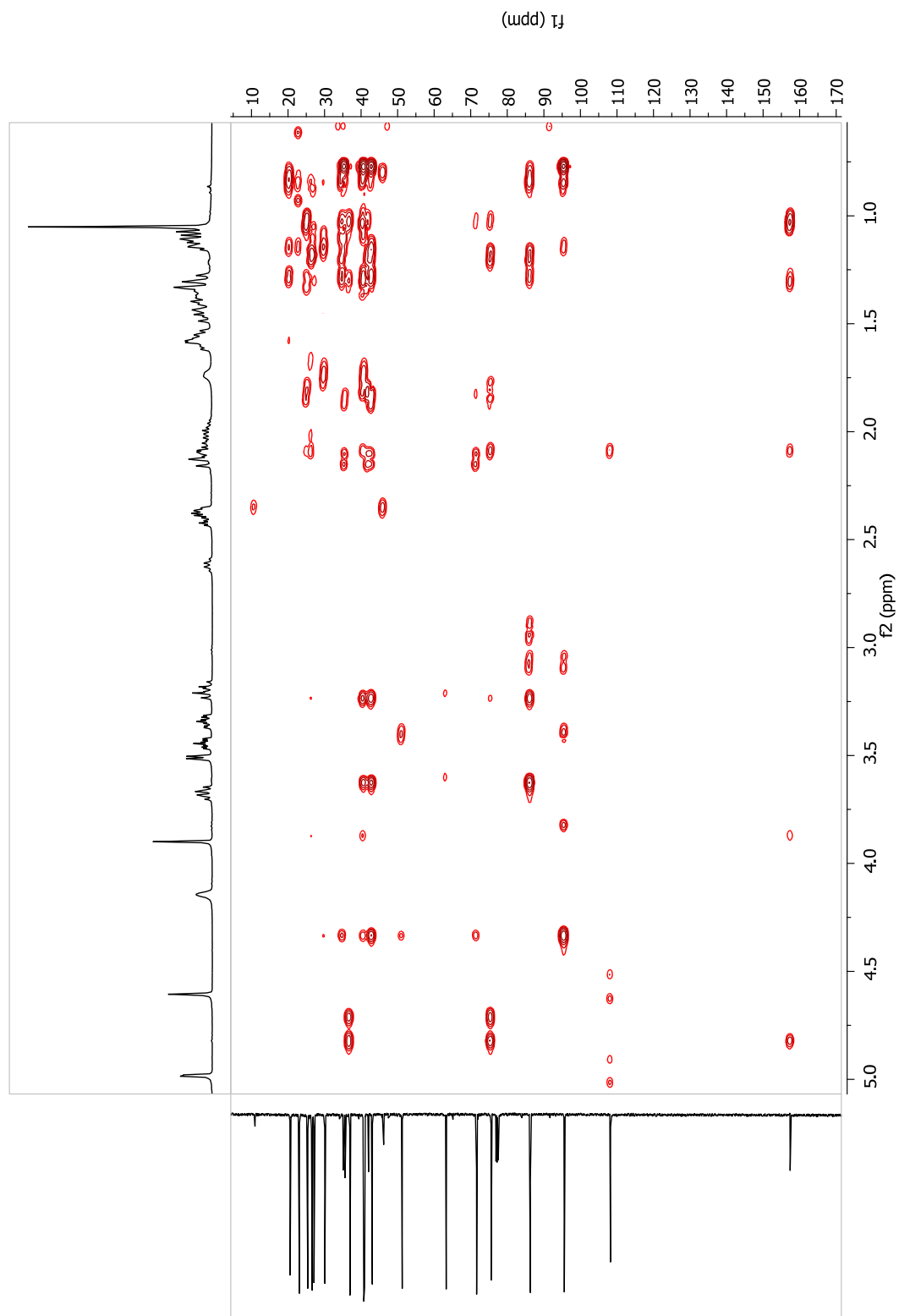
A2-3 $^1\text{H} - ^1\text{H}$ COSY spectrum of delphatisine D (77), 400 MHz, in CDCl_3



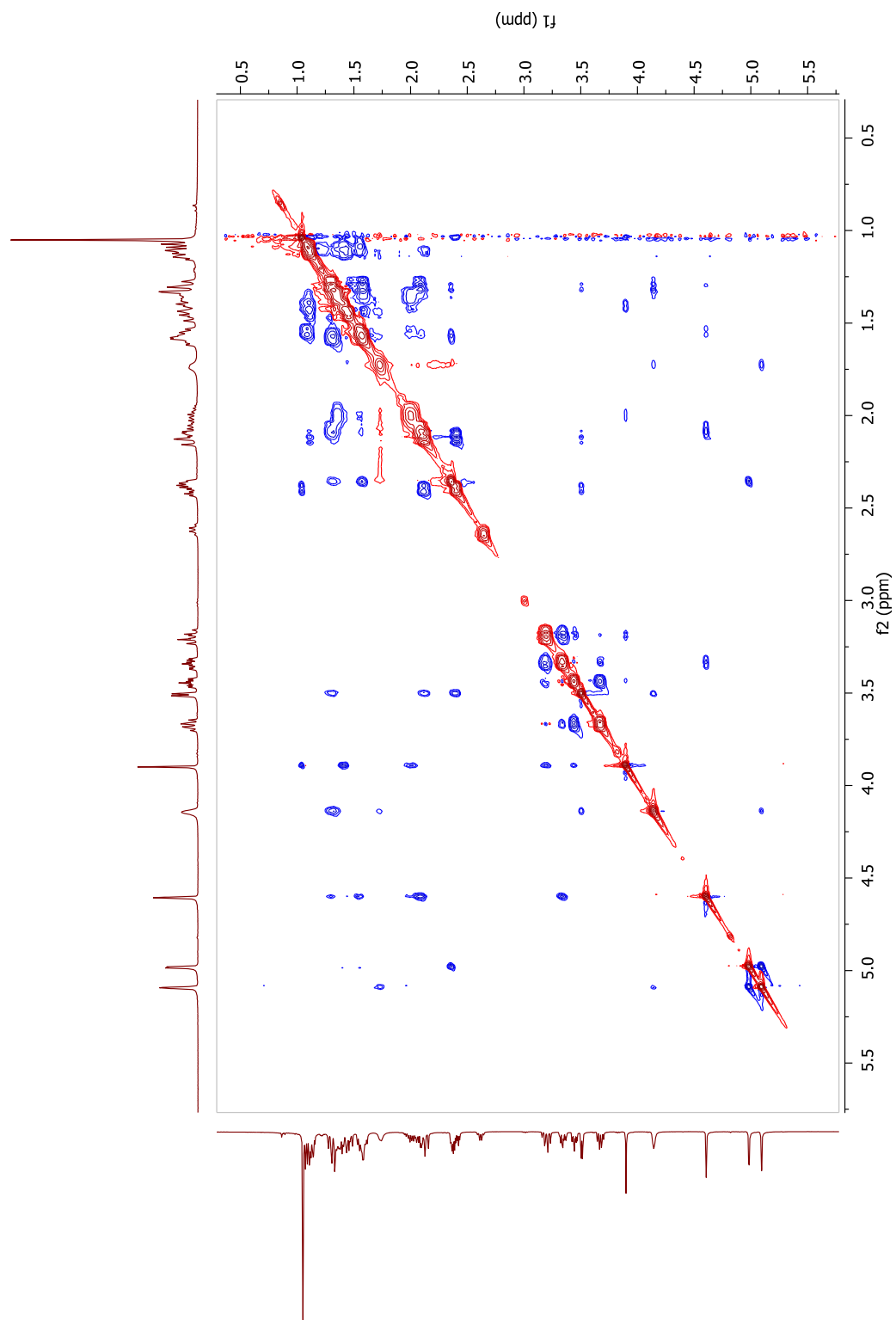
A2-4 HSQC spectrum of delphatisine D (77), 400 MHz, in CDCl₃



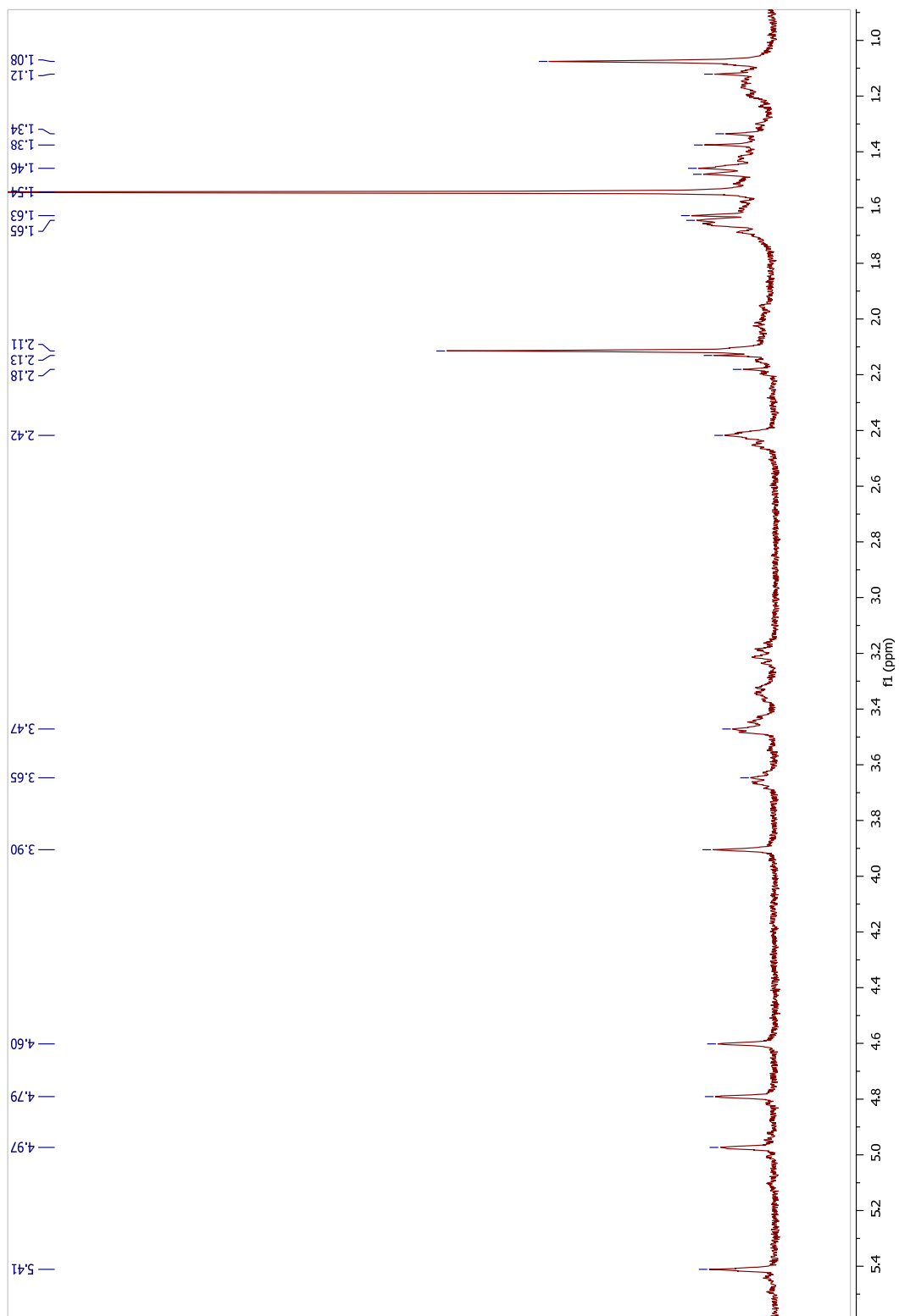
A2-5 HMBC spectrum of delphatisine D (77), 400 MHz, in CDCl₃



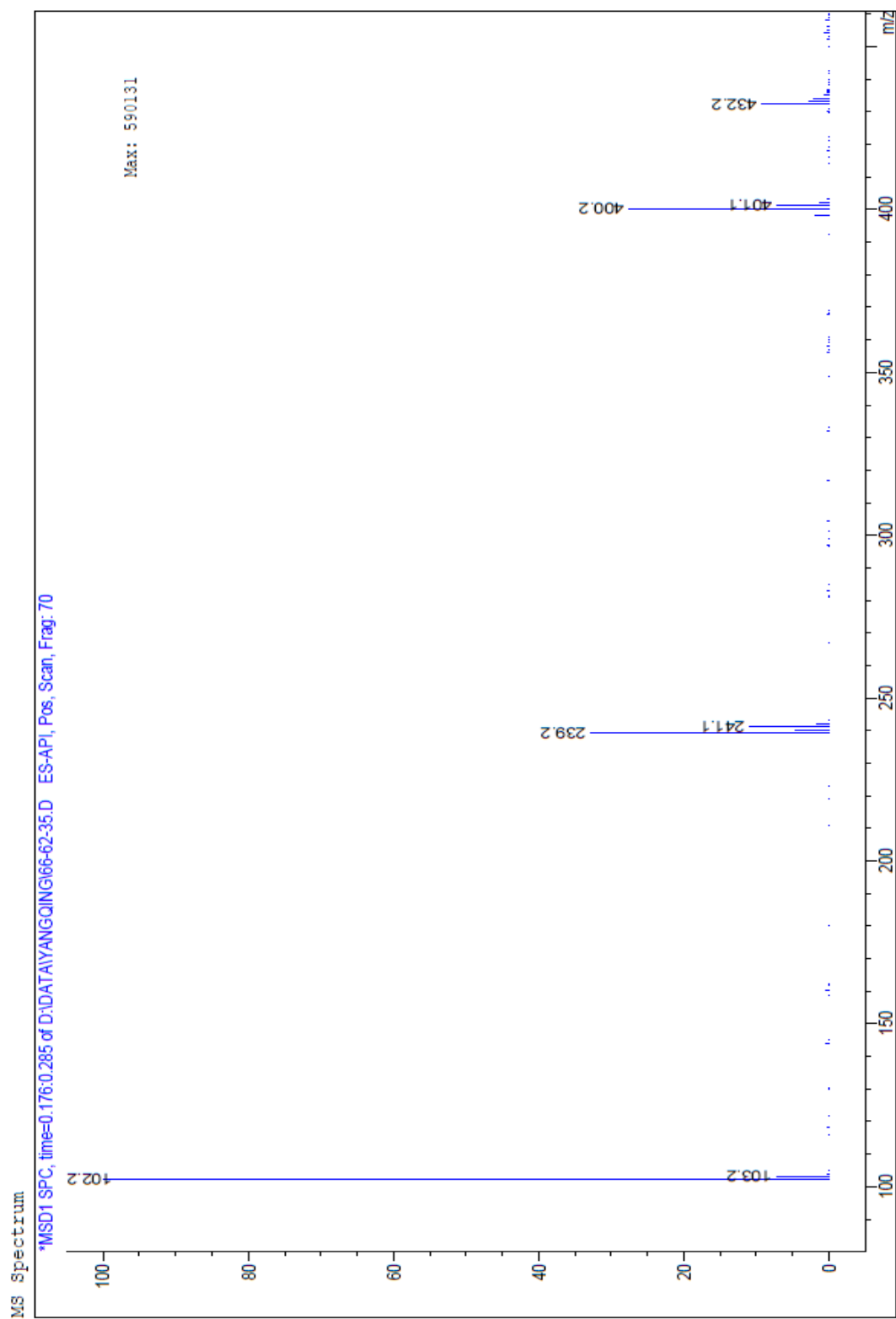
A2-6 NOESY spectrum of delphatisine D (77), 400 MHz, in CDCl₃



A2-7 ^1H NMR spectrum of 77 after estification, 400 MHz, in CDCl_3

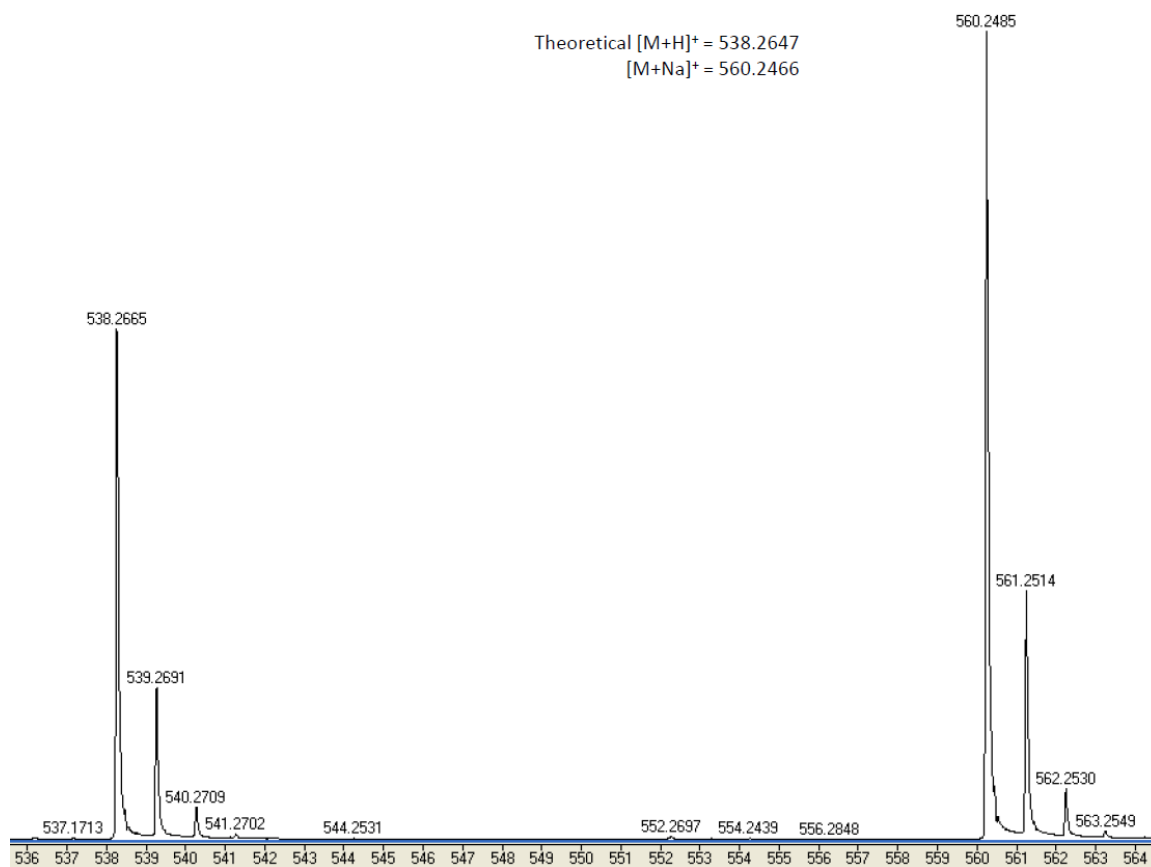


A2-8 ESIMS spectrum of 77 after estification.

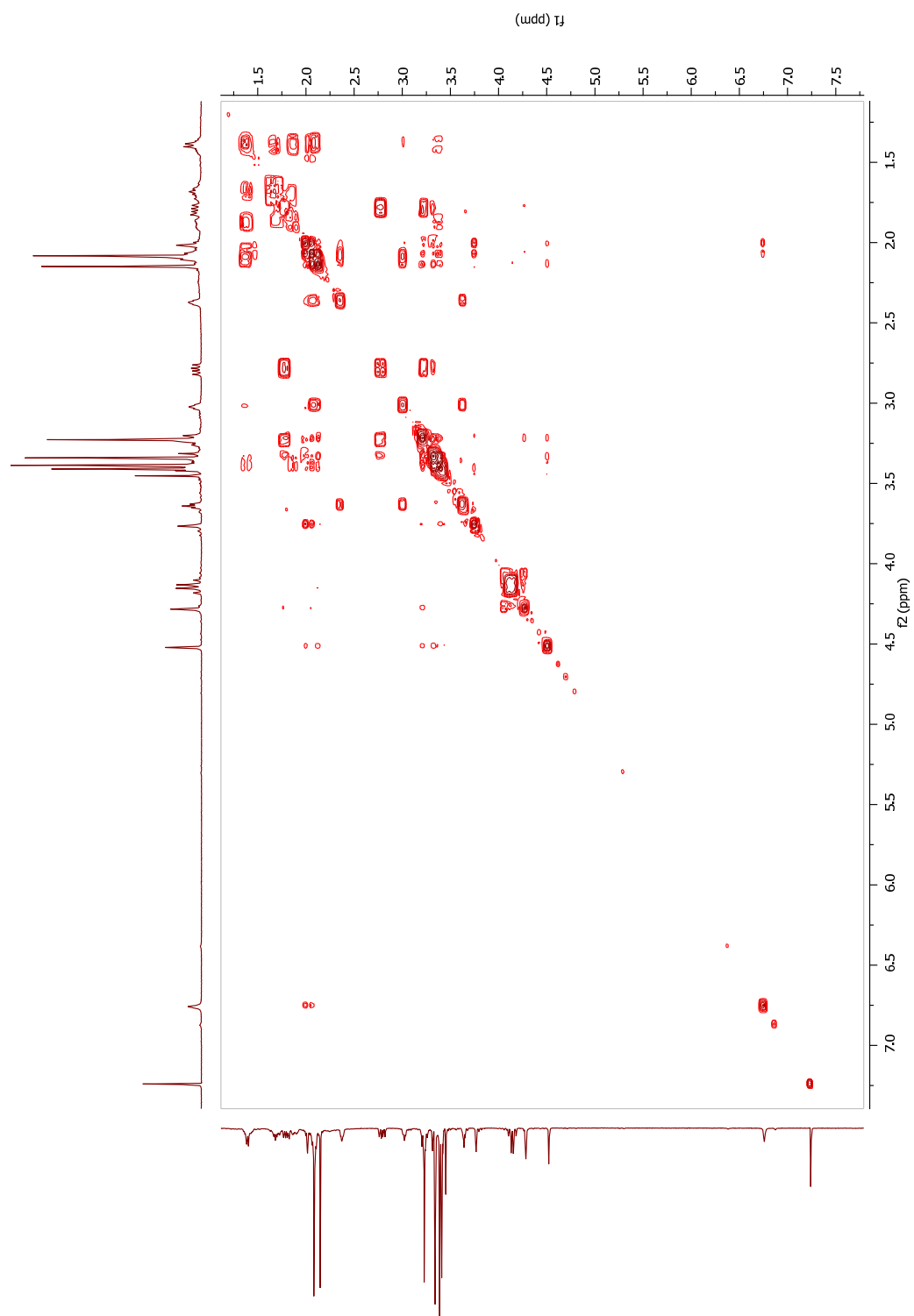


A2-9 HRESIMS spectrum of chrysotrichumine A (78)

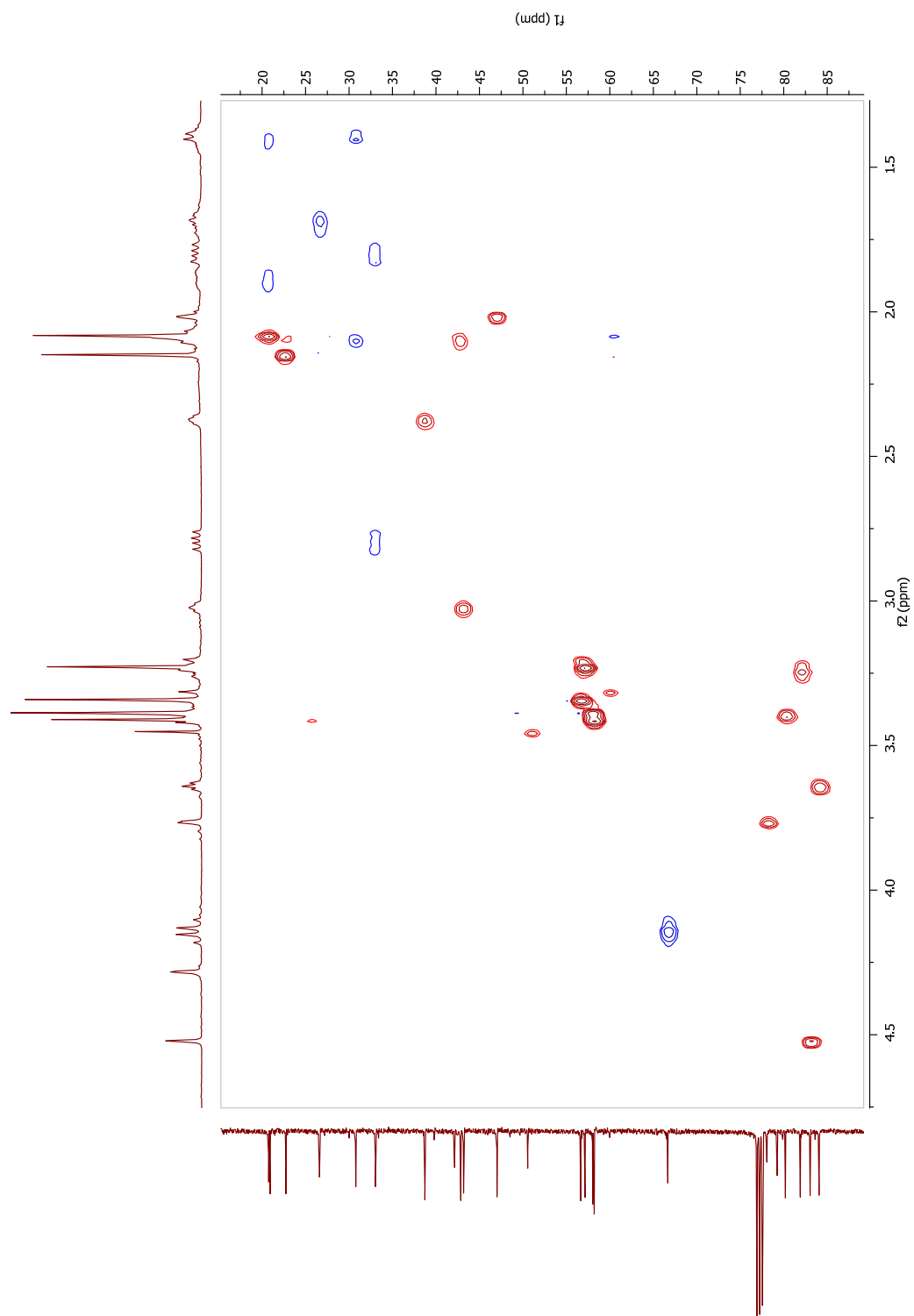
+ESI Scan (0.166-0.199 min, 3 scans) Frag=120.0V 19801_A-E-67-30_ESI.d Subtract



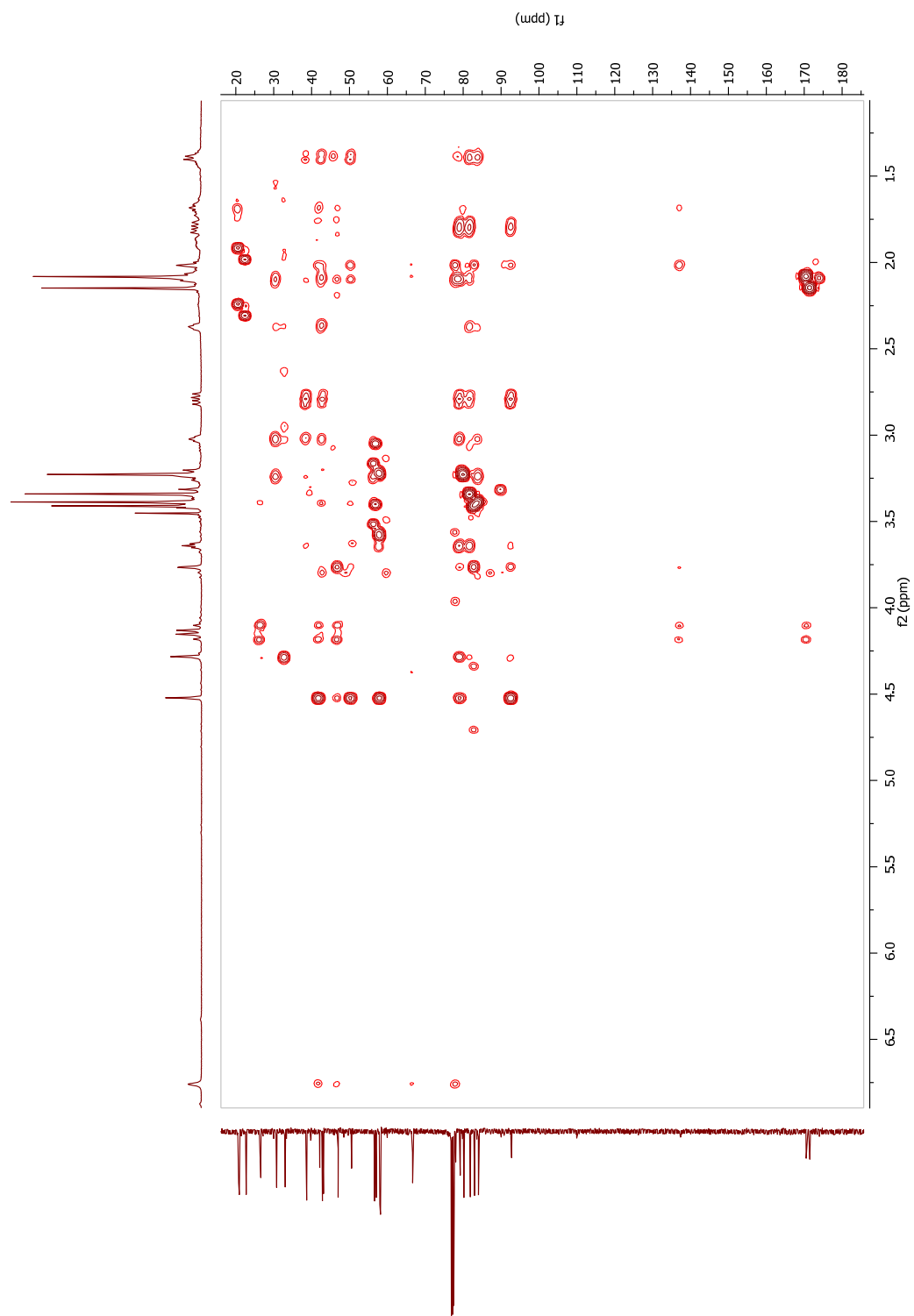
A2-10 $^1\text{H} - ^1\text{H}$ COSY spectrum of chryso-trichumine A (78), 400 MHz, in CDCl_3



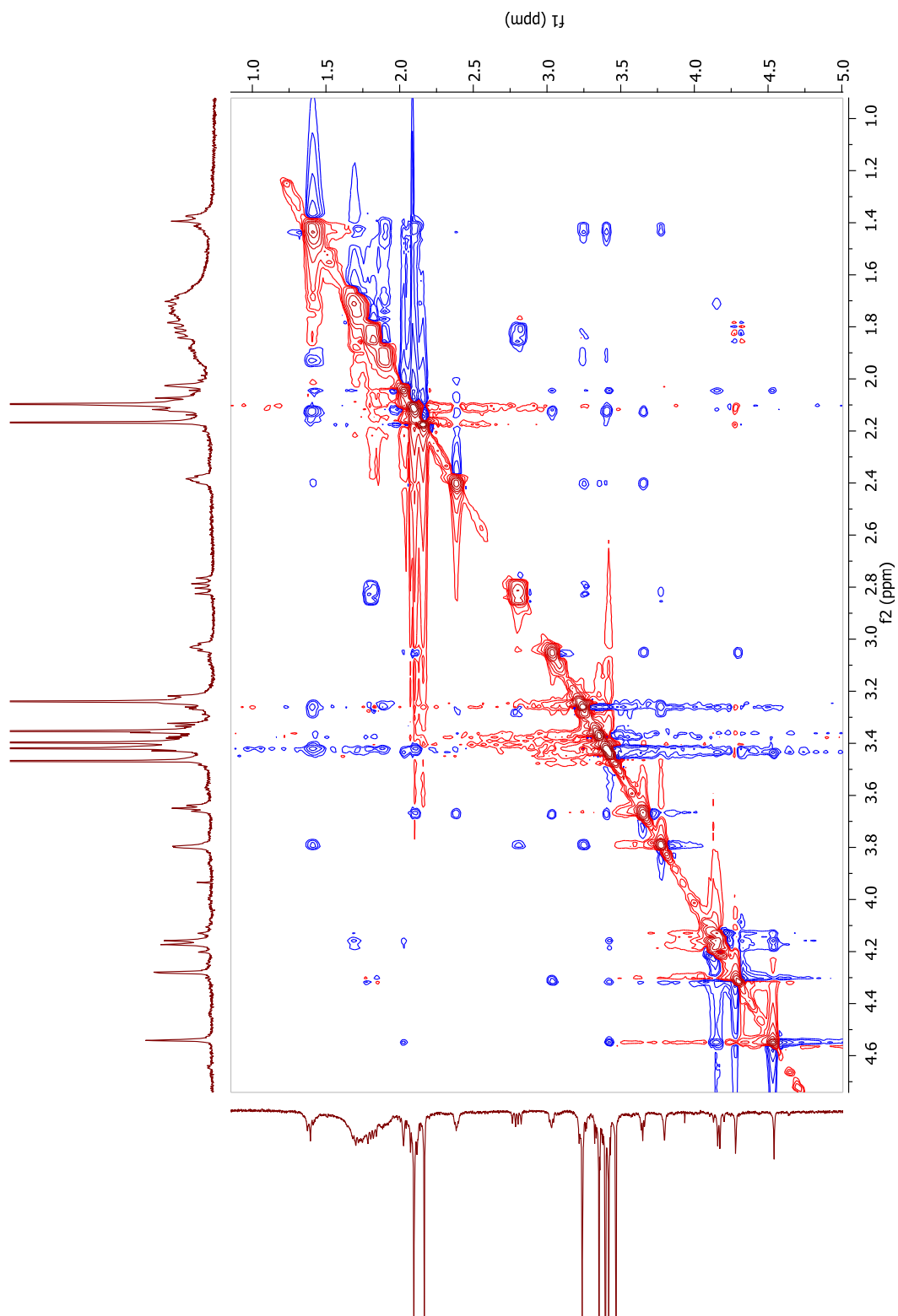
A2-11 HSQC spectrum of chrysotrichumine A (78), 400 MHz, in CDCl₃



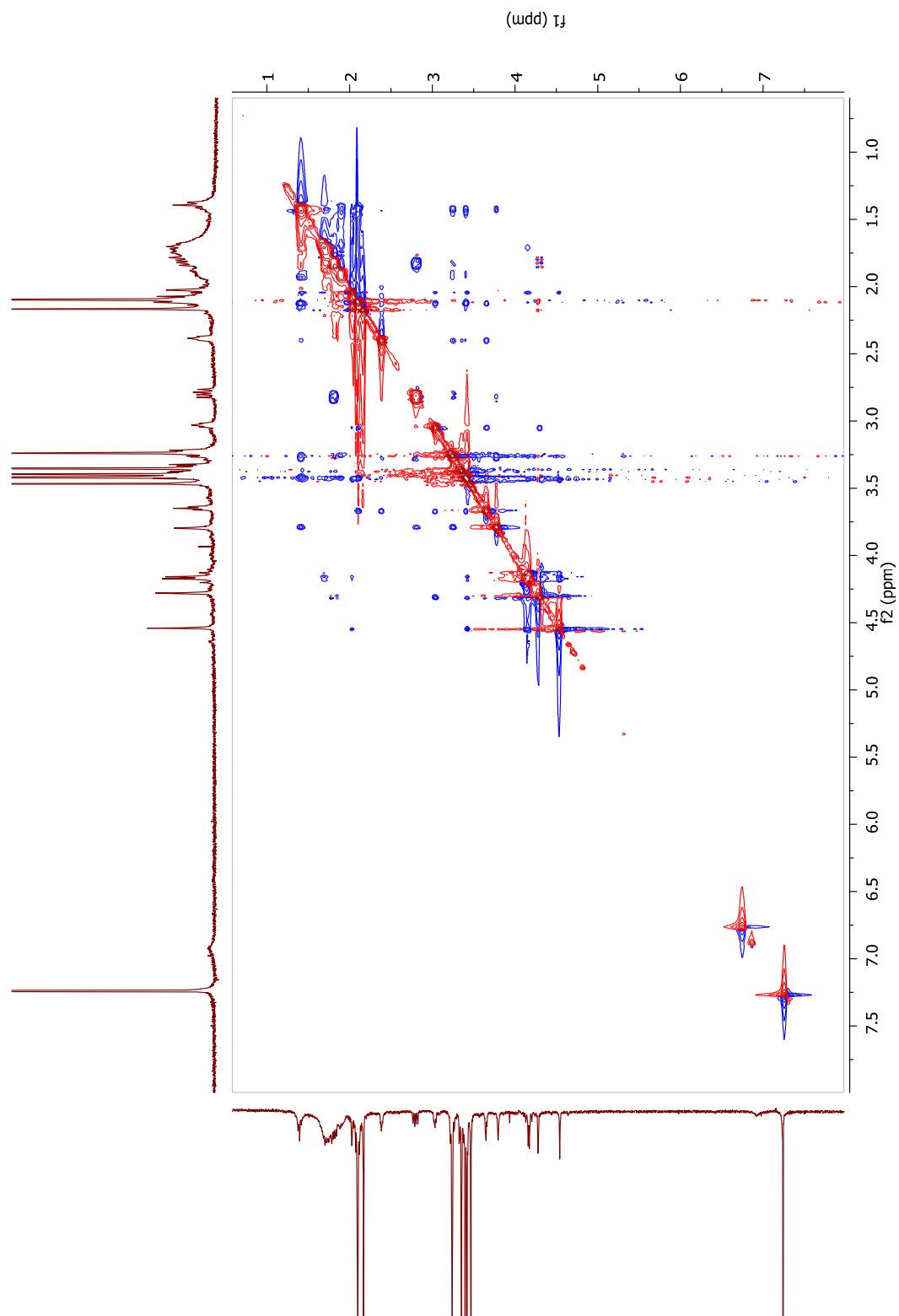
A2-12 HMBC spectrum of chrysotrichumine A (78), 400 MHz, in CDCl₃



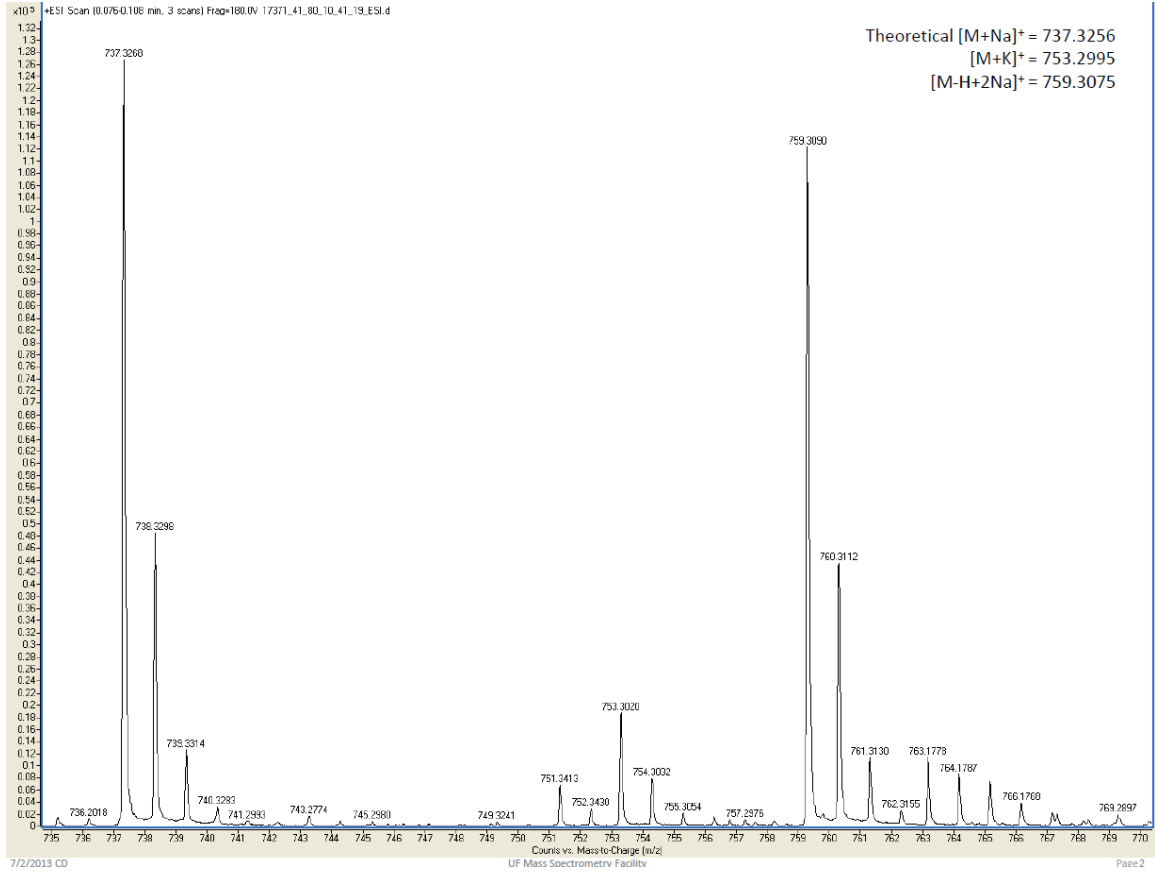
A2-13 EXPENDED ROESY spectrum of chrysochumine A (**78**) in CDCl₃



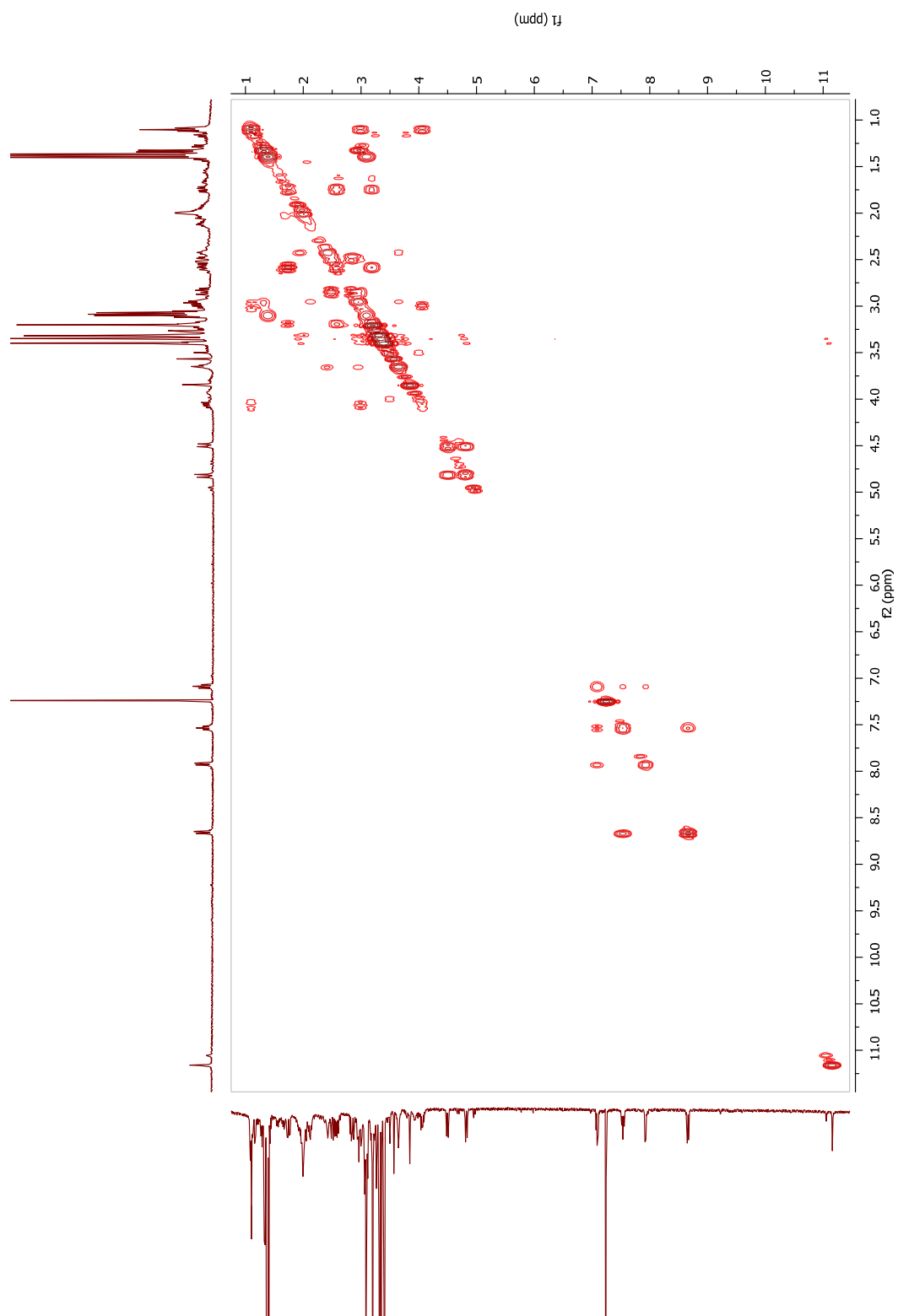
A2-14 ROESY spectrum of chrysostrictumine A (**78**), 400 MHz, in CDCl₃



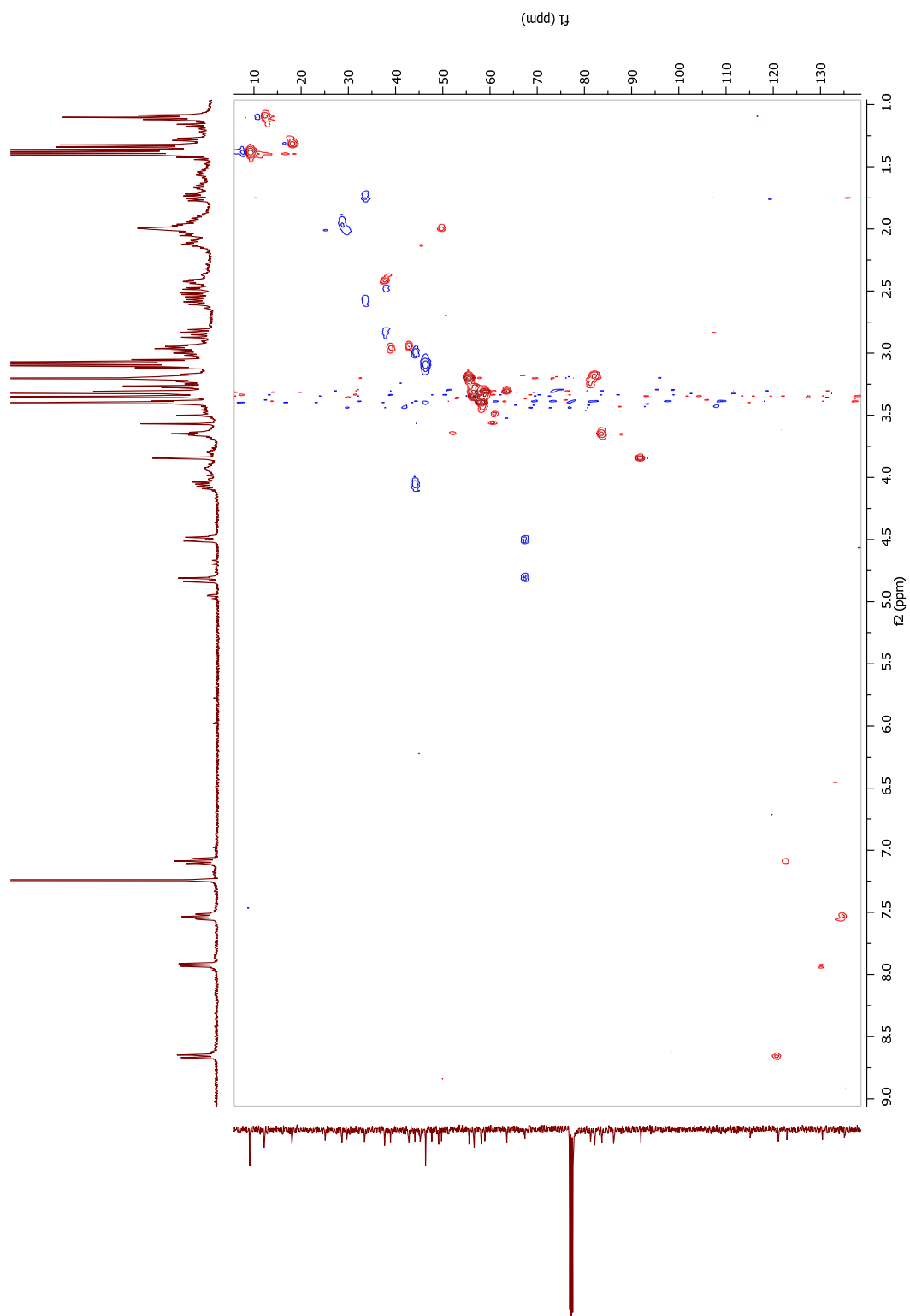
A2-15 HRESIMS spectrum of chrysostrictumine B (79)



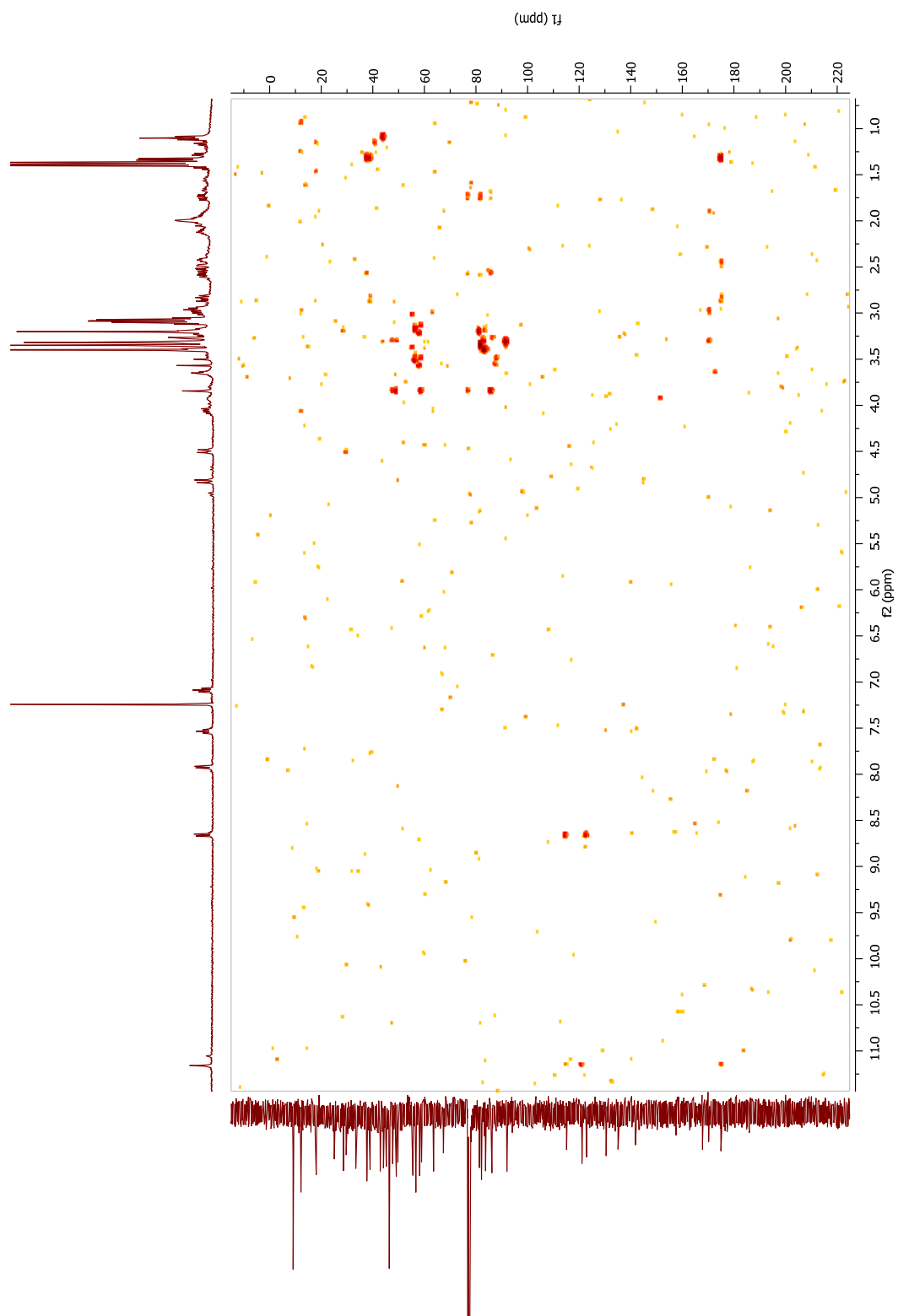
A2-16 $^1\text{H} - ^1\text{H}$ COSY spectrum of chryso-trichumine B (79), 400 MHz, in CDCl_3



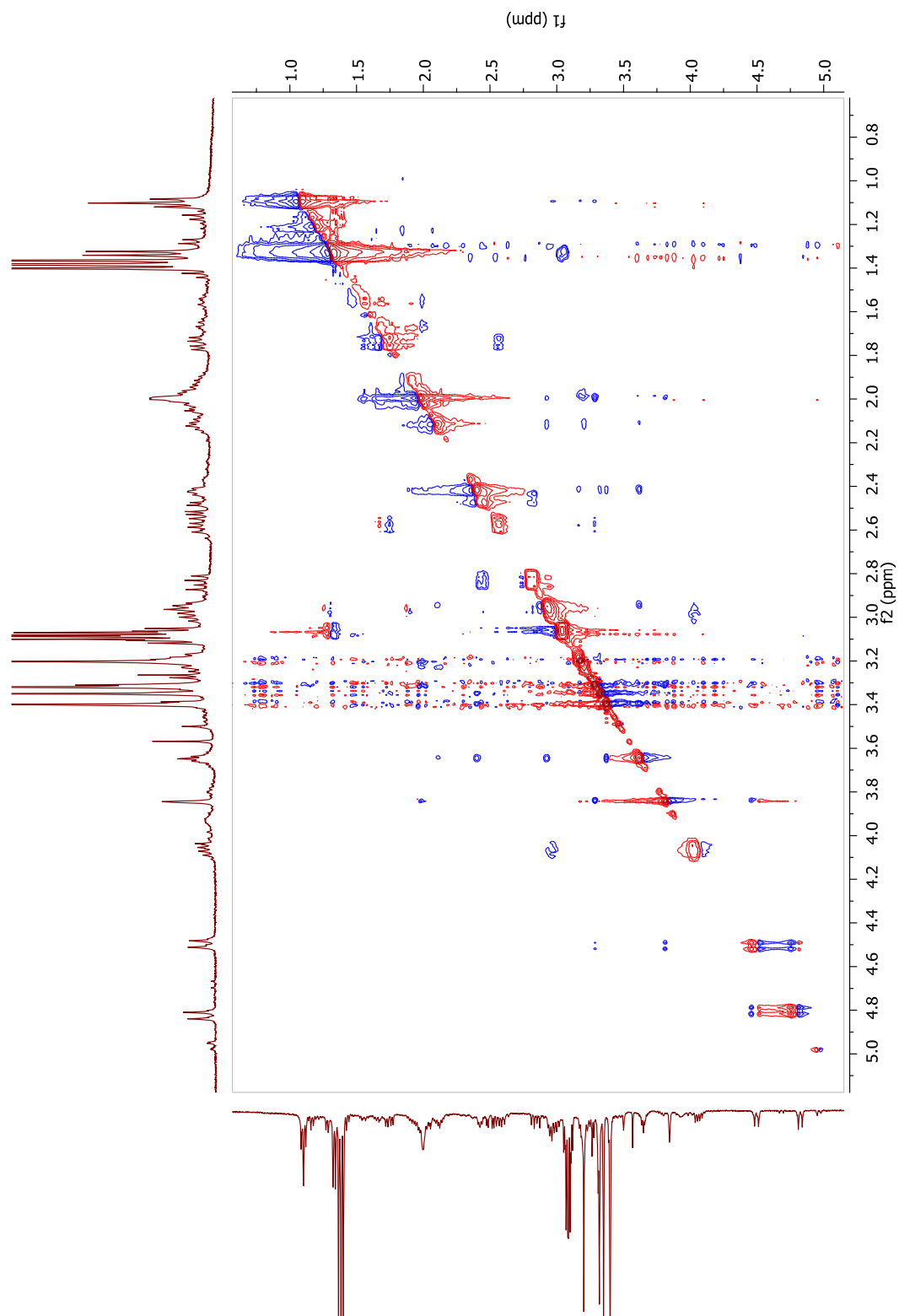
A2-17 HSQC spectrum of chrysotrichumine B (79), 400 MHz, in CDCl₃



A2-18 HMBC spectrum of chrysotrichumine B (79), 400 MHz, in CDCl₃



A2-19 NOESY spectrum of chrysostrictumine B (79), 400 MHz, in CDCl₃



REFERENCES

1. Lee, D.; Kang, S. J.; Lee, S. H.; Ro, J.; Lee, K.; Kinghorn, A. K. *Phytochemistry* **2000**, *53*, 405-407.
2. Kamei, A.; Hisada, T.; Iwata, S. *J. Ocul. Pharmacol.* **1987**, *3*, 239-248.
3. He, H.; Yang, X.; Zeng, X.; Shi, M.; Yang, J.; Wu, L.; Li, L.; *J. Pharm. Pharmacol.* **2007**, *59*, 1297-1305.
4. Nakagawa, T.; Yokozawa, T.; Yamabe, N.; Rhyu, D. Y.; Goto, H.; Shimada, Y.; Shibahara, N. *J. Pharm. Pharmacol.* **2005**, *57*, 1205-1212.
5. Seeram, N. P.; Schutzki, R.; Chandra, A.; Nair, M. G. *J. Agri. Food Chem.* **2002**, *50*, 2519-2523.
6. Qian, D. S.; Zhu, Y. F.; Zhu, Q. *China J. Chin. Mater. Med.* **2001**, *26*, 859-862.
7. Liou, S. S.; Liu, I. M.; Hsu, S. F.; Cheng, J. T. *J. Pharm. Pharmacol.* **2004**, *56*, 1443-1447.
8. Vareed, S. K.; Reddy, M. K.; Schutzki, R. E.; Nair, M. G. *Life Sci.* **2006**, *78*, 777-784.
9. Yamabe, N.; Kang, K. S.; Goto, E.; Tanaka, T.; Yokozawa, T. *Biol. Pharm. Bull.* **2007**, *30*, 520-526.
10. Wang, W.; Sun, F. L.; An, Y.; Ai, H. X.; Zhang, L.; Huang, W. T.; Li, L. *Eur. J. Pharmacol.* **2009**, *613*, 19-23.
11. Bas, E.; Recio, M. C.; Manez, S.; Giner, R. M.; Escandell, J. M.; Gines, C. L.; Rios, J. L. *Eur. J. Pharmacol.* **2007**, *555*, 199-210.

12. Diaz, A. M.; Abad, M. J.; Fernandez, L.; Recuero, C.; Villaescusa, L.; Silvan, A. M.; Bermejo, P. *Biol. Pharm. Bull* **2000**, *23*, 1307-1313.
13. Isiguro, K.; Yamaki, M.; Takagi, S.; Ikeda, Y.; Kawakami, K.; Ito, K.; Nose, T. *Chem. Pharm. Bull.* **1986**, *34*, 2375-2379.
14. Mouries, C.; Rakotondramasy, V. C.; Libot, F.; Tillequin, F.; Deguin, B. *Chem. Biodiver.* **2005**, *2*, 695-703.
15. Yokozawa, T.; Yamabe, N.; Kim, H. Y.; Kang, K. S.; Hur, J. M.; Park, C. H.; Tanaka, T. *Bio. Pharm. Bull.* **2008**, *31*, 1422-1428.
16. Lin, M. H.; Liu, H. K.; Huang, W. J.; Huang, C. C.; Wu, T. H.; Hsu, F. L. *J. Agric. Food Chem.* **2011**, *59*, 7743-7751.
17. Lee, K. Y.; Sung, S. H.; Kim, S. H.; Jang, Y. P.; Oh, T. H.; Kim, Y. C. *Arch. Pharm. Res.* **2009**, *32*, 677-683.
18. Yamabe, N.; Kang, K. S.; Matsuo, Y.; Tanaka, T.; Yokozawa, T. *Biol. Pharm. Bull.* **2007**, *30*, 1289-1296.
19. Kang, D. G.; Moon, M. K.; Lee, A. S.; Kwon, T. O.; Kim, J. S.; Lee, H. S. *Biol. Pharm. Bull.* **2007**, *30*, 1796-1799.
20. Jiang, W. J.; Chen, X. G.; Zhu, H. B.; Hou, J.; Tian, J. W. *Pharmacology* **2009**, *84*, 162-170.
21. Xu, H. Q.; Hao, H. P. *Biol. Pharm. Bull.* **2004**, *27*, 1014-1018.
22. Jayaprakasam, B.; Olson, L. K.; Schutzki, R. E.; Tai, M. H.; Nair, M. G. *J. Agric. Food Chem.* **2006**, *54*, 243-248.
23. Cho, K.; Lee, H. J.; Lee, S. Y.; Woo, H.; Lee, M. N.; Seok, J. H.; Lee, C. J. *Phytother. Res.* **2011**, *25*, 760-764.

24. Gao, D. G.; Li, Q. W.; Li, J.; Han, Z. S.; Fan, Y. S.; Liu, Z. W. *Therapy* **2008**, *5*, 697-705.
25. Tanaka, N.; Tanaka, T.; Fujioka, T.; Fujii, H.; Michashi, K.; Shimomura, K.; Ishimaru, K. *Photochemistry* **2001**, *57*, 1287-1291.
26. Zhang, Y. E.; Hu, L. E.; Jun, L. H.; Ping, L. *Chin. J. Nat. Med.* **2009**, *7*, 365-367.
27. He, Y. Q.; Ma, G. Y.; Peng, J. N.; Ma, Z. Y.; Hamann, M. T. *Bioch. Bio. Acta* **2012**, *1820*, 1021-1026.
28. Stermitz, F. R.; Krull, R. E. *Biochem. Syst. Ecol.* **1998**, *26*, 845-849.
29. Xu, H. Q.; Hao, H. P.; Zhang, X.; Pan, Y. *Acta Pharmacol. Sin.* **2004**, *25*, 412-415.
30. Vareed, S. K.; Schutzki, R. E.; Nair, M. G. *Phytomedicine* **2007**, *14*, 706-709.
31. Xu, H.; Shen, J.; Liu, H.; Shi, Y.; Li, L.; Wei, M. *Can. J. Pharm. Pharmacol.* **2006**, *84*, 1267-1273.
32. Xie, X. Y.; Wang, R.; Shi, Y. P. *Biochem. Syst. Ecol.* **2012**, *45*, 120-123.
33. Wang, M. Y.; Zhao, F. M.; Cai, B. C.; *Chin. Arch. Traddit. Chin. Med.* **2008**, *12*, 204-209.
34. Dong, M.; He, X. J.; Liu, R. H. *J. Agric. Food Chem.* **2007**, *55*, 6044-6051.
35. Ahmad, N. S.; Farman, M.; Najmi, M. H.; Mian, K. B.; Hasan, A. *J. Ethnopharmacol* **2008**, *117*, 478-482.
36. Matsuda, H.; Ninomiya, K.; Shimoda, H.; Yoshikawa, M. *Bioorg. Medicinal Chem.* **2002**, *10*, 707-712.
37. Sultana, N.; Lee, N. H. *Phytother. Res.* **2007**, *21*, 1171-1176.
38. Zhang, W.; Hong, D.; Zhou, Y.; Zhang, Y.; Shen, Q.; Li, J. Y.; Hu, L. H.; Li, J. *Bioch. Bio. Acta* **2006**, *1760*, 1505-1512.

39. Tanaka, N.; Nishikawa, K.; Ishimaru, K. *J. Agric. Food Chem.* **2003**, *51*, 5906-5910.
40. Fan, C.; Xiong, Q. Y. *Am. J. Bot.* **2001**, *88*, 1131-1138.
41. Mau, J.; Chen, C.; Hsieh, P. *J. Agric. Food Chem.* **2001**, *49*, 183-188.
42. Jayaprakasam, B.; Vareed, S. K.; Olson, L. K.; Nair, M. G. *J. Agric. Food Chem.* **2005**, *53*, 28-31.
43. Piccinini, P.; Vidari, G.; Zanoni, G. *J. Am. Chem. Sci.* **2004**, *126*, 5088-5089.
44. Marino, S. D.; Borbone, N.; Zollo, F.; Ianaro, A.; Meglio, P. D.; Iorizzi, M. *J. Agric. Food Chem.* **2004**, *52*, 7525-7531.
45. Sefton, M. A.; Francis, L.; Williams, P. J. *J. Agric. Food Chem.* **1990**, *38*, 2405-2049.
46. Nawwar, M. A.; Buddrus, J.; Bauer, H. *Phytochemistry* **1982**, *21*, 1755-1758.
47. Hillis, W. E.; Yazaki, Y. *Phytochemistry* **1973**, *12*, 2969-2977.
48. Nomiya, T.; Bruemmer, D. *Curr. Atheroscler. Rep.* **2008**, *10*, 88-95.
49. Jensen, S. S.; Kirk, O.; Nielsen, B. J.; Norrestam, R. *Phytochemistry* **1987**, *26*, 1725-1731.
50. Vieira, I. J.; Mathias, L.; Braz-Filho, R.; Schripsema, J. *Org. Lett.* **1999**, *1*, 1169-1171.
51. Berkowitz, W. F.; Choudhry, S. C.; Hrabie, J. A. *J. Org. Chem.* **1982**, *47*, 824-829.
52. Marinos, V. A.; Tate, M. E.; Williams, P. J. *Phytochemistry* **1992**, *31*, 2755-2759.
53. Li, Y.; Ishibashi, M.; Satake, M.; Oshima, Y.; Ohizumi, Y. *Chem. Pharm. Bull.* **2003**, *51*, 1103-1105.
54. Ono, M.; Oishi, K.; Abe, H.; Masuoka, C.; Okawa, M.; Ikeda, T.; Nohara, T. *Chem. Pharm. Bull.* **2006**, *54*, 1421-1424.

55. Alley, M. C.; Scudiero, D. A.; Monks, A.; Hursey, M. L.; Czerwinski, M. J.; Fine, D. L.; Abbott, B. J.; Mayo, J. G.; Shoemaker, R. H.; Boyd, M. R. *Cancer Res.* **1988**, *48*, 589-601.
56. Pelletier, S. W.; Mody, N. V.; Joshi, B. S.; Schramm L. C. In *The Alkaloids: Chemical and Perspectives*; Pelletier, S. W., Ed.; Wiley: New York, 1983; Vol. 1, pp 153-210.
57. Wang, F. P.; Liang, X. T. In *The Alkaloids: Chemical and Biology*; Cordell, G. A., Ed.; Elsevier Science: New York, 2002; Vol. 59, pp 1-280.
58. Wang, W. C.; Wamock, M. In *Flora of China*; Wu, Z. Y., Raven, R., Hong, D. Y., Eds.; Science: Beijing, 2004; Vol. 6, pp 223-248.
59. The Flora Committee of Chinese Academy of Science. In *The Chinese Flora*; Guan, K. X., Ed.; Science: Beijing, 1979; Vol. 27, pp 365-366.
60. Joshi, B.; Pelletier, S. W.; Zhang, X. L.; Synder, J. K. *Tetrahedron* **1991**, *47*, 4299-4316.
61. He, Y. Q.; Wei, X. M.; Han, Y. L.; Gao, L. M. *Chin. Chem. Lett.* **2007**, *18*, 545-547.
62. He, Y. Q.; Ma, Z. Y.; Wei, X. M.; Du, B. Z.; Jing, Z. X.; Yao, B. H.; Gao, L. M. *Fitoterapia* **2010**, *81*, 929-931.
63. Deng, W.; Sung, W. L. *Heterocycles* **1986**, *24*, 873-876.
64. Pelletier, S. W.; Mody, N. V.; Joshi, B. S.; Schramm L. C. In *The Alkaloids: Chemical and Biological Perspectives*; Pelletier, S. W., Ed.; Wiley: New York, 1984; Vol. 2, pp 206-462.
65. Ata, A.; Conci, L. J.; Betteridge, J.; Orhan, I.; Sener, B. *Chem. Pharm. Bull.* **2007**, *55*, 118-123.

66. Zhang, C. Y.; Sung, W. L.; Chen, D. H. *Fitoterapia* **1993**, *64*, 188-189.
67. Liang, X. X.; Chen, D. L.; Wang, F. P. *Chin. Chem. Lett.* **2006**, *17*, 1473-1476.
68. Pelletier, S. W.; Marraz, F. M.; Badawi, M. M.; Tantiraksachai, S.; Wang, F. P.; Chen, S. Y. *Heterocycles* **1986**, *24*, 1853-1865.
69. Pelletier W. S.; Joshi, B. S. In *The Alkaloids: Chemical and Biological Perspectives*; Pelletier, S. W., Ed.; Wiley: New York, 1991; Vol. 7, pp 297-564.
70. Desai, H. K.; Pelletier, W. S. *J. Nat. Prod.* **1993**, *56*, 1140-1147.
71. Li, C.; Hirasawa, Y.; Arai, H.; Aisa, H. A.; Morita, H. *Heterocycles* **2010**, *80*, 607-612.
72. Desai, H. K.; Jiang, Q. P.; Pelletier W. S. *J. Nat. Prod.* **1990**, *53*, 1374-1378.
73. Node, M.; Hao, X. J.; Zhou, J.; Chen, S. Y.; Taga, T.; Miwa, Y.; Fuji, K. *Heterocycles* **1990**, *30*, 635-643.
74. Hao, X. J.; Hong, X.; Yang, X. S.; Zhao, B. T. *Phytochemistry* **1995**, *38*: 545-547.
75. Zhou, X. L.; Chen, Q. H.; Wang, F. P. *Chem. Pharm. Bull.* **2004**, *52*, 456-458.
76. Grandez, M.; Madinaveitia, A.; Gavin, J. A.; Fuenta, G. D. *J. Nat. Prod.* **2002**, *65*, 513-516.
77. Gu, D. Y.; Aisa, H. A.; Usmanova, S. K. *Chem. Nat. Comp.* **2007**, *43*, 298-301.
78. Shrestha, P. M.; Katz, A. *J. Nat. Prod.* **2004**, *67*, 1574-1576.
79. Wang, F. P.; Pelletier, S. W. *Acta Bot. Sin.* **1990**, *32*, 733-736.
80. Coates, P. A.; Blagbrough, I. S.; Hardick, D. J.; Rowan, M. G.; Wonnacott, S.; Potter, B. V. *Tetrahedron Lett.* **1994**, *35*, 8701-8704.